A University of Sussex PhD thesis

Available online via Sussex Research Online:

http://sro.sussex.ac.uk/

This thesis is protected by copyright which belongs to the author.

This thesis cannot be reproduced or quoted extensively from without first obtaining permission in writing from the Author

The content must not be changed in any way or sold commercially in any format or medium without the formal permission of the Author

When referring to this work, full bibliographic details including the author, title, awarding institution and date of the thesis must be given

Please visit Sussex Research Online for more information and further details

Tensile properties and associated cellular composition of axon bundles in the desert locust and other orthopteroid insects

Siân Maeve Lyons

University of Sussex

This thesis is submitted to the University of Sussex in application for the degree of Doctor of Philosophy

December 2018

Declaration

This thesis is the result of my own work and includes nothing which is the outcome of work done in collaboration with others except where specifically indicated in the text. No part of this dissertation has been submitted to any other university in application for a higher degree.

Signature:

Sian Lyons

20th December, 2018

Summary

Axons are known to be under tension during growth and development for guidance of the growth cone, synapse formation and stretch growth. Tension is also present during adulthood, but its role is unclear. Here we investigate whether axon bundles in the desert locust are under tension. We then determine whether this tension is reflected in the composition of the axon bundle and/or individual axons.

We used microdissection and nerve cutting to observe tension in axon bundles connected to the metathoracic ganglion of adult gregarious desert locusts (*Schistocerca gregaria*). We show variable levels of tension in three axon bundles, with the highest level in the connectives between the meso- and metathoracic ganglia.

Transmission electron microscopy (TEM) allowed us to compare these bundles at the gross anatomical, cellular and sub-cellular levels. Gross anatomical differences in bundle size do not account for the results from the microdissections. Instead, the number of microtubules per axon and the relationship between microtubule number and axon size are the main factors that correlate with results from microdissection. This suggests that the tension of the entire axon bundle is mediated by the cellular cytoskeleton. We use *ex vivo* uniaxial loading to link microdissection and TEM findings to mechanical properties. We find that high-tension bundles withstand the highest forces prior to failure.

We repeated our microdissection nerve cutting across growth stages (instars) immediately prior to and after moulting. This showed that tension does not change during periods of growth. We performed microsurgery on third instar *S. gregaria*, cutting one of the high-tension connectives to expose the second to greater force. We then

resealed the cuticle and allowed the locusts to grow to adulthood. Despite morphological changes, there was no change in *in vivo* tension in surgery locusts. TEM revealed that the remaining connective had a higher density and count of microtubules than shams or controls, suggesting these had been actively upregulated in response to changing forces.

Finally, we repeated the microdissections on solitary phase *S. gregaria* and *Locusta migratoria*. We found no differences in tension held in the connectives between the meso- and metathoracic ganglia and those of gregarious desert locusts. We expanded to other orthopteroids (*Gryllus bimaculatus*, *Periplaneta americana*) that differ in the extent to which their metathoracic ganglion is fused. In both species the connectives between the meso- and metathoracic ganglia are under less tension than in locusts. This was reflected in TEM results: connectives in locusts had a higher number of microtubules per axon than other species. However uniaxial loading experiments did not reflect microdissection results, which suggests mechanical properties of axons do not necessarily reflect *in vivo* forces experienced.

We suggest in this thesis that axonal tension is a variable property of axons that is correlated with the density of microtubules in the longitudinal orientation. We propose that individual axons have a 'set-point' of tension that is actively maintained throughout growth and in response to injury. Combined these results suggest that axonal tension is likely functional, rather than universal, property of axons that is capable of responding to selective pressures.

Acknowledgments

I think this must start with Jeremy. I spent my entire PhD trying to find a gap in this man's knowledge, it was never going to be any topic of science but apparently it's not literature, history, art, or even comic books: I might be ahead on true crime knowledge but he's catching up. Jeremy Niven is truly the best supervisor I have encountered, unwaveringly interested and enthusiastic and a perfect balance of giving freedom while providing support. He has also gone above and beyond his duties and I can safely say I would not have made it through without him. I am sorry for what I've put him through, but eternally grateful that he was the one there.

Next, my secondary supervisor Guy Richardson provided me not just with guidance but also let me wreck his lab a few times. I need to thank Richard, Other Richard and Other Sian in the Richardson lab – your lab is insane but half my PhD couldn't have happened without it. My thesis committee members, Louise Serpell and Jonathon Bacon: occasionally Jeremy is so enthusiastic is causes worry that you might be living in a shared delusion, thank you for supporting it.

To my office mates. The list of things I need to apologise for is extensive. I'm messy and loud and distracting and annoying but you were all still there. Adrian taught me everything when I first started and I'm still learning all the ways that was wrong. Sofia joined me in a lot of hatred but was also the only one who actually knew anything about anything. James and Alex were both just far too nice for the rest of us. Marta was intimidating and awesome and will firmly leave the rest of us in the dust. Doran, you don't even go here but I'm glad you're around. And Craig, honestly I'm torn whether to

say something nice or mean because they both feel wrong. You helped me get through this and be myself, but I'm not sure that was a good thing.

Outside of the lab there are so many other people who have made this a far more pleasant and interesting journey. Paul Graham helped me find my love of teaching both inside and out of the university settings. Other EBE or not EBE folk; Jamie, Josie, Beth, Caroline, Jorn – whether through drinking or crafting or moaning or getting women's rage on; I needed all of you. My fellow Sussex neuroscience PhD people, Ola, Saskia and Meike (and of course those from other years). We went through a weird experiment together but it seems like we're all making it. Meike, for some reason you even decided to put up with me at home. My other housemates, equally, made home a safe and fun place to escape to: Joe, Chelsea and Vangelis. I will miss our attic.

Somehow, I managed to have hobbies through this, and the ones I found were filled with some of the best people around who kept me from losing myself in the stress. Mermaids; Amy, Claire, Kitty, Abi, Sofia (again!), and everyone else there, you guys made me feel like I could actually accomplish things. I'm also forever grateful for all the people who have played D&D with me over the years and given me a really stupid way of escaping. My DMs, Steve, Josh, Iain and Nate and all the players in those games. The insanity definitely has helped me stay sane.

This work is dedicated to my family. Lyn and Doug kept me safe while I was so far away from home, they helped me explore this new place and find happiness within it. Kieran seems kind of on board with the whole thing, even though I'm sure he mostly thinks it's silly. My Nana Cherry, sadly no longer here but I try to approach life as I think she would (by saying HELLO and giving it a nickname). My parents, Dave and Sue, have

been hugely supportive in the most wonderfully weird ways and I wouldn't ask for anything else. Saved until last, James. You have been with me every step of the way, you put up with me leaving our home for four years to poke bugs and have never complained. You've believed in me far more than I have ever believed in myself and have only been a bit smug about being proven right so far. I am going to spend the rest of our lives trying to be as good to you as you have been to me.

Contents

1 General Introduction

1.1 Physical forces in biological research

The study of biology and, therefore, the nervous system has largely focused on physiological, biochemical, molecular and genetic processes when trying to answer research questions. This is true from early embryogenesis, to growth, to normal functioning, to disease processes. However, in many fields it is impossible to ignore the importance of physics. Approaches and theories derived from physics have always existed to an extent, including Hooke's work in microscopy and optics and his mechanistic theory of memory formation (Hooke, 1665; Hintzman, 2003). Physical properties of biological materials have been exploited in techniques such as X-ray crystallography (Bragg and Bragg, 1915; Kendrew *et al.*, 1958) or electrophysiology (Galvani, 1791; Hodgkin and Huxley, 1939) to answer biological questions. Physics is also central to entire fields of biology, such as perception (Fatt and Weissman, 1992) and biomechanics (Alexander, 1983; Vogel, 2003). In biomechanics questions range from how organisms create forces, such as the study of flight (Wootton *et al.*, 2003), but also how forces may be utilised in biological systems alongside chemical cues and genetic programmes (Franze and Guck, 2010; Franze, 2013; Lemke and Schnorrer, 2017; Loza and Thompson, 2017). From D'Arcy Thompson's On Growth and Form (1917) onward there has been interest in the role of mechanical forces in shaping organisms. The morphology of many structures is dictated by the mechanical properties of the tissues rather than being driven purely by chemical cues, including the formation of vertebrate

gut loops which has been successfully modelled based on physical parameters alone (Savin *et al.*, 2011).

1.2 Tension, stress and strain

This thesis predominantly focuses on tension, which in the literature it is sometimes used interchangeably with stress. Tension describes pulling forces exerted on a material. Stress may refer to either the internal forces acting within a material, the residual stress after external causes have been removed, or to broader forces including tension (pulling), compression (pushing) and shear (sliding) (Gere, 2004). Strain refers to the deformation of a material caused by external stress, such as tension. The relationship between stress and strain is important for understanding the properties of the material tested such as its elasticity and stiffness. Elastic materials recover after stress is removed, whereas stiff materials require greater stress to deform. Stress-strain responses have been particularly important in the study of traumatic brain injury (TBI), which typically involves a complex mix of tension, compression and shear forces (Laplaca *et al.*, 2005; Mcintosh *et al.*, 2014; Sahoo *et al.*, 2016; Elkin *et al.*, 2018). Materials that are under tension will release that tension when cut, producing a gap between the cut edges. This technique has been used in biological research to identify areas of stress and tension in tissues (Dorfman and Cherdantzev, 1975; Xu *et al.*, 2009, 2010; Luna *et al.*, 2013; Nia *et al.*, 2018 and reviewed in Sugimura *et al.*, 2016).

Direct testing by stretching has been performed on axons. Generally, axons behave like a viscoelastic material (they exhibit both viscous and elastic responses to deformation (Gere, 2004)), and the relationship between force and extension are non-linear (Galbraith *et al.*, 1993; Miller and Chinzei, 2002; Gefen and Margulies, 2004; Bernal *et al.*, 2007; Tamura *et al.*, 2008; Javid *et al.*, 2014). The viscoelastic response is

complex and often incorporates elements of responses of other materials. For example, at low level forces it may behave more like a pure elastic material whereas at higher forces it may behave partially elastic and partially viscous (Alexander, 1983; Figure 1-1). Viscoelastic materials also often undergo 'creep' in response to sustained or repeated stresses, this is a lack of full recovery but is not necessarily associated with failure of the material (Gere, 2004; Grevesse *et al.*, 2015).

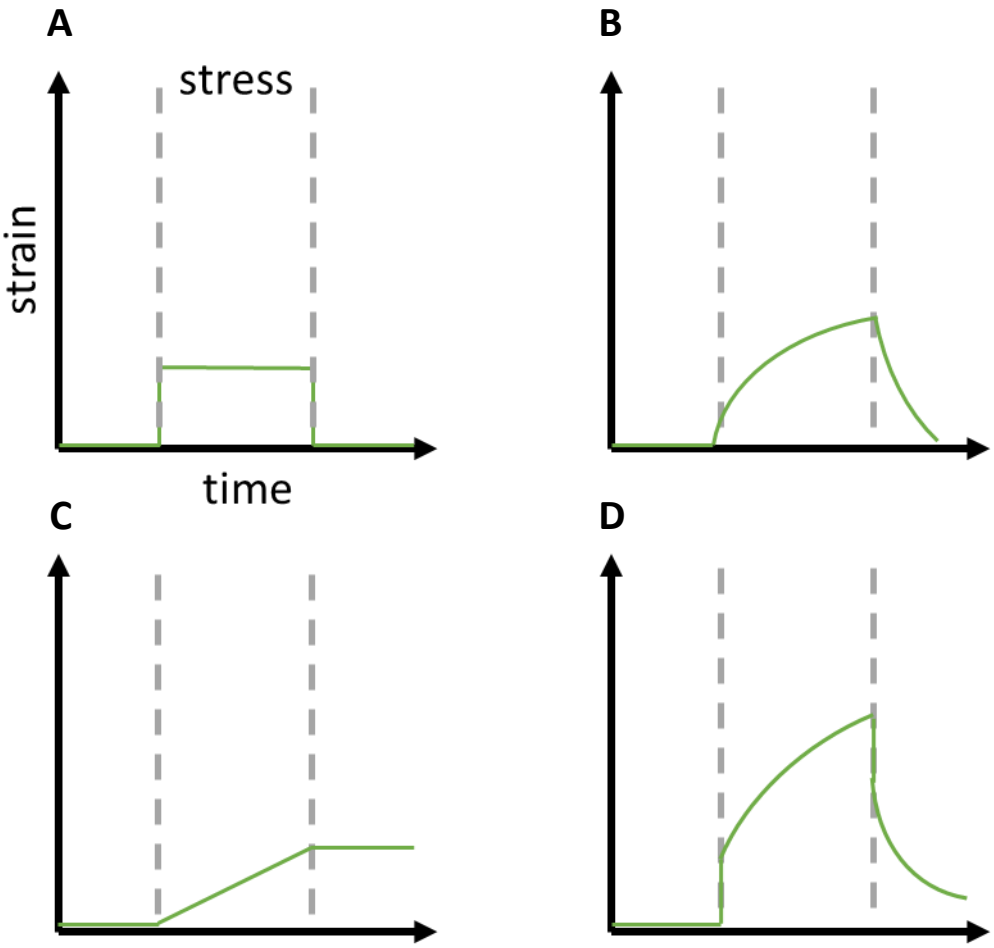

Figure 1-1: Schematics of strain against time for viscoelastic materials when experiencing a uniaxial stress. A is an example of instantaneous elastic strain, B shows slow elastic strain, C shows viscous flow and D shows a viscoelastic strain which involves all components of A-C and shows an incomplete recovery or 'creep'. Image based on Alexander, 1983, pg 93.

1.3 Mechanisms of cellular tension

Typically, tension is studied in cells that are dynamic and changing, such as dividing, growing or motile cells (reviews include Bray and White, 1988; Cramer, 2013; Munoz-Diz *et al.*, 2013; Akhshi *et al.*, 2014; Sens and Plastino, 2015; Cheffings *et al.*, 2016; Löffek *et al.*, 2016; Lemke and Schnorrer, 2017; Guo *et al.*, 2018). As such, the maintenance of tension at a consistent level is less clear than how it changes, although active contraction of cytoskeleton and differential growth have both been theorised (Xu *et al.*, 2009). The production and maintenance of tension can generally be attributed to the actions of the cytoskeleton; the individual components and their regulation, interactions between these components (Chang and Goldman, 2004), and their interactions with the cell membrane and other structures (Inoue and Salmon, 1995). Other factors that influence cell forces include the substrate on which the cell is growing (Pelham and Wang, 1997; Engler *et al.*, 2004).

The intracellular components of tension are primarily the cytoskeleton, which includes (from largest to smallest) microtubules, intermediate filaments and actin (Alberts *et al.*, 2015). Microtubules were named and described in the 1960s with the advent of electron microscopy and glutaraldehyde fixation (Ledbetter and Porter, 1963; Slautterback, 1963). Most microtubules are tubes formed of 10 to 15 protofilaments (Ledbetter and Porter, 1964; Phillips, 1966; Tilney *et al.*, 1973) approximately 25 nm in diameter, although in certain cases, such as during cell division or within cilia and flagella, they can form doublets or triplets that contain the original 10-15 protofilament tube and then one or two additional 10 protofilament attachments (Tilney *et al.*, 1973). The protofilaments are formed of tubulin, originally identified by its binding with colchicine (Borisy and Taylor, 1967; Mohri, 1968). Later, α and β tubulin subunits were

identified and shown to form dimers that produce the protofilaments (Bryan, 1972; Lee and Frigon, 1973; Luduena and Woodward, 1973). Microtubules may also include γ, δ, and ε tubulin as well as ζ tubulin, which is not found in placental mammals (Oakley and Oakley, 1989; Burns, 1991; Dutcher and Trabuco, 1998; Chang and Stearns, 2000; Findeisen *et al.*, 2014; Turk *et al.*, 2015). Microtubules are usually polarised, with most growth occurring at the plus end where β subunits are exposed (Allen and Borisy, 1974; Weisenberg *et al.*, 1976; Chretien *et al.*, 1995).

Microtubules are rarely stable, instead undergoing a motion called treadmilling (Margolis and Wilson, 1978) in which tubulin loss at one end is balanced by gain at the other resulting in equilibrium, in movement of the entire microtubule (Rodionov and Borisy, 1997), or in dynamic instability (Mitchison and Kirschner, 1984b, 1984a) where microtubules first undergo shortening 'catastrophe' and then 'rescue' growth (Horio and Hotani, 1986; Walker *et al.*, 1988; Kerssemakers *et al.*, 2006). In general, dynamic instability is considered to occur more frequently than treadmilling, which requires constant energy consumption (evidence reviewed in Cassimeris *et al.*, 1987). *In vivo,* however, assembly and disassembly is controlled tightly, predominantly at microtubule organisation centres (MTOCs) to ensure proper cellular function (more about the control and regulation can be found in a recent review Akhmanova and Steinmetz, 2015). Microtubules can generate force in two ways. Firstly, through controlled changes in polymerisation and depolymerisation (evidence reviewed in Inoue and Salmont, 1995). Polymerisation can create pushing forces, moving structures potentially including organelles (Kulic *et al.*, 2008), and even pushing through the membrane (Goldberg, 1992), while depolymerisation can produce pulling forces when the end of the microtubule is linked to an object during depolymerisation, such as the chromosomes

during mitosis (Inoue *et al.*, 1975; Salmon, 1976; Gordon *et al.*, 2001). Secondly, through associated motor proteins (Gibbons and Rowe, 1965; McIntosh *et al.*, 1969) that can modulate or impede the growth of microtubule filaments depending upon whether they are unipolar, bipolar and configured in the right way; certain motor proteins may also be involved in the specialisation of axons (Jakobs *et al.*, 2015).

The intermediate fibres (IFs) have a diameter of around 10 nm, intermediate between microtubules and actin microfilaments (structure reviewed in Parry and Steinert, 1999). They were likely first observed via silver staining as part of tonofibrils (Wilson, 1928), then later via x-ray diffraction (Astbury and Street, 1930; Astbury, 1939) and electron microscopy (Fraser and Macrae, 1961; Ishikawa *et al.*, 1968; Cooke, 1976). Unlike actin filaments and microtubules, there are many different IF proteins (some are reviewed and categorised in Steinert and Roop, 1988) including lamins that are present in only animals (Devine and Anderson, 1957; Mercer, 1958; Fawcett, 1966; Erber *et al.*, 1999; evidence for the absence of lamins in plants and unicellular organisms is discussed in Meier, 2007; Melcer *et al.*, 2007). An early proto-lamin is thought to be the progenitor of most if not all IFs given that all organisms known to possess IF proteins also have lamin proteins (Dodemont *et al.*, 1990; Doring and Stick, 1990; Erber *et al.*, 1999 and discussed in Dittmer and Misteli, 2011).

The IFs are generally much more flexible than either actin or microtubules but vimentin-based IFs have been shown to produce ‘strain stiffening’ under high stress (Janmey *et al.*, 1991). Due to their relative stability, insolubility and apolar properties, IFs were originally considered to be purely a scaffold (Starger *et al.*, 1978; Soellner *et al.*, 1985). However, there is evidence that IFs are dynamic, can move and may be involved

in cell shaping (Goldman and Follett, 1970; Yoon *et al.*, 1998, 2001; Windoffer and Leube, 1999). Their resistance to deformation, presence as a scaffolding and connections to other elements of the cytoskeleton providing cross-talk may allow for cells to respond to perturbations (Chang and Goldman, 2004; Koster *et al.*, 2015).

The actin family of proteins form the smallest filaments of the cytoskeleton at between 5-7 nm, they are monomeric and as filaments are known as F-actin (Hanson and Lowy, 1963; Alberts *et al.*, 2015), these along with myosin form the actomyosin complex (Huxley, 1969; Ecken *et al.*, 2016; Chugh and Paluch, 2018). Actomyosin is found in different arrangements such as sarcomeres in striated muscle (Smith, 1972), bundles in smooth muscle (Gunst and Zhang, 2008; Lavoie *et al.*, 2009), a thin network at the cell cortex (Usukura and Kusumi, 2006; Estecha *et al.*, 2009; Tooley *et al.*, 2013) and rings during cell division (Schroeder, 1972, 1990; Lewellyn *et al.*, 2010, 2011). Actin was first identified as distinct from myosin in the 1940s (Straub, 1942, 1943) then the structure described using X-ray analysis (Kabsch *et al.*, 1990). Like microtubules, F-actin is polarised and can undergo rapid assembly and disassembly in the form of treadmilling (Wegner, 1982; Neuhaus *et al.*, 1983; Wang, 1985). F-actin polymerisation is thought to have a major role in cell migration via actin flow and exploratory protrusions (Abercrombie *et al.*, 1971; Theriot and Mitchison, 1991; Lin *et al.*, 1996; Loisel *et al.*, 1999; Piel *et al.*, 2011; Suraneni *et al.*, 2012; Ridley *et al.*, 2016). Actin is involved in transport via the movement of transport myosin proteins. In muscle cells the association with myosin is key to muscle contraction (Huxley, 1969). Non-muscular myosins also have contractile properties and are involved in forces generated for cell adhesion and migration (Evans *et al.*, 1998; Rogers and Gelfand, 1998; Tabb *et al.*, 1998; Mehta *et al.*, 1999; Vicente-manzanares *et al.*, 2010) and during cytokinesis (Ma *et al.*, 2012).

How these components interact with each other, the cell membrane and other cellular components to produce, maintain and respond to force is still far from fully understood (Yusko and Asbury, 2014). Directly applied forces to cells show that the actin network has a large role in responsive stiffness (Jonas and Duschl, 2010). In this study both actin destabilising and stabilising drugs altered responsive stiffness, but actin and microtubules were required to produce opposing forces to those applied. Another study (Kraning-rush *et al.*, 2011) showed that disrupting actin, myosin or microtubules altered force generation in 2D and 3D environments. The cell membrane itself has some role in tension by interactions with extracellular materials, the cytoskeleton, and by linking the two (Grashoff *et al.*, 2010; Carisey *et al.*, 2013; Ciobanasu *et al.*, 2014; Demali *et al.*, 2014; Pyrpassopoulos *et al.*, 2016).

1.4 Tension in biological research

Tension is an important force in many biological processes. During embryonic development it plays several roles. For example, tension plays an important role in cell organisation and forming the boundaries between compartments; adjacent, nonmixing, groups of cells (Garcia-Bellido *et al.*, 1973; Kiecker and Lumsden, 2005). During development local increases in tension are found along compartment boundaries, preventing mixing (Landsberg *et al.*, 2009; Vincent and Irons, 2009; Martin and Wieschaus, 2010; Aliee *et al.*, 2012). This has been linked to contractile actomyosin filaments in the cortices of bordering cells (Winter *et al.*, 2001; Major and Irvine, 2006) and the physical properties and proliferation of cells (Farhadifar *et al.*, 2007; Brodland, 2016). In the fruit fly, *Drosophila melanogaster*, local increases in cell junction tension caused by the differential expression of genes such as *engrailed* and *invected* and

subsequent cell arrangements has also shown to prevent cell mixing (Umetsu *et al.*, 2014).

Another process in embryogenesis that requires tension is dorsal closure in *Drosophila* (Kiehart et al., 2000; Hutson et al., 2003), the closure of an elliptical gap in dorsal midline of the epidermis over the amnioserosal sheet. This process has been particularly focussed on due its similarities with wound closure (similarities reviewed in Martin and Parkhurst, 2004), another process that depends on tension and mechanical properties of tissues. The process of dorsal closure can be split into four phases: initiation, epithelial sweeping, zippering and termination (for a review with novel findings see: Jacinto et al., 2002). Each phase involves cells initiating and responding to mechanical forces.

During initiation most of the closure is due to contraction of the amnioserosa (Kiehart *et al.*, 2000). Recent work (Pasakarnis *et al.*, 2016) suggests that contraction of amnioserosa may be the driving force of the entirety of dorsal closure. In the sweeping phase cells on the epithelial edge become polarised, actin and myosin builds up on the free edge forming a cable (Edwards *et al.*, 1997; Kaltschmidt *et al.*, 2002). This was the first example of molecular motor involvement in morphogenesis (Young *et al.*, 1993). Currently, it is thought that this cable is unnecessary for dorsal closure but does ensure that no scarring occurs via regulation of cell level forces (Magie *et al.*, 1999; Jacinto, Wood, *et al.*, 2002; Ducuing and Vincent, 2016). Filopodia, structures containing high levels of actin, also protrude from the leading edge in this phase (Jacinto *et al.*, 2000). When the filopodia from each edge can touch the zippering phase of dorsal closure begins. The filopodia ensure segmentation remains continuous (Jacinto *et al.*, 2000;

Millard and Martin, 2008) while the force of closure comes from the contractile amnioserosa and actin cable (Kiehart *et al.*, 2000; Harden *et al.*, 2002; Hutson *et al.*, 2003). Microtubules are also essential for the zippering process, because colcemid (a drug that depolymerises microtubules) prevents zippering from occurring but does not affect other steps (Jankovics and Brunner, 2006). In the termination phase the seam is joined and junctions between the amnioserosa and leading edge are replaced by junctions between pairs of leading edge cells (Jacinto *et al.*, 2000; Wada *et al.*, 2007; H. Lu *et al.*, 2015), there must be no overshooting of the leading edge to ensure a continuous seam without scarring; the actin cable likely limits cell migration by exerting forces (Martın-Blanco *et al.*, 1998; Jacinto, Woolner, *et al.*, 2002).

Tension is also important in adult animals because it is central to muscle function. All muscles use the same basic mechanisms for force generation but there is substantial variation in the structure, function and physiology of muscles (differences in mammalian skeletal muscles reviewed in Schiaffino and Reggiani, 2018). Some produce large amounts of force briefly before becoming fatigued, such as jaw muscles, and others are high endurance, such as the heart or flight muscles (Gotz, 1987; Lehmann and Dickinson, 1997). In all cases, myofibrils (Draper and Hodge, 1949, 1950), which contain actin, myosin (Hodge *et al.*, 1953) and titin (Wang *et al.*, 1979; Ziegler, 1994), are required for force generation in muscles. In striated and cardiac muscles the myofibrils are arranged into subunits called sarcomeres (Smith, 1972). The sliding filament hypothesis, that actin and myosin slide relative to each other, was first proposed in 1954 (Huxley and Hanson, 1954; Huxley and Niedergerke, 1954). Although it has been refined and added to (for historical reviews see Squire, 2016; Remedios and Gilmour, 2017), it is still the basis of how we understand force generation by muscle. The myosin heads

attach to actin, undergo a conformational change producing force, detach and then reattach further along the actin filament (Huxley, 1969; Huxley and Simmons, 1971; Reconditi *et al.*, 2011), which is powered by ATP hydrolysis. The force produced by muscles can be adjusted by a variety of physiological and environmental factors, such as length and velocity of muscle fibres (Gordon *et al.*, 1966; Bahler *et al.*, 1968; Arnold *et al.*, 2013) and temperature (Clarke *et al.*, 1958; Ranatunga and Wylie, 1983; Ranatunga and Offer, 2017). Force generation and maintenance in muscles is of relevance to this thesis, because it is an example of the composition and force generation of individual cells influencing the forces within an entire tissue in adulthood.

As well as transiently generated forces involved in muscle contraction, skeletal muscles are also under passive tension at rest (Magid and Law, 1985). This is tension does not involve the active process of contraction of the sarcomeres (Huxley and Hanson, 1954; Granzier and Wang, 1993; Linke *et al.*, 1994). Instead, passive tension most closely reflects the elasticity and stress-strain responses of titin (Linke *et al.*, 1998 and reviewed in Lindstedt and Nishikawa, 2017). Passive tension increases velocities of myocytes (Sweitzer and Moss, 1993), but also makes muscles more prone to damage, as myofibril rupture releases the passive tension making it difficult for reattachment to occur (Eccles, 1943; Hersche and Gerber, 1998; Davidson *et al.*, 2000).

1.5 Axonal structure and its relation to tension

Axons are the long protrusions from neural cell bodies that may branch into telodendria and end in synapses (Deiters, 1865; Cajal, 1897, 1911). Variation in axon morphology is extensive even within a single organism (Peters *et al.*, 1991). The diameter, length and extent of myelination can all differ depending on the role of the neuron, the tissue it is innervating, the anatomy of the species and a myriad of other factors (Wang *et al.*,

2008). The longest axon, while not directly measured, is likely to be the dorsal root ganglion (DRG) neuron of the blue whale, which may be as long as to 30 m (calculated in Smith, 2009), while the smallest will only be a few microns in length in tiny insects and spiders (Niven and Farris, 2012). Diameter also varies as wildly, with the classic squid giant axon at 1 mm and axons in the mammalian brain reaching only 0.08 µm (Pumphrey and Young, 1938; Berbel and Innocenti, 1988; Faisal *et al.*, 2005).

Yet, despite this, axons are often treated as highly homogenous. Indeed, axons share a range of characteristics and functions. They contain the transport system that connects the cell body and soma to the synapse (Kapitein and Hoogenraad, 2011). They propagate action and/or graded potentials (Hodgkin and Katz, 1948; Hodgkin and Huxley, 1952; Burrows, 1979; Protti *et al.*, 2000) with differing degrees of speed and efficiency depending on the aforementioned variations (Hursh, 1939; Perge *et al.*, 2012; Horowitz and Barazany, 2014; Arancibia-ca *et al.*, 2017 reviewed in Seidl, 2014). They are also a major cellular sub-compartment involved in embryogenesis (Lowery and Van Vactor, 2009; Athamneh and Suter, 2015), growth (Pfister, Bonislawski, *et al.*, 2006; Loverde *et al.*, 2011) and repair (Hellal *et al.*, 2012; W. Lu *et al.*, 2015).

Axons have also been known to maintain tension longitudinally for a long time (Dennerll *et al.*, 1988; Lamoureux *et al.*, 1989), and more recently it has been suggested that they maintain tension in the circumferential direction too (Fan *et al.*, 2017), although the how and why of this are not fully known. For all this to be achieved with a single set of mechanisms that remains consistent from the smallest nematode axon to those of the blue whale seems remarkable. In the previous section, we discussed the mechanisms behind cellular tension in general. As well as these more universal

mechanisms for stiffness and tension mediated by the cytoskeleton, there is some evidence that axons differ from other neuronal sub-compartments. Studies using advanced imaging techniques including atomic force microscopy (AFM) and computational modelling have shown that axons in the rat hippocampus have a unique array of actin rings connected by spectrin filaments and associated with ankyrin along the axon (Xu *et al.*, 2013; Zhang *et al.*, 2017), also finding the axon to be much stiffer than either the soma or the dendrites. While this array has not been found in invertebrates, ankyrin lattices have been found in *Drosophila* axons and synapses (Pielage *et al.*, 2009). In the nematode worm, *C. elegans*, loss of β-spectrin has no effect on axonal outgrowth, but in mature axons it leads to breakages in response to strain by muscle contraction (Hammarlund *et al.*, 2007). Together this evidence suggests that specific cytoskeleton components and arrangements are necessary for mature axons to maintain structural integrity and function.

1.6 Axonal tension in development and growth

1.6.1 Embryogenesis

In the case of neurons, the vast majority of tension research has focussed on embryogenesis and the growth cone, which both responds to and uses tension (Lowery and Van Vactor, 2009; Betz *et al.*, 2011; Dent *et al.*, 2011; Athamneh and Suter, 2015). During this period, the neuron behaves more like a motile cell, so it is unclear how these mechanisms translate into the generation and maintenance of tension after connection and synaptic stabilisation, through growth and into adulthood. Bray (1984) was the first to find that applying stretch to axons via the growth cone could induce growth *in vitro*.

Indeed, this is so reliable that high-throughput methods are being designed that allow the control of cultured neuronal circuits based on tension (Nguyen *et al.*, 2013).

Tension has been shown to guide and encourage soma migration (Hanein *et al.*, 2011) and neurite growth (Rajagopalan *et al.*, 2010; Loverde and Pfister, 2015). During neurite growth, external pulling on the cell membrane reduces the compressive force on microtubules, thereby allowing for increased microtubule assembly and growth (Tanaka *et al.*, 1995; Conde and Cáceres, 2009). Microtubule stabilisation may be sufficient in allowing a growing neurite to specialise into an axon (Witte *et al.*, 2008). Tau, a microtubule stabiliser, has been found in mechanically-induced growing axons (Nguyen *et al.*, 2013). Growing neurites and axons also produce their own pulling force via the growth cone (Lamoureux *et al.*, 1989; Bridgman *et al.*, 2001), allowing them to explore and move along a substrate. Briefly, actin polymerises at leading edges of filopodia and is pulled back by myosin motors creating a backward F-actin flow. This is coupled via adhesion receptors to other cellular components and via the membrane to the substrate, creating a pulling force on the substrate (Lin et al., 1996; Bard et al., 2008; reviewed in Athamneh and Suter, 2015). A pushing force by polymerisation of microtubules (reviewed in Inoue and Salmont, 1995) may also contribute to axonal growth via responses to cues such as nerve growth factor (NGF) (Zhou *et al.*, 2004; Dingyu *et al.*, 2016). The presence of tension in axons is also sufficient to stimulate vesicle accumulation at the formation of a synapse (Ahmed *et al.*, 2012, 2013; Ahmed and Saif, 2014).

A macroscopic link between axonal tension and morphology has also been hypothesized to contribute to the formation of the sulci and gyri (grooves and ridges of the vertebrate cortex), and in shaping the central nervous system more generally (Van

Essen, 1997). While this hypothesis has been modified since its original formulation, it posits that connections formed between neurons cause stretch upon each other, with large axonal tracts pulling more forcefully than smaller ones, creating the buckling seen in the cortex (Van Essen, 1997). Along with the theory of gyro- or morphogenetics, which posits that the sulci and gyri are genetically predetermined and patterned (Toro and Burnod, 2005), the tension hypothesis (Van Essen, 1997) has been largely replaced with the idea of tangential cortical expansion (Xu *et al.*, 2010; Ronan and Fletcher, 2014; Kasthuri *et al.*, 2015; Razavi, Zhang, Liu, *et al.*, 2015).

1.6.2 Stretch-growth

Axonal tension likely also plays a role in axon elongation during development and growth (Bray, 1984). The growth of axons integrated into neural circuits is not well understood and has been ignored in comparison to growth from growth cones. During development and growth neurons that are already part of a functional circuit must grow, for example the DRG in a child is much shorter than in an adult. There must be a mechanism allowing for growth without affecting function. One theory is stretch growth; axons are stretched by surrounding growing tissue and grow to compensate for the stretch. Stretch growth was first observed in embryonic chick sensory axons (Bray, 1984; Lamoureux *et al.*, 1989; Zheng *et al.*, 1991). It has also been established that the new material is added non-uniformly and interstitially across the length of the axon (Zheng *et al.*, 1991). Previously, it was thought that microtubules were only added at the growth cone as it was towed forwards (Van Veen and Van Pelt, 1994). The realisation that this was not the case in embryonic axons informed how integrated axons might also grow although stretch growth in integrated axons was not established until much later (Smith *et al.*, 2001).

The mechanisms of stretch growth in integrated axons are poorly understood, although the process has been observed (Pfister, 2004). It has been suggested that stretch and thinning leads to slight breakage or blockage of the cytoskeleton, leading to an accumulation of transported molecules at the area which are incorporated into the membrane (Heidemann and Bray, 2015). This hypothesis fits with the observation that stretched axons grow at seemingly random points along their length (Zheng *et al.*, 1991). It is also supported by previous findings of cytoskeletal remodelling acting to convert force signals to biochemical changes (reviewed in Vogel, 2006). However, there are also contradictory lines of evidence. Firstly, neurons remain functional during stretch-growth (Pfister *et al.*, 2006; Loverde and Pfister, 2015) but breakages and blockages of the cytoskeleton may well effect activity. It has also been criticised for being reliant upon axonal transport and the fastest estimates of axonal transport fall short of the speeds required for growth to occur in this way (Litchy and Brimijoin, 1983; Lasek *et al.*, 1993). Smith (2009) uses the extreme example of the blue whale to illustrate these faults, pointing out that these axons must grow around 3 cm per day (Bannister *et al.*, 1996) outstripping neurite outgrowth (Harris *et al.*, 1987; Smirnov *et al.*, 2014) and repair (Jin *et al.*, 2009), and rivalling growth of cancerous cells (Clarkson *et al.*, 1965). A more recent study (Oyama *et al.*, 2015), has shown that micro heating neurites by about 5 ˚C can produce and induce growth speeds of around 10 µm per minute, but this is only very short term and based largely on the dynamics of materials already present. Such a speed would likely not last as materials were used faster than could be supplied, yet even this is under half what must occur in the blue whale. Another criticism of the cytoskeleton-breakage model put forward by Heidemann and Bray (2015) is that after axons are

initially thinned by stretching, their diameter then increases (Pfister, 2004; Pfister, Iwata, *et al.*, 2006) that would require a second mechanism across the whole axon.

Purohit and Smith (2016) suggest a slightly different model in which stretch induces microtubule polymerisation primarily at the junction between the axon and soma to increase length and occurs to a lesser extent throughout the axon to maintain and increase diameter. Rather than being dependent on breakages and blockages of the cytoskeleton they offer an alternative; the tension-dependent opening of mechanosensitive ion channels (Sigurdson and Morris, 1989; Franze *et al.*, 2009; Tojkander *et al.*, 2012) cue polymerisation. This hypothesis partially addresses the transport speed issue; that growth of axons may outstrip the speed of axonal transport (Smith, 2009). If polymerisation and growth is primarily at the junction between soma and axon it does not need to be transported the length of the axon, however, this model has yet to be experimentally validated. Despite the lack of understanding around stretch-growth, it has been exploited to produce faster growing and longer axons in cell culture and is being investigated as a method of producing transplantable tissue for nervous system injury (Xu *et al.*, 2014; Li *et al.*, 2016).

1.7 Axonal tension in adults and disease

Whilst investigating the hypothesis put forward by Van Essen (1997), tension in axons of adult mammals has been found. Axonal tract tension is present in the central nervous system. The brain has been directly tested and found to be under tension (Xu *et al.*, 2009, 2010) while evidence points to similar results in the spinal cord (Koser *et al.*, 2015). Xu *et al.* (2009) found that axon tracts in the adult mouse brain were under tension in the circumferential direction in the coronal cerebral plane, and that this stress was coupled with compressive stress on the grey matter. They suggest that most of this

residual stress is caused by differential growth rather than active contraction of the axons because there are relatively low amounts of myosin II in the white matter as previously established (Kioussi *et al.*, 2007). In the spinal cord, white matter produces a strain stiffening response that increased as indentations increased (Koser *et al.*, 2015). The strain stiffening response paired with the transversely isotropic property of the axons suggests the possibility of tension (Cheng *et al.*, 2008; Koser *et al.*, 2015). Tension has also been found in the spinal cord of lamprey larvae (Luna *et al.*, 2013); the spinal cord is 'prestressed' by 10% *in vivo* increasing to 15% when in a swimming position indicating that the cord is both under tension and exposed to increased forces.

Additional studies have been carried out investigating the biomechanical properties of white matter in the brain and spinal cord. These studies focus upon testing the materials' responses to perturbation; for example via direct uniaxial loading *in vitro* (Miller and Chinzei, 2002; Angelillo, 2006; Shreiber *et al.*, 2009; Rashid *et al.*, 2014; Okazaki *et al.*, 2018 and reviewed in Cheng *et al.*, 2008). Although such studies provide information regarding the behaviour of tissues and are important for understanding injury and repair, they provide little insight into how these materials behave *in vivo.*

Currently, no function is attributed to the presence of tension in adult tissues, although as discussed above mammalian axons have a unique actin array (Zhang *et al.*, 2017). This may influence the arrangement of Na^+ channels making firing more efficient or reliable; however, this has yet to be demonstrated directly. This lack of hypothesised function is interesting, particularly regarding the brain, where the axons do not have to adapt to external forces barring severe injury. It could be that tension is an emergent property that is due to the growth and structure of the surrounding tissues. However, if

this is the case it conflicts with the passive stretch model of axon growth (Bray, 1984; Smith, 2009; Loverde *et al.*, 2011). Alternatively, this tension could be actively generated and maintained by the axons themselves (O'Toole *et al.*, 2015; Polackwich *et al.*, 2015).

There is evidence that alterations in the cytoskeleton that lead to a loss of tension may be linked to certain diseases and injuries. In neurodegenerative diseases such as Alzheimer's disease, tau dysfunction is a major contributor (Hong *et al.*, 1998). Tau stabilises microtubules and their destabilisation leads to loss of transport function (Drechsel *et al.*, 1992; Ishihara *et al.*, 1999; Zhang *et al.*, 2005; Duan *et al.*, 2012; Stokin *et al.*, 2014), although not all microtubule loss is linked to tau dysfunction (Cash *et al.*, 2003). When it is considered that microtubules are force generators (Inoue and Salmon, 1995; Keener and Shtylla, 2014; Jakobs *et al.*, 2015), their loss may lead to loss of tension in axonal tracts as well. Other diseases such as amyotrophic lateral sclerosis (ALS; reviewed by Zarei *et al.*, 2015), loss of tension of the cytoskeleton is more clearly involved. ALS is partially characterised by issues in axonal transport (reviewed by Ikenaka *et al.*, 2012). This includes tangles of neurofilaments (Carpenter, 1968; Chou and Fakadej, 1971; Hirano *et al.*, 1984; reviewed in Hirano, 1995) that are known to play an important role in the diameter of axons (Marszalek *et al.*, 1996; Zhu *et al.*, 1997; Elder *et al.*, 1998). Disruption of the transport system in axons is implicated in other neurodegenerative diseases, including congenital diseases such as some forms of spinal and bulbar muscular atrophy and spastic paraplegia (for a review with associated mutations see Chevalier-larsen and Holzbaur, 2006). However, it is difficult currently to distinguish whether loss of tension or loss of other functionality of the cytoskeleton produces symptoms in neurodegenerative diseases.

Axonal tension is often studied in injury and repair as axonal damage is one of the major consequences of traumatic brain injury (TBI) (Johnson *et al.*, 2013). It is unclear why repair after injury does not occur readily in the human CNS compared to the periphery. Many factors have been implicated including the presence of NOGO (a growth inhibitor), the formation of glial scars, the lack of Schwann cells for guidance (reviews include Grandpré *et al.*, 2001; Navarro *et al.*, 2007; Allodi *et al.*, 2012; Gonzalez-perez *et al.*, 2013). It has been suggested that if axons are under tension or pre-stress *in vivo* then damage will actually cause them to recoil a much greater distance and make any regeneration much slower and more difficult (Luna *et al.*, 2013). In TBI, diffuse axonal injury (DAI) frequently occurs with clear pathologies such as axonal swelling injuries (Christman *et al.*, 1994). It is also thought to play a role in the possibly controversial (Randolph, 2018) disease chronic traumatic encephalopathy (CTE), a neurodegenerative disorder caused by repeated trauma (reviewed by Ling *et al.*, 2015). DAI is seemingly caused by the sudden loading of force on axons causing the strain-stiffening previously discussed (Shahinnejad *et al.*, 2013; Koser *et al.*, 2015) and subsequent ruptures within the cytoskeleton (Christman *et al.*, 1994; Stone *et al.*, 2004). This leads to interruption to axonal transport, and axonal misalignment and undulations (Christman *et al.*, 1994; Smith *et al.*, 1999). The latter is thought to be caused by the immediate breaking of microtubules at points along the axon; these microtubules then disassemble allowing for a slow relaxation and recovery to occur but at the cost of transport which can lead to axonal degeneration (Tang-Schomer *et al.*, 2010). Thus, the biomechanics of the axons in the central nervous system may be detrimental when surviving a severe insult; the stress-strain response makes axons more likely to rupture and being under tension may hinder any repair processes.

1.8 Insects as a model system

Insects provide a powerful model for many areas of research (North and Greenspan, 2007). This project takes advantage of the morphology of the nerve cord within and between species (Burrows, 1996; Niven *et al.*, 2008). We also take advantage of the relatively short developmental periods and clearly defined growth stages in hemimetabolous insects (Chapman, 2013). Insects have been important model systems in neuroscience and cell biology (Krogh, 1929). Fruit flies (*Drosophila melanogaster*) offer a powerful model in which to study genetics and development and, more recently, neurobiology (Nüsslein-Volhard and Wieschaus, 1980; Nüsslein-Volhard *et al.*, 1980; Santamaria and Nüsslein-Volhard, 1983; Wieschaus *et al.*, 1984; Song *et al.*, 2002; Tracey *et al.*, 2003). However, historically other insects have also proven invaluable for electrophysiological research (Horridge, 1960, 1964; Wolbarsht, 1960; Burrows, 1996). Insects have also been used frequently in electron microscopy studies (EM), although the blood-brain barrier still produces a challenge for proper fixation (Keil and Steinbrecht, 2010). In this thesis, we focus on the ventral nerve cord, which varies greatly among insect species (Niven *et al.*, 2008). For our purposes specifically, the insects we have chosen possess axon bundles that are clearly distinguished from the cell bodies located in the ganglia, and that are easily identifiable using standard light microscopy.

1.9 The ventral nerve cord

1.9.1 Ventral nerve cord anatomy

There has been interest in the ventral nerve cord (VNC) since the 1800s (Prosser, 1934), from comparative morphology and evolutionary patterns to early neurobiology. The VNC is segmental, formed from a chain of neuromeres (aggregations of neurons) that

correspond to each anatomical segment (Bullock and Horridge, 1965). These neuromeres process sensory signals and are responsible for motor control of that segment often containing central pattern generators (CPGs) (Miller, 1960a, 1960b; Wilson, 1961; Vierk *et al.*, 2009; Ayali and Lange, 2010; da Silva and Lange, 2011; Wong and Lange, 2014). There are also ascending and descending connections to other ganglia within the VNC and to the brain. In the locust there are thought to be six neuromeres within the brain (Scholtz and Edgecombe, 2006), three within the suboesophageal ganglion (S1-3), three thoracic (T1-3) and eleven abdominal (A1-11). Each neuromere is connected by two connectives formed primarily of axons. In some hexapods, such as silverfish, the majority of these neuromeres form a ganglion that are all separated and parallel with the structures they innervate (Niven *et al.*, 2008). In other species, fusions occur among neuromeres to form composite ganglia containing multiple neuromeres. In these fusions the connective axon bundles are reduced to tracts within the neuropil; these fusions shift the nerves innervating of some peripheral structures away from parallel.

In this study, we take the definition of a fused ganglion from Niven *et al.* (2008): a fusion occurs when adjacent neuromeres are close enough to distort their edges, forming a composite ganglion with a distortion of both/all outlines with at most a small indentation to differentiate between the neuromeres. Furthermore, there are no visible connective tracts when observing the intact fused ganglion. It is unclear what the driver is for certain morphological differences in the VNC among species. There appears to be a general evolutionary trend towards an anterior shift and fusion of ganglia (Niven *et al.*, 2008). For example, in higher flies, such as *Drosophila melanogaster*, there is total fusion of all the thoracic and abdominal ganglia with no clear distinction among them possible.

The morphology of the VNC reflects peripheral anatomy to some extent. For example, ganglia fusions may be linked the presence of peripheral structures such as wings (Niven *et al.*, 2008).

The ganglia of the nerve cord are bilateral and composed of an outer layer of neuronal cell bodies, with the core containing axon tracts, commissures and neuropil regions (Burrows, 1996). Axon tracts are found in the anterior/posterior direction and are extensions of the connectives to adjacent ganglia, the commissures are also found in discreet layers but are axons that cross the ganglion from left to right (and vice versa), and the neuropil regions can be functionally and topographically identified. For example, sensory neuropils tend to be found in the ventral medial region (Smarandache-Wellman, 2016), whilst for interneurons and motor neurons individual cell types or even individual cells can be reliably identified between individuals (Hoyle and Burrows, 1973; Watson and Burrows, 1982; Pflüger and Watson, 1988; Burrows, 1996; Castillo *et al.*, 2018). The thoracic neuromeres each have six pairs of lateral nerves and the median nerve while each abdominal neuromere or unfused ganglia has only two pairs of lateral nerves but two median (Burrows, 1996).

The connectives themselves have been less frequently researched in terms of anatomy, though Rowell (1967) described the composition thoroughly in the desert locust, *Schistocerca gregaria*. The connectives are comprised of a neural lamella, considered part of the insect blood brain barrier, approximately 2-3 microns thick (Hindle and Bainton, 2014). A further layer of perineural cells around 1 micron wide is lined with glial cells that send processes into the connective to surround axons (Rowell and Dorey, 1967). Larger axons tend to receive more wrapping and investment than smaller ones.

The composition of the main connective varies in regions; in some areas the density of axons is low with around 70% of the space taken up by glial cells, but in other regions the opposite is true. Overall, around 40% of the connective is glia. This varies slightly between the different connectives in the VNC. Rowell (1967) also described the axons, finding that a region of small axons contained 40% of the axons, most of these being less than 1 micron in diameter and not wrapped by glial processes, the large axons represented a smaller number of axons with only 3% being larger than 5 µm. There was no evidence of axonal branching, or of vesicles suggesting that synapses are absent within the connectives. Thus, the connectives are formed of a neural lamella, a glial sheath and then a mix of glial cells and straight parallel axons.

1.9.2 Development of the ventral nerve cord

Insects, like all arthropods, are bilateral gastroneuralian animals. The nervous system arises from the neuroectoderm that has neurogenic regions either side of a centralised population of midline cells. In vertebrates, this structure folds producing the neural tube but in insects the neural tissue eventually detaches to form the rope-ladder like structure of the VNC (Arendt and Nübler-jung, 1999). The neurogenic regions of the neuroectoderm give rise to multipotent neural progenitors including neuroblasts then ganglion mother cells. Post mitotic neurons then differentiate and migrate towards the body cavity producing distinct layers. Hox genes begin to differentiate regions of the nervous system in the anterior-posterior direction (Mallo and Alonso, 2013), sonic hedgehog and BMP4 pattern the nervous system dorsoventrally and factors released from the midline pattern laterally.

In insects, individual neuroblasts are repeated segment to segment, embryo to embryo within the same species, and the pattern if not the number is consistent across

species (Bate, 1976; Doe and Goodman, 1985; Bastiani *et al.*, 1986; Meier *et al.*, 1993; Zacharias *et al.*, 1993; Condron and Zinn, 1994; Zinn and Condron, 1994; Burrows, 1996). Growth cones of the midline precursor cells extend to form the scaffolding of the longitudinal tracts of the connectives between neuromeres. The peripheral nerves are pioneered by sensory neurons in the peripheral tissues that project into the central nervous system: neurons that develop later arising from target ganglia then follow this path outward to the periphery (Kutsch, 1989). This has been described in detail in the hind limb where Ti1 cells are formed near the tip of the limb bud, approximately 200 µm from the central nervous system (Caudy and Bentley, 1986). The Ti1 cells establish Nerve 5B1, while Nerve 5B2 (a and b) is formed by Ti2, Ta1 and Ta2 neurons; these all eventually converge on the C12 motor neuron that forms the main branch of nerve 5 (Bate, 1976; Keshishian, 1980; Keshishian and Bentley, 1983; Bentley and Toroian-Raymond, 1989; Burrows, 1996).

1.10 Orthopteroid Insects

Although this thesis focusses primarily upon desert locusts, migratory locusts, cockroaches and crickets are also used for experimental work. These are all orthopteroids, which refers to their 'straight wings'. Historically all of these insects were in the order Orthoptera (Linnaeus, 1758), but some have since been reclassified into different orders so that orthopteroid insects include those within the Blattodea, Dermaptera, Grylloblattodea, Mantodea, Mantophasmatodea, Orthoptera and Phasmatodea (Cochran, 2009; Ingrisch and Rentz, 2009). This thesis includes work on *Schistocerca gregaria* (Forskål, 1775)*, Locusta migratoria* (Linnaeus, 1758) and *Gryllus bimaculatus* (De Geer, 1773) that are all in the order Orthoptera, and *Periplaneta*

americana (Linnaeus, 1758) that is now placed within the Blattodea (Wheeler *et al.*, 2001). The species we focus upon represent a range of variables, including those with similar anatomy but differences in behaviour, lifestyle and genetics to those with different VNC anatomy and morphology differences.

1.10.1 The desert locust

Our primary model organism is the desert locust, *Schistocerca gregaria*. This insect has been used as a model organism in physiology, neuroscience (Burrows, 1996; Castillo *et al.*, 2018) and ecology (Lomer *et al.*, 2001; Miller *et al.*, 2008; Anstey *et al.*, 2009a; Sword *et al.*, 2010). Locusts are hemimetabolous, lacking a pupal stage, and undergoing a series of moults in which the nymphs resemble the adults though they lack wings. During the larval stages they undergo hormone-controlled moulting, which is accompanied by changes in morphology and body size (Chapman, 2013). The phases between moults are called instars. In the desert locust there are six instars including adulthood, although the number of instars can be altered hormonally or in certain living conditions (Uvarov, 1966; Pélissié *et al.*, 2016). In this project, the youngest locusts used are third instar. These locusts can be easily distinguished from fourth instars by a much smaller (almost hard to see) wing budding, and from second instars due to size and body proportion changes, and the emergence of the small wing buds (Figure 1-2). The time between moults varies depending on temperature, food and water availability as well as health of individual locusts. Once locusts have reached adulthood, where wings are present, they become fertile around a week later and live for around one to two months depending upon conditions (Burrows, 1996).

Locusts were identified as a potential model system due to the morphology of the VNC (Niven *et al.*, 2008), which contains both unfused and fused ganglia that we

hypothesised may create regions of tension (Figure 1-3). The locust VNC, when accessed from the ventral surface, lies beneath the cuticle, behind a layer of connective tissue and part of the a tracheal/air sac system. It comprises the brain, the suboesophageal, pro-, meso- and metathoracic ganglia along with five abdominal ganglia. The suboesophageal ganglion is a fusion of the three suboesophageal neuromeres, the metathoracic ganglion is a fusion of the T3 and A1-A3 neuromeres but is located within the thorax, and the terminal ganglion is a fusion of A8-11 neuromeres (Burrows, 1996). We focus particularly upon the metathoracic ganglion because it extensively fused and also positioned anteriorly to many of the structures it innervates (Figure 1-4).

Locusts also provided a contrast between the ganglia and axon bundles of the thorax and those of the abdomen. The cuticle of the thorax is stiff forming a box-like structure with an internal space filled with haemolymph with space between organs. In contrast, the abdominal cuticle is markedly softer, extensible, and the abdomen is filled with the gut, reproductive structures and fat with little unoccupied space. We are also able to contrast bundles in the VNC with peripheral nerves, such as nerve 5, which are exposed to the motion of peripheral structures.

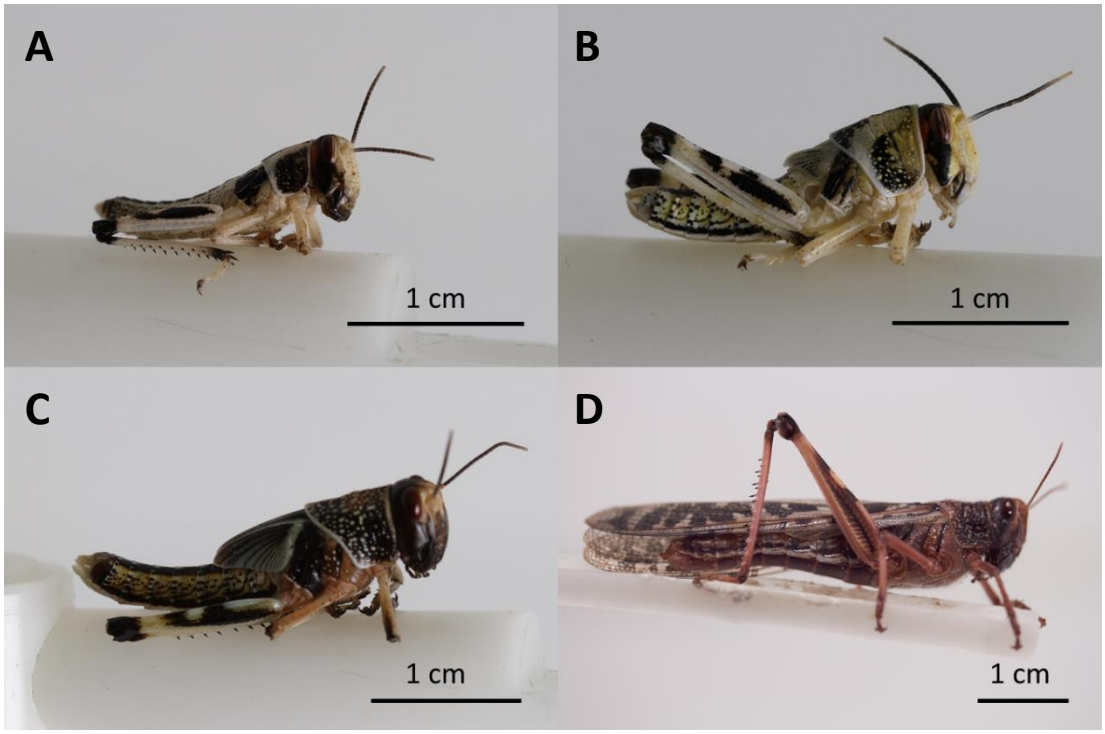

Figure 1-2: Desert locust instars undergo distance morphological changes. Pictured are desert locust instars used in this thesis. A is a third instar locust with small wing buds. B is a fourth instar, larger and with more prominent wing buds. C is a fifth instar with large wing buds and D is an adult with wings and pinker colouring.

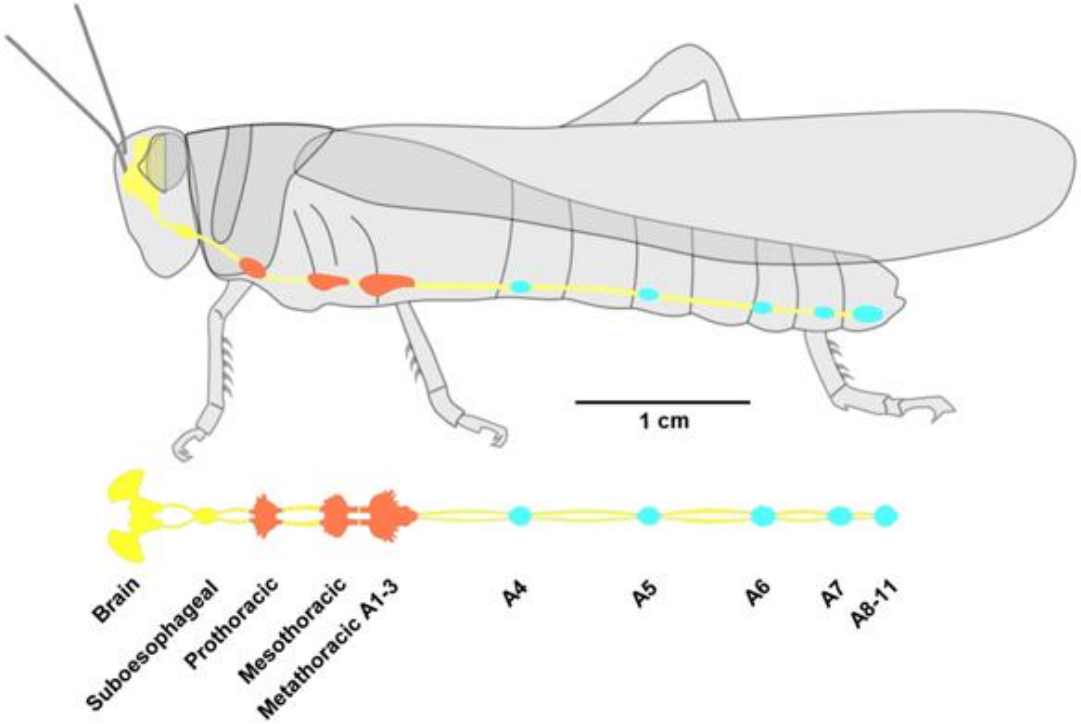

Figure 1-3: The ventral nerve cord of the desert locust and its positioning within the body. Image shows a lateral schematic of the desert locust and the positioning of the VNC and (below) a ventral view of the VNC (adapted from Castillo *et al.*, 2018)

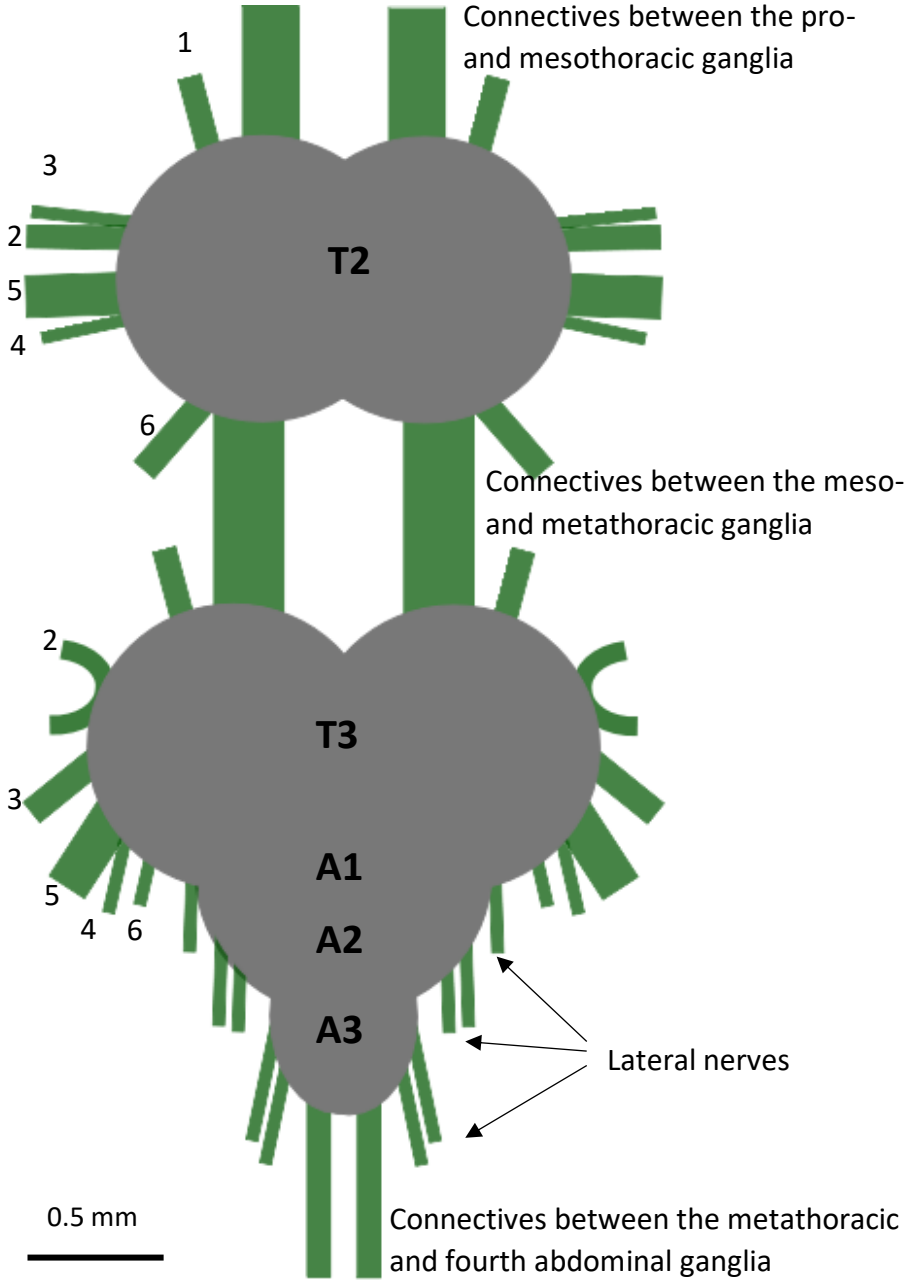

Figure 1-4: The mesothoracic and metathoracic ganglia of the desert locust. The mesothoracic ganglion (grey) is formed of 1 neuromere (T2) and has 6 pairs of lateral nerves (green) and 1 median nerve (not shown). The metathoracic ganglion (grey) is formed of 4 neuromeres (T3, A1-3). Axon bundles are shown in green. The T3 neuromere has 6 pairs of lateral nerves (1-6) and each abdominal neuromere has 2 pairs (labelled), except for A1 where lateral nerve 1 has fused to nerve 6 of T3. The connectives of the ventral nerve cord to other ganglia are also shown (green). The T3 neuromere largely innervates the wing and hindlimb, nerve 2 is purely sensory and 6 connects to 1 of the next segment. 1 has some neurons from the mesothoracic ganglion in it and innervates the hindwing, nerves 3 and 4 innervate both the hindwing and hindlimb while nerve 5 innervates just the hindlimb. The abdominal neuromere nerves pairs are dorsal and ventral (image based on those in Burrows, 1996; Bevan and Burrows, 2003; Castillo *et al.*, 2018).

1.10.2 Solitary and gregarious desert locusts

For the majority of our experiments we used the gregarious desert locust. However the desert locust can also be found in the solitarious phase. Despite being the same species, these locusts have remarkably different anatomy, physiology and behaviour. In laboratory conditions it is difficult to claim locusts are ever truly gregarious or solitarious and the terms 'crowded' and 'isolated' are often used instead (Pener, 1991), however the literature is inconsistent in these terms and to reduce confusion we will stick to a single set of terms 'gregarious' and 'solitary/solitarious'. The solitarious phase locusts can be transformed into the gregarious phase in a density-dependent manner. Currently, it is thought that a mix of olfactory cues and hind femur stimulation (Simpson *et al.*, 2001) trigger serotonin-mediated hormonal cascades (Anstey *et al.*, 2009b) that alter appearance, physiology and behaviour. Pener and Simpson (2009) have produced a thorough review on the polyphenism. Outwardly there are many obvious anatomical and morphological differences between solitary and gregarious locusts. The solitarious females are larger than gregarious, while the males are slightly smaller and there are many variations in morphometrics (Pener and Simpson, 2009). The VNC also differs; gregarious locusts have around a 30% larger brain overall (Ott and Rogers, 2010).

1.10.3 Other species

Other species selected for this project were chosen predominantly due to the morphology of the nerve cord (Figure 1-5), body size and morphology and that all had had some attention in regards to VNC anatomy (Gregory, 1974; Eibl and Huber, 1979; Burrows, 1996). The first species we selected was *Locusta migratoria* which belongs to the same family as *S. gregaria*. This species has largely the same gross anatomy as *S. gregaria*, the same VNC morphology and also undergoes phase change. However, there

are also many differences. By comparing species with similar morphology and anatomy, but that were still different species, we are able to draw conclusions about the role of anatomy in the axonal forces we examine. The second species was *Gryllus bimaculatus*, another reasonably common model species. This species has a metathoracic ganglion that is formed of a fusion of three neuromeres (Figure 1-5) and has another fusion at the terminal ganglion. The cricket is also very anatomically distinct from the locusts. The very stiff cuticle of the thorax in locusts is not present in crickets, although the external anatomy of the thorax is broadly similar. The abdomen is also much less motile in crickets and of course there is difference in wing anatomy: the cricket forewing is an elytra and used by males for the chirping noises they produce (Simmons and Zuk, 1992; Ferreira and Ferguson, 2002).

Our final species studied was *Periplaneta americana* (Linnaeus, 1758), known as the American cockroach. Unlike our other species, *P. americana* has a highly variable number of moults, anywhere between 6 and 14, often around 13 (Roth, 1982). Our interest in *P. americana* was based on the fusion of the metathoracic ganglion, which in this species is a fusion of two neuromeres (Figure 1-5) as well as a further departure from the locust thorax and abdominal anatomy. The cockroach lacks the large hind limbs of the locust and cricket, and has a much thinner ventral cuticle covering the VNC (personal observation) with instead the coxae offering some protection.

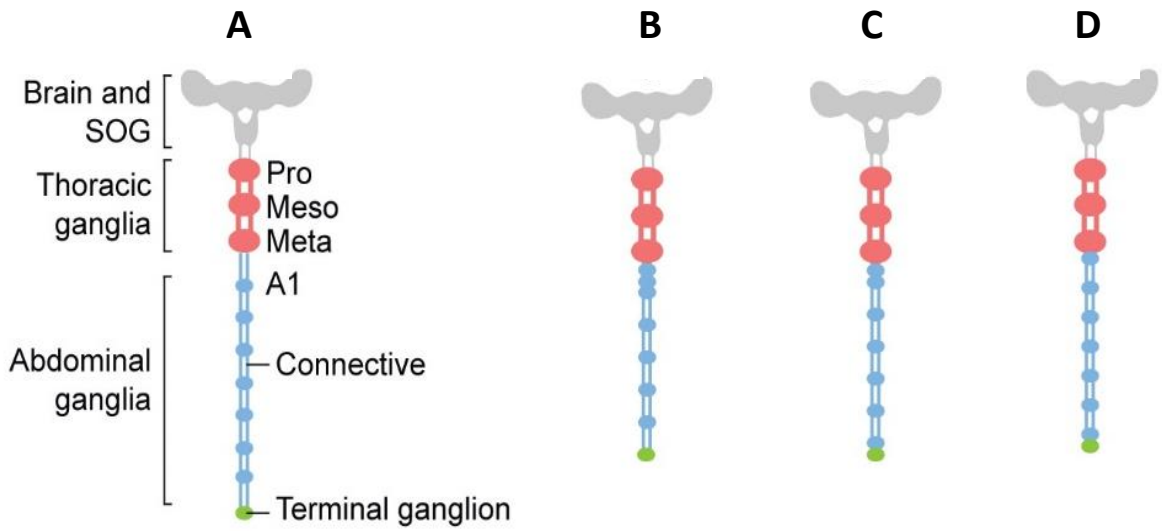

Figure 1-5: Stylised graphical representation of the ventral nerve cord of several insects. The anatomy of the VNC differs across species, *Japyx spp*. (Diplura) has no fusions and is used for reference (A). *Schistocerca gregaria* (Orthoptera) has a fusion of four neuromeres shared with *Locusta migratoria* (B). *Gryllus bimaculatus* contains two fusions, two at the metathoracic ganglia and one at the terminal ganglia (C). *Periplaneta Americana* has a single fusion at the metathoracic ganglia and one at the terminal ganglia (D). Image modified from Niven *et al.* (2008).

1.11 Summary of contributions

This thesis discusses several novel contributions to the study of tension and forces in the central nervous system. We develop, to our knowledge, the first experimental model of physical tension in whole axon bundles in invertebrates by locating a region under tension in adult desert locusts (*S. gregaria)*: the connectives between the meso- and metathoracic ganglia. We were able to ascertain that the tension is partially mediated by a posterior pull on the connectives. Further microdissections allowed for identification of varying tensile properties in two other axon bundles connecting to the metathoracic ganglion.

We use transmission electron microscopy (TEM) to compare these bundles at the gross anatomical, cellular and sub-cellular levels. The number of microtubules per axon and the relationship between microtubule number and axon size are the main factors that correlate with results from microdissection, rather than gross anatomical differences. This suggests that the macroscopic mechanical properties of axon bundles are mediated by the cytoskeletons of individual axons. By imposing a uniaxial loading upon the axon bundles and measuring the force in response, we find that all bundles were viscoelastic and that high-tension bundles can withstand the highest forces prior to critical failure.

We repeated our microdissection nerve cutting throughout growth from third instar. We found no change in tension in the connectives between the meso- and metathoracic ganglia during growth. We performed microsurgery on third instar *S. gregaria*, cutting one of the high-tension connectives to expose the second to greater force. This produced adults with a range of morphological differences including a smaller body size yet a longer connective between the meso- and metathoracic ganglia.

However, tension in the connective was the same as in controls. This suggests that tension in axon bundles is actively maintained. This is further supported by TEM studies that showed locusts that had undergone the third instar surgery had an increased density and number of microtubules in axons of the remaining bundle.

We repeated the microdissections to study tension in the connectives between the meso- and metathoracic ganglia in solitary *S. gregaria* and in *L. migratoria*. These did not differ from previous results. We expanded to two other orthopteroids; *G. bimaculatus* and *P. americana*. In both of these species, the connectives between the meso- and metathoracic ganglia are under less tension than in locusts. Using TEM, we showed that microtubule number in axons reflected the tension in the connectives most closely. Once again, all bundles display viscoelastic behaviour, however, their strength and elasticity do not correlate to the results of microdissection and TEM.

Overall we show that axonal tension is highly variable even within the same species. We provide evidence that the cytoskeleton, particularly microtubules, are reflective of *in vivo* tensile properties at the macroscopic scale. We suggest that axonal tension is not simply a universal property of axons or solely a response to their growth environment but is actively regulated and maintained throughout development and in response to injury.

2 Methods

2.1 Abstract

In this thesis, a wide range of techniques are used to study axonal tension in entire axon bundles: (1) *Microdissection* allows access to axonal bundles with high and low axonal tension *in vivo*, and to manipulate tension through ablation of specific bundles; (2) *Transmission electron microscopy* (*TEM*) permits direct comparison of gross axon bundle structure with the cellular and sub-cellular composition of axons within these bundles; (3) *Uniaxial loading* is used to investigate other physical properties of the axon bundles, such as elasticity and strength; (4) *Growth-stage comparisons* allows for the study of tension throughout growth and also in response to injury; (5) *Phylogenetic comparisons* are used to investigate the universality of findings and other factors that may affect axonal tension. This chapter describes the varied techniques that are used throughout the thesis.

2.2 Main

Below I present the details of the methods used throughout the thesis. Where specific variants of the methods arise, they are described within the relevant chapters.

2.2.1 Animals

Gregarious phase *Schistocerca gregaria* (Forskål, 1775) and *Locusta migratoria* (Linnaeus, 1758)

Animals were purchased at various growth stages (instars) from Blades Biological (Kent, UK), Pets at Home (Handforth, UK) or Peregrine Food Supplies Ltd. (Magdalen Laver, UK). These commercial suppliers each maintain crowded colonies of locusts in the gregarious phase. Locusts were then kept at the School of Life Sciences, University of Sussex, UK in heated tanks (160 x 100 x 120 mm, 24°C) and given a diet of wheatgerm, organic lettuce and water to which they had *ad libitum* access unless otherwise specified. Locusts were maintained in crowded conditions at all times.

Solitary phase *Schistocerca gregaria*

Solitary locusts were bred at the University of Leicester by Dr Swidbert Ott (methods described in Roessingh *et al.*, 1993), who gifted us several individuals along with colony- and age-matched gregarious locusts. Once at the University of Sussex, the solitary locusts were kept in separate rooms and fed on a diet of bran and organic lettuce. Experiments were carried out within 10 days to reduce the possibility that phase change could have occurred through exposure to olfactory or visual cues (Lester *et al.*, 2005). Gregarious locusts from the University of Leicester were kept according to our normal protocol (see above).

Periplaneta americana (Linnaeus, 1758)

Animals were purchased as adults from Blades Biological (Kent, UK). They were then maintained under crowded conditions at the School of Life Sciences, University of Sussex, UK in heated tanks (160 x 100 x 120 mm, 24°C) and fed a diet of wheatgerm, organic lettuce and apple, dried dogfood, and water to which they had *ad libitum* access.

Gryllus bimaculatus (De Geer, 1773)

Crickets were purchased as adults from Peregrine Food Supplies Ltd. (Magdalen Laver, UK). They were kept at the School of Life Sciences, University of Sussex, UK in heated tanks (160 x 100 x 120 mm, 24°C) and fed a diet of wheatgerm, organic lettuce and apple, and water to which they had *ad libitum* access. Animals were maintained in low-density crowded conditions.

2.2.2 Identifying insect sex

Throughout all experiments insects were differentiated by sex, allowing us to determine whether sex differences contributed to tension within axonal bundles.

S. gregaria and *L. migratoria*

Male and female locusts were differentiated through their abdominal anatomy (Albrecht, 1953; Uvarov, 1966). Females have large, visible ventral and dorsal valves at the posterior tip of their abdomen. In contrast, males have a generally smoother appearance due to the sub-genital plate and smaller abdominal segments. These anatomical differences are clear in both solitary and gregarious *S. gregaria* and in *L. migratoria*. They are present throughout development (personal observation). Overall

body size can also be an indication, female gregarious *S. gregaria* tend to be larger than males and males can become yellow upon maturation (Uvarov, 1966; Pener, 1991; Pener and Simpson, 2009). However, these was not considered definitive due to variations and abdominal anatomy was primarily used.

P. americana sex differentiation

Male and female cockroaches are easily distinguishable due to the presence or absence of the styli, which are only found in males, and the ovipositor, which is present only in females (Bell and Adiyodi, 1982; Chapman, 2013). Females are also generally broader around the seventh abdominal segment but this is not definitive.

G. bimaculatus sex differentiation

Black crickets show clear sexual dimorphism. Females are typically larger and entirely black, whereas males are smaller with brown wings. The best indication of sex is the presence or absence of the large ovipositor found in females (Snodgrass, 1933).

2.2.3 Identifying instar and stage

Desert locusts have morphological features that allow for clear identification of instar (Figure 1-2). A major one is the presence and size of wing buds. These first appear at third instar and are very small, at fourth instar they are clearly visible cuticle and at fifth instar they reach the tip of the hindlimb when in a relaxed position. Size can also be a guide, although just prior to and after moulting stages can be difficult to distinguish. We categorised each instar into 'mid' and 'late'. 'Mid' instars referred to animals at least 72

hours post-moult, whereas ‘late’ was categorised as pharate individuals when the appearance of the folded procuticle beneath the old cuticle (Figure 2-1). Despite this method of categorisation, some variability still remains because moulting could be delayed due to food access, health and temperature. Consequently, the appearance of these sub-cuticular folds does not necessarily mean moulting was imminent, although it would usually occur within 48 hours of the folds appearing.

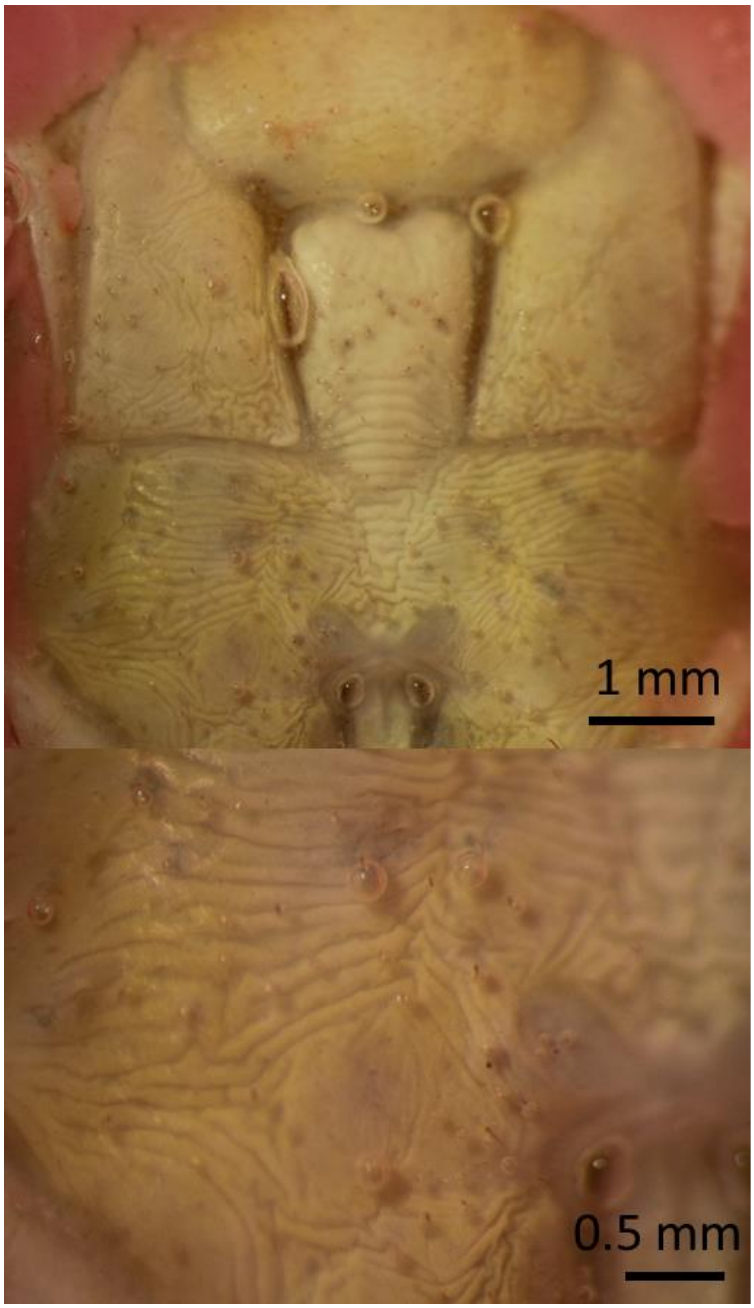

Figure 2-1: Example of 'late' stage locust cuticle. New procuticle is clearly visible in folds beneath the exocuticle. This example is taken from a pharate fifth instar male *Schistocerca gregaria*.

.

2.2.4 Image and video capture of microdissections

Images and videos were recorded using a Canon EOS 70D camera (Canon Inc., Ōta, Tokyo, Japan) and a Leica MZ12.5 dissecting microscope (Leica, Germany). Images were taken at a resolution of 1080 pixels and videos at 30 frames per second (fps). These were scaled using a 1 mm micrometer stage graticule (Scientific & Chemical Supplies Ltd., Wolverhampton, UK). Videos were captured in .mov format. To permit analysis using ImageJ and FIJI (Schindelin *et al.*, 2012; Schneider *et al.*, 2012; Rueden *et al.*, 2017) these were converted into uncompressed .avi files via Emicsoft Video Converter (version 5.0.6, Emicsoft Studios) and VirtualDub (version 1.10.4, by Avery Lee). The resulting .avi files were too large to store permanently, so only the original .mov files and .jpeg images of the frames used for analysis have been stored for future analysis.

2.2.5 Image analysis

All images were measured using FIJI (Schindelin *et al.*, 2012). Images were scaled using the micrometer to ensure accurate and consistent measuring of the regions of interest. In the case of videos, snapshots of the frame of video being measured were taken and retained. Measurements were then analysed Graphpad Prism 7 (version 7.00 for Windows, GraphPad Software, La Jolla California USA).

2.2.6 Ventral dissections and variants

Ventral dissections were carried out on adult gregarious desert locusts (*S. gregaria*) (Chapters 3 and 4), immature gregarious desert locusts (*S. gregaria*) (Chapter 5), and crickets (*G. bimaculatus*), cockroaches (*P. americana*), migratory locusts (*L. migratoria*) and solitarious desert locusts (*S. gregaria*) (Chapter 6) to assess whether tension is present in the pair of connectives between the meso- and metathoracic ganglia. Variants

of this microdissection were also carried out on gregarious desert locusts to assess tension within axon bundles also connected to the metathoracic ganglion (Nerve 5, and the pair of connectives between the metathoracic and fourth abdominal ganglia) (Chapter 3).

Desert locust ventral dissection

The following protocol was used for adult desert locusts (both gregarious and solitarious) and forms the basis of several variants found in the other results chapters (Chapters 3-6).

Animals were mounted ventral surface uppermost in Newplast Modelling Clay (Newclay Products Limited, Newton Abbot, UK) to expose the thorax (Figure 2-2). Animals were photographed next to a ruler to obtain gross anatomical measurements. Locust physiological saline (Table 1, adapted from Maddrell and Klunsuwan, 1973) was applied and replaced as necessary. The dissection was carried out in stages (adapted from Hoyle and Burrows, 1973); the cuticle was removed along with three sternal apophyses that penetrate into the thorax at the anterior end, and two similar sternal apophyses present at the posterior end near the abdomen (Figure 2-3). Air sacs, trachea and viscera were removed to expose the meso- and metathoracic ganglia along with the connectives and peripheral nerves. A small marker was placed to serve as a stable reference point. At this point, the dissections vary depending upon the experiment being performed.

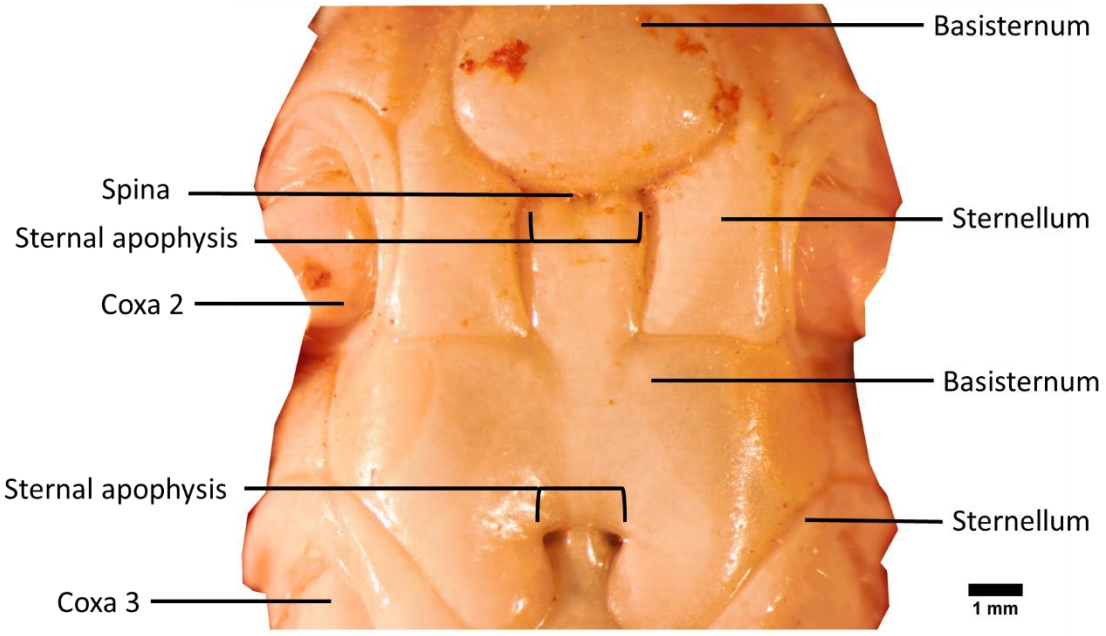

Figure 2-2 Anatomy of the ventral thorax of *Schistocerca gregaria.* The example shown is an adult gregarious female. Based on diagrams and designations from (Albrecht, 1953; Chapman, 2013).

Table 1 Saline recipe. Recipe was used for *S. gregaria* (both gregarious and solitary) and for *P. americana*.

Ingredients	g/L
Sodium chloride	5.73
Potassium chloride	0.3
Calcium chloride	2.04 mL/L
Sodium bicarbonate	1.86
(Mono)sodium phosphate	1.09
Magnesium chloride	0.19
Glucose	1.8
Sodium glutamate	0.83
Sodium citrate	0.88
DL-malic acid disodium salt	0.37
pH approx 7.2	

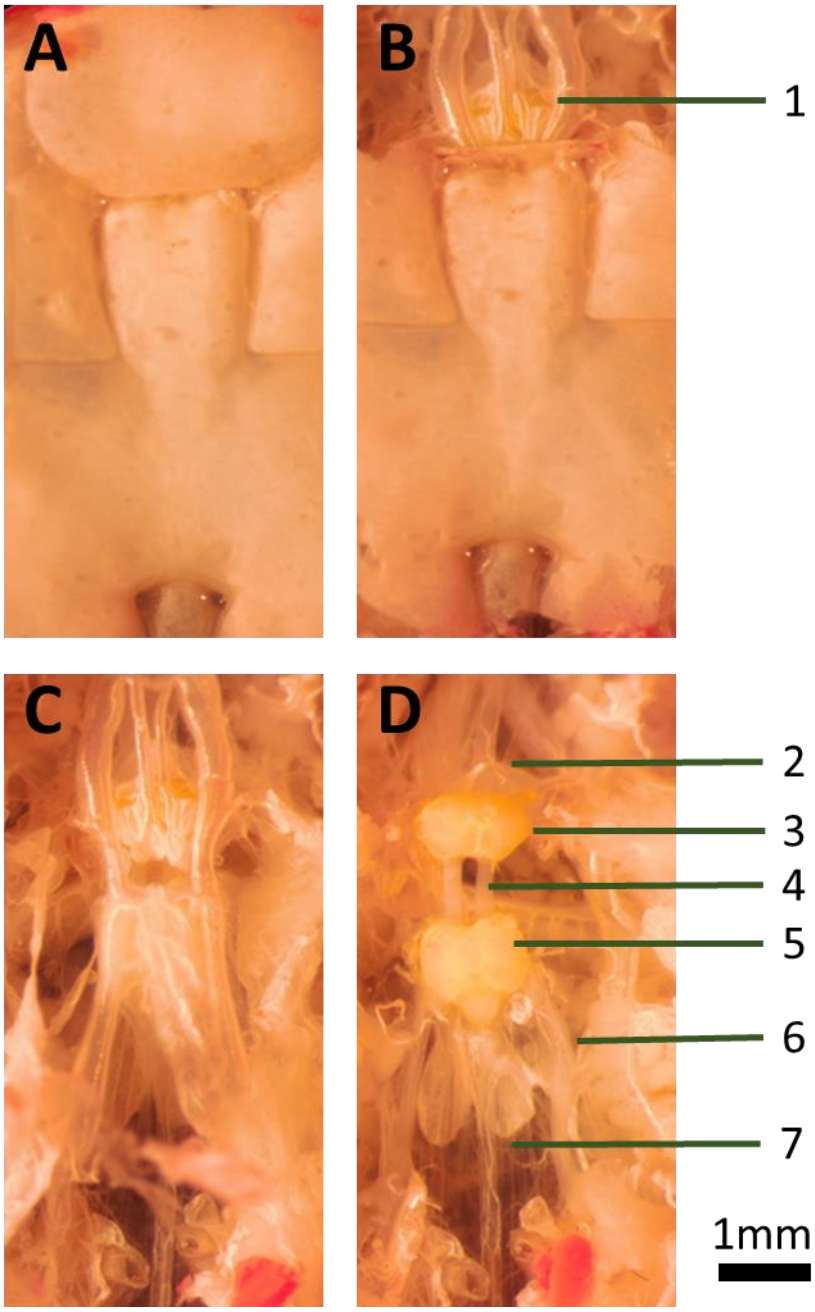

Figure 2-3: Stages of basic ventral dissection of *Schistocerca gregaria*. A Incisions were made to form two rectangles. A small rectangle was cut anterior to the spina and anterior sternal apophyses, and a larger one cut posterior to the posterior sternal apophyses. **B** The rectangle of cuticle largely comprised of the anterior basisternum was removed exposing the mesothoracic ganglia and tracheal system. **C** The spina and all sternal apophyses were cut by inserting microscissors beneath the cuticle via the incisions, the cuticle was then lifted away exposing the metathoracic ganglia and nerve cord descending to the abdomen. **D** The tracheae were removed along with air sacs and fat. Features are numbered. 1: trachea, 2: connectives to the prothoracic ganglion, 3: the mesothoracic ganglion, 4: connectives between the mesothoracic and metathoracic ganglia, 5: the metathoracic ganglion, 6: nerve 5, 7: the connectives to the fourth abdominal ganglion.

Severing the connectives between the meso- and metathoracic ganglia

After the ventral dissection is carried out, there were several different possible variants. The first is the severing of the connectives between the meso- and metathoracic ganglia (Figure 2-4). This forms the basis of the work in Chapter 3 and permits investigation of whether there is tension held in the connectives between the meso- and metathoracic ganglia. It is also used in Chapters 5 and 6 as a control. After performing the preliminary ventral dissection, the region containing the meso- and metathoracic ganglia was photographed. Animals were left to rest for 10 minutes. At the end of this period, the ganglia were filmed at 30 fps with the micrometer in place. The micrometer was removed and the intact ganglia-connective-ganglia complex recorded for 30 seconds. The left connective between the meso- and metathoracic ganglia was cut and filmed for 1.5 minutes, the right connective was then also cut and the recording allowed to reach 5 minutes.

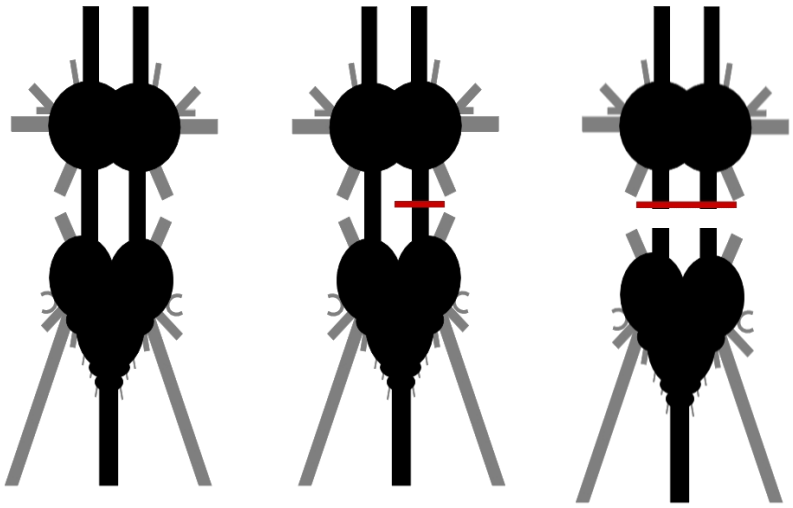

Figure 2-4: Schematic of severing the connectives between the meso- and metathoracic ganglia in *Schistocerca gregaria.* The schematic shows the cutting of first the left connective (mirrored due to the position of the locust) then the right, fully separating the two ganglia.

Time-lapse microdissection

In Chapter 3 we investigate the timeframe of the results seen from severing the connectives between the mesothoracic and metathoracic ganglia. In these experiments ganglia were exposed as normal and the animal allowed to rest for 10 minutes. Both left and right connectives were cut concurrently whilst filming at 30 fps, recording continued for a further minute.

Severing the connectives between the mesothoracic and metathoracic ganglia after initially severing selected axon bundles surrounding the meso- and/or metathoracic ganglia

In Chapter 3, we investigate the relative contributions of surrounding bundles to the results from our initial experiments. This was completed in two rounds of experiments. The first assessed the contributions of the peripheral nerve bundles surrounding our region of interest (Figure 2-5). In these experiments, we carried out the preliminary microdissection and then severed either the peripheral nerves connected to the mesothoracic ganglion, the metathoracic ganglion or both (a diagram of these can be found in General Introduction; Figure 1-4). We then severed the connectives between the two ganglia as usual. The second set of experiments assessed the relative contribution of the VNC itself (Figure 2-6). Once again, the preliminary microdissection was carried out, but was followed by severing the pair of connectives between the meso- to the prothoracic ganglia, the connectives between the metathoracic to the fourth abdominal ganglia, or both.

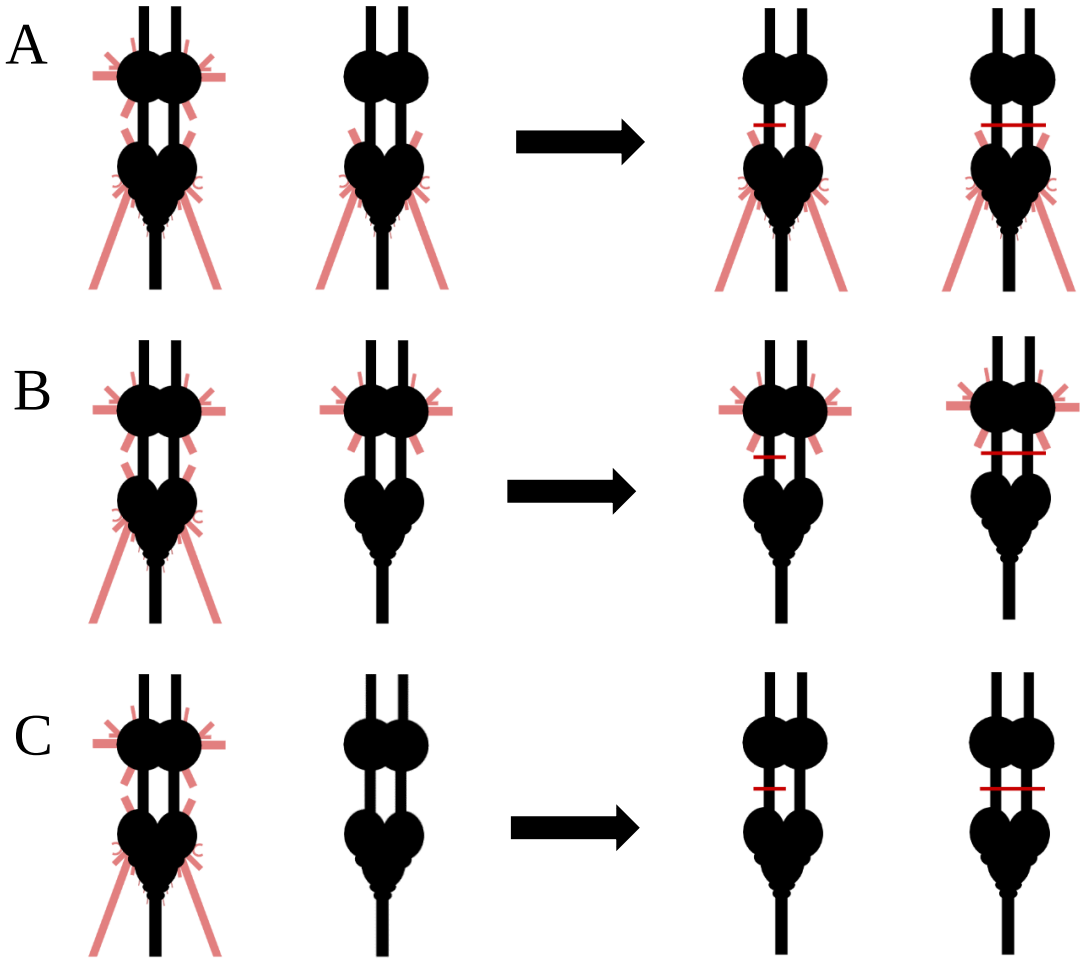

Figure 2-5: Testing the contributions of peripheral nerves. Testing the contributions of the peripheral nerves was done by first severing the nerves from the ganglion they were attached to. This was done in three studies, first the nerves around the mesothoracic ganglion **(A)**, metathoracic ganglion **(B)** and then both **(C)**. The connectives between the meso- and metathoracic ganglia were then severed as described previously.

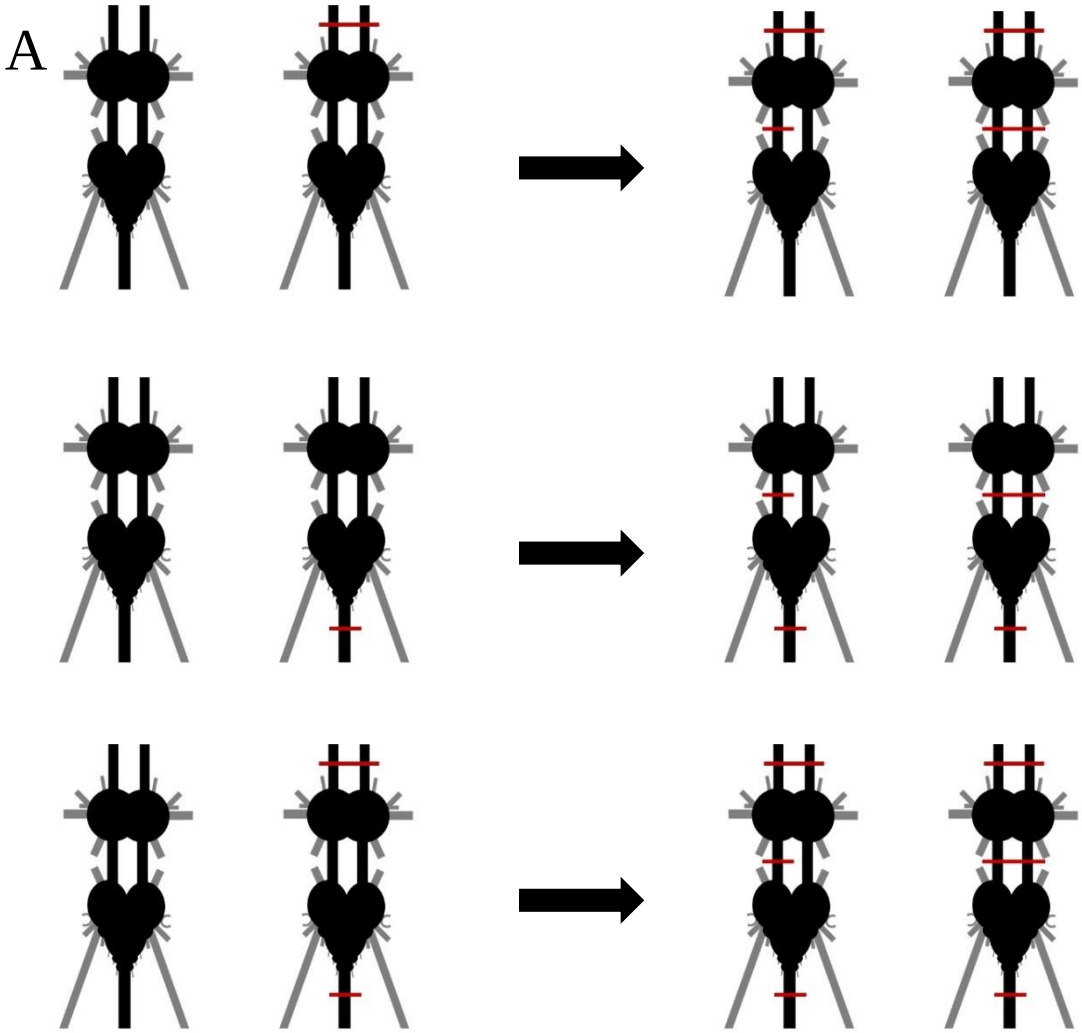

Figure 2-6 Testing the contribution of the nerve cord. To assess the role of the nerve cord in the tension between the meso- and metathoracic ganglia, three sets of experiments were carried out. First **(A)** the nerve cord anterior to the mesothoracic ganglion was severed, then **(B)** the nerve cord posterior to the metathoracic ganglion and **(C)** both were severed. The connectives between the meso- and metathoracic ganglia were then severed as described previously.

Severing peripheral nerve 5 (N5)

To explore whether axonal tension was also present in peripheral nerves, we tested Nerve 5 a large nerve between the metathoracic ganglion and the locust hindlimb (Burrows, 1996). Only individuals with two fully intact hindlimbs were selected for these experiments to ensure no neuropathy had occurred. The ganglia were exposed using the ventral dissection. The dissection window was then laterally and posteriorly expanded to reveal peripheral nerve 5 on the left and right of the metathoracic ganglion. After nerve 5 on both sides was exposed and photographed, animals were left to acclimate for 10 minutes. Next, the nerves were filmed with the micrometer in place. The micrometer was removed and the intact nerves filmed for 30 seconds at 30 fps. The left nerve 5 was cut, followed by the right and the recording left for 5 minutes. Because nerve 5 pairs are on opposite sides of the body they were treated as individual data points.

Severing the connectives between the metathoracic and fourth abdominal ganglia

We also tested the connectives between the metathoracic and fourth abdominal ganglia. A ventral dissection was carried out and extended posteriorly to the abdomen to view the entire connectives as well as fourth abdominal ganglion itself. After the ganglia and connectives were exposed and photographed, animals were left to rest for 10 minutes. Next, the region was filmed with the micrometer in place. The micrometer was removed and the connectives between the metathoracic and fourth abdominal ganglia filmed at 30 fps for 30 seconds. Both connectives were cut at the same time, and the recording continued for five minutes.

Variation of the ventral dissection in *P. americana* and *G. bimaculatus*

All work with American cockroaches (*P. americana*) and crickets (*G. bimaculatus*) is described in Chapter 6 in the context of cross-species comparisons. Protocols for dissection were developed in-house to permit direct comparison with locust preparations. Animals were mounted and photographed as for locusts. Ventral dissection was carried out to expose the meso- and metathoracic ganglia. For cockroaches, saline (Table 1) was applied as necessary throughout. The cuticle was removed by cutting the apophyses between the metathorax and first abdominal sternum, then the spina between the metathorax and mesothorax and gently peeling away the thin cuticle (Chapman, 2013). The connectives between the meso- and metathoracic ganglia are situated directly underneath the cuticle in this region so that no extra tissue had to be removed to expose the axon bundles. More cuticle and tissue were removed around the ganglia until the region around the ganglia was accessible. A small marker was placed to serve as a stable reference point.

For crickets, saline (Table 2) was again applied as necessary throughout. The apophyses between the metathorax and abdomen were removed first allowing for removal of the cuticle in this region, the area was then cleared of fatty tissue to expose the metathoracic ganglion. Scissors were then inserted just below the cuticle to cut the remaining apophyses between the meso- and metathorax surrounding the connectives. The cuticle above the mesothoracic ganglion was then removed. Cuticle was still present around and underneath the connectives, this was trimmed away until the region was exposed. A small marker was then added to serve as a stable reference point.

Table 2: Cricket saline recipe. Recipe used for *Gryllus bimaculatus.* Taken from Matsumoto *et al,* 2003

Ingredients	g/L
Calcium chloride (1 M in water)	5 ml/L
Potassium chloride	0.671
Sodium chloride	8.766
Sodium bicarbonate	0.168
Glucose	7.21
Sodium hydroxide	until pH= 7.2

2.2.7 Microsurgeries

Microsurgeries were carried out on third instars where no folding was present under the cuticle. Animals were mounted as described and locust saline (Table 1) was applied as necessary. A small window was cut between the anterior apophysis on the animal's left hand side and lifted to expose the trachea and the left connective between the meso- and metathoracic ganglia. Scissors were inserted and the connective cut. The cuticle flap was repositioned and the saline removed. The animal was left for half an hour allowing the cuticle to dry, then Loctite® super glue ULTRA gel control™ (Loctite, Düsseldorf, Germany) was used to seal the cuticle. Sham operations were conducted as above, with all tools inserted, but the connective was left uncut.

2.2.8 Adult ventral microdissections after surgery

Locusts that had undergone surgery at third instar were collected again as adults. These underwent the ventral dissection as described. Additional photographs were taken to examine any morphological changes caused by the surgery prior to the removal of the

trachea. The severing of the connectives between the meso- and metathoracic ganglia was identical to that described previously. However the left connective was missing and/or replaced by other tissue.

2.2.9 Transmission electron microscopy

Transmission electron microscopy work was performed at the University of Sussex's Electron Microscopy Imaging Centre (EMC), funded by the School of Life Sciences, the Wellcome Trust (095605/Z/11/A, 208348/Z/17/Z) and the RM Phillips Trust.

Preliminary ventral dissections were carried out as described above. The connectives of interest were removed with some excess nervous tissue and pinned on a sylgard 184 (Dow Corning, Midland, Michigan, USA) coated petri dish using straight minuten pins (10mm, 0.15mm 0.0175mm; Fine Science Tools GmbH, Heidelberg, Germany) to ensure the connective remained straight but not stretched. These were placed in a fume cupboard and fixed in a solution of 2.5% glutaraldehyde, 0.1 M sodium cacodylate for two hours. The samples were then washed in 0.1 M sodium cacodylate and transferred into 1.5 ml TubeOne® microfuge tubes (STARLAB, Milton Keynes, UK). Samples were then left in an osmium mix (2 ml of 4% osmium tetroxide, 5 ml H_2O, 800 µl of 1 M sodium cacodylate) for two hours, washed in a 0.1 M sodium cacodylate solution three times and then placed in a fridge at 4 °C overnight. Samples were dehydrated in an ethanol series (5 minute emersions in 50%, 70%, 80% and 90% ethanol in water then two 10 minute emersions in 100% ethanol) culminating in two 10 minute emersions in propylene oxide before being added to a resin mix (11.8 g EPON, 14.35 g DDSA, 2.98 g MNA, 0.6 ml DMP.30; TAAB Laboratories Equipment Ltd, Aldermaston, UK)

of 1 part resin to 1 part propylene oxide for 2 hours, followed by a 3:1 mixture for 4 hours and 100% resin overnight at room temperature. Samples were embedded in fresh resin the next day and bases for the sample made of the same resin were prepared and polymerised at 60°C for 24 hours (Goodyear *et al.*, 2005).

Samples embedded in resin were cut to separate the connectives between the mesothoracic and metathoracic ganglia, nerve 5 and the connectives between the metathoracic and fourth abdominal ganglia. Each axon bundle was reattached to a resin base in an orientation to ensure sections were cut perpendicular to the connective. Sections for TEM were transverse through the connectives (clearly visible in the resin due to the black staining). The region of interest was reached by making preliminary sections using glass knives made using the LKB 7800 knifemaker (LKB Bromma, Sweden). Once reached, sections were taken using a DiATOME Ultra diamond knife (DiATOME, Hatfield, PA, USA) producing 'gold' coloured sections with a thickness of approximately 100 nm. Once a ribbon had formed, the sections were transferred onto a 300 or 100 GSM copper grid (Agar Scientific Ltd, Essex, UK). Typically, five such grids were produced per axon bundle per animal.

Grids were imaged using a JEOL JEM1400-Plus (JEOL, Tokyo, Japan) electron microscope at 120kV with Lab6 and a Gatan OneView 4K CMOS digital camera (Gatan, Pleasanton, USA). Single images were taken using the software GMS3 (Gatan, Pleasanton, USA) at magnifications of around 200x to allow for a full image of the connective, then at 500-600x to view a singular grid square. Montages were then produced at 20,000x magnification using Shot Meister (JEOL, Tokyo, Japan) software. These montages were produced using the deflector to produce 5x5 grids and the motor

to produce 2x2 of these covering 20 μm^2 region comprising of 100 images each. For each bundle around 6 such montages were completed that included the blood-brain barrier and core regions of the connective.

In the case of three *G. bimaculatus* samples were instead imaged using an Orius SC1000 (Gatan, Pleasanton, USA) at 80 kv, and images were taken individually between 3500x and 5000x with no montages due to a change in available equipment.

Microtubule quantification

In Chapters 4, 5 and 6 we count the number of microtubules in individual axons. We focus on microtubules that are oriented perpendicularly to the plane of sections, thus in the same direction as tension observed. Microtubules in this orientation are easily distinguished in sections due to precise circular appearances (Figure 2-7).

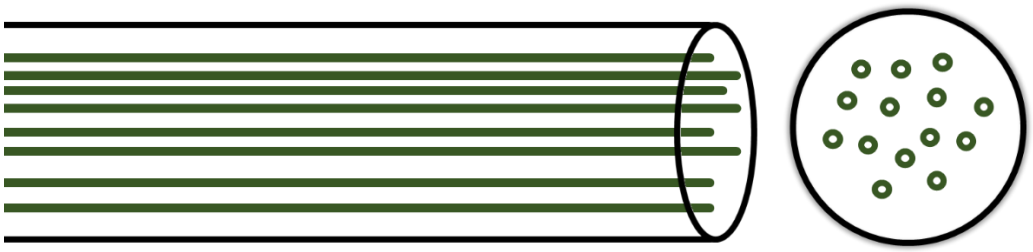

Figure 2-7: Diagram of microtubules counted in TEM images. We count only the microtubules in precise orientation that is perpendicular to the sections cut and the plane of tension observed and in the same longitudinal direction as the axon in the connective.

2.2.10 Direct tensile testing

To determine the forces that axon bundles were exposed to *in vivo*, and to find critical failure points of the system, *ex vivo* bundles were stretched and the forces experienced recorded. This was done with all axon bundles investigated and results can be found in Chapters 4, 5 and 6.

Tissue was glued to a plain microscope slide on one end and to a pin attached to an S256 10 g load cell (Strain Measurement Devices Ltd, Chedburgh, UK) on the other using Loctite® super glue ULTRA gel control™ (Loctite, Düsseldorf, Germany). The force sensor was mounted on an in-house designed mount (Figure 2-8) designed on Openscad software (Kintel and Wolf) and constructed with 3D printer slicing software Cura 3.4.1 and an Ultimaker 2 with polylactic acid (PLA) material (Ultimaker, Geldermalsen, Netherlands). This allowed the force sensor to be attached to an IVM single axis motorised micromanipulator mounted to an LBM-7 manual manipulator via an IVM-LBM-7 fixed mount and controlled LinLab software (Scientifica Ltd, Uckfield, UK). This micromanipulator allowed the force sensor to be moved away from the tissue in discreet horizontal steps, producing a force that could be measured.

The force sensor was powered by a 9 V battery that would then produce an output in mv depending on the force applied. This was calibrated daily. The output signal was processed using an LHBF-48X (high pass filter 0.1 Hz, low pass 20 Hz, gain 1000, offset range ±0.1 V; npi electronic GmbH, Tamm, Germany). The signal was analogue to digital converted using a Micro1401-3 board (Cambridge Electronic Design Limited, Cambridge, UK), as was the simultaneous output from the IVM motorised micromanipulator. Signals were displayed using Spike2 software (version 8.13, Cambridge Electronic Design Limited, Cambridge, UK). Throughout this process, the

tissue being stretched was also filmed simultaneously using the camera and software described in 2.2.5.

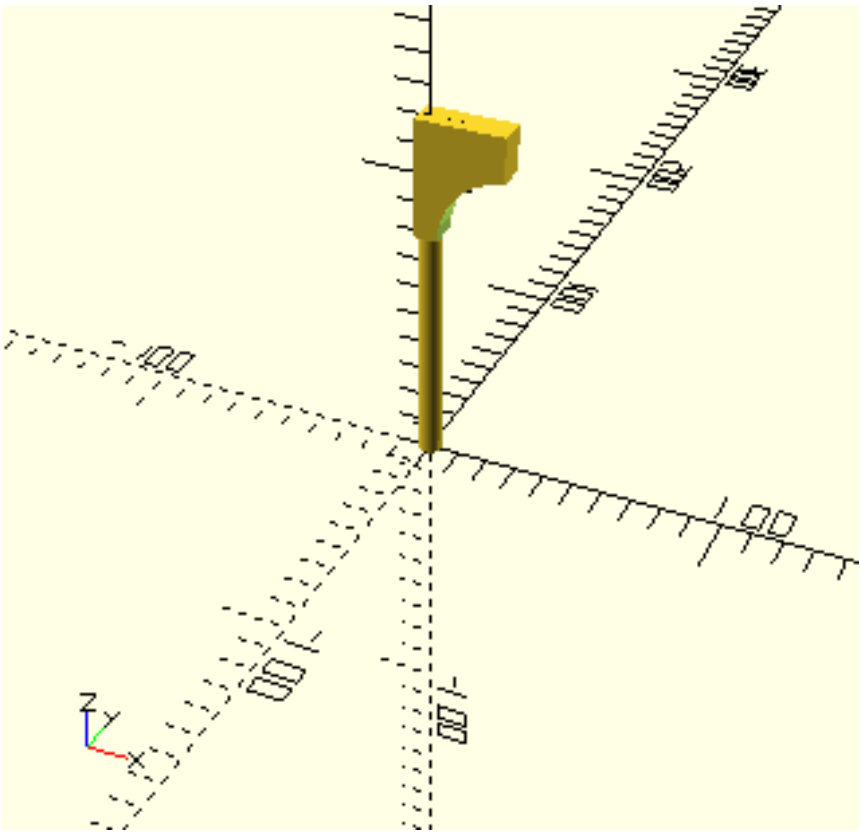

Figure 2-8: Bespoke mount design from OpenScad. The mount consisted of three OpenScad elements. A 10 cm cylinder (radius 4 mm), with a 3 cm x 1 cm x 4 cm cuboid, a cylinder (4 cm with a radius 2.5 cm) was removed from the cube to create an arc. Axes are in mm.

Testing the connectives between the meso- and metathoracic ganglia

Uniaxial loading on the connectives between the mesothoracic and metathoracic ganglia were carried out on gregarious desert locust adults (healthy, those who had undergone third instar surgery and sham operations), adult black crickets and adult cockroaches. In each case, a ventral dissection was carried out as described previously and the ganglia photographed *in vivo,* the meso- and metathoracic ganglia along with the connectives between them were then removed. The mesothoracic ganglion attached to the slide and the metathoracic ganglion to the force sensor, saline was then applied. Filming and recording via Spike2 began and the micromanipulator was stepped away from the tissue in 50 µm stages at 3 second intervals until the force returned to zero or the connectives were completely free, whichever occurred last.

We also tested other axon bundles in gregarious desert locusts. The connectives between the metathoracic and fourth abdominal ganglia were tested as above with the metathoracic ganglion attached to the glass slide. Nerve 5 was dissected out prior to any branching still attached to the metathoracic ganglion. The ganglion was attached to the glass slide and the severed end to the pin.

Testing full recovery after single steps

In gregarious desert locust adults, we tested the time it took for the force to return to zero after individual steps. This was carried out on the connectives linking the meso- to metathoracic ganglia and the preparation the same as above. A 50 µm step was applied, and the connectives monitored until the connective fully recovered and the force returned to zero. This was repeated twice more.

3 Axon bundles in *Schistocerca gregaria* are under differing levels of tension

3.1 Abstract

Axonal tension is present during development and growth, and plays key roles in these processes. It has also been found in adult axonal tracts but there is currently no explanation of its function or the structures that generate it. To investigate the role of tension in adult nervous systems, we developed an experimental model using microdissection methods. Arthropods offer a powerful model for studying axonal tension due to the clear separation of axonal bundles (connectives or peripheral nerves) from the accretions of cell bodies, dendrites and axons in the ganglia of the ventral nerve cord (VNC). We identified a region within the VNC of the desert locust, *Schistocerca gregaria*, where the morphology suggested a region of tension between the meso- and the metathoracic ganglia. Here, using microdissection techniques, we have shown that the axon bundles between the meso- and metathoracic ganglia do indeed experience tension. We identify two other axon bundles in this region that are under less tension: the connectives between the metathoracic and fourth abdominal ganglion which contribute to the tension between the meso- and metathoracic ganglia, and nerve 5 which does not. Further microdissections showed some but not all of the tension was mediated by the VNC posterior to the metathoracic ganglion, and that neither feeding nor egg laying altered the tension observed.

3.2 Introduction

Tension is a pulling force that exerts stress upon a material (Gere, 2004). One indication of a tissue being under tension is that cutting or puncturing it produces a large gap (Dorfman and Cherdantzev, 1975; Xu et al., 2009, 2010; Luna et al., 2013; Nia et al., 2018 and reviewed in Sugimura et al., 2016). Tension is present in tissues such as muscle (Huxley, 1969; Magid and Law, 1985), and has several roles in other tissues during embryogenesis (Siechen *et al.*, 2009; Aliee *et al.*, 2012; Pasakarnis *et al.*, 2016). Axonal tension has been implicated during embryogenesis and later during growth through stretch growth (Pfister, 2004; Smith, 2009; Lamoureux *et al.*, 2010; Polackwich *et al.*, 2015). During embryogenesis the main role of axonal tension is the growth and guidance of the axon itself (Sabry *et al.*, 1991; Dingyu *et al.*, 2016).

Van Essen (1997) hypothesized that axonal tension also plays a role in shaping the nervous system by exerting pulling forces. He proposed that the tensile forces of axonal tracts were responsible for the formation of sulci and gyri of the mammalian brain. This is only one of several hypotheses that attempt to explain the formation of the sulci and gyri in humans, including that they may be formed by genetic patterning or that other mechanical properties of the human brain such as stiffness or differential growth may cause the emergence of the folded cortices (Toro and Burnod, 2005; Ronan and Fletcher, 2014; Ronan *et al.*, 2014; Razavi, Zhang, Li, *et al.*, 2015).

Among the research that seemed to support Van Essen's (1997) hypothesis of axonal tension leading to the formation of sulci and gyri and shaping nervous system morphology were several studies that identified axonal tension in white matter tracts (Xu *et al.*, 2009, 2010; Luna *et al.*, 2013; Koser *et al.*, 2015). In the ferret (Xu *et al.*, 2010) and mouse brain (Xu *et al.*, 2009), and in the lamprey spinal cord (Luna *et al.*, 2013),

tension was found by cutting axonal tracts in various planes and measuring the subsequent gap. In the lamprey spinal cord, it was found that axons are prestressed to about 10-15% of their maximum before breaking. In mouse spinal cords, tension was inferred from stiffness results (Koser *et al.*, 2015). However, not all of these lines of evidence supported the hypothesis that axonal tension would lead to the cortical folding in the brain fully; the axonal tension found in the ferret brain was not in the right orientation to explain the folding morphology (Xu *et al.*, 2010). If axonal tension does not drive morphology yet still occurs, it likely has an alternate function yet this is currently unknown.

Two models of stretch-growth, or the growth of integrated axons, describe the process as a passive response to stretch. In the first model, it is hypothesised that stretch caused by the growth of surrounding tissue causes small breaks in the axonal cytoskeleton which then leads to accumulation of transported materials that are then integrated into the axonal membrane (Heidemann and Bray, 2015). In a second model, the growth of surrounding tissues is hypothesised to stretch the axons, causing opening of mechanosensitive ion channels along the axon that signal for growth to occur primarily at the junction between the axon and soma (Purohit and Smith, 2016). In both models, growth is a response to stretch and neither account for axons being under tension in the absence of growth.

There are some potential theories for the function of axonal tension. Studies have found the presence of actin rings throughout rat axons that, coupled with spectrin and ankyrin, may lead to a stable and efficient arrangement of sodium channels thus may improve firing (Xu *et al.*, 2013; Zhang *et al.*, 2017). Spectrin and ankyrin have also

been shown to have importance in the structure and integrity of arthropod axons (Hammarlund *et al.*, 2007; Pielage *et al.*, 2009).

Loss of tension due to dysfunction of the cytoskeleton is also implicated in some human diseases, such as amyotrophic lateral sclerosis (ALS). In this disease it is thought that the loss of tension in the cytoskeleton leads to neurofilament tangles, effecting both axonal integrity and transport (Hirano *et al.*, 1984; and reviewed in Hirano, 1995; Ikenaka *et al.*, 2012). However, tension is likely maintained by a cytoskeletal structure that is also involved in axonal transport (Alberts *et al.*, 2015 and General Introduction), so it is difficult to disentangle the failure of which function causes the disease state. This difficulty is exacerbated by the lack of understanding of the normal functional role of tension, if indeed there is one.

Invertebrates offer a system in which to study axonal tension due to the morphology of their nervous system (Niven *et al.*, 2008; discussed further in General Introduction). Here we focus on the desert locust. The mesothoracic ganglion and those ganglia anterior to it are all positioned adjacent to the peripheral structures that they innervate. This is similar to the anatomy of the VNC from more basal insect lineages, such as silverfish (Niven *et al.*, 2008). In contrast, the metathoracic ganglion is shifted anteriorly to the majority of peripheral structures it innervates. This includes the hindlimbs of the locust, which are primarily innervated by nerves 3, 4 and 5 from the metathoracic ganglion (Figure 1-4). The metathoracic ganglion is formed through a fusion of four neuromeres, T3 and A1-A3 (Figure 1-4; General Introduction). We hypothesised that due to this anatomy there would be tension exerted on the metathoracic ganglion by posterior peripheral structures ‘pulling’ on the anteriorly

shifted metathoracic ganglion and subsequently on the connectives between the meso- and metathoracic ganglia.

We have investigated the presence of tension in the locust by cutting specific nerves. We focus on axon bundles, collections of axons running in parallel and wrapped in a sheath not embedded in other neuronal tissue. Such axon bundles can be peripheral nerves or connectives linking the ganglia of the VNC. If tension is present in axon bundles then a gap should appear between the severed ends upon cutting (Dorfman and Cherdantzev, 1975; Xu et al., 2009, 2010; Luna et al., 2013; Nia et al., 2018 and reviewed in Sugimura et al., 2016). We show that tension is present in the connective between the meso- and metathoracic ganglia that is largely a posterior 'pull' but one that originates from the VNC not the peripheral nerves.

3.3 Methods

The methods used here are outlined in Chapter 2, specifically sections 2.2.4 to 2.2.6.

3.4 Results

3.4.1 Tension in the connectives between the meso- and metathoracic ganglia

The meso- and metathoracic ganglia of the adult locusts are separated by connectives approximately 1 mm long (0.99±0.070 mm; mean ± SD; Figure 3-1). Severing a single connective produced no significant increase in the distance between the connectives in either males or females (two-way Repeated Measures Analysis of Variance (RM ANOVA) intact vs left cut, males, n=8, $p>0.999$; females, n=8, $p>0.999$; Figure 3-1). Following severing of both connectives, we observed a pulsating movement of the metathoracic ganglion. Consequently, we measured when the ganglion was at its most anterior position (creating the smaller gap) and posterior position (creating the larger gap). Severing both connectives increased the separation of the ganglia in both sexes (intact vs both cut, males, n=8, small $p<0.0001$, large $p<0.0001$; females, n=8, small $p<0.0001$, large $p<0.0001$; Figure 3-1). In females, the smallest and largest separations were significantly different (small vs large, females $p=0.0474$, males $p=0.6439$).

To separate the different contributions of the pulsating movement from the retraction of the axons within the connectives, we measured the length of the connectives before and after cutting (Figure 3-2). In both males and females, the retraction of axons within the connectives was significantly smaller than the total separation (paired two-tailed T-tests; males $t=6.245$, $df=7$, $p=0.0004$; females, $t=8.445$, $df=6$, $p=0.0002$). The retraction in axon length within the connectives was normalised to the overall separation of their severed ends and represented as a percentage. Retraction of the axons within the connections did occur, accounting for approximately 13% of the overall separation of the severed ends of the connectives after they were cut (males,

n=8, 13.6±12.8%, mean ± SD; females, n=8, 12.7±13.3%). The expansion was rapid (Figure 3-3), occurring 1-2 seconds after the microscissors obscured accurate measurements, and then remaining stable afterwards.

We assessed the movement of the ganglia by comparing their positions to a fixed point on the thorax (Figure 3-4). The mesothoracic ganglion moves anteriorly to a small extent, whereas the metathoracic ganglion moves posteriorly by a significantly larger amount (two-way RM ANOVA, $F(7,98) = 31.93$, $p<0.0001$; Sidak's post hoc test, smallest distance moved by meso- vs metathoracic ganglion males $p=0.0026$, females $p=0.0157$, greatest distance moved by meso- vs metathoracic ganglion males $p<0.0001$, females $p<0.0001$). These measurements were taken at points throughout the microdissection, before and after the 10 minute rest period (0-10), then between the end of the rest period and after severing both connectives (measuring the smallest and largest gap), and finally comparing the difference between the smallest and largest gap.

A

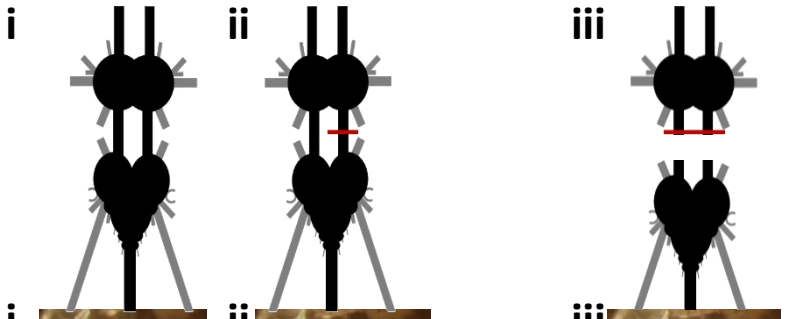

B

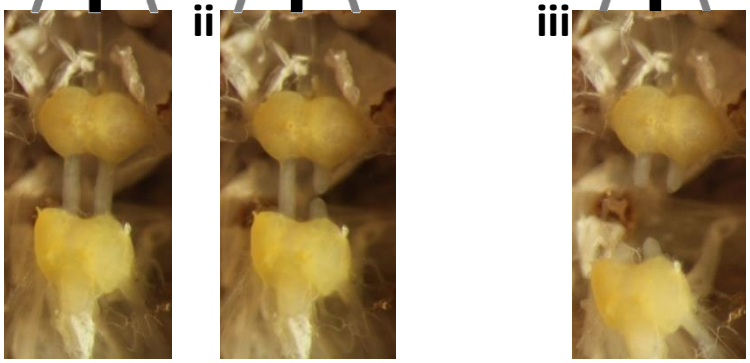

C

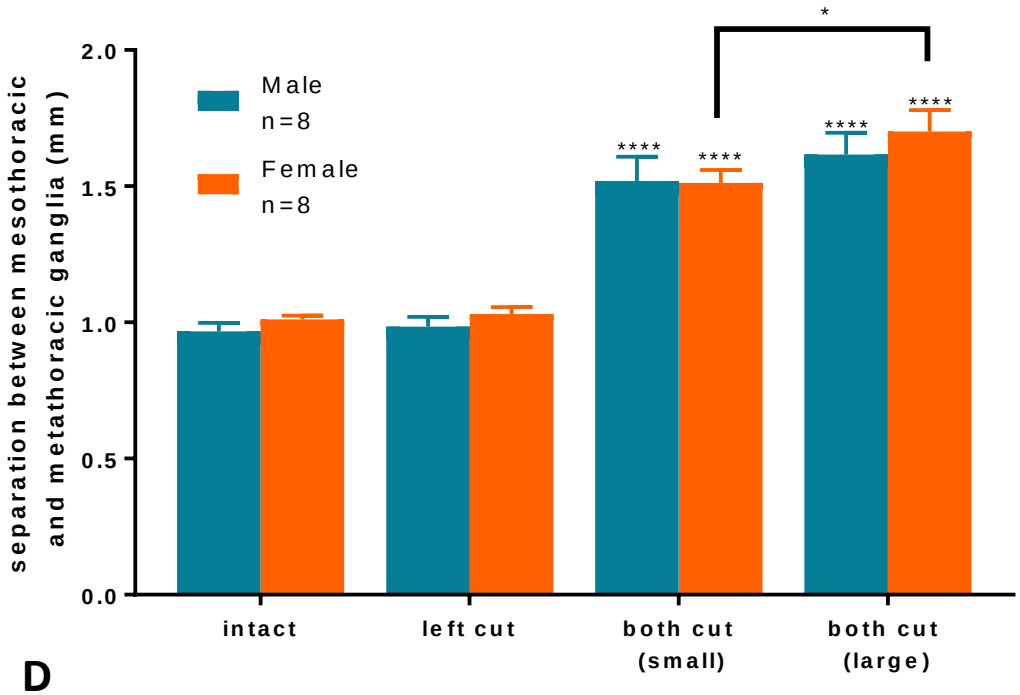

D

	Male		Female	
	Mean	SD	Mean	SD
intact	0.97	0.09	1.01	0.04
left cut	0.98	0.10	1.03	0.07
both cut (small)	1.52	0.25	1.51	0.13
both cut (large)	1.62	0.23	1.70	0.22

Figure 3-1 The effect of cutting connectives upon the position of the meso- and metathoracic ganglia. **A**i-iii. A stylised schematic of this region showing the experimental design. Connectives and nerves are in grey, ganglia in black and the cutting location in red. i is the intact state, ii shows the left connective cut, and iii shows both cut and a clear separation between the severed ends. **B**i-iii. An example of the connective cutting *in vivo*. The meso- and metathoracic ganglia are a clear bright yellow while the connectives are a semi-translucent white. i shows the connectives intact, ii shows the left cut and iii shows both cut and a clear gap has formed between the two ganglia. **C**. The size (mean ± SD) of the gap between the ganglia at each stage. Data were divided into male and female. After both connectives were severed a movement was apparent so measurements were taken at the two extremes. (two-way RM ANOVA, *p<0.05, ****p<0.0001 compared to intact same-sex state). **D:** mean ± SD of the separation of the meso- and metathoracic ganglia (mm).

A

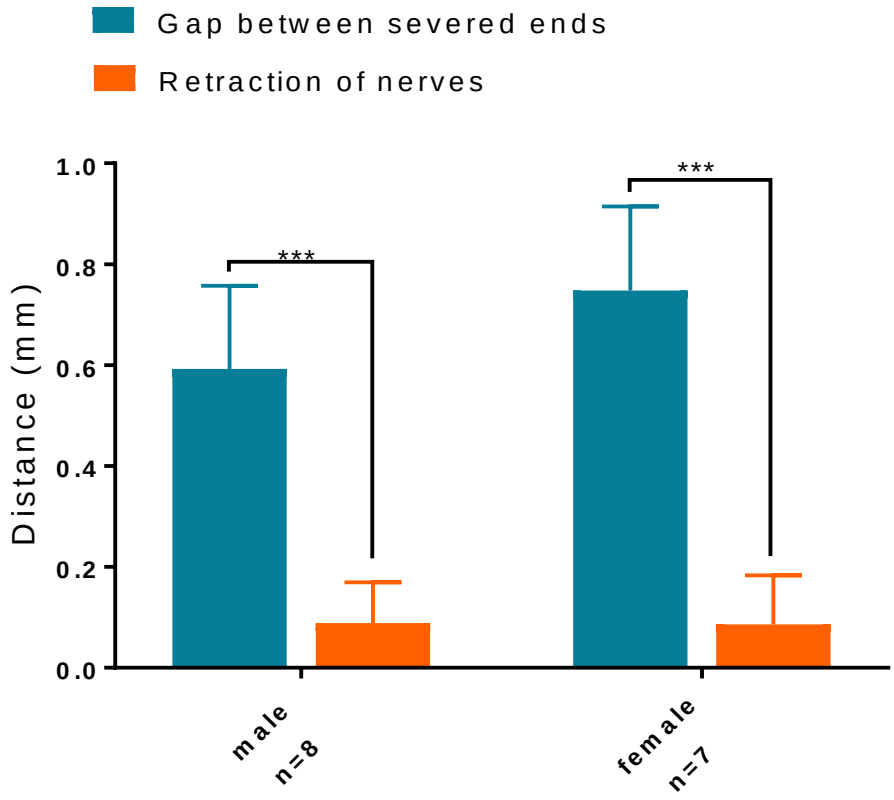

B

	Gap between severed ends		Retraction of nerves	
	Mean	SD	Mean	SD
male	0.59	0.16	0.09	0.08
female	0.75	0.17	0.09	0.10

Figure 3-2 Retraction of the axons within the connectives contributes to the separation of the ganglia after connective cutting. A: The total gap produced by cutting the connectives between the meso- and metathoracic ganglia is significantly larger than the gap that is formed due to retraction of these cut axons (paired two-tailed T-tests were done for males and female separately, *** $p<0.001$, data is mean ± SD). **B:** mean ± SD of the separation of the severed ends of the connectives between the meso- and metathoracic ganglia (mm) and the retraction of axons (mm).

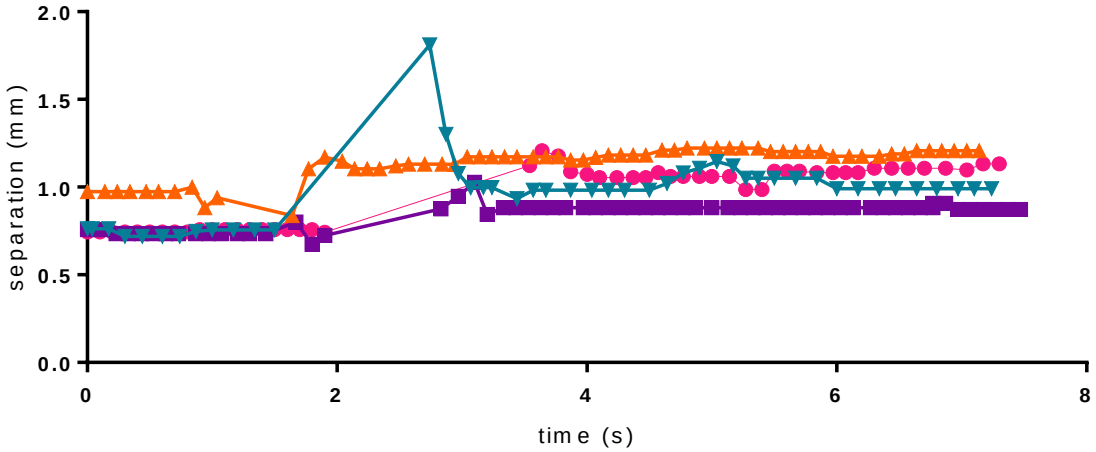

Figure 3-3: Separation of the meso- and metathoracic ganglia occurs rapidly after severing the connectives. Measurements were taken approximately every 100 milliseconds in four animals, the gaps in data collection are due to scissors obscuring the ganglia.

A

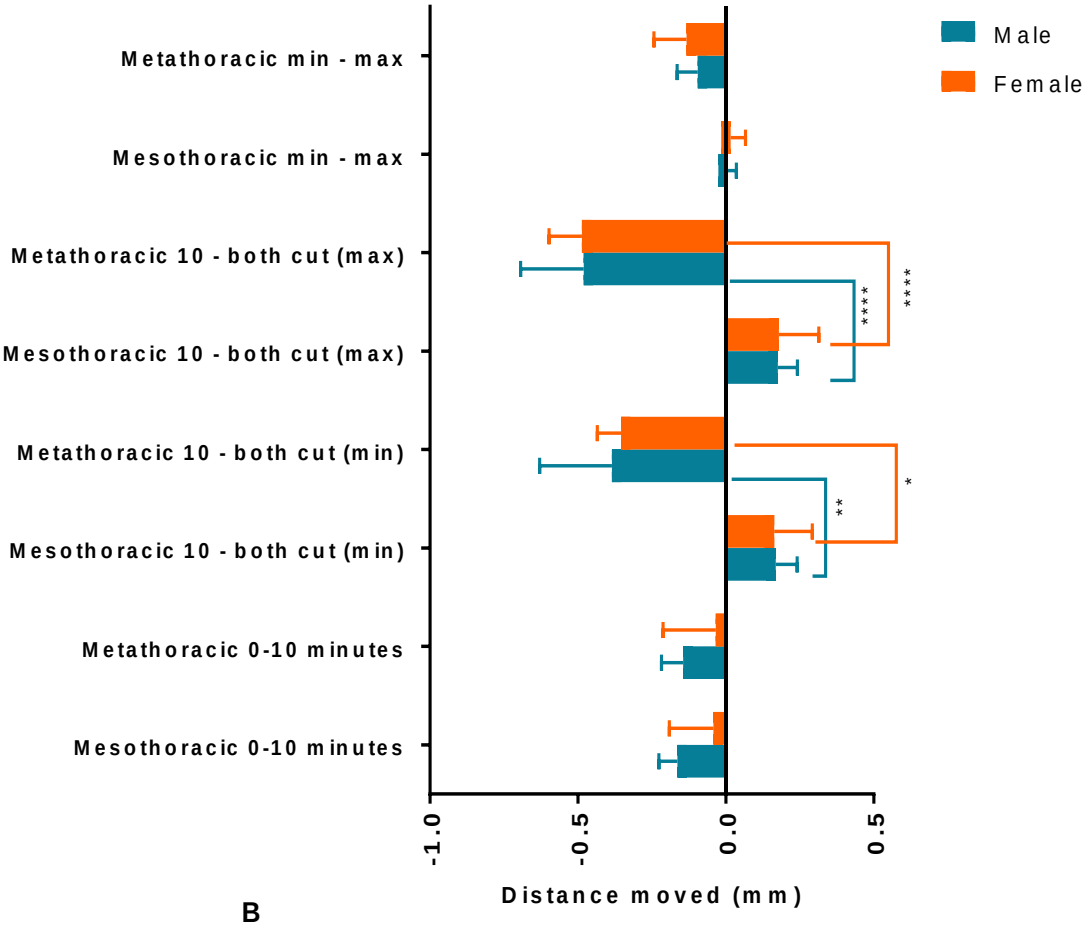

B

	Male		Female	
	Mean	SD	Mean	SD
Mesothoracic 0-10 minutes	0.164	0.062	0.042	0.149
Metathoracic 0-10 minutes	0.144	0.073	0.034	0.178
Mesothoracic 10 - both cut (min)	0.169	0.072	0.164	0.128
Metathoracic 10 - both cut (min)	0.385	0.244	0.354	0.081
Mesothoracic 10 - both cut (max)	0.176	0.066	0.180	0.134
Metathoracic 10 - both cut (max)	0.480	0.214	0.486	0.111
Mesothoracic min - max	0.007	0.029	0.016	0.050
Metathoracic min - max	0.095	0.070	0.133	0.111

Figure 3-4. The metathoracic ganglion moves more than the mesothoracic ganglion after the connectives between them are cut. A: Data, divided into male and female, shows the movement of the ganglia between different stages of the surgery as well as the direction (negative = posterior, positive = anterior). The steps are between timepoint 0 and the 10 minute rest, between the 10 minute rest and both of the connectives cut both at the point where the separation was smallest and largest due to visible oscillations after cutting and the difference between the two. In males but not females differences were seen between the extent of movement between the meso- and metathoracic ganglia (data was all made positive to compare distance moved regardless of direction, Two-way RM ANOVA and Sidak's multiple comparisons, *p<0.05,**p<0.01 ****p<0.0001).)data is mean ± SD. **B:** mean ± SD of the movement of the meso- and metathoracic ganglia (mm). Absolute values are shown for direct comparisons.

3.4.2 Separation of the meso- and metathoracic ganglia following connective cutting is partially caused by other axon bundles

We severed the nerve bundles linked to the meso- and metathoracic ganglia to identify the source of the tension (Figure 3-5). When we severed the peripheral nerves connected to the mesothoracic ganglion (meso peripherals) there was no change in the separation between the meso- and metathoracic ganglia upon cutting the connectives between them. Likewise, when the peripherals around the metathoracic ganglion (meta peripherals) were cut or all the peripherals around the meso- and metathoracic ganglia were cut there was no change in the separation between the meso- and metathoracic ganglia upon cutting the connectives between them(all peripherals) (Kruskal Wallis test $H=42.35$, $n=16$ in all groups, followed by Dunn's post hoc test against control animals, no significance (n.s)).

When we severed the connectives between the pro- and mesothoracic ganglia (pro-meso) prior to severing the connectives between the meso- and metathoracic ganglia there was also no significant change in the gap that formed. Conversely, when we severed the connectives between the metathoracic and fourth abdominal ganglia or both those connectives and those between the pro- and mesothoracic ganglia there was a significant decrease in the gap formed when the connectives between the meso- and metathoracic ganglia were severed (meta-ab4, $p=0.0064$; both cord, $p=0.0002$).

We examined how first severing these different surrounding bundles (peripheral nerves and the connectives to other ganglia) affected the extent and direction of movement of the meso- and metathoracic ganglia. Measurements of movements were taken at the same points as described above (Figure 3-4). Cutting all the peripheral nerves around the meso- and metathoracic ganglia did not change the motion in comparison to

controls in either males or females at any point measured (two- way RM ANOVA tests followed by Sidak's multiple comparisons were carried out control vs peripherals cut males $F(1,14)=0.2435$, $p=0.6293$, females $F(1,14)=1.709$, $p=0.2122$, post-hoc comparisons were done at different stages, no significant differences were found,

Figure 3-6, Figure 3-7). Likewise, severing the peripherals around the mesothoracic ganglion, metathoracic ganglion or both did not change the movement of the metathoracic ganglion (one-way ANOVA with Tukey's post hoc test, Figure 3-8).

Severing both the connectives between the meso- and prothoracic ganglia and the connectives between the metathoracic and fourth abdominal ganglia reduced the movement of the meta- but not the mesothoracic ganglion. There was a significantly greater effect in males in which there were differences between both the smallest distance moved by the metathoracic ganglion after cutting the connectives between it and the mesothoracic ganglion, and the largest distance (two-way RM ANOVA, $F(1,14)=19.72$, $p=0.0006$; Sidak's post hoc test to compare control vs nerve cord cut at each stage of dissection; smallest distance $p<0.0001$, largest distance $p<0.0001$; Figure 3-9). In females, severing the connectives to the prothoracic ganglion and those to the fourth abdominal ganglion causes a significant reduction in the movement of the metathoracic ganglion (two-way RM ANOVA, $F(1,14)=7.584$, $p=0.0155$; Sidak's post hoc test to compare control vs nerve cord cut at each stage of dissection, control vs cord cut effected the distance moved by the metathoracic ganglion $p=0.0002$; Figure 3-10).

We examined the movement of the metathoracic ganglion when only the connectives between the pro- and mesothoracic ganglia, the connectives between the metathoracic and fourth abdominal ganglia or both were cut. Severing either the

connectives between the metathoracic and fourth abdominal ganglia or the connectives between the pro- and mesothoracic ganglia reduced the movement and cutting both produced the largest decrease (one-way ANOVA, $F(3,60)=13.11$, $p<0.0001$; Tukey's post hoc test, all groups n=8, pro-meso $p=0.0027$, meta-fourth abdominal $p=0.006$ and both $p<0.0001$; Figure 3-11).

A

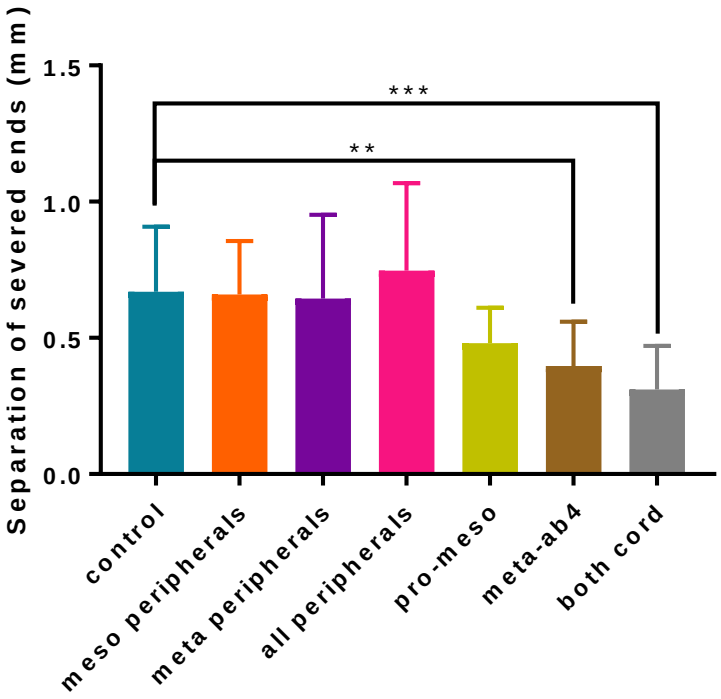

B

control	0.6698	0.2382
meso peripherals	0.6593	0.1963
meta peripherals	0.6449	0.3073
all peripherals	0.7464	0.3212
pro-meso	0.4809	0.1303
meta-ab4	0.3964	0.1626
both cord	0.3111	0.1599

Figure 3-5: Effect of severing surrounding axon bundles prior to cutting the connectives between the meso- and metathoracic ganglia on the separation that forms between the severed ends. A: The total separation of the severed ends of the connectives between the meso- and metathoracic ganglia was measured after the connectives were cut (mean ± SD). 'Meso peripherals' are all peripheral nerves connected to the mesothoracic ganglion, 'meta peripherals' are all the peripheral nerves connected to the metathoracic ganglion and 'all peripherals' are both of these together. 'Pro-meso' are the connectives between the pro- and mesothoracic ganglia, 'meta-ab4' are the connectives between the metathoracic and fourth abdominal ganglia and 'both cord' is both of these. Prior to the nerve cutting different axon bundles were severed. Severing the peripheral nerves around the meso- and/or the metathoracic ganglia had no effect on the gap that formed, however cutting the nerve cord posterior to the metathoracic ganglion and cutting both this and the nerve cord anterior to the mesothoracic ganglion made the gap significantly smaller when compared to the control (Kruskal Wallis test with Dunn's Multiple comparisons, **p<0.01, ***p<0.001). **B:** mean ± SD of the separation of the severed ends of the connectives between the meso-metathoracic ganglia when other bundles are severed first (mm).

A

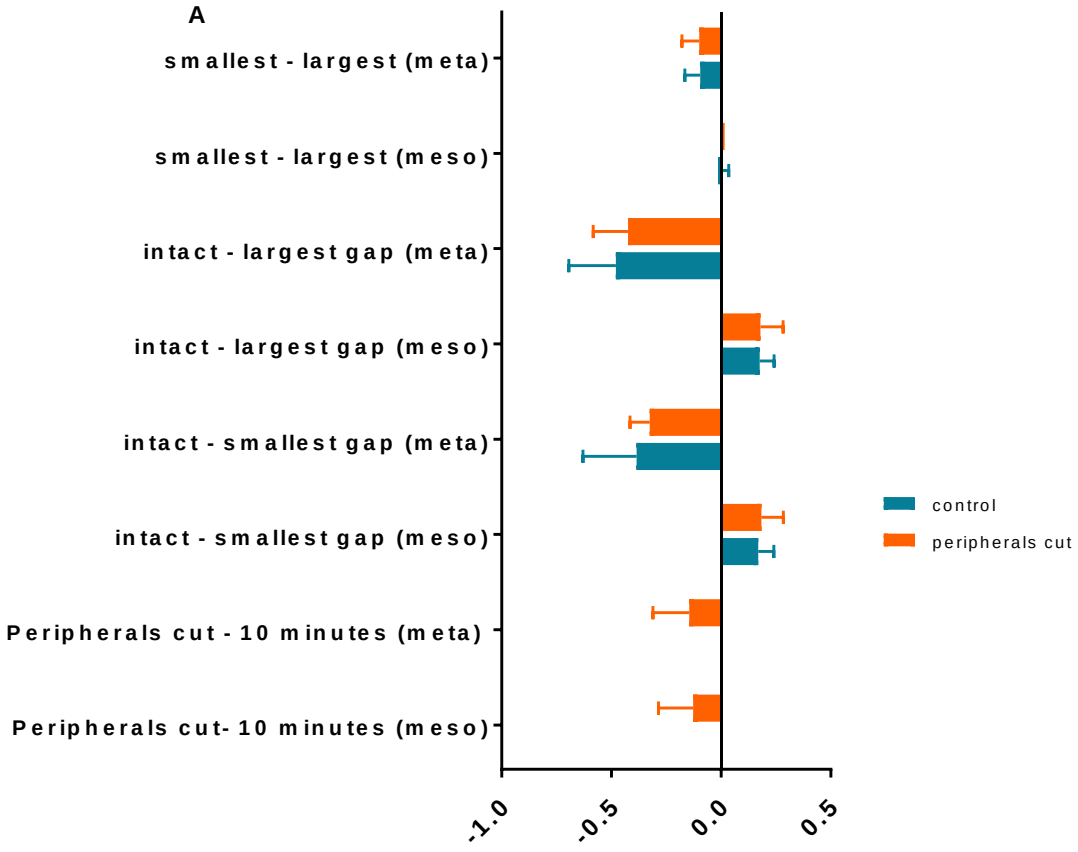

B

	control		peripherals cut	
	Mean	SD	Mean	SD
Peripherals cut- 10 minutes (meso)			0.128	0.158
Peripherals cut - 10 minutes (meta)			0.145	0.166
intact - smallest gap (meso)	0.169	0.072	0.184	0.100
intact - smallest gap (meta)	0.385	0.244	0.325	0.090
intact - largest gap (meso)	0.176	0.066	0.180	0.103
intact - largest gap (meta)	0.480	0.214	0.424	0.158
smallest - largest (meso)	0.007	0.029	0.004	0.016
smallest - largest (meta)	0.095	0.070	0.099	0.080

Figure 3-6: Movement of ganglia after cutting the connectives between the meso- and metathoracic ganglia when all connected peripheral nerves are cut (males). A: Cutting the peripherals around the meso- and metathoracic ganglia had no effect on any movements of either ganglia at any stage of the microdissection (mean ± SD, two-way RM ANOVA with Sidak's multiple comparisons). Movement was measured between the peripherals being cut and the 10 minute rest, 'intact – smallest gap' and 'intact – the largest gap' are measured before the connectives between the meso- and metathoracic ganglia are cut to the smallest/largest separation between the two and then 'smallest-largest' is the movement between these states. **B:** absolute mean ± SD of the movements of the meso- and metathoracic ganglia after severing the connectives between them (mm).

A

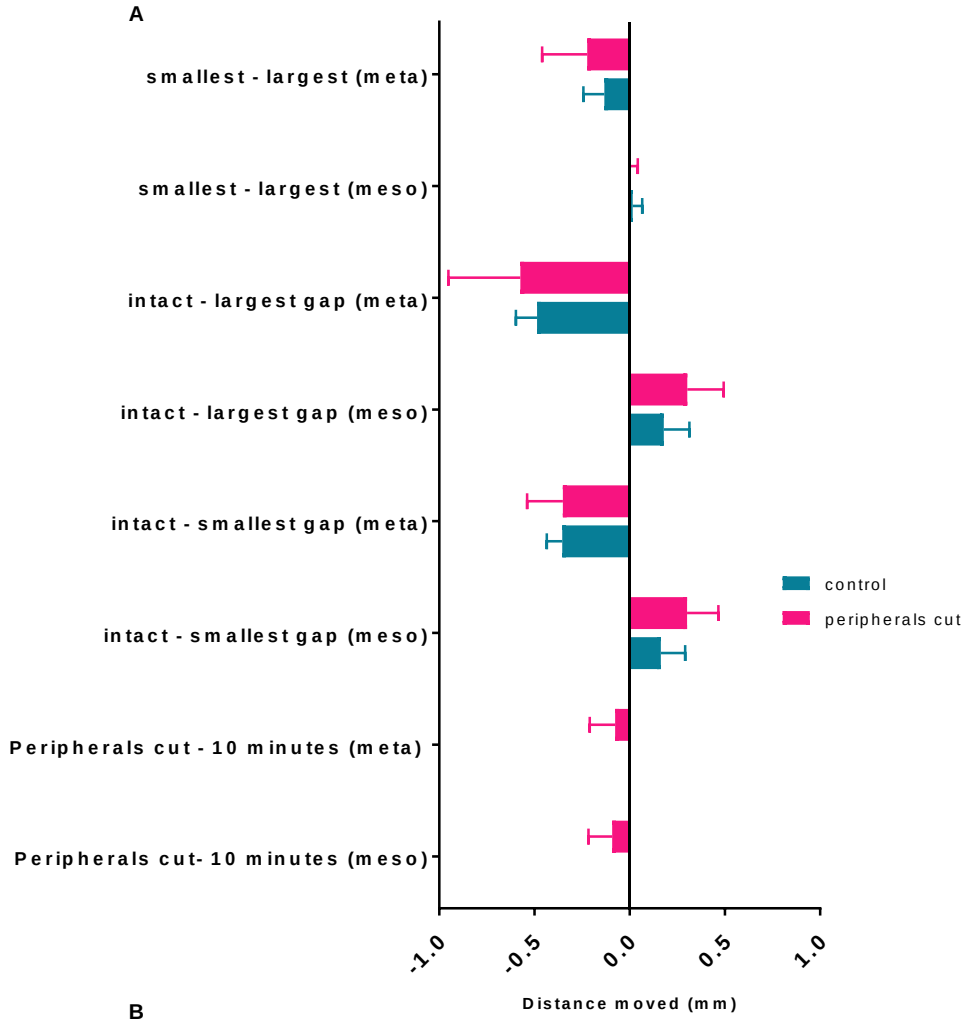

B

	control		peripherals cut	
	Mean	SD	Mean	SD
Peripherals cut- 10 minutes (meso)			0.092	0.125
Peripherals cut - 10 minutes (meta)			0.076	0.134
intact - smallest gap (meso)	0.164	0.128	0.302	0.164
intact - smallest gap (meta)	0.354	0.081	0.351	0.188
intact - largest gap (meso)	0.180	0.134	0.302	0.191
intact - largest gap (meta)	0.486	0.111	0.574	0.377
smallest - largest (meso)	0.016	0.050	2.500e-004	0.042
smallest - largest (meta)	0.133	0.111	0.223	0.237

Figure 3-7: Movement of ganglia after cutting the connectives between the meso- and metathoracic ganglia when all connecting peripheral nerves are cut (females). A: Cutting the peripherals around the meso- and metathoracic ganglia had no effect on any movements of either ganglia at any stage of the microdissection (mean ± SD, Two-way RM ANOVA with Sidak's multiple comparison). Movement was measured between the peripherals being cut and the 10 minute rest, 'intact – smallest gap' and 'intact – the largest gap' are measured before the connectives between the meso- and metathoracic ganglia are cut to the smallest/largest separation between the two and then 'smallest-largest' is the movement between these states. **B:** absolute mean ± SD of the movement of the meso- and metathoracic ganglia after the connectives between them are severed.

A

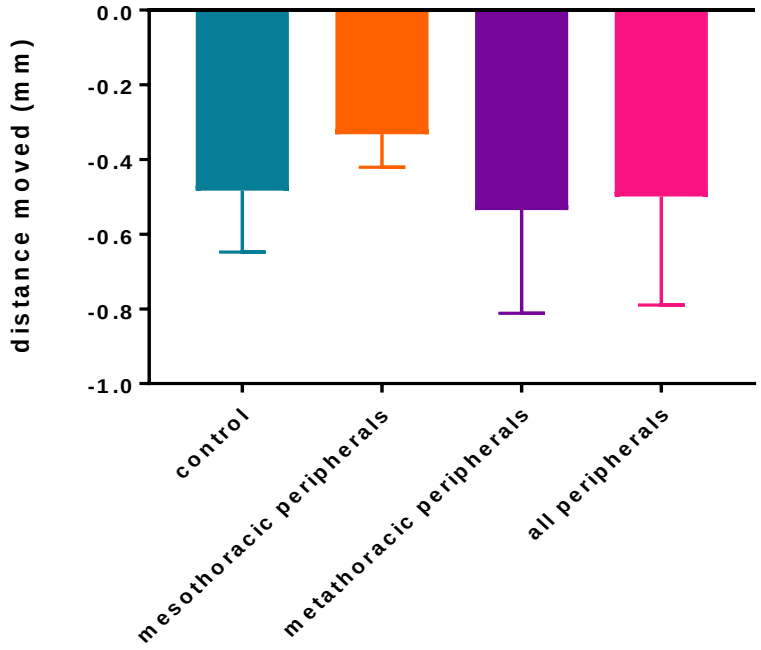

B

control	-0.4831	0.16440
mesothoracic peripherals	-0.3323	0.08845
metathoracic peripherals	-0.5354	0.27590
all peripherals	-0.4992	0.29010

Figure 3-8: Cutting the peripheral nerves connected to either the mesothoracic ganglion, metathoracic ganglion or both has no effect on the movement of the metathoracic ganglion after cutting the connectives between it and the mesothoracic ganglion. A: The movement (mean ± SD) of the metathoracic ganglion measured from a stable starting point. Male and female data was merged as there were no differences between them (data not shown, one-way ANOVA with Tukey's post hoc tests). No significant differences were found (one-way ANOVA and Tukey's post hoc tests). **B:** mean ± SD of the movements of the metathoracic ganglion in the posterior direction after connectives between the meso- and metathoracic ganglia are severed.

A

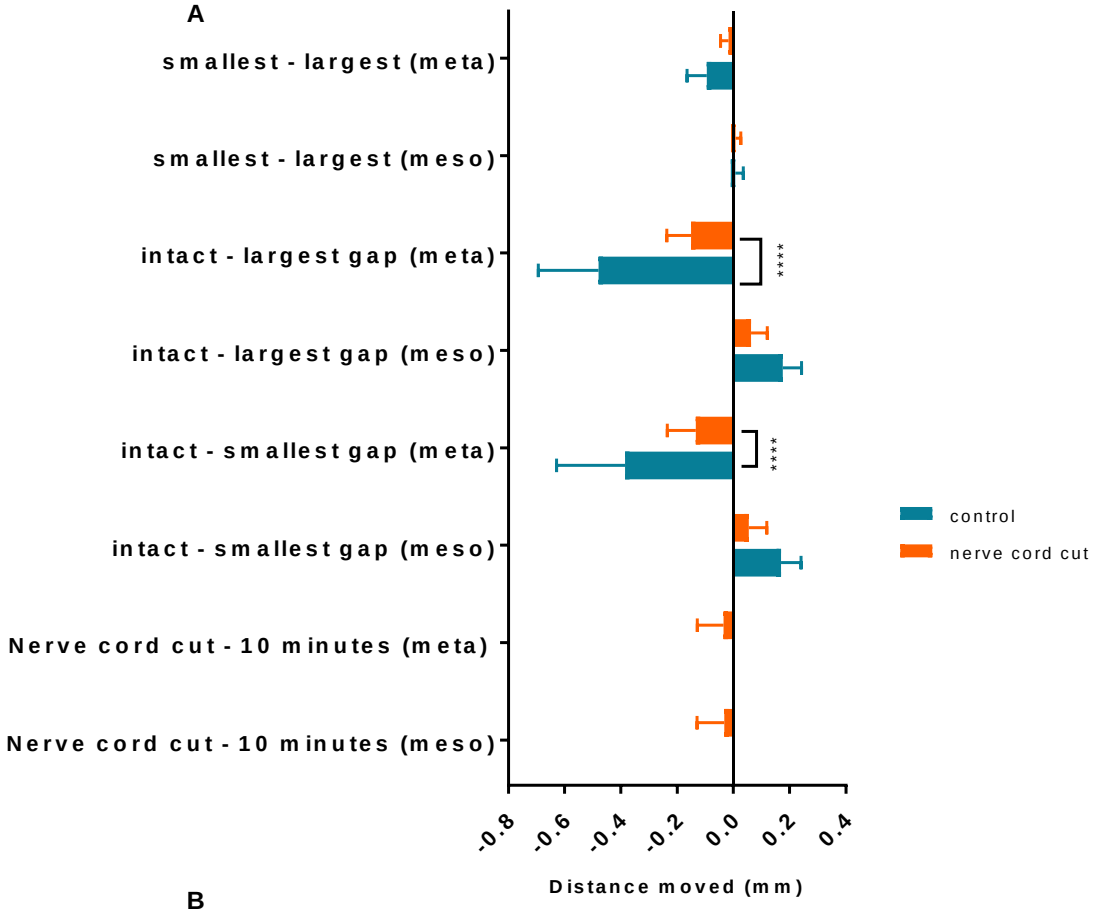

B

	control		nerve cord cut	
	Mean	SD	Mean	SD
Nerve cord cut - 10 minutes (meso)			0.032	0.097
Nerve cord cut - 10 minutes (meta)			0.035	0.094
intact - smallest gap (meso)	0.169	0.072	0.055	0.064
intact - smallest gap (meta)	0.385	0.244	0.133	0.101
intact - largest gap (meso)	0.176	0.066	0.062	0.058
intact - largest gap (meta)	0.480	0.214	0.151	0.086
smallest - largest (meso)	0.007	0.029	0.008	0.018
smallest - largest (meta)	0.095	0.070	0.017	0.028

Figure 3-9: Cutting the ventral nerve cord between the pro- and mesothoracic and the metathoracic and fourth abdominal ganglia reduces the movement of the metathoracic ganglion in the posterior direction (males) when the connectives between it and the mesothoracic ganglion are severed. A: Cutting the nerve cord posterior to the metathoracic ganglion and anterior to the mesothoracic ganglion causes a decrease in the movement of the metathoracic ganglion when the connectives between it and the mesothoracic ganglion are cut in males (two-way RM ANOVA with Sidak's post hoc test, ****$p<0.0001$, data shown is mean ± SD, negative shows movement to the posterior and positive to the anterior) Movement was measured between the VNC being cut and the 10 minute rest, 'intact – smallest gap' and 'intact – the largest gap' are measured before the connectives between the meso- and metathoracic ganglia are cut to the smallest/largest separation between the two and then 'smallest-largest' is the movement between these states. **B:** absolute mean ± SD of movements (mm).

A

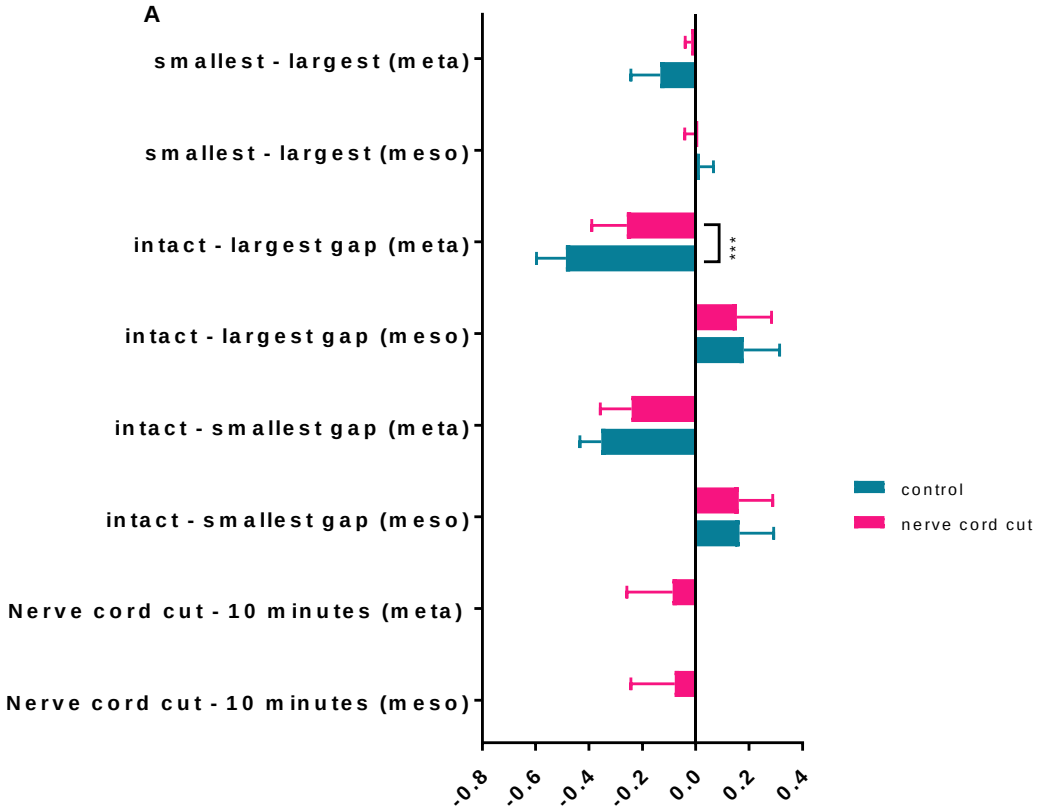

B

	control		nerve cord cut	
	Mean	SD	Mean	SD
Nerve cord cut - 10 minutes (meso)			0.079	0.164
Nerve cord cut - 10 minutes (meta)			0.087	0.172
intact - smallest gap (meso)	0.164	0.128	0.162	0.127
intact - smallest gap (meta)	0.354	0.081	0.241	0.117
intact - largest gap (meso)	0.180	0.134	0.155	0.129
intact - largest gap (meta)	0.486	0.111	0.258	0.132
smallest - largest (meso)	0.016	0.050	0.007	0.034
smallest - largest (meta)	0.133	0.111	0.017	0.022

Figure 3-10: Cutting the ventral nerve cord between the pro- and mesothoracic and the metathoracic and fourth abdominal ganglia reduces the movement of the metathoracic ganglion in the posterior direction (females) when the connectives between it and the mesothoracic ganglion are severed. A: Cutting the nerve cord posterior to the metathoracic ganglion and anterior to the mesothoracic ganglion causes a decrease in the movement of the metathoracic ganglion when the connectives between it and the mesothoracic ganglion are cut in females (two-way RM ANOVA with Sidak's post hoc test, *** $p<0.001$, data shown is mean ± SD, negative shows movement to the posterior and positive to the anterior) Movement was measured between the VNC being cut and the 10 minute rest, 'intact – smallest gap' and 'intact – the largest gap' are measured before the connectives between the meso- and metathoracic ganglia are cut to the smallest/largest separation between the two and then 'smallest-largest' is the movement between these states. **B:** absolute mean ± SD of the movement of ganglia (mm).

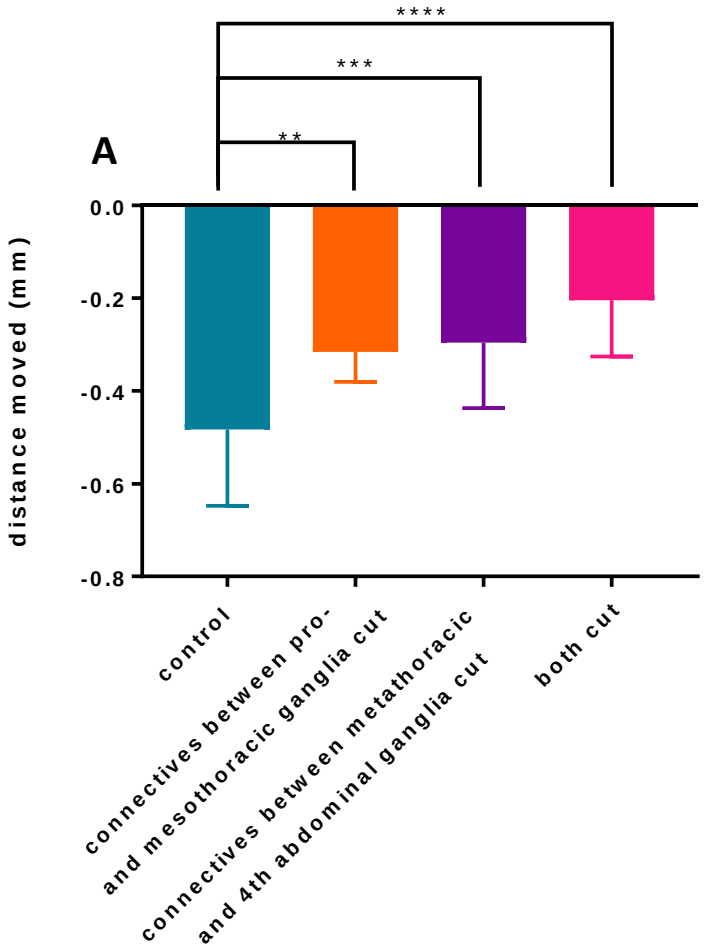

B

	movement (mm)	
	mean	SD
control	-0.4831	0.1644
connectives between pro- and mesothoracic ganglia cut	-0.3159	0.0647
connectives between metathoracic and 4th abdominal ganglia cut	-0.2954	0.1414
both cut	-0.2044	0.1211

Figure 3-11: Cutting the nerve cord anterior to the mesothoracic ganglion, posterior to the metathoracic ganglion or both decreases the distance moved by the metathoracic ganglion after the connectives between it and the mesothoracic ganglion are cut. A: Males and females were combined as there were no differences between the two (data not shown, ANOVA with Tukey's post hoc showed no significant differences). Cutting either of the regions of the nerve cord or both caused a decrease in the movement of the metathoracic ganglion (one-way ANOVA and Tukey's post hoc test, **p=0.0027, ***p=0.006 and ****p<0.0001, data shown is mean ± SD and negative shows a posterior direction moved). **B:** mean ± SD of the movement of the metathoracic ganglion after the connectives between the meso- and metathoracic ganglion are severed (mm).

3.4.3 Other tissues do not contribute to the separation of the meso- and metathoracic ganglia after the connectives between them are severed

To investigate the roles of tissues other than the VNC, we repeated our connective cutting experiments with starved adult locusts, and with adult females that had been separated from males during the fifth instar to ensure no mating or egg laying occurred. No eggs were found ruling out parthenogenesis, which can occur in *S. gregaria* (Hamilton, 1953). We measured the distance between the meso- and metathoracic ganglia when intact, and then again after both connectives had been cut, calculating the percentage increase for each locust.

Starved locusts showed no significant change in the separation when compared to sex-matched locusts with *ad libitum* access to food (two-tailed T-tests were carried out in males control vs starved ($t=0.7406$, $df=14$, $p= 0.4712$) and females control vs starved ($t=0.4034$, $df=14$, $p=0.6927$), Figure 3-12, controls for this experiment are taken from data obtained in Figure 3-1). Virgin females were also not significantly different when compared to age matched females with access to mating and egg laying sites (two-tailed T-test, $t=0.04148$, $df=18$, $p=0.9674$; Figure 3-13), we compared both of these sets to our previously obtained results (Figure 3-1) and found no significant differences between those either (data not shown, one-way ANOVA, $F(2,25)=0.001468$, $p=0.9985$).

A

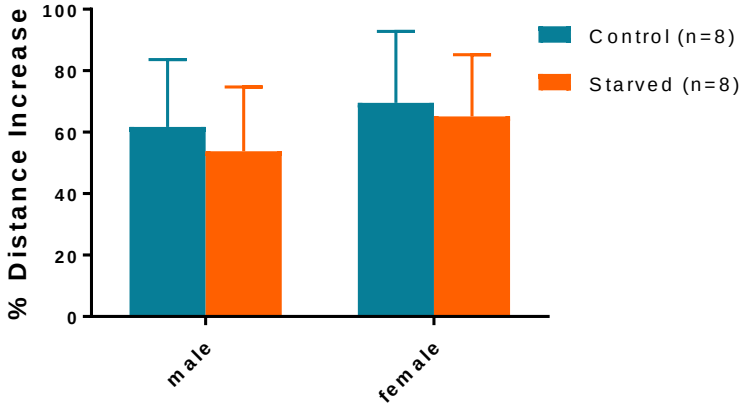

B

	male		female	
	Mean	SD	Mean	SD
Control (distance before cutting (mm))	0.97	0.09	1.01	0.04
Starved (distance before cutting (mm))	1.51	0.24	1.65	0.21
Control (distance after cutting (mm))	1.62	0.23	1.70	0.22
Starved (distance after cutting (mm))	0.92	0.09	0.99	0.07
Control (percentage increase)	61.74	21.86	69.53	23.26
Starved (percentage increase)	53.83	20.86	65.15	20.05

Figure 3-12: Starvation does not affect the separation of the mesothoracic and metathoracic ganglia when the connectives between the two are cut. A: Neither males nor females show any changes in the tension held in the connectives between the mesothoracic and metathoracic ganglia (mean ± SD, two-tailed T-tests n.s). **B:** mean ± SD of the separation between the meso- and the metathoracic ganglia before connectives are cut (mm), after connectives are cut (mm) and the change as percentage increase.

A

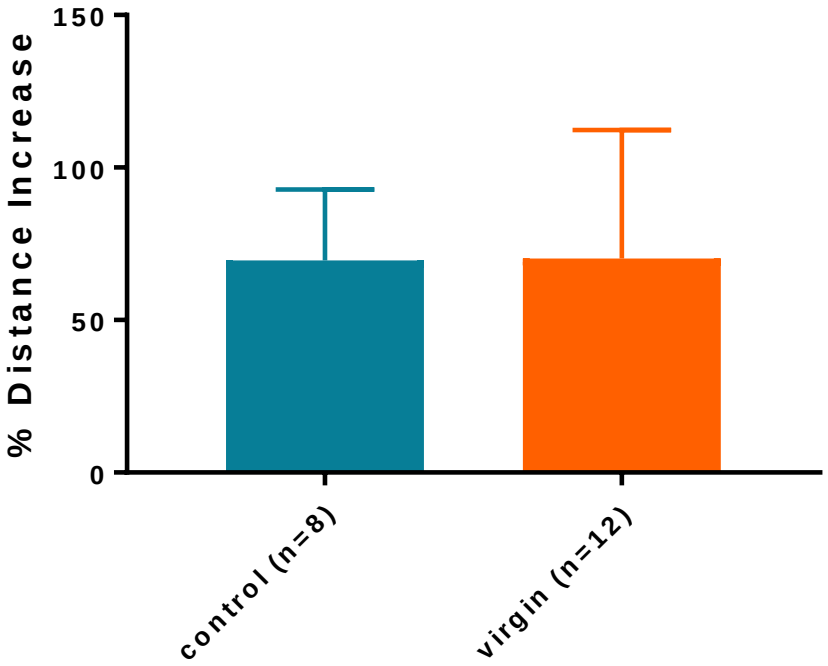

B

	Mean	Std. Deviation
control (distance before cutting (mm))	1.011	0.0407
virgin (distance before cutting (mm))	1.012	0.07926
control (distance after cutting (mm))	1.7	0.2236
virgin (distance after cutting (mm))	1.705	0.4241
control (% increase)	69.53	23.26
virgin (% increase)	70.21	42.08

Figure 3-13: Access to mating and egg laying sites does not affect the separation of the meso- and metathoracic ganglia when the connectives between the two are cut. A: Females separated from males and egg laying sites at 5th instar and age matched controls with access to these show no difference in the tension held in the connectives between the meso- and metathoracic ganglia (data is mean ± SD, two-tailed T-test n.s). **B:** mean ± SD of the separation between the meso- and metathoracic ganglia before connectives are cut (mm), after connectives are cut (mm) and the difference represented as a percentage increase.

3.4.4 Other axon bundles in *Schistocerca gregaria* are under less tension *in vivo* than the connectives between the meso- and metathoracic ganglia

To assess the differences between axon bundles, we cut either nerve 5 or the connectives between the metathoracic and fourth abdominal ganglia, and measured the gap formed between the severed ends. We compared this to the connectives between the meso- and metathoracic ganglia (Figure 3-2). The separation between the connectives between the meso- and metathoracic ganglia was significantly larger when severed than either of the two other bundles (one-way ANOVA, $F(2,37)=22.21$, $p<0.0001$, post-hoc Tukey's HSD showed the gap formed in the connectives between the meso- and metathoracic ganglia was significantly larger than nerve 5 $p<0.0001$, and meta-a4 $p=0.0003$; Figure 3-14).

A

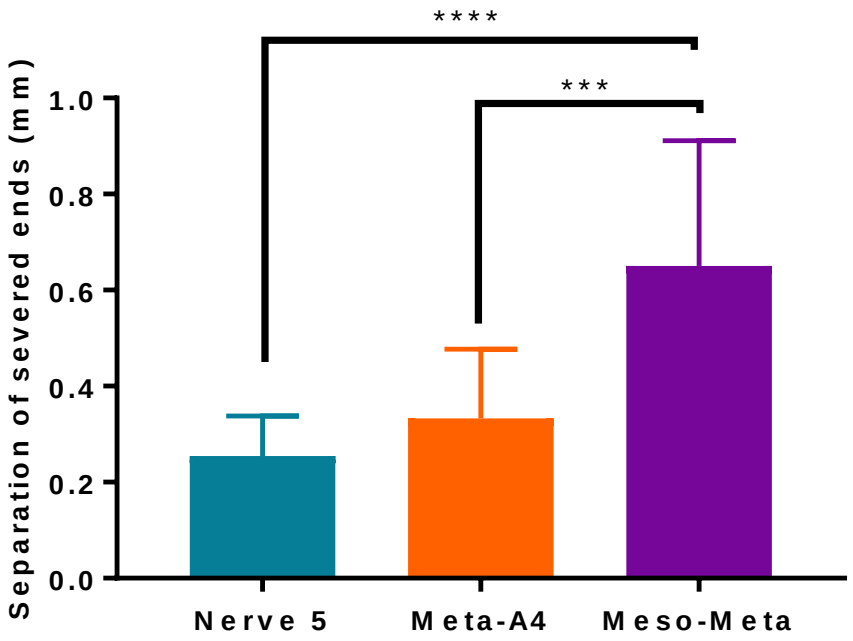

B

	Nerve 5	Meta-A4	Meso-Meta
Mean	0.2548	0.333	0.65
Std. Deviation	0.08285	0.1444	0.2616

Figure 3-14: Separation of severed ends of axon bundles in adult male locusts. A: The gap between the severed ends of nerve bundles were measured 1 minute after cutting. Data shown is mean ± SD. For the connectives between the metathoracic and fourth abdominal ganglia (Meta-A4) and the connectives between the meso- and metathoracic ganglia (Meso-Meta) both connectives provided one data point, whereas each individual provided two data points for nerve 5. The gap between the meso-meta severed ends was significantly larger than both other connectives which were not significantly different from each other (one-way ANOVA and Tukey's post hoc tests, **** $p<0.0001$, *** $p=0.0003$). **B:** mean ± SD of the separation between severed ends of axon bundles in the desert locust (mm).

3.5 Discussion

To our knowledge tension in entire axon bundles has not been reported or investigated in adult invertebrates before, so our finding of tension in the connectives between the meso- and metathoracic ganglia is the first such example. However, the tension of individual axons has been studied in developing insects and is found to have an important role in embryogenesis in the growth and guidance of neurites (Bray, 1984; Rajagopalan *et al.*, 2010) and synapse formation (Siechen *et al.*, 2009). There is evidence that tension in other invertebrate tissues during embryogenesis has a role in morphology, such as forming compartment boundaries (Aliee *et al.*, 2012) or dorsal closure in *Drosophila* (Jacinto, Woolner, *et al.*, 2002). In the desert locust, tension of individual axons has been shown to drive their geometric morphology (Condron and Zinn, 1997). Based on these findings and the hypothesis of axonal tension driving nervous system morphology (Van Essen, 1997), we hypothesised that adult invertebrates would possess axon bundles under tension.

Severing the connectives between the meso- and metathoracic ganglia demonstrates that tension is present in these axon bundles. This is evident from the separation between the severed ends of the connectives, which is only partially explained by the retraction of the damaged axons. We sought to isolate the tissues that contributed to the posterior pull. Severing the peripheral nerves connected to either the meso- or metathoracic ganglia had no effect on the separation after cutting the connectives between the two, nor did first severing the connectives between the pro- and mesothoracic ganglia. However, severing the connectives between the metathoracic and fourth abdominal ganglia before cutting the connectives between the

meso- and metathoracic ganglia led to a reduction in the gap formed. Thus, some of the tension can be attributed to the VNC posterior to the metathoracic ganglion.

We also studied other possible sources that may have contributed to the tension. We found that starvation did not reduce the gap seen and there was no difference between virgin females and those with access to mating and egg laying. We also investigated nerve 5 and the connectives between the metathoracic and fourth abdominal ganglia and found that no separation occurred between the severed ends. Therefore, tension in adult axon bundles in the desert locust varies across axon bundles.

3.5.1 Tissues contributing to tension in the connectives between the meso- and metathoracic ganglia

Tension is present in the connectives between the meso- and metathoracic ganglia and is largely mediated by a posterior pull on the metathoracic ganglion by the VNC. However, the nerve cord cannot be the only structure involved in this tension because first severing the connectives between the metathoracic and fourth abdominal ganglia did not completely eliminate the separation of the meso- and metathoracic ganglia when the connectives between them were cut.

Here we must consider the reproductive, respiratory, circulatory and digestive systems, which are all present in the thorax and abdomen near the VNC. These systems are dynamic and cause some level of mechanical motion (Uvarov, 1966). We determined that neither food intake nor access to mating and egg laying altered the extent of separation or motions of the metathoracic ganglion seen after separation from the mesothoracic ganglion. Although we cannot definitively show that the females in the egg laying group had all laid eggs. However, the females in the control group had a

smaller range of responses than the virgins, indicating that egg laying did not significantly alter the tension.

However, our negative findings do not exclude the possibility that these other organ systems are involved; the nerve cord is not protected from the effects of the rest of the body any organ or system that creates small movements within the locust body likely causing slight stresses and tension to the nerve cord. In the lamprey, for example, the motions caused by swimming increase the prestress exhibited in the spinal cord from 10-15% (Luna *et al.*, 2013). It is therefore possible that movements, such as ventilatory movements (Hamilton, 1964; Hustert, 1975; Burrows, 1996), peristalsis (Uvarov, 1966) or the abdominal movements associated with egg laying (Snodgrass, 1933) will cause stress upon the locust VNC.

3.5.2 Tension is not sexually dimorphic

Throughout our experiments we separated males from females and only combined data if there were no significant differences. We did this because we suspected that there may be sexual dimorphism due to the different roles the sexes undertake in adulthood. During mating the males extend their abdomen in order to reach the females (Uvarov, 1966; Burrows, 1996). However, during egg laying the females extend their abdomen from around 30 mm to 130 mm and can retract a fully extended abdomen almost instantaneously (Vosseler, 1905; Uvarov, 1966; Burrows, 1996). Egg laying behaviour is usually prevented by descending inhibition, and can be released by severing the nerve cord below T3 such as the connectives between the metathoracic and fourth abdominal ganglia (Thompson, 1986). It is possible that the exaggerated pulsations of the

metathoracic ganglion seen in females when the connectives between the meso- and metathoracic ganglia were severed was caused by partial loss of descending inhibition and the initiation of some abdominal movements associated with egg laying.

How this extension occurs with regards to both the cuticle and musculature of the abdomen is understood (Vincent and Wood, 1972; Jorgensen and Rice, 1983; Hackman and Goldberg, 1987), but the behaviour of the nerve cord during this process is unknown. However, it seems likely that the female nerve cord must be able to withstand sudden changes in forces exerted upon it. We expected to see this reflected in gross differences between the sexes in the tension exhibited, however only subtle differences were observed.

3.5.3 Tension may be linked to ventral nerve cord morphology

We hypothesised that the connectives between the meso- and metathoracic ganglia would be under tension due to a posterior pull on the metathoracic ganglion, due to a pulling force from the peripheral structures innervated by the metathoracic ganglion. This was because the metathoracic ganglion is an example of a fused ganglion, in which several neuromeres fuse together with the connectives between them becoming enmeshed with the neuropil of the ganglion (Niven *et al.*, 2008). Fused ganglia are common in insects, but also highly variable. Often, but not always, fusions occur in the anterior direction. The fruit fly (*Drosophila melanogaster*) is an extreme example of this, with all neuromeres fused anteriorly and no visible connectives (Niven *et al.*, 2008). With anterior fusions, peripheral structures innervated by the ganglion are posterior to the ganglion. In the case of *S. gregaria* this includes the hindlimbs, which are connected to

the metathoracic ganglion by several nerves including the very large nerve 5 (Burrows, 1996).

The lack of contribution to tension by the peripheral nerves may be explained by the development of the nervous system; the VNC develops from neuromeres that are first separate and then fuse to produce the metathoracic ganglion. This takes place prior to the innervation of peripheral structures. Furthermore, the peripheral nerves develop and migrate from 'the outside in': they start from the peripheral structure and grow and move into the VNC (Bate, 1976; Kutsch, 1989; Burrows, 1996). Thus, the peripheral nerves grow to the already fused ganglia during embryogenesis, meaning there is little to suggest developmentally that they would then pull on the ganglion.

3.5.4 Comparison with tension in vertebrate axons

Tension has been found in vertebrate axonal tracts (Xu et al., 2009, 2010; Luna et al., 2013). In this study we found that the same amount of tension did not appear to be present in every axon bundle, with the connectives between the meso- and metathoracic ganglia producing a far larger separation than either of the other bundles considered. This is the case in mammalian brains as well, with only certain tracts in certain planes showing evidence of tension (Xu *et al.*, 2009, 2010). As such it appears that tension is not merely a universal property of all axons. Instead, it may be caused by the surrounding tissue or something that is actively regulated and developed. Currently, there is no specified function of tension in axons, although it is possible that it protects against neurofilament tangling (Ikenaka *et al.*, 2012) or may ensure efficient arrangement of axon components such as sodium channels (Zhang *et al.*, 2017).

If axons under tension do have a functional benefit it would suggest there is also a risk otherwise all axons would share this property. Tension in axons may make them more vulnerable to irreparable damage and more difficult to repair due to the large separation of damaged ends (Luna *et al.*, 2013), similar to tearing muscle tissue (Eccles, 1943; Hersche and Gerber, 1998; Davidson *et al.*, 2000). So far axonal tension has only been found in vertebrate central nervous systems, which are protected from external forces by bone. Our results show that the connectives under tension (the meso- to metathoracic connectives) are also those exposed to the least external force because the connectives between the metathoracic and fourth abdominal ganglia sit in the soft and motile abdomen and the peripheral nerve 5 is exposed to the motion of the hindlimb (Burrows, 1996).

3.5.5 Tension in adult axonal bundles contradicts current theories of stretch-growth

The existence of axonal tension in adults seems to contradict the theory of stretch growth. Stretch-growth is the growth of integrated axons caused by the pulling of surrounding growing tissues (Pfister, 2004). Currently the mechanisms of stretch-growth are unknown, although there are two alternative hypotheses (Heidemann and Bray, 2015; Purohit and Smith, 2016). Despite this, researchers take advantage of its existence to produce cultures of long axons (Pfister, Iwata, *et al.*, 2006; Xu *et al.*, 2014; Li *et al.*, 2016). Currently the hypotheses for stretch-growth describe a passive phenomenon, with axons growing in response to external stresses. However, this does not fit with our finding of tension in the connectives between the meso- and metathoracic ganglia, nor

the findings of others (Xu *et al.*, 2009, 2010; Luna *et al.*, 2013), that axonal tension persists into adulthood.

It is possible in these studies that the axons are actively contracting (Bray, 1979), therefore stretch-growth would not occur. However, we have found the tension in the connectives between the meso- and metathoracic ganglia is partially caused by a posterior pull mediated by the nerve cord. This is an external stretch, yet the axons in the connectives between the meso- and metathoracic ganglia do not grow in response to it. Neither of the current hypotheses suggest a threshold of force required to initiate growth or regulatory mechanisms, however, it seems likely that one or both of these are necessary to explain the tension observed in the locust axon bundles.

4 Anatomical, physiological and mechanical differences associated with differences in tension among axon bundles in *Schistocerca gregaria*

4.1 Abstract

We seek to find a cellular basis for the differences in tension among axon bundles in *Schistocerca gregaria* observed through microdissection (Chapter 3). We use transmission electron microscopy (TEM) techniques to look at anatomical features of the axon bundle; the thickness of the blood brain barrier, the diameter of the bundles, and the density and size of axons located within. We also counted microtubules orientated longitudinally with respect to individual axons to determine the cellular basis of macroscopic bundle properties. Although most anatomical features do not reflect the tension within the axon bundle revealed through microdissection, those connectives under high tension contained more microtubules per axon than bundles with low tension. Moreover, the relationship between microtubule number and axon size is significantly steeper in bundles under tension. These results show that microtubules oriented longitudinally reflect the tension an axon bundle is subjected to *in vivo*. Uniaxial loading using a 10 g force sensor coupled to micromanipulator to stretch the axon bundles allowed us to determine the force required to break the axon bundles as well as their viscoelastic properties. Those axon bundles under tension were less elastic than

those under low tension, and also resisted stretch with a higher force. Our results suggest that tension in bundles is produced by their intracellular composition, specifically microtubules in the longitudinal orientation, which may also cause stiffer and stronger bundles. Together these results suggest that tension is actively maintained within axon bundles.

4.2 Introduction

Tension is not the same in all axon bundles but is instead highly variable, with even axon bundles in the same region of the desert locust (those connecting to the metathoracic ganglion) having different properties (Chapter 3). To find a cellular basis for this variability in tension and to measure the mechanical properties (stiffness, strength and elasticity) directly, we use transmission electron microscopy (TEM) and uniaxial loading *ex vivo*, respectively.

The main molecular structures that generate, oppose and respond to tension in cells are the elements of the cytoskeleton (Alberts *et al.*, 2015; see General Introduction). Actin can rapidly polymerise or depolymerise to produce forces (Wegner, 1982; Neuhaus *et al.*, 1983; Wang, 1985), as well as interact with myosin to produce active contractions (Huxley, 1969; Evans *et al.*, 1998). Likewise, microtubules can polymerise and depolymerise to produce forces (Goldberg, 1992; Inoue and Salmon, 1995; Kulic *et al.*, 2008), and intermediate filaments have dynamic properties (Goldman and Follett, 1970; Yoon *et al.*, 1998, 2001; Windoffer and Leube, 1999). Intermediate filaments also provide the scaffold for crosstalk between the membrane and other elements of the cytoskeleton (Chang and Goldman, 2004; Koster *et al.*, 2015).

Axons are known to maintain tension both longitudinally (Dennerll *et al.*, 1988; Lamoureux *et al.*, 1989) and circumferentially (Fan *et al.*, 2017). When considering entire axonal bundles, however, there are many other, non-neural components including glia, the blood-brain barrier and extracellular material (Rowell and Dorey, 1967). Moreover, the axon bundles may also differ in diameter. These factors can contribute to the tension present in the entire axon bundle and, as such, have been addressed in this chapter.

We have focussed on microtubules, which are known to contribute to force generation, responses in growth cone growth and guidance (Sabry *et al.*, 1991; Rauch *et al.*, 2013), and axonal injury (Johnson *et al.*, 2013; Lazarus *et al.*, 2015). Theories of stretch growth have also included roles for microtubules (Heidemann and Bray, 2015). Furthermore, microtubules increase in number with axon calibre (Fadic *et al.*, 1985; Saitua and Alvarez, 1988), allowing for comparisons of this relationship between bundles. Within axons microtubules are arranged longitudinally (reviewed in Conde and Cáceres, 2009), so they align with the longitudinal orientation of the tension we have previously observed. Finally, microtubules are clearly visible via TEM imaging, allowing them to be measured along with other elements from the same images. This makes microtubules an ideal candidate to begin looking for any intracellular basis of whole axon bundle tension.

Axon and axon bundle properties have been investigated previously using shear stress tests (Cohen *et al.*, 2008), strain-stiffening tests (Koser *et al.*, 2015), and uniaxial loading tests (Luna *et al.*, 2013). To our knowledge, this has never been paired with measures of the intracellular composition of axon bundles. It is unnecessary for the tension experienced *in vivo* to be reflected in other mechanical properties because these

can exist distinctly. In biological materials, however, we may expect tissues to have evolved properties to withstand or compensate for the forces they experience. We also expect that the connectives between the meso- and metathoracic ganglia, which are under tension, will experience a greater strain-stiffening response than bundles under low tension. Our previous findings did not account for all of the tension in this region (see Chapter 3); the separation between the meso- and metathoracic ganglia was reduced by first severing the connectives between the metathoracic and fourth abdominal ganglia, but did not completely eliminate the separation. This suggests that some of the tension is generated elsewhere, such as the axons themselves via contraction (Tofangchi *et al.*, 2016). This would indicate a presence of cytoskeletal components such as actin, microtubules and intermediate filaments which are known to have strain-stiffening responses (Janmey *et al.*, 1991; Jonas and Duschl, 2010; Kraning-rush *et al.*, 2011).

Here, using TEM, we show that the number of microtubules orientated longitudinally in axon bundles relates closely to tension revealed by microdissections. This suggests that microtubules in individual axons influence the macroscopic properties of axon bundles. Using uniaxial loading, we find that these properties are also reflected in the strength and elasticity of bundles which suggests that mechanical properties are influenced by forces experienced *in vivo*.

4.3 Methods

Methods for this chapter are found in the Methods 2.2.9, 2.2.10.

4.4 Results

4.4.1 Anatomical features of axon bundles do not reflect microdissection results

We took images at a variety of magnifications to allow for comparisons between gross structural attributes (Figure 4-1). We found the diameters of the axon bundles differ (one-way ANOVA, $F(2,20)=29.87$, $p<0.0001$ followed by Tukey's post hoc tests; Figure 4-2). The connectives between the meso- and metathoracic ganglia (Meso-Meta) were larger in diameter than the connectives between the metathoracic and fourth abdominal ganglia (Meta-A4; $p<0.0001$) and Nerve 5 ($p=0.0043$). Nerve 5 also had a statistically significantly larger diameter than connectives between Meta-A4 ($p=0.0028$). There were no significant differences in the thickness of the blood brain barrier around any of the connectives (one-way ANOVA, $F(2,19)=0.7265$, $p=0.4966$, Figure 4-3) or in the density of axons within the bundle (one-way ANOVA, $F(2,40)=2.36$, $p=0.1074$; Figure 4-4). The axons in the connectives between the meso- and metathoracic ganglia had significantly larger transverse areas than those in nerve 5 (Kruskal Wallis, $H=7.232$, $p=0.0269$, Dunn's multiple comparison $p=0.0359$; Figure 4-5; Table 3). The axons in the connectives between the metathoracic and fourth abdominal ganglia were not significantly different in area from either nerve 5 ($p>0.999$) or the connectives between the meso- and metathoracic ganglia ($p=0.2101$). These results do not explain the tension observed by microdissections.

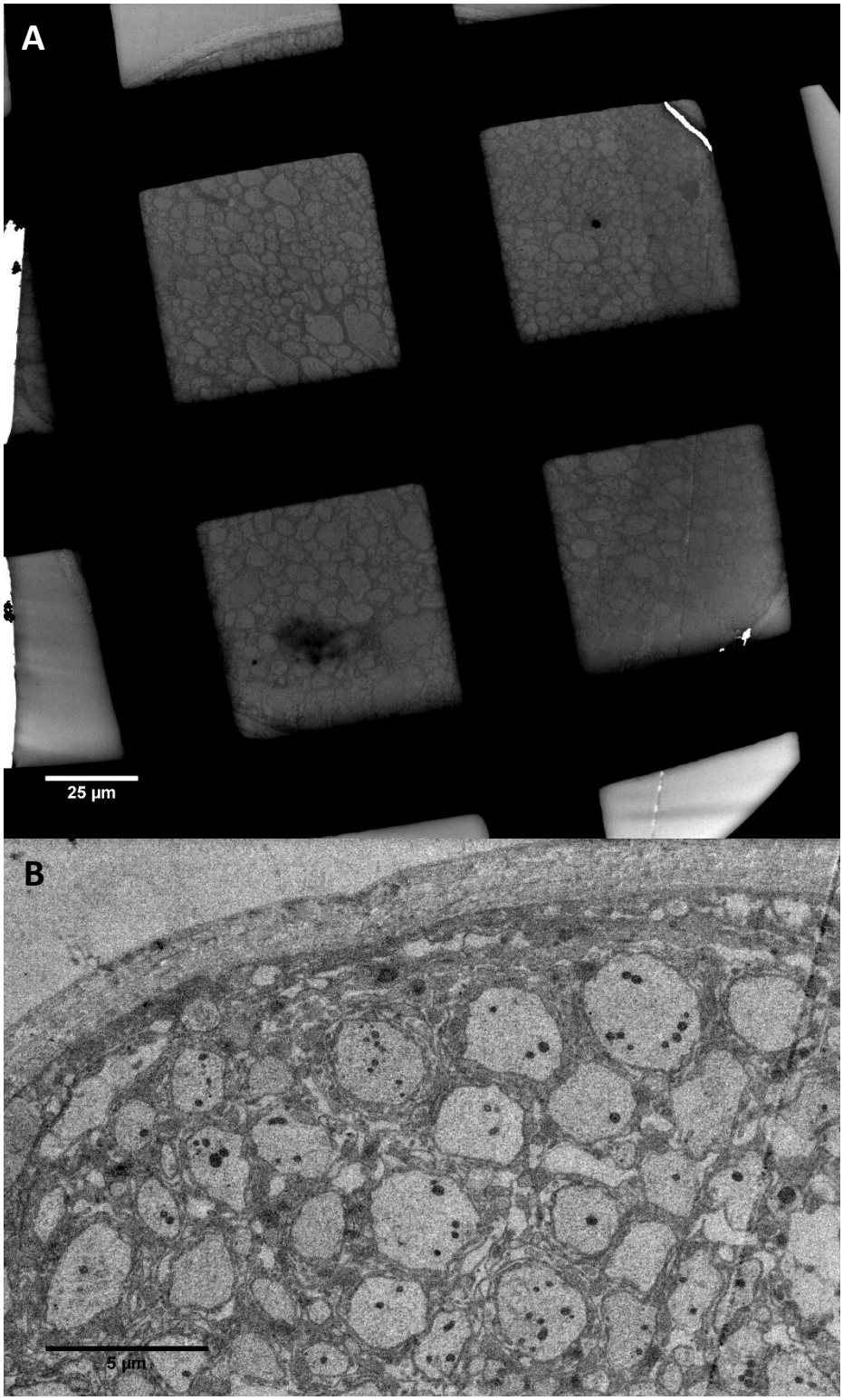

Figure 4-1: Example TEM images of a connective between the mesothoracic and metathoracic ganglia of the desert locust. Low magnification images (A) allow for measurement of the size of the connectives while higher magnification images allow for measurement of the BBB and counting and measuring of axons (B). Contrast in A has been increased using imagej for the purpose of printing, while image B is from a sample stained using uranyl acetate and lead citrate for the same reason.

A

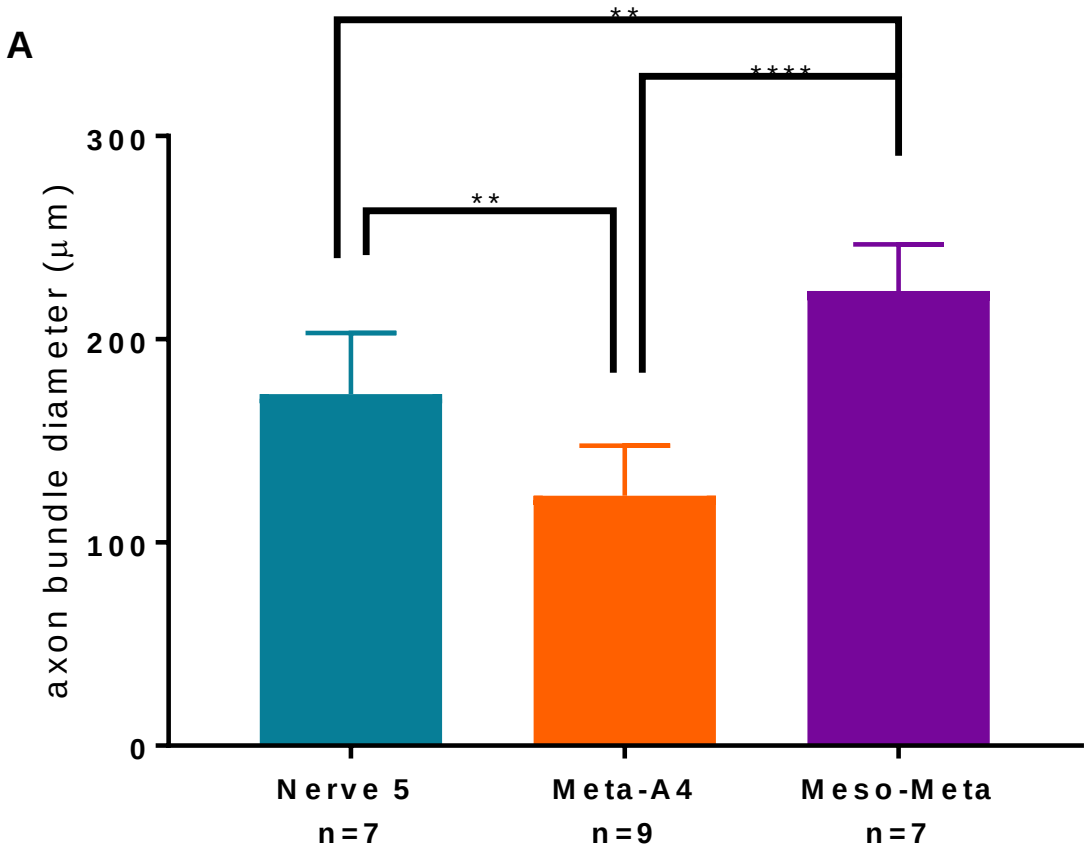

B

	Nerve 5 n=7	Meta-A4 n=9	Meso-Meta n=7
Mean	173.1	123	223.8
Std. Deviation	29.97	24.77	22.96

Figure 4-2: Diameter of axon bundles of the desert locust. A: The axon bundles (nerve 5, the connectives between the metathoracic and fourth abdominal ganglia (Meta-A4) and the connectives between the meso- and metathoracic ganglia (Meso-Meta)) significantly differed in diameter (one-way ANOVA ****$p<0.0001$, **$p<0.01$). Data shown is mean ± SD. **B:** mean ± SD of the diameter of the different axon bundles in the desert locust (µm).

A

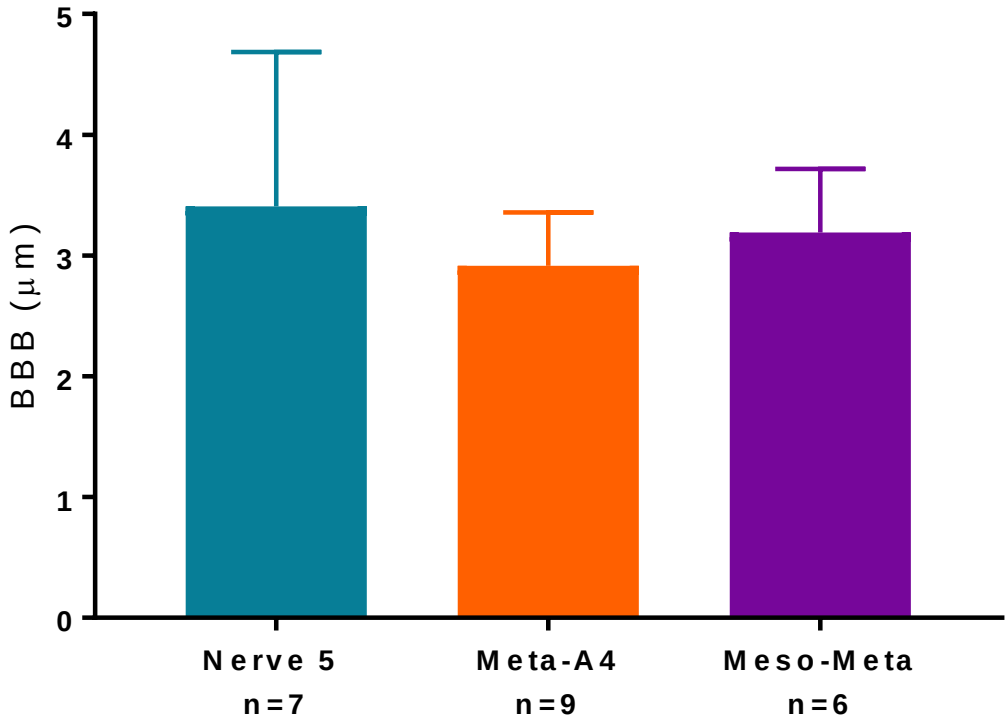

B

	Nerve 5 n=7	Meta-A4 n=9	Meso-Meta n=6
Mean	3.408	2.914	3.19
Std. Deviation	1.279	0.4434	0.5283

Figure 4-3: There is no difference in the thickness of the blood brain barrier (BBB) between axon bundles in the desert locust. A: The thickness of the BBB was measured in each bundle (nerve 5, the connectives between the metathoracic and fourth abdominal ganglia (Meta-A4) and the connectives between the meso- and metathoracic ganglia (Meso-Meta)), no significant differences were found between the bundles studied (one-way ANOVA, n.s) data is mean ± SD. **B:** mean ± SD of BBB diameter in the three axon bundles studied in the desert locust (µm).

A

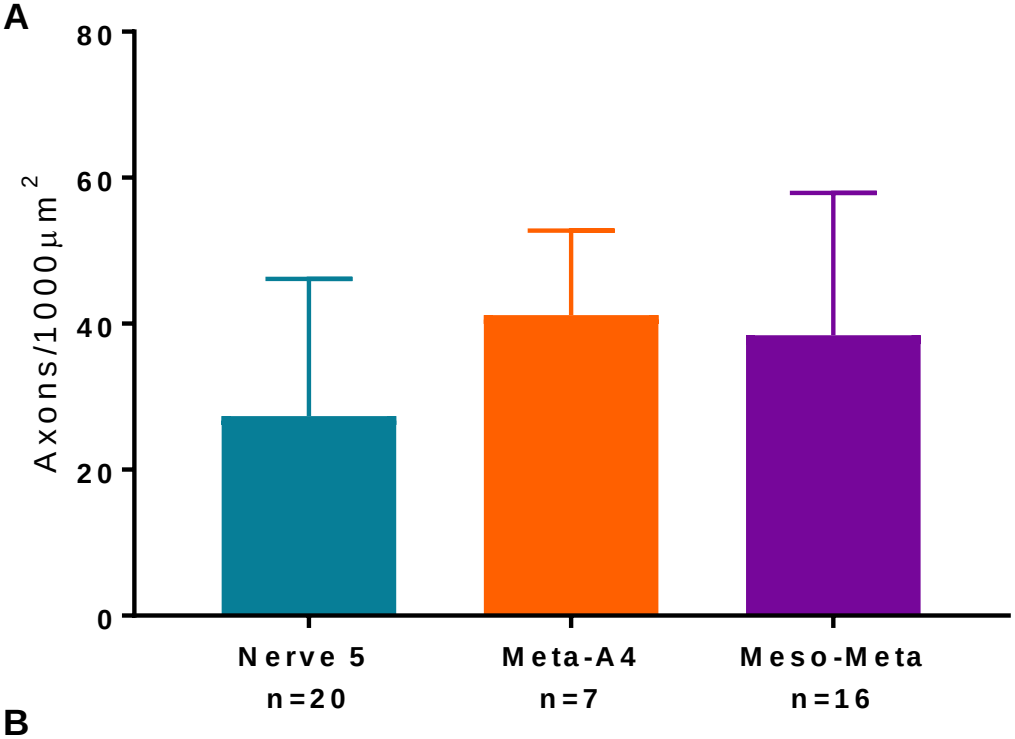

B

	Nerve 5 n=20	Meta-A4 n=7	Meso-Meta n=16
Mean	27.33	41.17	38.44
Std. Deviation	18.84	11.61	19.47

Figure 4-4: There is no difference in axon density between axon bundles in the desert locust. **A:** The number of axons were counted per grid square containing axons, only the axons that were not touching the mesh grid were counted. These counts were then normalised to axons/mm^2. No differences were found between the three bundle (nerve 5, the connectives between the metathoracic and fourth abdominal ganglia (Meta-A4) and the connectives between the meso- and metathoracic ganglia (Meso-Meta); one-way ANOVA, n.s) data is mean ± SD. **B:** mean ± SD of axon density in axon bundles in the desert locust (axons per 1000 µm^2).

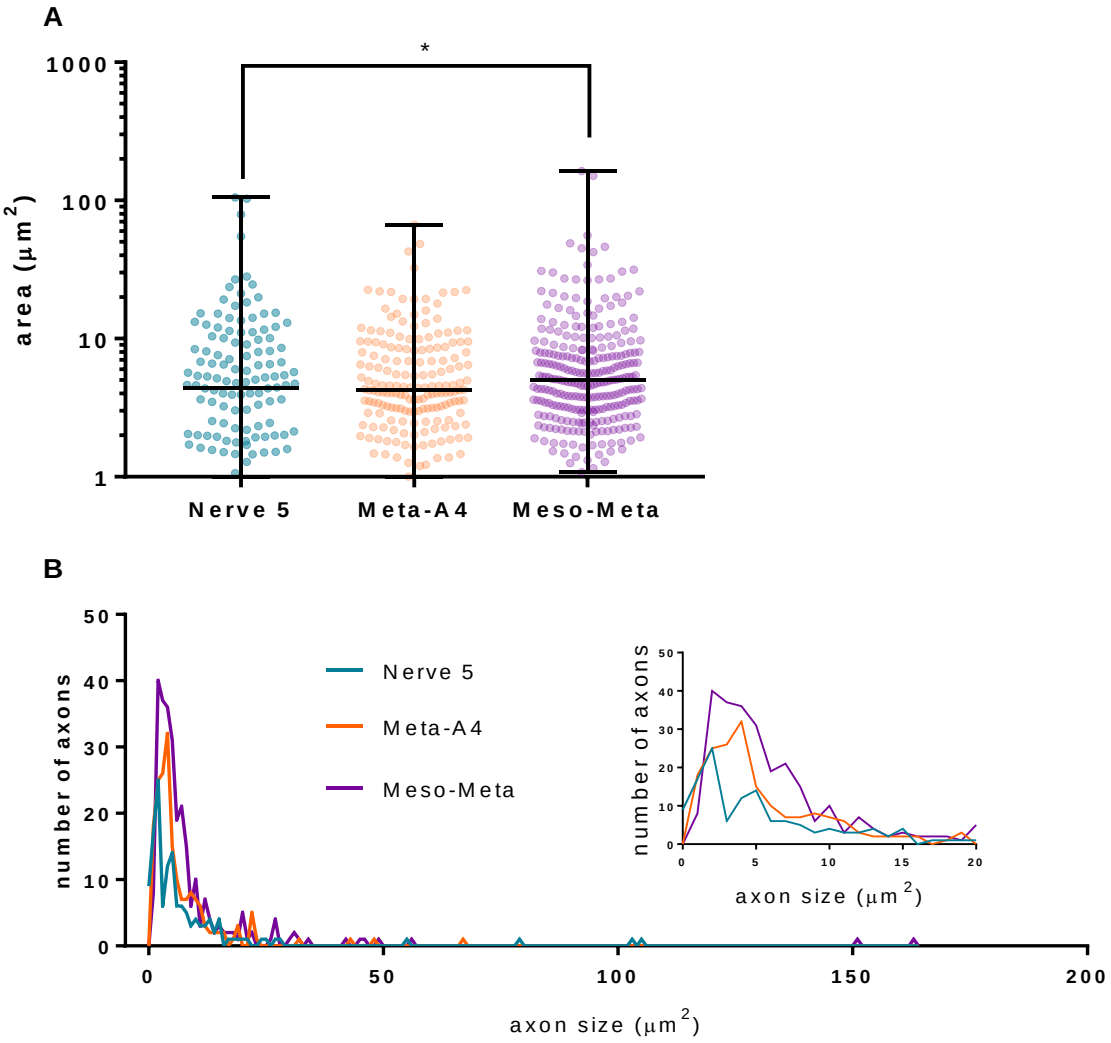

Figure 4-5: Axons in the connectives between the meso- and metathoracic ganglia are larger than those in nerve 5. **A:** Axons were measured in each connective, axons in the connectives between the meso- and metathoracic ganglia were larger than those in nerve five while the axons in the connectives between the metathoracic and fourth abdominal ganglia were not different from either other bundle (nerve 5, the connectives between the metathoracic and fourth abdominal ganglia (Meta-A4) and the connectives between the meso- and metathoracic ganglia (Meso-Meta); Kruskal Wallis with Dunn's multiple comparison * $p<0.05$; data shows median and range). **B**: distribution of axon sizes in each bundle in full and those near zero (inset).

Table 3: Axon area in axon bundles in the desert locust has a high positive skew. Data on transverse axonal area from Figure 4-5 shows all axon bundles have a positive skew in the distribution of axon cross-section areas.

	Nerve 5	Meta-A4	Meso-Meta
Mean (μm^2)	8.369	6.848	8.777
SD (μm^2)	15.15	8.028	15.2
cv	181.07%	117.24%	173.21%
skew	4.81	3.944	7.32
n	136	186	274

4.4.2 Microtubules number and density varies in axon bundles

We used montage software (see Methods 2.2.9) to produce images with a high resolution that allowed us to identify the individual microtubules in the entire axon cross-sections (Figure 4-6A). We counted only those microtubules that were in the orientation of the tension observed from microdissections (see Chapter 3). Specifically, these were the microtubules whose cross-section was visible in the slice, appearing as sharp dots or rings. Microtubules in which a 'tail' was present were excluded because this indicates an orientation that is not perpendicular (Figure 4-6B-D).

We counted the microtubules in individual axon cross-sections, then normalised each axon to microtubules per μm^2. There was no significant difference between the density of microtubules in a perpendicular orientation in any of the bundles (Kruskal-Wallis, H=3.276, p=0.1944; Figure 4-7; Table 4). We also calculated the average number of microtubules per axon. The connectives between the meso- and metathoracic ganglia had significantly more microtubules per axon than either of the other two axon bundles (Kruskal Wallis, H=15.59, p=0.0004; Dunn's multiple comparisons, connectives between the meso- and metathoracic ganglia *versus* the connectives between the metathoracic and fourth abdominal ganglia p=0.0121, and against nerve 5 p=0.0011; Figure 4-8).

We investigated the relationship between microtubule number and axon size in each bundle (Figure 4-9). Microtubule number increased as axons increased in diameter (nerve 5 $Y=2.844*X+12.74$, $R^2=0.5728$, $F=179.7$, $DF = 134$, $p<0.0001$; meta-a4 $Y=3.405*X+6.26$, $R^2=0.5428$, $F=218.4$, $DF=184$, $p<0.0001$; meso-meta $Y=5.017*X+5.366$, $R^2=0.7618$, $F= 69.9$, $DF=272$, $p<0.0001$). However, the linear relationships between microtubule number and axon cross-section area differed across bundles (ANCOVA $F(2,590)=39.32$, $p<0.0001$; one-way ANOVA of slopes $F(2,590)=32.66$, $p<0.0001$

followed by Tukey's post hoc test). The connectives between the meso- and metathoracic ganglia had a significantly steeper relationship between microtubule number and axon cross-section area in comparison to nerve 5 ($p<0.0001$) and the connectives between the metathoracic and fourth abdominal ganglia ($p<0.0001$). Nerve 5 and the connectives between the metathoracic and fourth abdominal ganglia were not significantly different ($p=0.1901$).

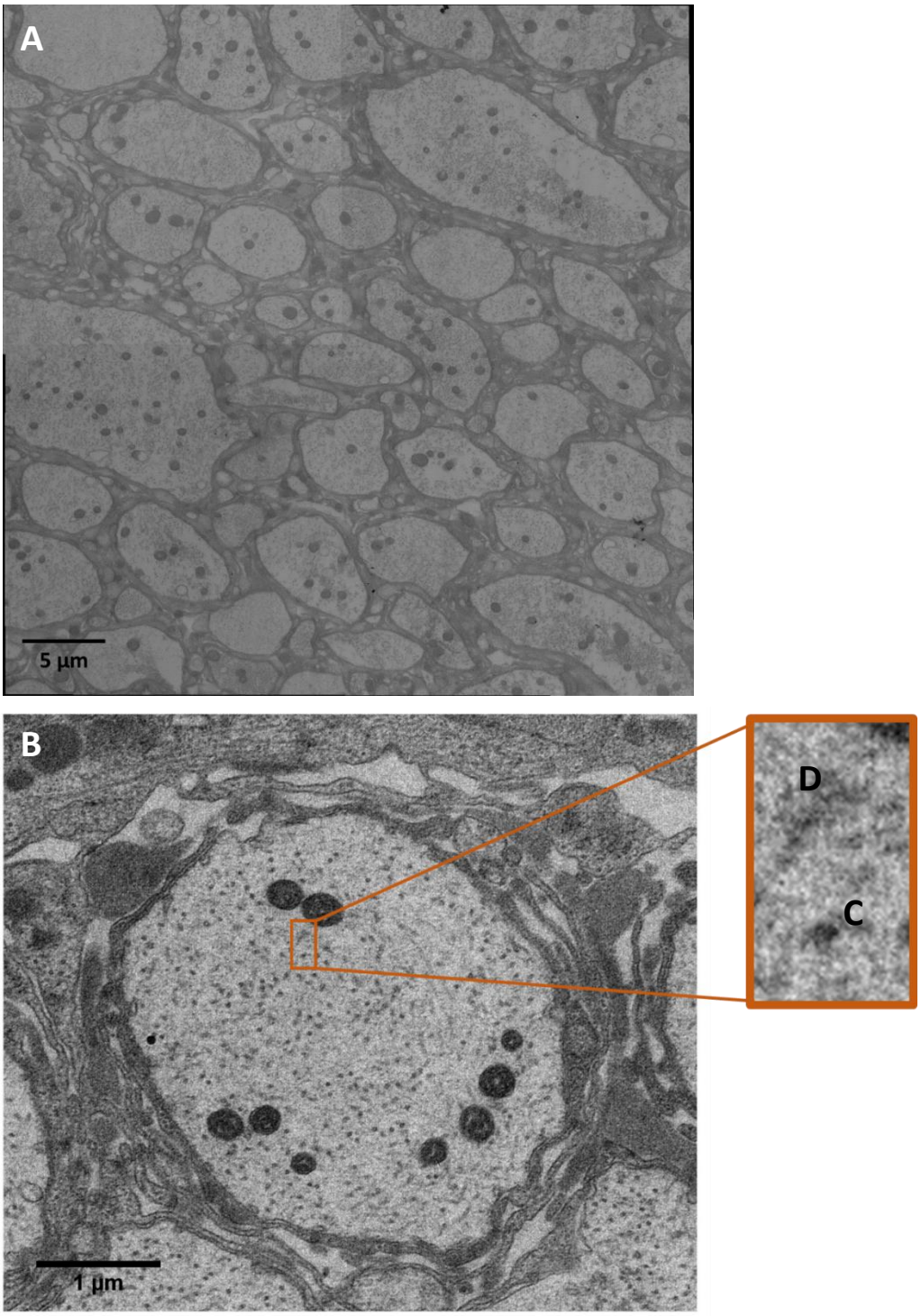

Figure 4-6: Example images for microtubule counts. Montages containing multiple cells at high resolution were created (A, contrast enhanced using Fiji for printing purposes). Microtubules in cells (B, stained with uranyl acetate and lead citrate for printing purposes) were counted if in the correct orientation (C) but not if there was a 'tail' visible behind (D). Examples shown are from the connectives between the meso- and metathoracic ganglia in desert locust.

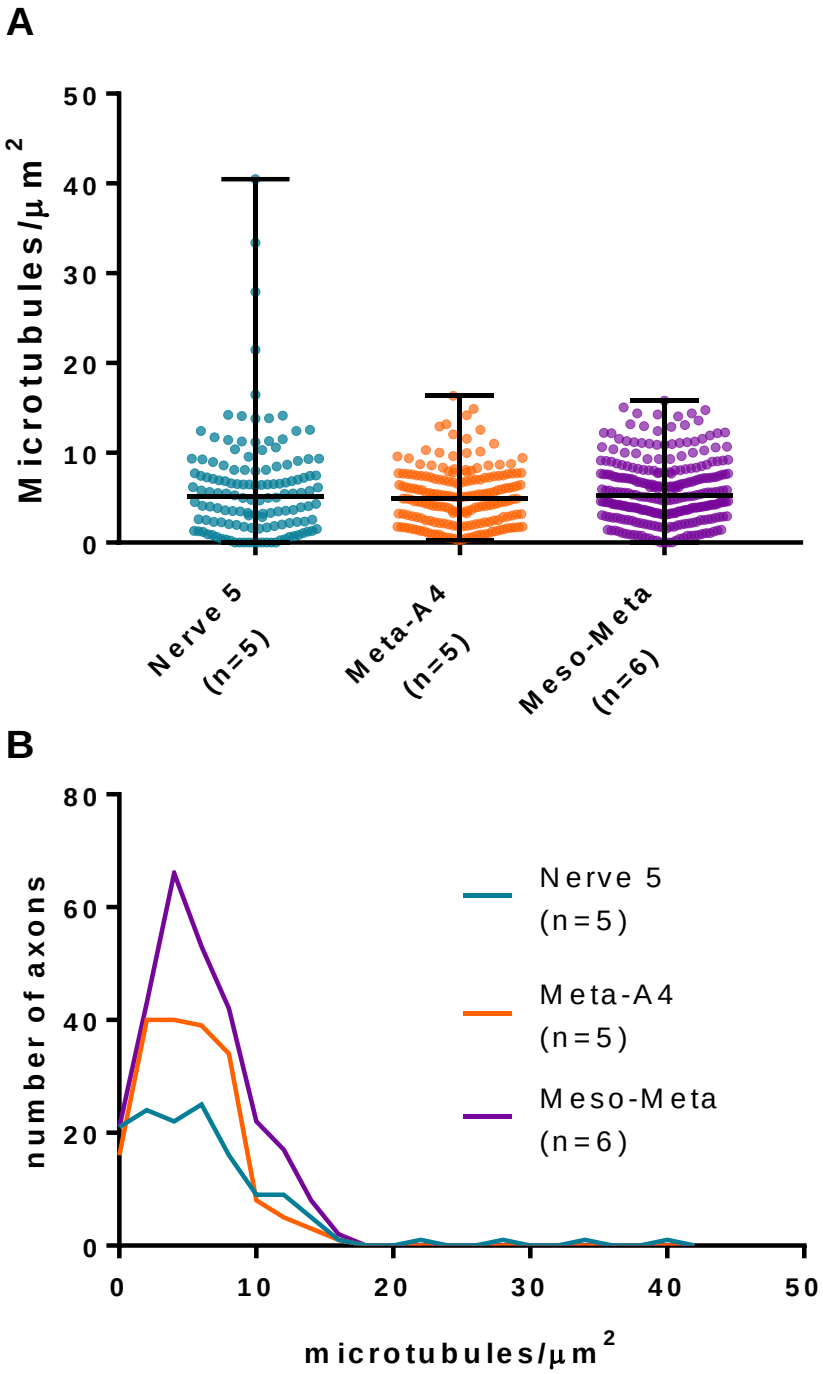

Figure 4-7: Microtubule density in the perpendicular orientation is consistent across axon bundles in the desert locust. A: There is no difference between density of microtubules in the orientation consistent with the plane of tension (Kruskal-Wallis n.s) data shows median and range. **B:** distribution of microtubule densities in each bundle.

Table 4: The microtubule density is positively skewed in the connectives between the meso- and metathoracic ganglia in the desert locust. Data from Figure 4-7 shows that the connectives between the meso- and metathoracic ganglia (Meso-Meta) has a positively skewed distribution of microtubule density.

	Nerve 5	Meta-A4	Meso-Meta
Mean (microtubules/μm^2)	6.024	5.056	5.712
SD (microtubules/μm^2)	5.956	3.169	3.49
cv	98.87%	59.86%	61.10%
skew	2.693	0.7527	0.5969
n	126	186	270

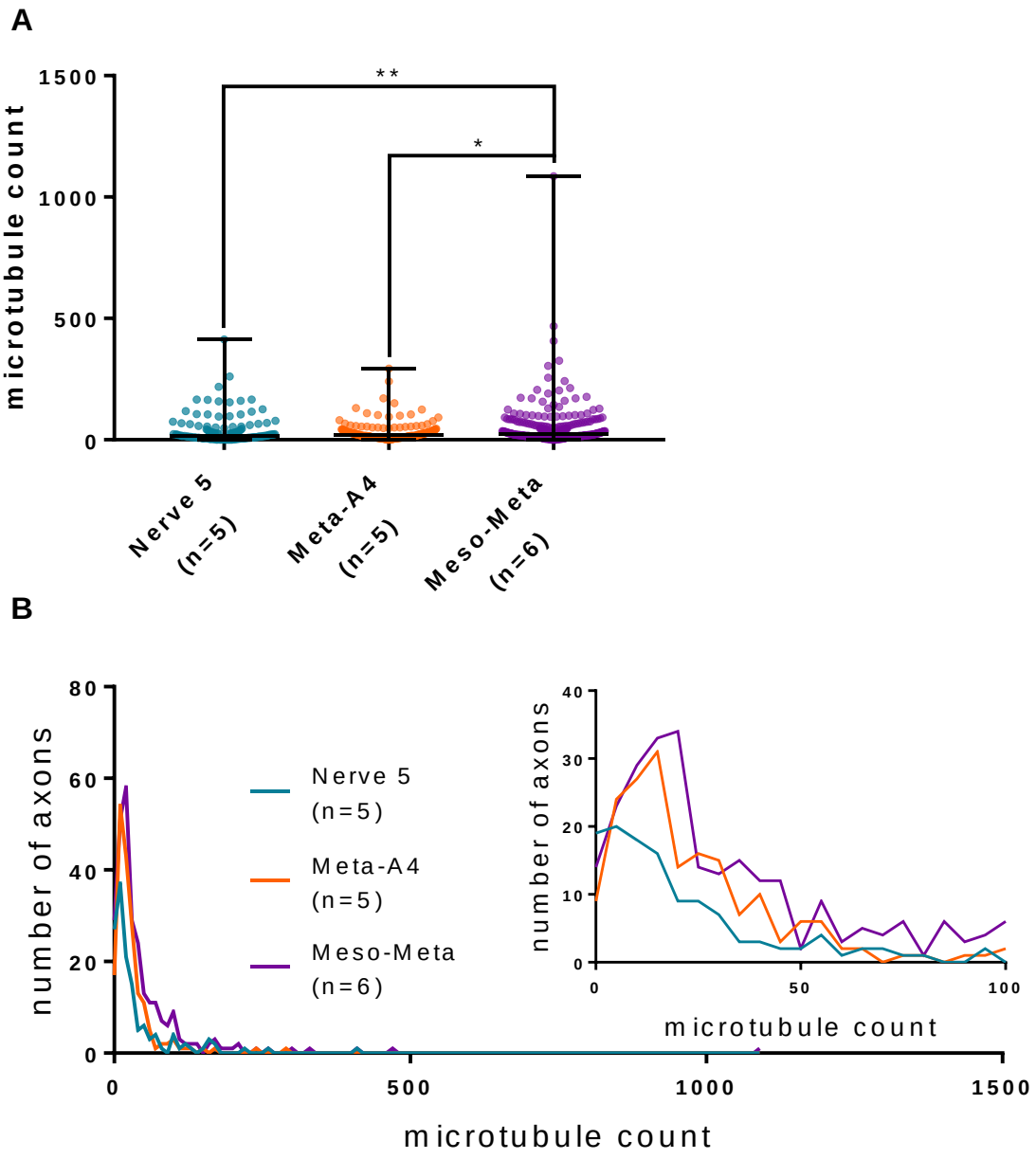

Figure 4-8: Microtubules per cell across the three bundles. **A:** There are more microtubules per cell in the connectives between the meso- and metathoracic ganglia (Kruskal Wallis and Dunn's multiple comparisons, * $p<0.05$, ** $p<0.01$); data shows median and range. **B:** distribution of number of microtubules per axon in each bundle in full and between 0-100 microtubules (inset).

Table 5: Axon bundles in the desert locust have positively skewed distributions of microtubules/axon. Data from Figure 4-8 shows the connectives between the meso- and metathoracic ganglia (Meso-Meta), the connectives between the metathoracic and fourth abdominal ganglia (Meta-A4), and nerve 5 also have a positive skew in the distribution of microtubules per axon.

	Nerve 5	Meta-A4	Meso-Meta
Mean (microtubules per axon)	36.54	29.58	49.4
SD (microtubules per axon)	56.95	37.11	87.39
cv	155.83%	125.45%	176.89%
skew	3.403	3.844	7.236
n	136	186	274

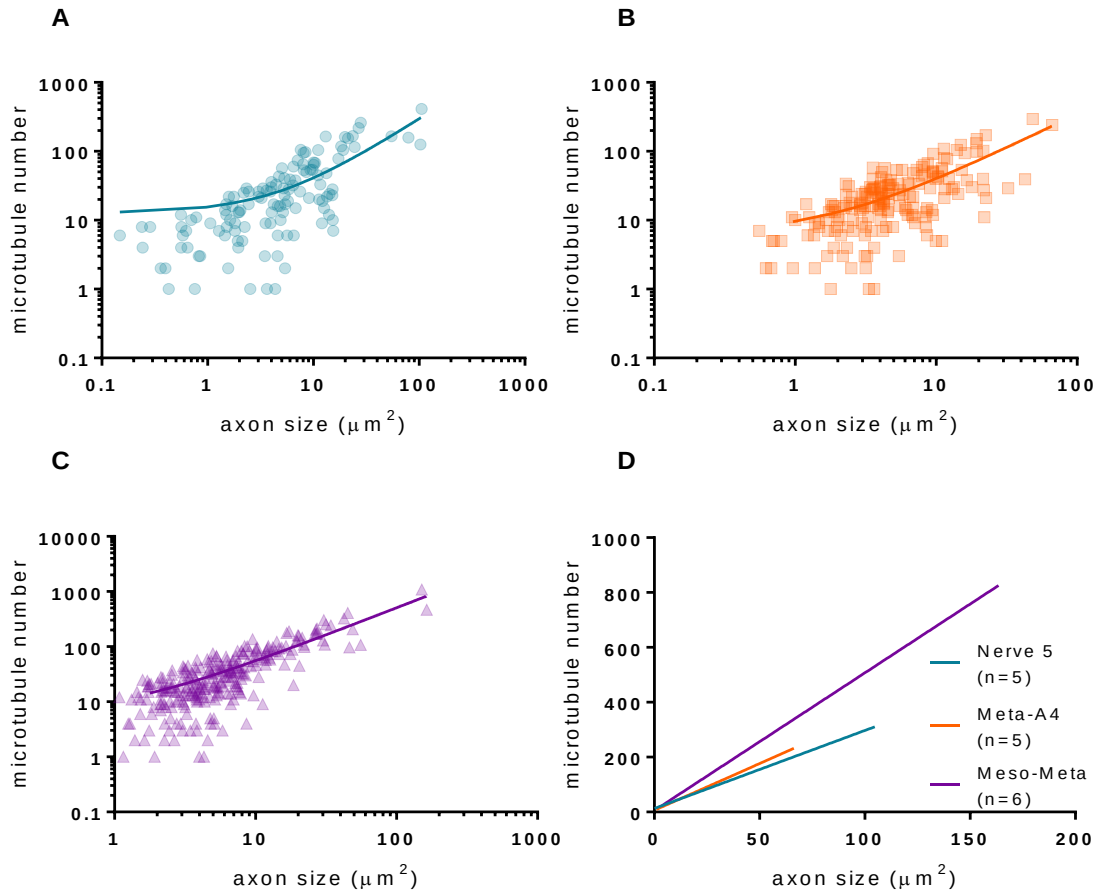

Figure 4-9: The relationship between microtubule number and axon size is significantly steeper in the connectives between the meso- and metathoracic ganglia. A: the microtubules per axon of nerve 5 on a log plot (symbols) and linear regression, R^2 nerve 5= 0.5728, **B:** the microtubules per axon of the connectives between the metathoracic and fourth abdominal ganglia on a log plot (symbols) and linear regression, R^2 meta-a4 = 0.5428, **C:** the microtubules per axon of the connectives between the meso- and metathoracic ganglia on a log plot (symbols) and linear regression, R^2 meso-meta Y = 0.7618. **D:** linear regressions of the relationship between microtubule number and axon size for each bundle. It was then determined that the relationship of microtubule number to axon size was significantly different in the connectives between the meso- and metathoracic ganglia.

4.4.3 Forces experienced in response to stretch differ across axon bundles

We used bespoke apparatus to stretch the axon bundles *ex vivo* by stretching the bundles in discreet horizontal steps of 50 µm every 3 seconds (see Methods 2.2.10). We measured the maximum force that could be applied before the bundle broke (Figure 4-10). Breakage was not always associated with a sudden decrease to zero force, rather there would be steps down as elements of the connective were torn apart. Consequently, we measured the maximum force recorded for the connectives between the meso- and metathoracic ganglia (Meso-Meta), the connectives between the metathoracic and fourth abdominal ganglia (Meta-A4) and nerve 5, separating the sexes.

Female connectives between the meso- and metathoracic ganglia withstood significantly higher forces than those in males (two-way ANOVA, interaction $F(2,56)=4.984$; $p=0.0102$, sex $F(1, 56)=7.244$, $p=0.0094$, bundle $F(2,56)=52.84$, $p<0.0001$; Tukey's multiple comparisons Meso-Meta male vs female $p=0.0016$). There were no significant differences between sexes for the other bundles (nerve 5 $p=0.9994$, Meta-A4 $p>0.9999$). Nerve 5 and the connectives between the metathoracic and fourth abdominal ganglia did not differ significantly from each other (male $p=0.9995$, female $p>0.9999$). The connectives between the meso- and metathoracic ganglia, however, withstood a much greater force than nerve 5 (male $p=0.0006$, female $p<0.0001$) and the connectives between the metathoracic and fourth abdominal ganglia (male $p=0.0023$, female $p<0.0001$) before breaking.

Measurement of the empirical breaking points did not account for nerve 5 being a single axon bundle whilst the VNC connectives are pairs. To account for this, we halved

the maximum force for these bundles. When we halved the maximum force the significant difference in maximum force found between the male connectives between the meso- and metathoracic ganglia and nerve 5 disappeared, however, all other significant and non-significant results remained (two-way ANOVA, interaction $F(2,56)=4.039$, $p=0.0230$, sex $F(1,56)=7.273$, $p=0.0092$, bundle $F(2,56)= 3.02$, $p<0.0001$; Tukey's multiple comparisons; Figure 4-11).

We measured the distance the bundle was stretched prior to breakage, which gives an indication of the overall elasticity of the bundle and/or its connections. This measure was obtained by counting the number of steps that increased the force to which the axon bundle was exposed up to and including the maximum force achieved. The connectives between the metathoracic and fourth abdominal ganglia were stretched significantly further in females than males before breakage (two-way ANOVA, interaction $F(2,53)=2.834$, $p=0.0677$, sex $F(1,53)=8.887$, $p=0.0043$, bundle $F(2,53)=134.4$, $p<0.0001$; Tukey's multiple comparison male vs female $p=0.0129$; Figure 4-12). There was no difference in distance stretched between males and females for the connectives between the meso- and metathoracic ganglia ($p=0.9977$) or nerve 5 ($p=0.8872$). The connectives between the metathoracic and fourth abdominal ganglia could be stretched significantly further than the connectives between the meso- and metathoracic ganglia (males $p<0.0001$, females $p<0.0001$) and nerve 5 (males $p=0.0011$, female $p<0.0001$). Nerve 5 could also be stretched a significantly greater distance than the connectives between the meso- and metathoracic ganglia (males $p<0.0001$, females $p<0.0001$).

Taking the empirical distance stretched does not account for the different lengths of the axon bundles. Consequently, we calculated the relative distance stretched as a percentage increase from *in vivo* measurements using only females. Using this measurement, we found no differences between the three connectives (one-way ANOVA, $F(2,24)=0.9355$, $p=0.4062$; Figure 4-13).

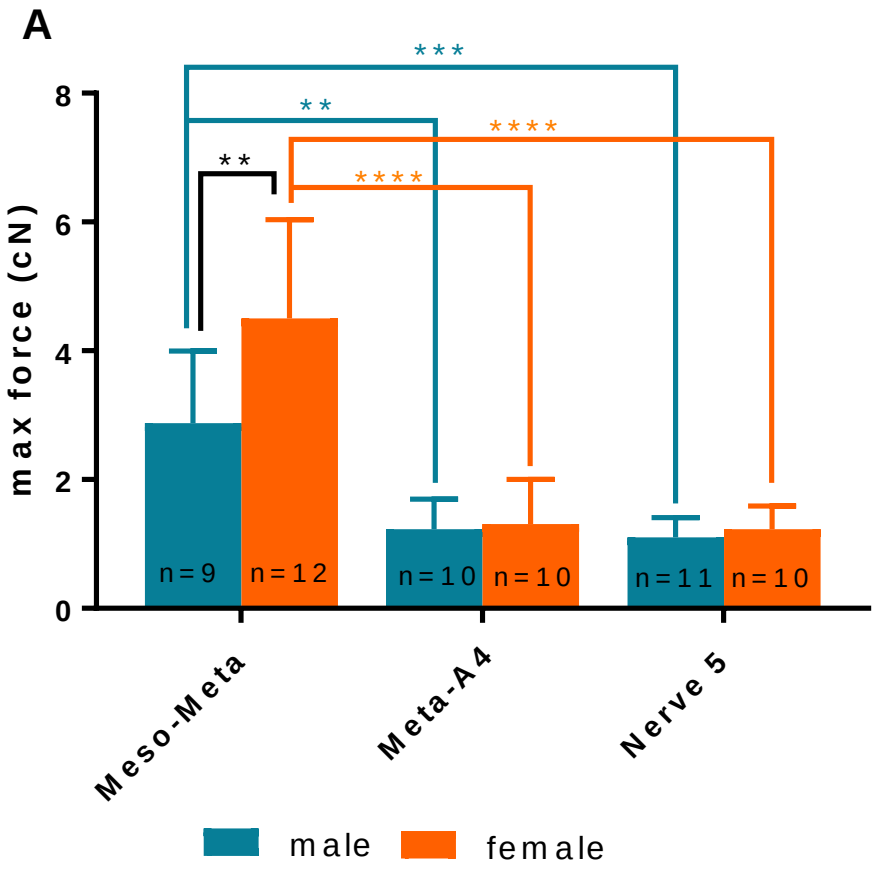

B

	Male		Female	
	Mean	SD	Mean	SD
Meso-Meta	2.88	1.12	4.50	1.54
Meta-A4	1.23	0.47	1.31	0.70
Nerve 5	1.10	0.31	1.23	0.36

Figure 4-10: Maximum force experienced by axon bundles before failure. A: The connectives between the meso- and metathoracic ganglia (Meso-Meta) experienced higher forces than other bundles before breaking, particularly in females (two-way ANOVA with Tukey's multiple comparisons,**p<0.01, *** p<0.001, **** p<0.0001, data is mean ± SD). **B:** mean ± SD of maximum force prior to critical failure (cN).

A

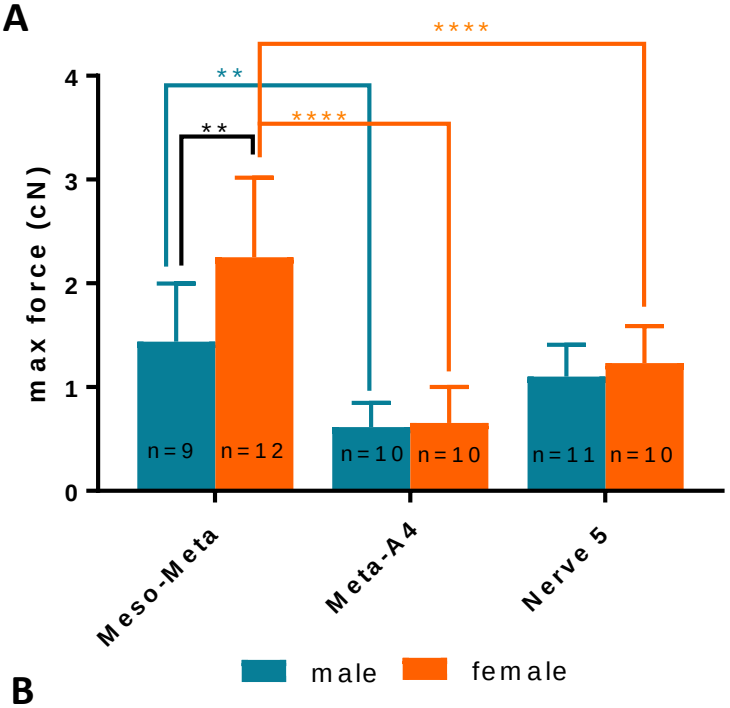

B

	Male		Female	
	Mean	SD	Mean	SD
Meso-Meta	1.44	0.56	2.25	0.77
Meta-A4	0.61	0.23	0.65	0.35
Nerve 5	1.10	0.31	1.23	0.36

C

	Meso-Meta		Meta-A4		Nerve 5
Meso-Meta	Male vs female p=0.0037				
Meta-A4	Male p=0.005	Female p<0.0001	Male vs female p>0.9999		
Nerve 5	Male p=0.610	Female p<0.0001	Male p=0.1917	Female p=0.0888	Male vs female p=0.9891

Figure 4-11: Maximum force experienced by singular bundles before breakage. A: When accounting for singular bundles the connective between the meso- and metathoracic ganglia still reach larger forces prior to breakage than other bundles in females, although only compared to the connective between the metathoracic and fourth abdominal ganglia in males (two-way ANOVA with Tukey's multiple comparisons; **p<0.01, ****p<0.0001; data is mean ± SD). **B:** mean ± SD of the max force experienced by single connectives (cN). **C:** Results of Tukey's multiple comparisons for all three axon bundles.

A

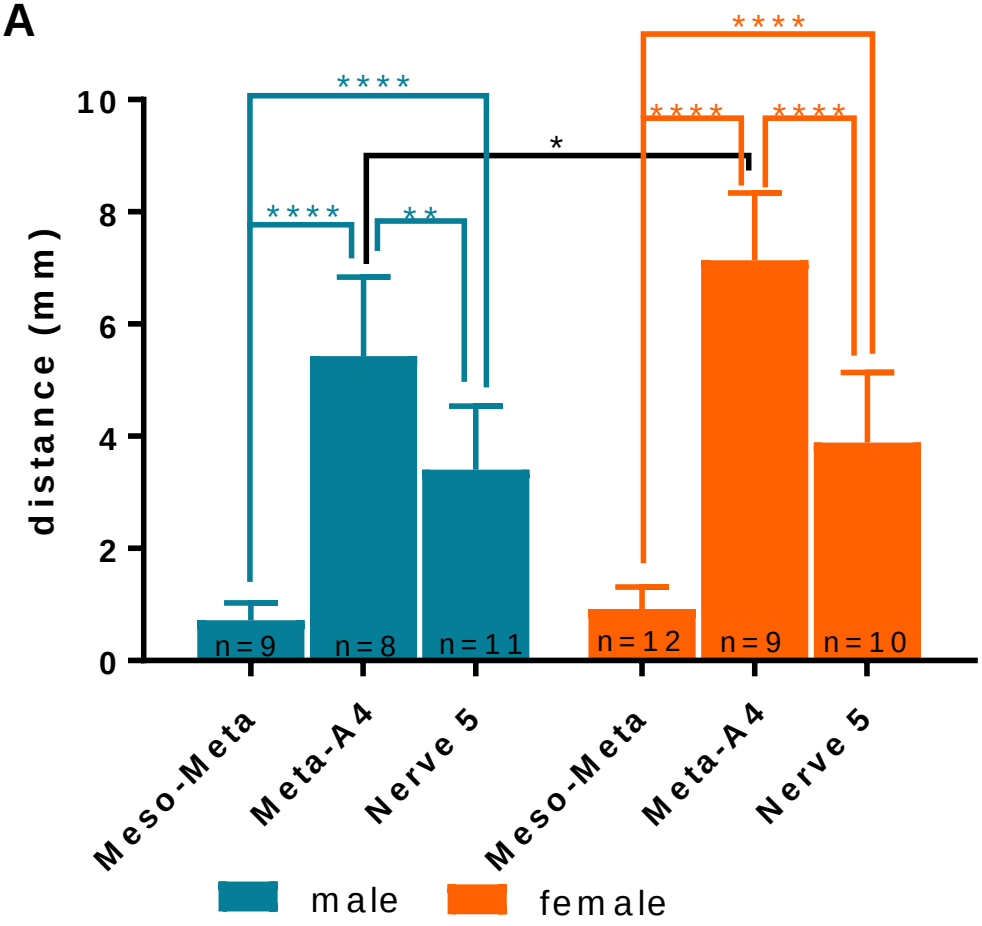

B

	Male		Female	
	Mean	SD	Mean	SD
Meso-Meta	0.72	0.31	0.92	0.39
Meta-A4	5.43	1.42	7.14	1.20
Nerve 5	3.40	1.13	3.89	1.26

Figure 4-12: Distance axon bundles were pulled prior to breaking. A: The connectives between the metathoracic and fourth abdominal ganglia were pulled the longest distance before breaking, particularly females, nerve 5 was next then the connectives between the meso- and metathoracic ganglia (two-way ANOVA with Tukey's multiple comparison; *p<0.05, **p<0.01, ****p<0.0001; data is mean ± SD). **B:** mean ± SD of the distance each axon bundle of the desert locust was stretched (mm).

A

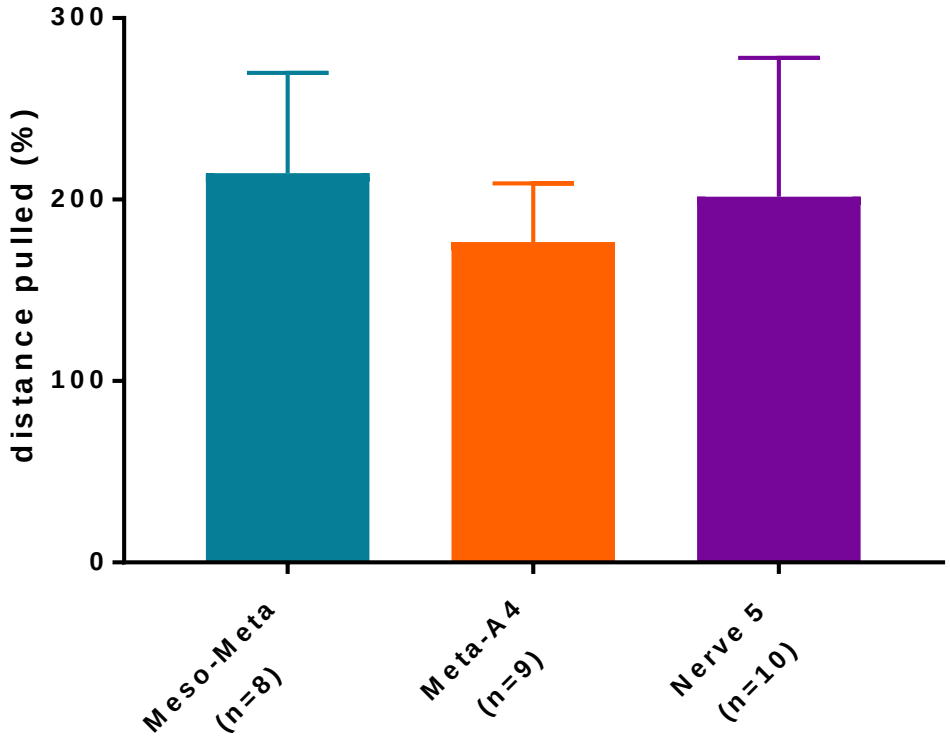

B

	Meso-Meta (n=8)	Meta-A4 (n=9)	Nerve 5 (n=10)
Mean	214.6	176.6	201.6
Std. Deviation	55.16	32.35	76.54

Figure 4-13: Distance pulled as a percent of the length of the axon bundle *in vivo*. A: We represent the distance the bundles were pulled prior to breaking as a percentage increase of their original length, there is no difference between them with all bundles being pulled approximately 100% more than their initial length (one-way ANOVA n.s; data is mean ± SD). **B:** mean ± SD of the distance axon bundles in the desert locust were stretched represented as a percentage increase from length *in vivo*.

4.4.4 Axon bundles in the desert locust are viscoelastic but vary in responses to uniaxial loading

We compared the traces obtained from uniaxial loading experiments with simultaneous video of connectives. We found that in all three axon bundles (the connectives between the meso- and metathoracic ganglia, the connectives between the metathoracic and fourth abdominal ganglia and nerve 5) the critical failure point when force began to decrease aligned with the clear separation of one or both of the axon bundles (Figure 4-14; Figure 4-15; Figure 4-16). In the connectives between the meso- and metathoracic ganglia the critical failure point was preceded by 'bulging' at the metathoracic ganglion as the connectives began to pull free, whereas in both nerve 5 and the connectives between the metathoracic and fourth abdominal ganglia, breakage usually occurred along the length of the axon bundle.

Considering the entire uniaxial loading experiment traces, the three different axon bundles respond to stretch differently. The connectives between the meso- and metathoracic ganglia rise steeply in the resistance force in a small number of steps (and therefore a short distance of stretch) before breaking, whereas in nerve 5 and the connectives between the metathoracic and fourth abdominal ganglia the increase is more gradual.

We isolated individual steps for each axon bundle, taking the first step to produce an increase in force and the step immediately prior to the critical failure. Nerve 5 and the connectives between the metathoracic and fourth abdominal ganglia show similar behaviour, both early steps and later steps produce a sudden increase in force and a gradual recovery, which is typical of a viscoelastic material (Figure 4-17). However, in the connectives between the meso- and metathoracic ganglia there appears to be no

recovery in the early steps. To confirm whether the connectives between the meso- and metathoracic ganglia recovered from early steps we carried out experiments where only a single step was applied to connectives (Figure 4-18). Consistent with the viscoelastic properties of axon bundles, we found that recovery did occur after two minutes.

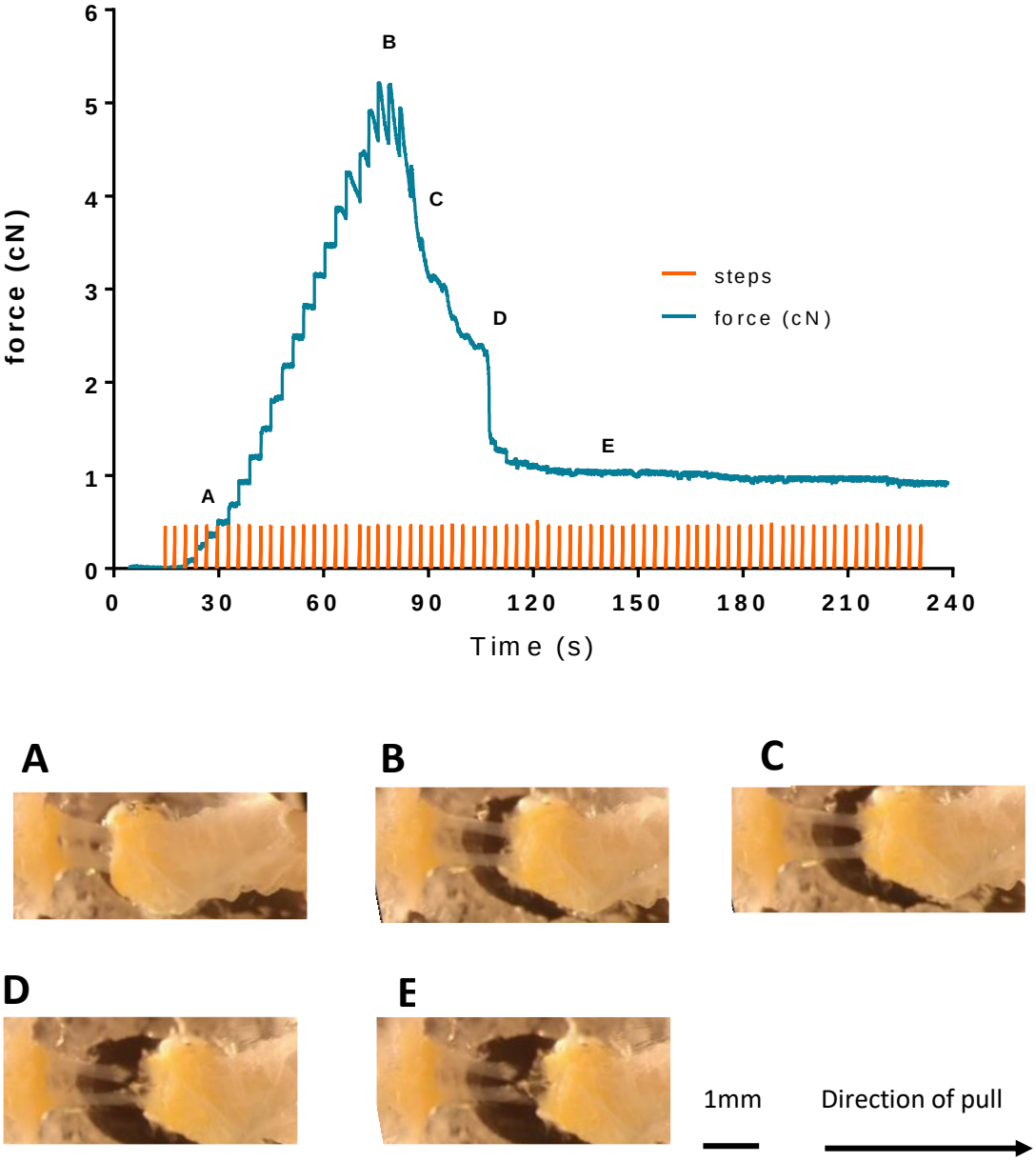

Figure 4-14: Example trace of the connectives between the mesothoracic and metathoracic ganglia undergoing stepped stretching and images of the region at certain points of interest. The trace (force (cN) in blue, steps in orange) and accompanying images show the first steps that exert force (A), the peak force exerted (B), the first loss of resistance (C), a dramatic loss of force associated with complete severing of one of the connectives (D) and the point at which both connectives are clearly severed on the video (E).

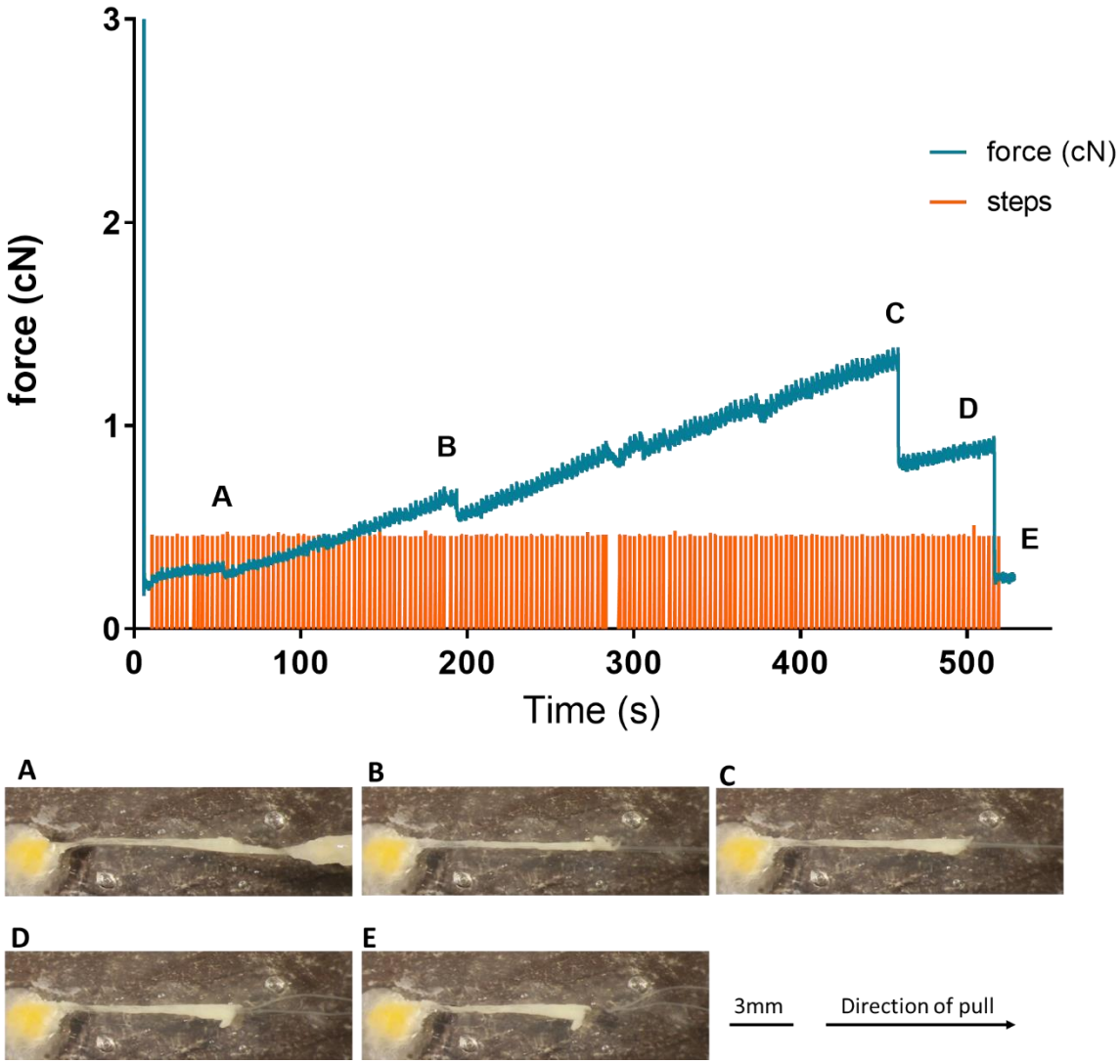

Figure 4-15: Example trace of the connectives between the metathoracic and fourth abdominal ganglia undergoing stepped stretching and images of the region at certain points of interest. The trace (force (cN) in blue and steps in orange) and accompanying images show the first steps that exert force (A), the breakage of the sheath around the connectives(B), the peak force (C), a dramatic loss of force associated with complete severing of one of the connectives (D) and the point at which both connectives are clearly severed on the video (E).

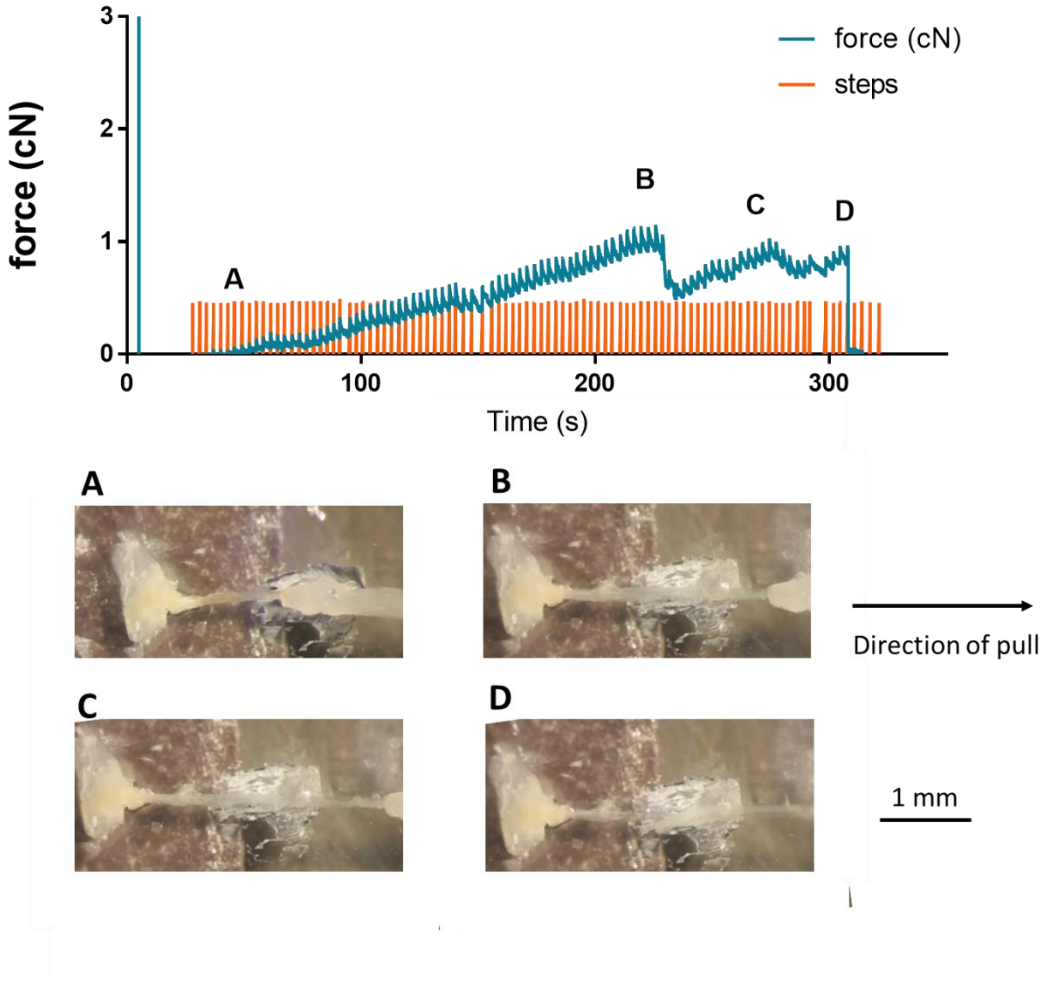

Figure 4-16: Example trace of the nerve 5 undergoing stepped stretching and images of the region at certain points of interest. The trace (force (cN) in blue and steps in orange) and accompanying images show the first steps that exert force (A), the peak force (B), the breakage of the sheath around the nerve and associated loss of force(C), a dramatic loss of force when the nerve breaks(D).

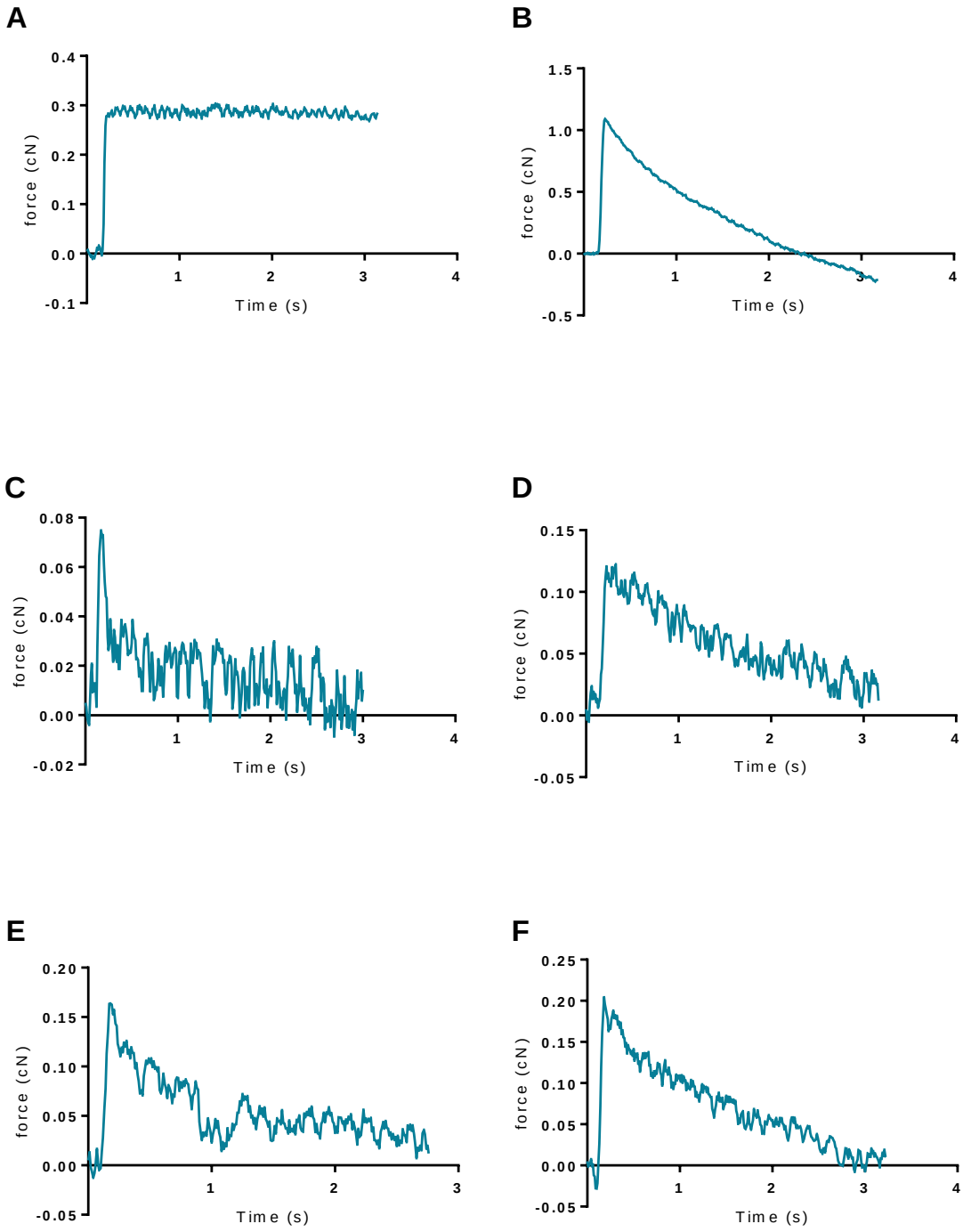

Figure 4-17: Examples of axon bundle responses to single pulling steps. Examples show early (A, C, E) steps when changes in force were first measured and late (B, D, F) steps just prior to the maximum force reached for the connectives between the meso- and metathoracic ganglia (A, B), the connectives between the metathoracic and fourth abdominal ganglia (C, D) and nerve 5 (E, F). All forces were normalised to start at 0 cN.

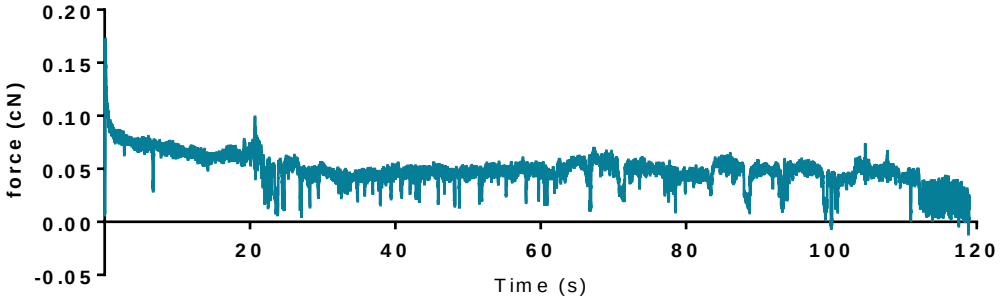

Figure 4-18: One pulling step on the connectives between the meso- and metathoracic ganglia. A singular step of 50 µm was made and the connective left to return to baseline, force is artificially normalised around 0 cN.

4.5 Discussion

To our knowledge, we have shown the first example of microtubule number being linked to tensile properties of an entire axon bundle and to the strength of axon bundles. We have shown that the linear relationship between the number of microtubules in longitudinal orientation and axon cross-section area differs among axon bundles in the desert locust. We also find this is reflected in mechanical properties of the axon bundles, specifically that the axon bundles with the steepest relationship between microtubule count and axon area (the connectives between the meso- and metathoracic ganglia) are able to withstand the greatest forces before breaking.

Previously we identified that the connectives between the meso- and metathoracic were under tension. We then found that the connectives between the metathoracic and fourth abdominal ganglia were not but contributed to the tension exerted on the connectives between the meso- and metathoracic ganglia, and that nerve 5 was not under tension and did not contribute. We assessed differences in anatomy and physiology at different organisational levels to correlate with the tension present. Using TEM imaging, we found that the primary feature of axon bundles that most closely reflects the tension to which they are exposed *in vivo* is the relationship between axon cross-section area and microtubule number. Using *ex vivo* uniaxial stretching, we also correlate strength but not elasticity to both the steepness of the relationship between microtubule number and axon area and to tension *in vivo.*

Using TEM we found other anatomical differences between the three bundles studied. The connectives between the meso- and metathoracic ganglia had the largest diameter followed by nerve 5 and then the connectives between the metathoracic and fourth abdominal ganglia. The connectives between the meso- and metathoracic ganglia

also contained axons with larger areas than nerve 5. These anatomical differences did not reflect the tension within their respective axon bundles, nor were they reflected in the strength determined by uniaxial loading. Using uniaxial loading, we found that all bundles were equally elastic when corrected for initial length. We also found that the connectives between the meso- and metathoracic ganglia were able to withstand more force than the other bundles and there was no difference between nerve 5 or the connectives between the metathoracic and fourth abdominal ganglia despite their differences in diameter.

4.5.1 Microtubules in orientation relate to the tension observed in nerve cutting experiments

By counting the number of microtubules in the longitudinal orientation of individual axons, we found a linear relationship between microtubule number and the cross-sectional area of axons in each of the three axon bundles. Microtubule numbers increased as axon cross-section areas increased. The slope of this relationship significantly differed among the axon bundles; the connectives between the meso- and metathoracic ganglia had a significantly steeper relationship than either the connectives between the metathoracic and fourth abdominal ganglia or peripheral nerve 5. A linear relationship has been found before in mammalian sensory neurons (Fadic *et al.*, 1985). In this study the slopes found between microtubule number and axon calibre were much steeper than ours, while the intercepts were similar. This study focuses on axons under 1.4 μm^2 which may explain the difference in slopes. Fadic *et al* (1985) find relatively consistent slopes across peripheral sensory neurons. Another study in the sural nerve of rats found that the relationship between microtubule number and axon calibre remains consistent throughout growth (Saitua and Alvarez, 1988). To our knowledge, however,

this is the first demonstration of differences in the relationship between microtubule count and axon area between axon bundles, particularly in the same species, and the first to suggest a functional reason for the differing slopes.

The connectives between the meso- and metathoracic ganglia are under tension *in vivo*, and have a significantly steeper relationship between microtubule number and axon area than the other bundles studied. Microtubules in orientation with tension have recently been linked to tensile properties of axons in *C. elegans* (Krieg *et al.*, 2017), which focussed on individual axons rather than bundles, using mutants to demonstrate a link between microtubule bundle stability and axonal resistance to stress. Microtubules are also implicated in embryonic towed growth, responding to force (Chada *et al.*, 1997). We suggest that the microtubule number is either enabling axons to withstand external forces (Krieg *et al.*, 2017) or involved in generating internal forces and producing stiffness (Inoue and Salmon, 1995; Rooij and Kuhl, 2018).

4.5.2 Critical failure points found via direct uniaxial loading *ex vivo* reflect microdissection and TEM results

Using uniaxial loading, we found that the connectives between the meso- and metathoracic ganglia withstood the highest force prior to breaking with no difference between the connectives between the metathoracic and fourth abdominal ganglia and nerve 5; this reflects the finding of high tension in these bundles. We found no differences in the elasticity of bundles when we represented the distance they could be stretched as a percentage increase of their initial length. In absolute terms, however, the connectives between the metathoracic and fourth abdominal ganglia could be stretched a greater distance. While uniaxial loading has been used to calculate *in vivo* stresses (Luna *et al.*, 2013), to our knowledge this is the first time that the strength and

elasticity of whole axon bundles has been related to the *in vivo* tension that bundles to which bundles are exposed.

In our experiments, we tested the critical failure point of the tissue, but not necessarily the tensile strength of the bundles themselves. The reason our experiments are not a true measure of tensile strength is two-fold. Firstly, in all cases the axon bundles remained connected to at least one ganglion that was used to affix the bundle to the equipment, this means the experiments may instead test the strength of the connections between the axon bundles and the ganglia. Secondly, true tensile strength testing requires strict dimensional properties to which our samples do not conform. The American Society for Testing and Materials (ASTM, currently the most frequently used standards, although does not directly refer to biological tissue) states the ratio required for the gauge:diameter of a rod being tested is 4 (Davis, 2004). This ensures comparisons are possible as the gauge length can alter the results of tensile testing, this is also true for biological materials such as tendons, where differences in gauge or cross-section can dramatically alter results (Legerlotz *et al.*, 2010).

There is currently no standardisation of miniature testing, although methods exist for non-biological materials (LaVan and Sharpe Jr, 1999; Gianola and Eberl, 2009). It is unlikely that the connectives between the meso- and metathoracic ganglia specifically would have a large enough gauge for valid tensile strength testing. In materials with a small gauge region and a large diameter compared to length, the forces can become more complex than simple tensile testing as the large 'shoulders' (in our case the ganglia) can constrain deformation (Davis, 2004). Other testing of miniature

biological materials often uses much longer and finer fibres, such as those in spider silk (Vehoff *et al.*, 2007).

4.5.3 Axon bundles in the desert locust respond variably to uniaxial loading

All three of the axon bundles studied exhibited typical viscoelastic responses to pulling forces (Alexander, 1983; General Introduction), however, there were differences in the responses. In response to stretching, the connectives between the meso- and metathoracic ganglia resist with high levels of force, whereas the other axon bundles showed relatively low levels of resistance. By examining the entire experimental traces, we observed that the connectives between the metathoracic and fourth abdominal ganglia and nerve 5 respond similarly, with gradual rise in force (cN) over the course of several minutes to a point where breakage occurs, often preceded by tearing of the sheath around the axon bundle. The connectives between the meso- and metathoracic ganglia respond quite differently, however, sharply increasing in force which peaks and then decreases more slowly than the other axon bundles, perhaps representative of a slower tearing of the various components and axons within the bundle rather than a sudden tearing of the entire structure.

Responses to individual discreet steps of 50 µm in nerve 5 and the connectives between the metathoracic and fourth abdominal ganglia show elastic strain responses of an initial increase in force and then a clear decreasing recovery although this does not return to baseline in our 3 second steps. This occurs in both steps early in the experimental procedure and continues until the critical failure point. The connectives between the meso- and metathoracic ganglia had different responses to the discreet

steps depending on whether they were early or late in the step sequence. The first steps to produce a force lead to a clear increase in force that appeared stable in our original experiment. However, when we applied a single step of 50 µm the connective did eventually recover after around two minutes, whereas at higher forces when already stretched the connectives recovered more quickly.

It is difficult to theorise why these differences may occur, largely because the dimensional differences between the bundles may be contributing to the differences seen. These bundles may have evolved these dimensions that may make them stiffer, stronger or more elastic which may relate to function. For example, the empirically larger distance that the connectives between the metathoracic and fourth abdominal ganglia may relate to the motility of the abdomen during mating and egg laying (Vosseler, 1905; Uvarov, 1966; Burrows, 1996). However, it does prevent direct comparisons of the mechanical properties of the axon bundles. Each bundle studied was stretched to around double its initial length prior to breaking, yet this stretching produced vastly difference responses and different forces.

4.5.4 Direct uniaxial loading revealed sexual dimorphisms

We separated the desert locusts by sex for the uniaxial loading experiments because of the sexual dimorphism in tension revealed by our microdissections (Chapter 3). We found that the connectives between the metathoracic and fourth abdominal ganglia in the desert locust in females could be stretched a greater distance than males indicating they were more elastic. We also found that the connectives between the meso- and metathoracic ganglia in females were stronger than those in males when looking at the force at which critical failure occurred.

Female desert locusts undergo drastic changes in the size of their abdomen during egg laying (Vosseler, 1905; Uvarov, 1966; Vincent and Wood, 1972; Jorgensen and Rice, 1983; Hackman and Goldberg, 1987), which may exert forces throughout the VNC (Burrows, 1996). The sexual dimorphisms in the VNC connectives may be adaptations to this. The connectives between the metathoracic and fourth abdominal ganglia must stretch to accommodate the increased length of the abdomen, whereas the connectives between the meso- and metathoracic ganglia sit in the thorax which does not extend, therefore instead being able to withstand changing forces is a useful adaptation.

5 Tension is maintained throughout growth even following ablation of a thoracic connective

5.1 Abstract

The connectives between the meso- and metathoracic ganglia of the desert locust, *Schistocerca gregaria*, are under tension. Here we investigate whether this tension is stable throughout post-embryonic growth, even when one of this pair of connectives is ablated. By severing the connectives between the meso- and metathoracic ganglia in growing locusts, starting at third instar, we assessed the tension to which they are exposed. We also performed surgeries on third instars, ablating one of the connectives. We then investigated any subsequent structural changes to the connectives in adulthood using TEM. Finally, we used uniaxial loading to compare the breakage point of the single remaining connective in adult locusts with those of controls. We found that tension is stable throughout growth. We also found that connective ablation at the third instar led to morphological changes while tension and physical properties, as ascertained by uniaxial loading, remained unchanged. After ablation, the remaining connective contained more microtubules in adults. Thus, whether tension is emergent or otherwise predetermined, it is likely actively maintained throughout development and is mediated by microtubules in individual axons.

5.2 Introduction

Axonal tension contributes to development, particularly during embryogenesis in which tension in the axon and growth cone is important for growth and guidance (Bray, 1984; Athamneh and Suter, 2015; Polackwich *et al.*, 2015), as well as synapse formation (Siechen *et al.*, 2009; Ahmed *et al.*, 2012). During embryogenesis axons actively regulate tension (Rajagopalan *et al.*, 2010) and externally applied tension can induce growth (Bray, 1984).

Axons also grow after integration into a network, and this is thought to also involve tension in the form of stretch growth. Stretch growth is the growth of integrated axons that occurs during growth (reviewed in Smith, 2009). Imposed stretch growth *in vitro* can produce cultures of long axons (Pfister, 2004; Pfister, Iwata, *et al.*, 2006; Xu *et al.*, 2014; Li *et al.*, 2016), but little is known about the mechanism underpinning it or whether it occurs *in vivo*. A current hypothesis suggests it is a largely passive mechanism, in which slight stretching of the axons caused by the growth of surrounding tissues creates small breaks in the cytoskeleton at the thinnest point (Heidemann and Bray, 2015). A build-up of transported cellular elements to this region leads to them being incorporated into the thinning cell membrane (Heidemann and Bray, 2015). However, this hypothesis has not been tested and has been challenged based on issues of timing; some animals grow far faster than a build-up of slowly transported cellular components would allow (Smith, 2009). A second hypothesis posits that stretch causes the opening of mechanosensitive channels in the axon which then signals for growth to occur largely at the junction between the soma and axon, eliminating the issue of transport speed (Purohit and Smith, 2016). Whichever mechanisms axons use to grow *in vivo*, this must

not disturb normal functioning of the neuron to a noticeable extent (Pfister, Bonislawski, *et al.*, 2006).

Like other the hemimetabolous insects, the desert locust (*Schistocerca gregaria*) undergoes ecdysis several times during post-embryonic growth (Burrows, 1996). Ecdysis is accompanied by stereotypical movements and expiratory contractions that inflate the gut and tracheal system, changing internal pressure (Chapman, 2013). The period prior to ecdysis is also important because the insect is outgrowing its outmost cuticle, suggesting its internal space is 'overcrowded'. Moulting takes place over a few hours, often occurring overnight (Chapman, 2013). How is the VNC affected by ecdysis? If it were the case that the nerve cord grows prior to moulting, it may be under less tension immediately before the moult begins. However, some tissue growth occurs between moults may serve to cause stretch-growth of the nerve cord because only regions with sclerotized cuticle undergo incremental growth (Nijhout and Callier, 2015).

The presence of tension in adult axon bundles, namely the connectives between the meso- and the metathoracic ganglia, suggests that it has some functional relevance because axons should grow until stretch was no longer experienced (Heidemann and Bray, 2015; Purohit and Smith, 2016). This may be partially due to active contraction of the axons within these connectives, but it is partially mediated by the VNC posterior to the metathoracic ganglion (see Chapter 3).

Is tension consistent or does it alter during growth periods? Can the tension we have observed change in response to an alteration of the forces experienced by the connectives? We address these questions by: (1) severing the connectives between the meso- and metathoracic ganglia in locusts during different growth stages; and (2)

ablating one of the connectives during the third instar and repeating our previous microdissection nerve cutting and TEM studies.

5.3 Methods

Methods can be found in Methods 2.2.6-2.2.10.

5.4 Results

5.4.1 Tension within the connectives between the meso- and metathoracic ganglia is consistent throughout growth

We measured the connectives between the meso- and metathoracic ganglia which increased from 0.2903 mm ± 0.04422 (mean + S.D) in third instars to 0.9888 mm ± 0.07022 in adults (Figure 5-1; blue bars). We found that the growth of the connectives from third instar was linear (mid and late stages merged Spearman's rank test rho=0.9151, $p<0.0001$; linear regression, $R^2=0.8552$). We also separated the instars into mid and late (pharate) stages to examine if there was evidence of incremental growth. There was no significant difference in the lengths of the connectives between the meso- and metathoracic ganglia within instars (one-way ANOVA, $F(6,114)=153.8$, $p<0.0001$; Tukey's post hoc tests mid vs late, third instar $p=0.9055$, fourth instar $p=0.9952$, fifth instar $p>0.9999$). There was a significant increase in the lengths of the connectives between the meso- and metathoracic ganglia between the late phase of the fourth instar and the mid-point of the fifth instar, and the late phase of fifth instar and adult (late third instar – mid fourth instar $p=0.0576$, late fourth instar – mid fifth instar and late fifth instar – adult $p<0.0001$).

We severed the connectives between the ganglia which we previously showed caused an increase in the separation between the meso- and metathoracic ganglia in adults (chapter 3). To allow for comparisons across growth stages we normalised the separation as a percentage increase of the length of the connectives prior to severing. If the tension these connectives were exposed to changed during growth, then the percentage increase as a result of severing the connectives would differ. We found no relationship between the percentage increase in length and instar (mid- and late stages

merged; Spearman's rank test r=0.1351, p=0.1464). We were interested if tension rapidly increased or decreased around moulting: there was a significant difference in the tension between two growth stages but no others (between late fourth instar and mid fifth instar; Kruskal Wallis, H=14.91, p=0.0210, Dunn's multiple comparison, p=0.0085).

A

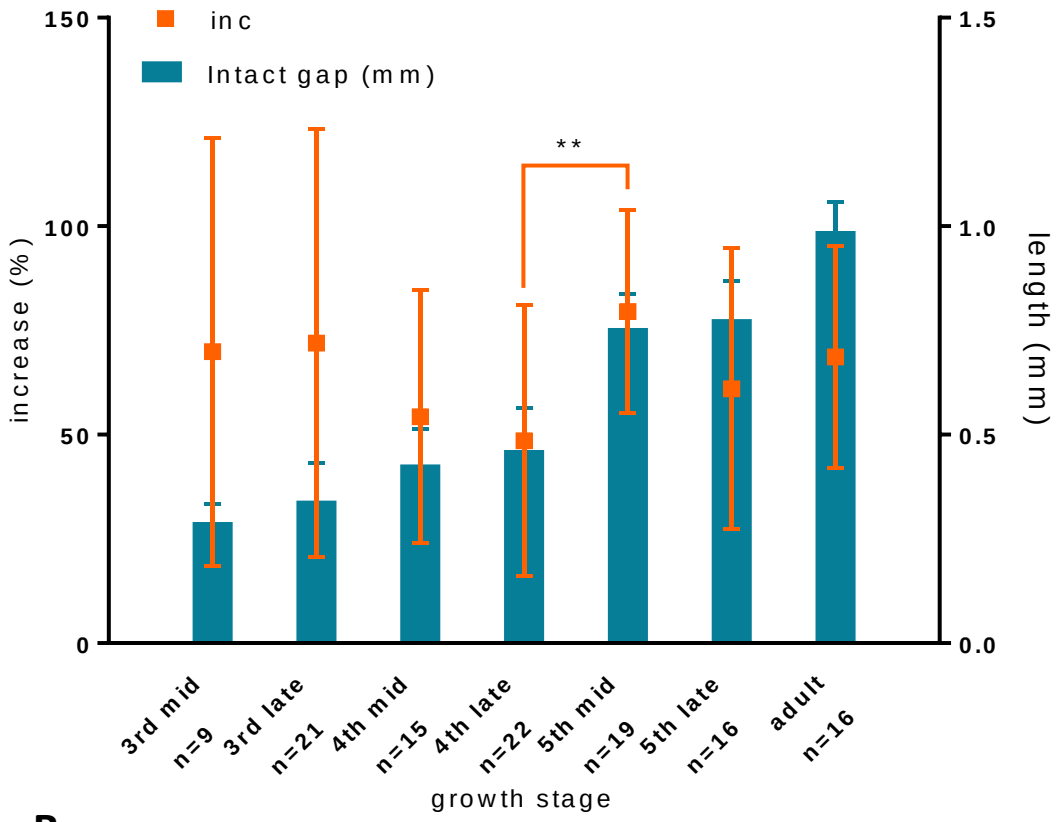

B

	3rd mid	3rd late	4th mid	4th late	5th mid	5th late	adult
Length of connectives (mm)	0.29 ± 0.044	0.34 ± 0.091	0.43 ± 0.086	0.46 ± 0.10	0.76 ± 0.083	0.78 ± 0.091	0.99 ± 0.070
Length after severing (mm)	0.48 ± 0.12	0.56 ± 0.28	0.66 ± 0.18	0.69 ± 0.22	1.43 ± 0.19	1.33 ± 0.17	1.66 ± 0.22
Percentage increase	69.92 ± 51.38	71.94 ± 51.27	54.26 ± 30.42	48.56 ± 32.49	79.51 ± 24.29	60.98 ± 33.73	68.67 ± 26.57

Figure 5-1: Distance between meso- and metathoracic ganglia increases during growth but percentage increase after severance of the connectives between does not. A: The percentage increase remained similar throughout growth except between late fourth instar and mid fifth instar (Kruskal Wallis and Dunn's multiple comparison, **p<0.01) data is mean ± SD. **B:** the means ± SD of the length of connectives at each growth stage, the distance between the meso- and metathoracic ganglia after connectives are severed, and the change represented as a percentage increase.

5.4.2 Ablation of a single connective between the meso- and metathoracic ganglia alters remaining connective length but not the tension

The microsurgery and sham surgery was undertaken as described in methods section 2.2.7. The body length of these locusts at adulthood was significantly smaller than controls but not significantly different from each other (one-way ANOVA, $F(2,36)=64.16$, $p<0.0001$, surgery vs controls $p<0.0001$, sham vs controls $p<0.0001$, surgery vs sham $p=0.7181$; Figure 5-2). This data included both male and female locusts because there was no significant difference in length between them (data not shown, Kruskal Wallis $H = 29.41$, $p<0.0001$, Dunn's multiple comparison surgery males vs female $p>0.9999$, sham males vs females $p=8018$, control males vs females $p>0.9999$).

Surgery produced striking changes in the anatomy of the thorax (Figure 5-3), including an infiltration of tracheal and fat tissue to the damaged area. Despite their similar body lengths, locusts that had undergone surgery had a significantly larger absolute distance between the meso- and metathoracic ganglia than their sham operated counterparts (one-way ANOVA, $F(2,43)=6.723$, $p<0.0001$, Tukey's multiple comparison post hoc test surgery vs sham, $p=0.0026$, vs control $p=0.0831$, sham vs control $p=0.2619$; Figure 5-4). The relative distance between the meso- and metathoracic ganglia of the surgery group was significantly larger than either the controls or the shams (one-way ANOVA, $F(2,36)=18.34$, $p<0.0001$; Tukey's multiple comparison test, surgery vs sham $p=0.0016$, surgery vs control, $p<0.0001$, sham vs control $p=0.2647$; Figure 5-5).

We severed the remaining connective between the meso- and metathoracic ganglia in the surgery locusts to measure the resulting separation. We represented this

as a percentage increase of the initial distance between the meso- and metathoracic ganglia to account for the morphological changes. We found that the extent the meso- and metathoracic ganglia separated after the connective cutting did not differ between the groups (one-way ANOVA, $F(2,43)=0.2991$, $p=0.7430$; Figure 5-6).

A

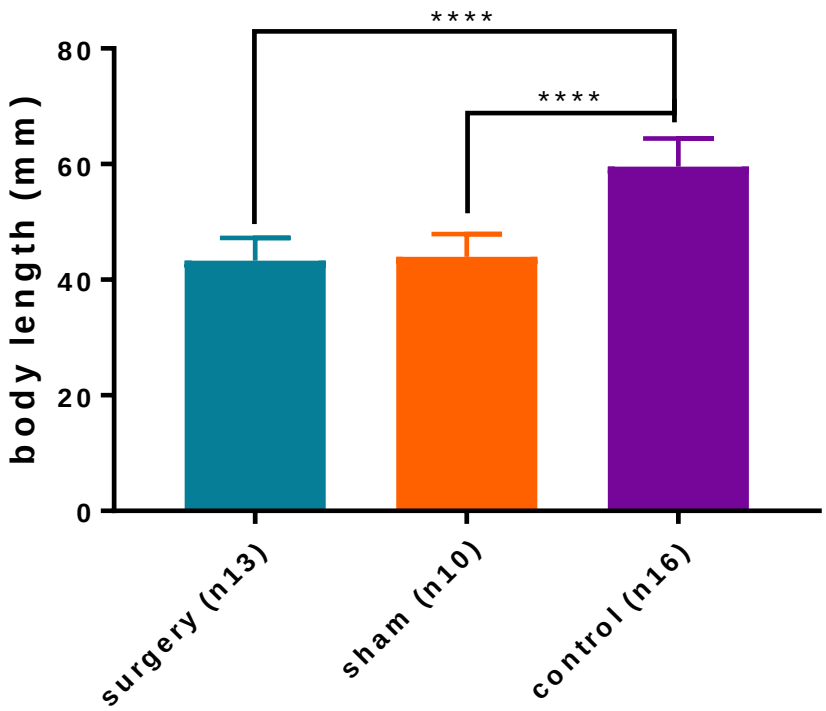

B

	surgery (n13)	sham (n10)	control (n16)
Mean	43.33	43.99	59.57
Std. Deviation	3.896	3.927	4.854

Figure 5-2: Both the full and sham surgery on juvenile desert locusts reduce adult body length. **A:** Both the full nerve cutting surgery and sham procedure at third instar produced locusts that were smaller than controls at adulthood (one-way ANOVA, ****p<0.0001) data is mean ± SD. **B:** the means ± SD (mm) of body lengths in each group.

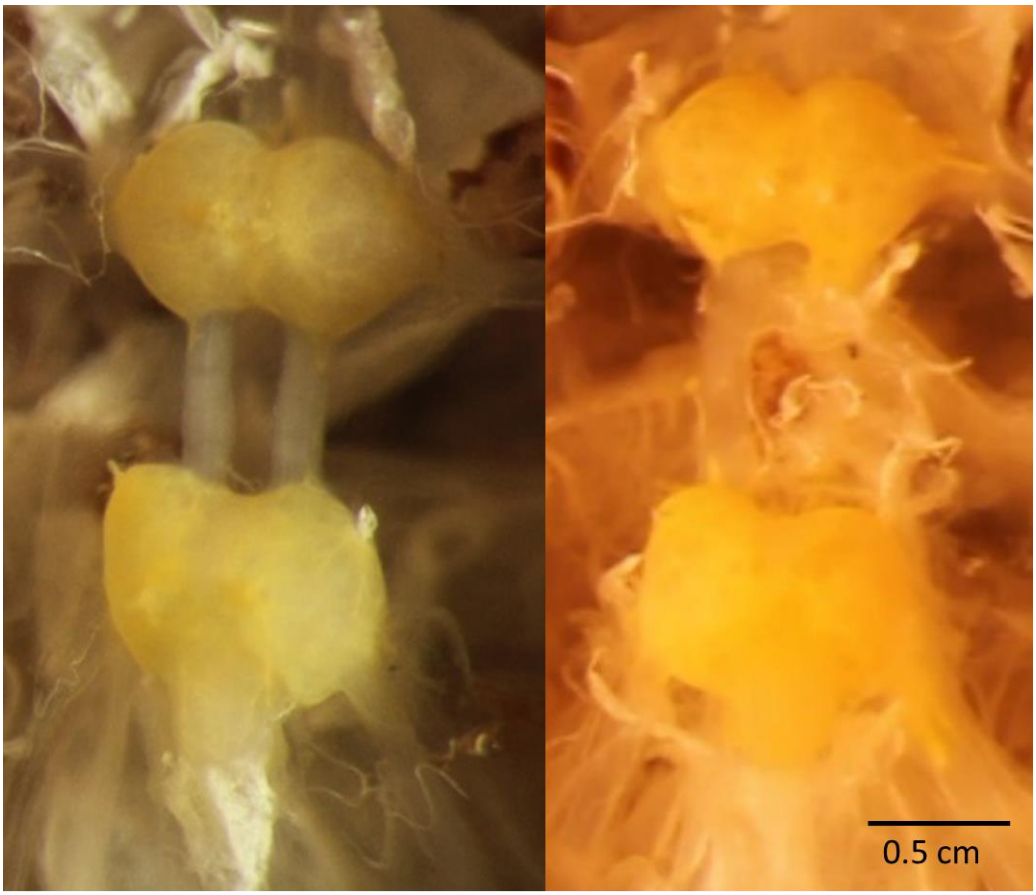

Figure 5-3: Examples of the meso-and metathoracic ganglia and connectives between of (A) a control adult and (B) an adult having undergone nerve cutting at third instar. A typical example of the changes seen in locusts that undergo cutting of the left connective at third instar. The area where the connective is missing/damaged is invaded by other tissue particularly tracheal and fat, the remaining right connective appears longer and bowed, yellow nerve tissue appears to have invaded into some of the nerve bundle space (particularly on the left-hand side into nerve 5 from the metathoracic ganglion and posteriorly from the mesothoracic ganglion). It also appears that the remaining right connective becomes broader towards the mesothoracic ganglion.

A

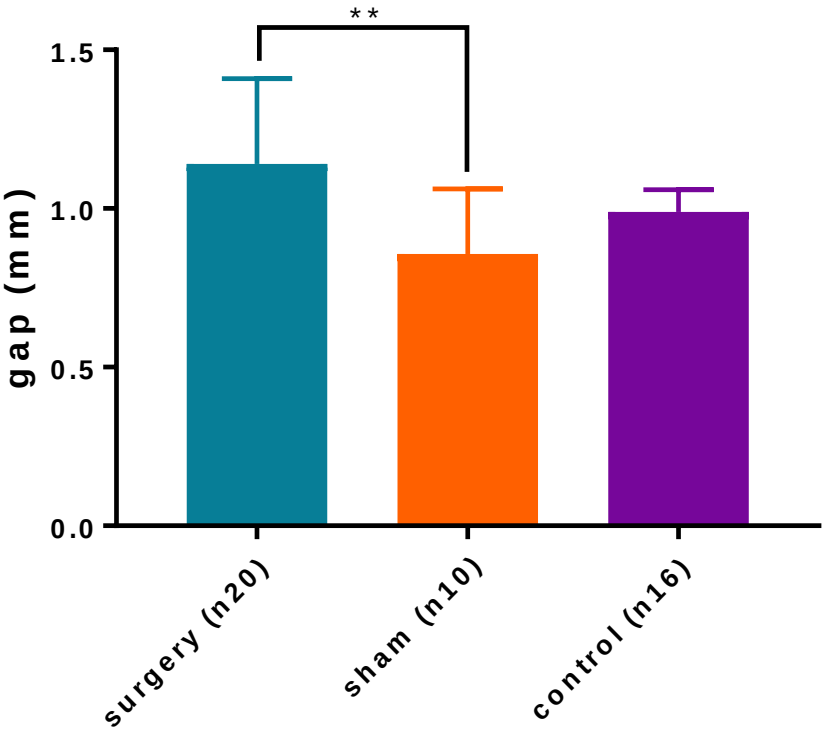

B

	surgery (n20)	sham (n10)	control (n16)
Mean	1.141	0.857	0.9888
Std. Deviation	0.2687	0.205	0.07022

Figure 5-4: Distance between the meso- and metathoracic ganglia increases in adult desert locust that undergo nerve cutting surgery at third instar. A: Locusts that had undergone the nerve cutting surgery had a significantly larger distance between the meso- and metathoracic ganglia at rest, neither were different when compared to controls (one-way ANOVA and Tukey's multiple comparison post hoc test, **p<0.01) data is mean ± SD. **B:** mean ± SD (mm) for each group.

A

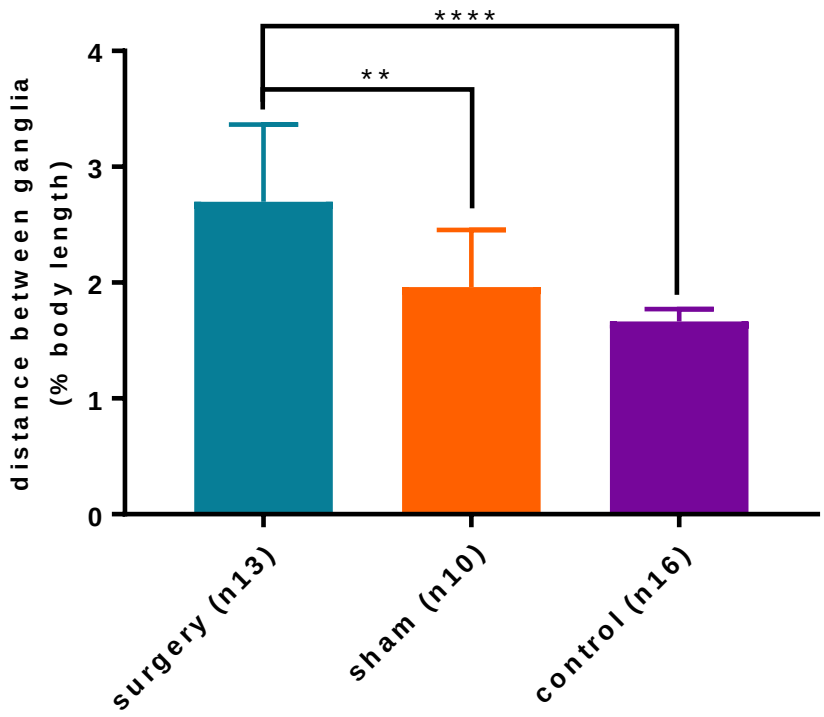

B

	surgery (n13)	sham (n10)	control (n16)
Mean	2.697	1.96	1.664
Std. Deviation	0.6669	0.4946	0.1081

Figure 5-5: The distance between the meso- and metathoracic ganglia as a percentage of overall body length increases in surgery locusts. A: Locusts that had undergone nerve cutting at third instar had a larger distance between the meso- and metathoracic ganglia when compared to shams and controls (one-way ANOVA and Tukey's multiple comparison test, **p<0.01, ****p<0.0001) data is mean ± SD. **B:** means ± SD of the lengths of the connectives between the meso- and metathoracic ganglia represented as a percentage of body length.

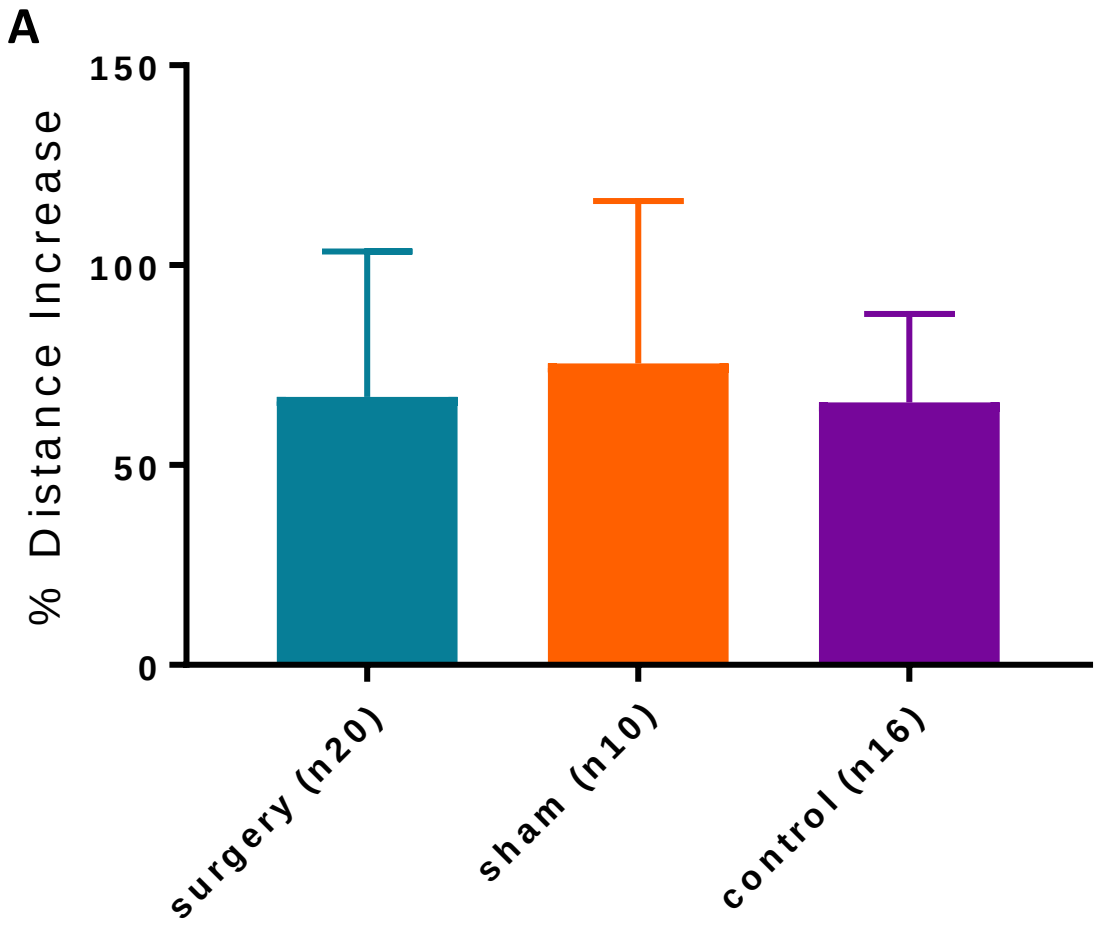

B

	Surgery	Sham	Control
Length of connectives (mm)	1.14 ± 0.27	0.86 ± 0.21	0.99 ± 0.07
Distance after severing connectives (mm)	1.85 ± 0.36	1.45 ± 0.28	1.66 ± 0.22
Distance as percentage increase	67.08 ± 36.38	75.48 ± 40.6	65.63 ± 22.17

Figure 5-6: Percentage increase in the gap between the meso- and metathoracic ganglia when the connectives between them are cut does not differ between groups. **A:** There is no difference in the percentage increase of the gap between the meso- and metathoracic ganglia when the connectives are cut when locusts undergo the cutting of the left connective at third instar or a sham procedure (one-way ANOVA, n.s) data is mean ± SD. **B:** means ± SD of the length of connectives (mm) in the surgery, sham and control groups, the distance between the meso- and metathoracic ganglia after the connectives are severed (mm) and that difference represented as a percentage increase.

5.4.3 Nerve cutting at third instar alters connective composition by increasing number of axons and decreasing the size of axons

We compared the structure of connectives from sham, surgery and unoperated control animals. The diameter of the remaining connective in operated animals did not significantly different from that of the shams or controls (control data from Chapter 4, Kruskal Wallis, H=0.7507, p=0.7056; Figure 5-7). There was also no significant difference in the thickness of the blood brain barrier between these three groups of locusts (Kruskal Wallis, H=5.002, p=0.0776; Figure 5-8).

However, there was a significant increase in the number of axons within a 1000 μm^2 area demonstrating an increase in axonal density in those locusts that had undergone surgery at third instar compared to both the shams and controls. The shams and controls were not significantly different from one another (one-way ANOVA $F(2,29)=9.11$, $p=0.0009$; Tukey's post hoc test surgery against control ($p=0.0013$) and against sham ($p=0.0033$) and sham against control ($p=0.9802$); Figure 5-9). There was also a significant difference in the cross-sectional area of axon size; the locusts that had undergone the surgery had markedly smaller axons than the other groups (Kruskal Wallis, $H=21.5$, $p<0.0001$, Dunn's post hoc surgery vs sham $p=0.0461$, surgery vs control $p<0.0001$, sham vs control $p = 0.0847$; Figure 5-10; Table 6).

A

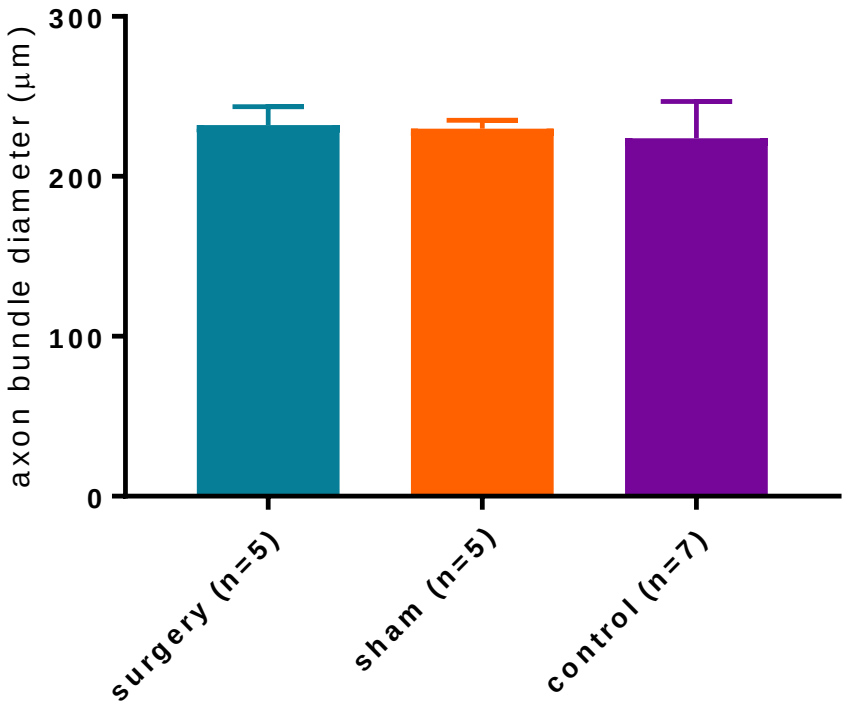

B

	surgery (n=5)	sham (n=5)	control (n=7)
Mean	232	229.9	223.8
Std. Deviation	11.51	5.096	22.96

Figure 5-7: Diameters of the connectives between the meso- and metathoracic ganglia do not differ among groups. A: Cutting the left connective at third instar had no effect on the diameter of the right connective at adulthood, nor did the sham procedure (Kruskal Wallis, n.s) data is mean ± SD. **B:** means ± SD (µm) of the diameter of the connectives between the meso- and metathoracic ganglia in surgery, sham and control desert locusts.

A

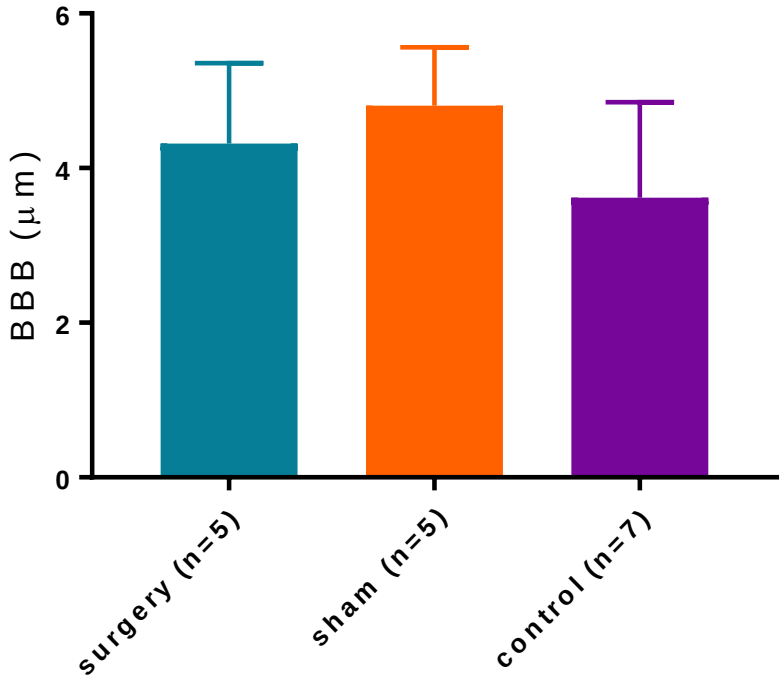

B

	surgery (n=5)	sham (n=5)	control (n=7)
Mean	4.316	4.808	3.619
Std. Deviation	1.041	0.7551	1.234

Figure 5-8: Blood brain barrier (BBB) thickness of the connectives between the meso- and metathoracic ganglia does not differ among groups. A: Cutting the left connective between the meso- and metathoracic ganglia at third instar does not alter thickness of the BBB when compared to shams or controls (Kruskal Wallis, n.s) data is mean ± SD. **B**: the mean ± SD (µm) of the thickness of the BBB in the surgery, sham and control groups.

A

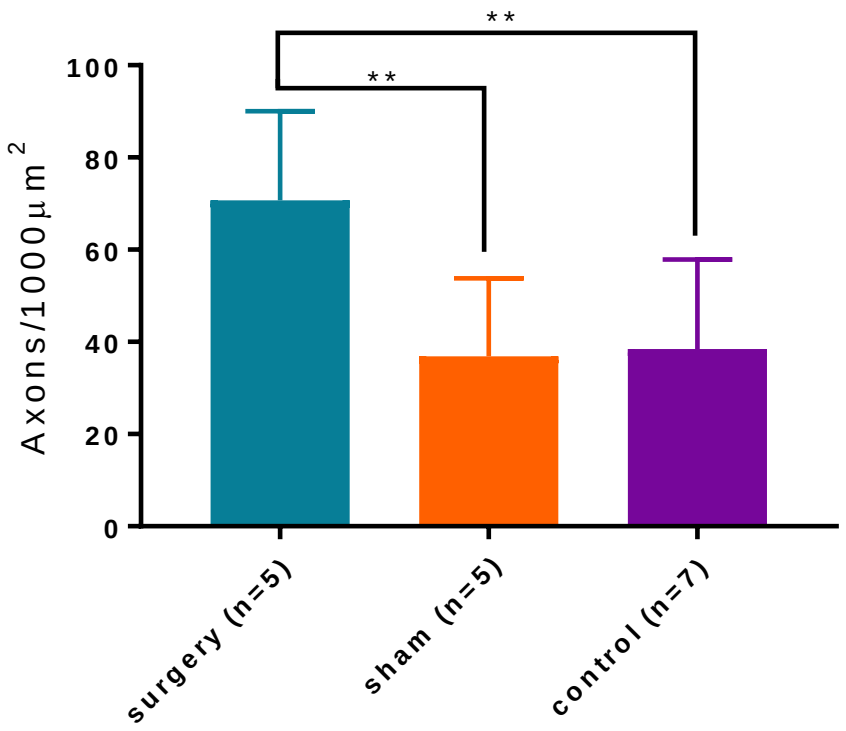

B

	surgery (n=5)	sham (n=5)	control (n=7)
Mean	70.72	36.89	38.44
Std. Deviation	19.29	16.91	19.47

Figure 5-9: Axonal density in the connective between the meso- and metathoracic ganglia is higher in the surgery group. **A:** Locusts that underwent connective cutting microsurgery at third instar had an increased axonal density within the remaining right connective when compared to controls and shams (one-way ANOVA and Tukey's post hoc test, **p<0.01) data is mean ± SD. **B:** the mean ± SD of axon density in surgery, sham and control groups.

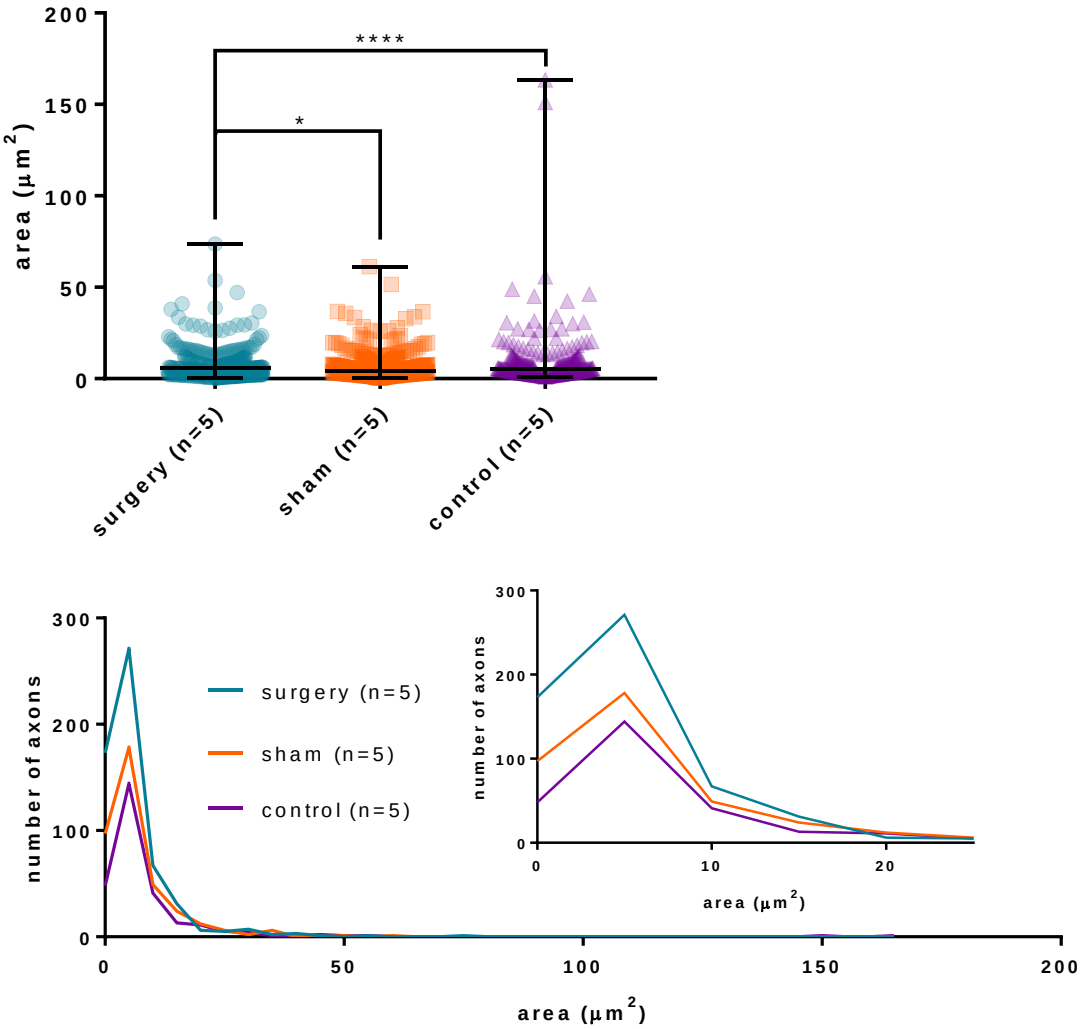

Figure 5-10: Size of axons in the connective between the meso- and metathoracic ganglia. A: Locusts that had undergone nerve cutting at third instar had axons with a smaller cross-sectional area when compared to controls or shams which were not different from each other (Kruskal Wallis and Dunn's post hoc, *p<0.05, ****p<0.0001) data is median and range. **B:** Distribution of axon area across the three connectives in full and below 25 µm^2 (inset).

Table 6: The distribution of axon cross-section area (μm^2) is positively skewed in all three groups. Data from Figure 5-10 shows the distribution of axon cross section area is positively skewed in control, sham and surgery groups.

	Surgery	Sham	Control
Mean (area μm^2)	5.987	6.855	8.777
Std. deviation	7.084	7.388	15.2
cv	118.32%	107.78%	173.21%
skew	3.984	3.058	7.32
n	568	376	274

5.4.4 Microtubule density and count are altered by nerve cutting at third instar

We compared microtubule density (microtubules/μm^2) and count (microtubules/axon) in axons in the surgery, sham and control groups. Surgery animals had a significantly higher density of microtubules than controls or shams (Kruskal Wallis, H=209.2, p<0.0001, Dunn's post hoc surgery vs sham p<0.0001, surgery vs control p<0.0001; Figure 5-11; Table 7). There was also a significant difference between shams and controls, with controls having a significantly higher density (p=0.0324). Connectives from sham operated locusts had significantly fewer microtubules per cell in comparison to surgery or control connectives (Kruskal Wallis H=71.52, p<0.0001, Dunn's Multiple comparison surgery vs sham p<0.0001, sham vs control p<0.0001; Figure 5-12; Table 8), whereas surgery animals had a greater number of microtubules than the controls (p=0.0064).

We fitted linear regression lines to examine the relationship between microtubule number and axon cross-section area in surgery animals (slope=8.719±0.2572, Y-intercept=3.216±2.384), shams (slope=3.936±0.2104, Y-intercept=4.301±2.119) and controls (slope=5.017±0.1701, Y-intercept=5.366±2.982), in all cases as axon area increase so did the number of microtubules (Figure 5-13). The relationship between microtubule number and axon size differed among the three groups (ANCOVA F(2,1212), p<0.0001). Each group was significantly different from each other group (one-way ANOVA of slopes F(2,1212)=119.8, p<0.0001; Tukey's post hoc test surgery against sham p<0.001, against control p<0.0001 and sham against control p=0.0166). The surgery group had the steepest relationship between microtubule number and axon area, followed by controls and finally shams.

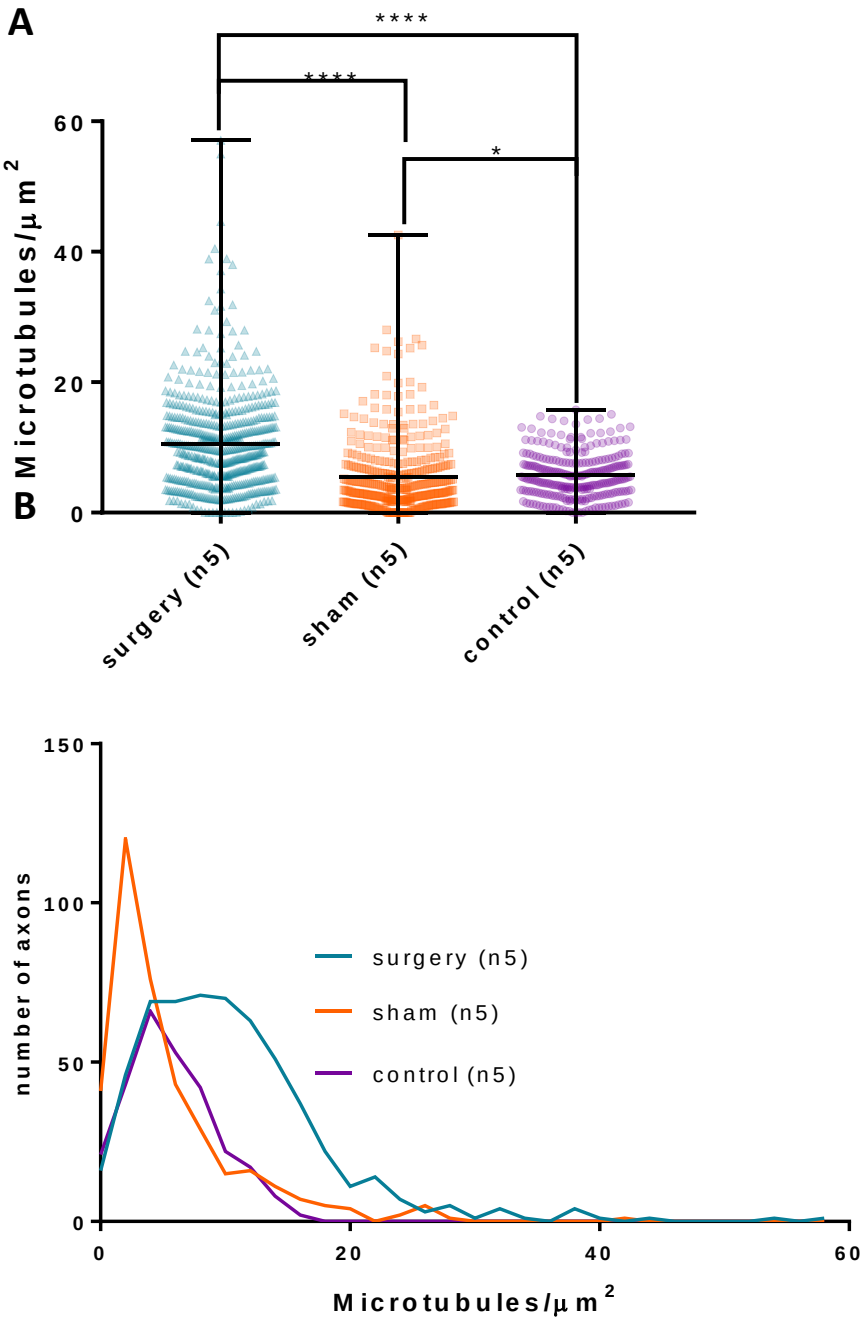

Figure 5-11: Microtubule density in the connective between the meso- and metathoracic ganglia. A: There is an increased microtubule density in the locusts that had undergone the microsurgery at third instar compared to both sham and controls. The controls also had a higher density than the shams (Kruskal Wallis and Dunn's post hoc, *p<0.05, ****p<0.0001) data is median and range. **B:** Distributions of microtubule density in each connective.

Table 7: Microtubule density has a positive skew in all groups. Data from Figure 5-11 shows that the distribution of microtubule density is positively skewed in control, sham and surgery locusts.

	Surgery	Sham	Control
Mean (microtubules/μm^2)	10.51	5.492	5.712
Std. deviation	7.421	5.604	3.49
cv	70.63%	102.03%	61.10%
skew	1.863	2.269	0.5969
n	568	376	274

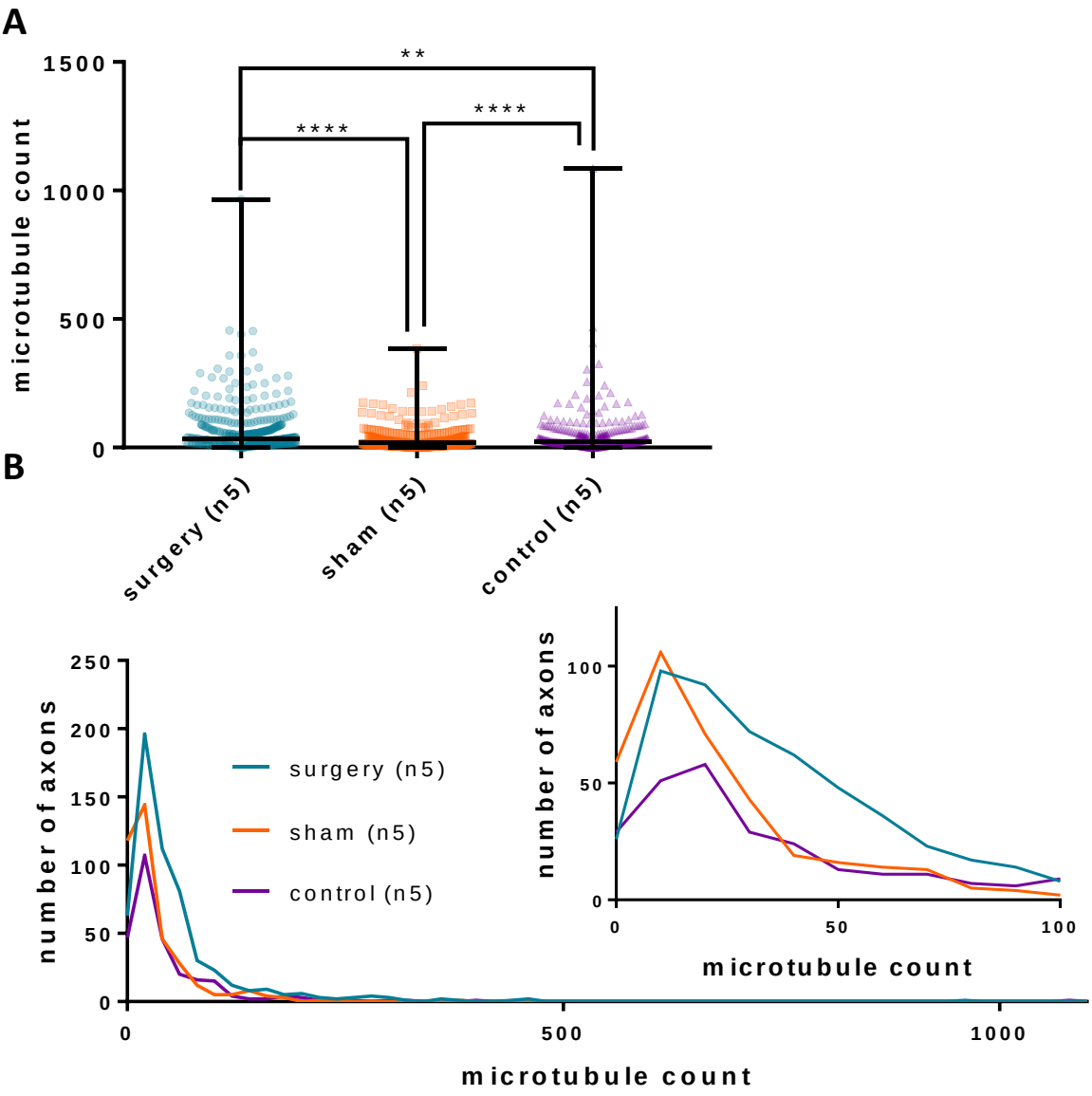

Figure 5-12: Number of microtubules per cell in the connective between the meso- and metathoracic ganglia. **A:** The average number of microtubules per axon significantly differed between all connectives. The sham group had significantly fewer microtubules than either the control or surgery group, while the surgery group also had significantly more than the control (Kruskal Wallis and Dunn's Multiple comparison, *p<0.01, ****p<0.0001) data is median and range. **B:** Distribution of microtubule number in axons in each connective in full and up to 100 microtubules/axon (inset).

Table 8: Distribution of microtubule count per axon is positively skewed across all groups. Using data from Figure 5-12 we see that control, sham and surgery locusts all have positively skewed distributions of microtubule counts.

	Surgery	Sham	Control
Mean (microtubule number)	55.42	31.28	49.4
Std. deviation	75.46	41.82	87.39
cv	136.16%	133.71%	176.89%
skew	4.975	3.37	7.236
n	568	376	274

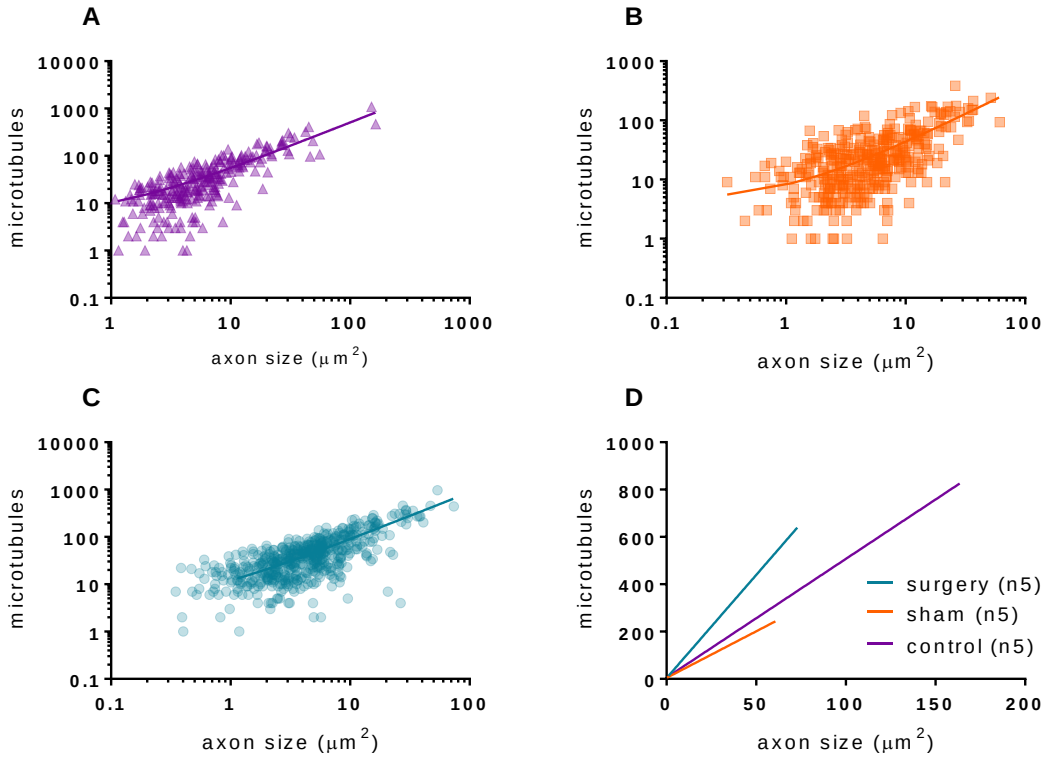

Figure 5-13: The relationship of microtubules and axon size differs among surgery, sham and control groups. Microtubule counts per axon are plotted against axon size for **(A)** control, **(B)** sham, and **(C)** surgery groups on log10 axes. D shows linear axes and the linear regression lines for each group; R^2: surgery = 0.67, sham = 0.4834, control = 0.7618.

5.4.5 Connectives remaining after third instar surgery are as strong as both connectives in control and sham desert locusts

We used uniaxial loading to test the maximum force that surgery, sham and control connectives could withstand. We compared the single remaining connective in the surgery locusts to the pairs of connectives in shams and controls. In comparison to controls, there was no significant difference in the total force (cN) prior to breakage in sham or surgery connectives (Kruskal Wallis, H=5.528, p=0.0630; Figure 5-14). The single remaining connective in surgery animals could be stretched a greater distance than the paired connectives of controls but not shams (Kruskal Wallis H=6.788, p=0.0336; Dunn's post hoc test surgery against control p = 0.0301 and sham p=0.9464 and control against sham p =>0.9999; Figure 5-15). When normalised as a percentage increase from *in vivo* length there was no significant difference between the elasticity of the groups (Kruskal Wallis, H=2.067, p=0.3746; Figure 5-16).

We also estimated the forces experienced by the connectives *in vivo*. We measured the length *in vivo*, then calculated the force required *ex vivo* for connectives to reach the same length. There were no differences between the forces experienced (Kruskal Wallis H=4.454, p=0.1074; Figure 5-17).

A

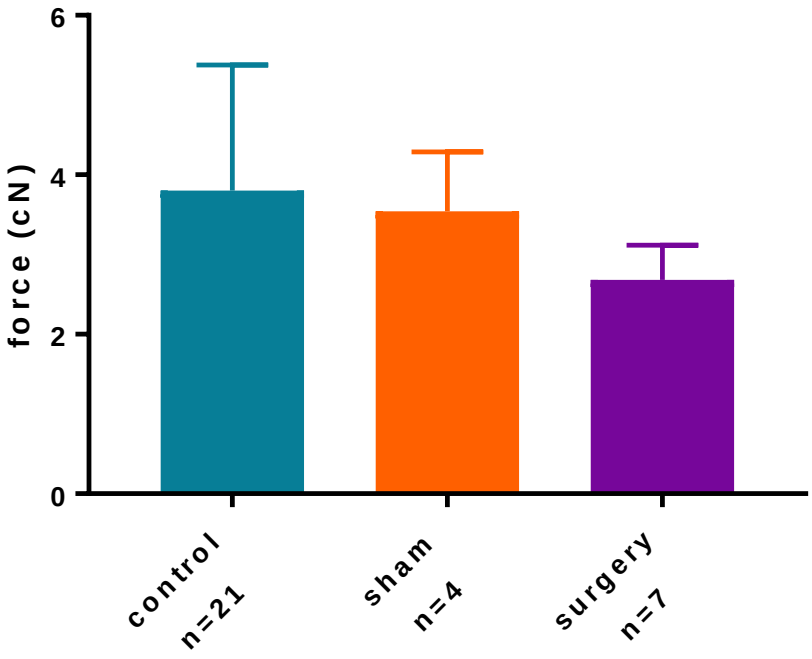

B

	control n=21	sham n=4	surgery n=7
Mean	3.805	3.543	2.685
Std. Deviation	1.574	0.7456	0.4342

Figure 5-14: The maximum force experienced by connectives between the meso- and metathoracic ganglia is not altered by third instar sham or full surgery. **A:** The force (g) experienced by the connectives just prior to breakage is no different across groups (Kruskal Wallis, n.s) data is mean ± SD. **B:** mean ± SD (cN) of the maximum force measured for each group.

A

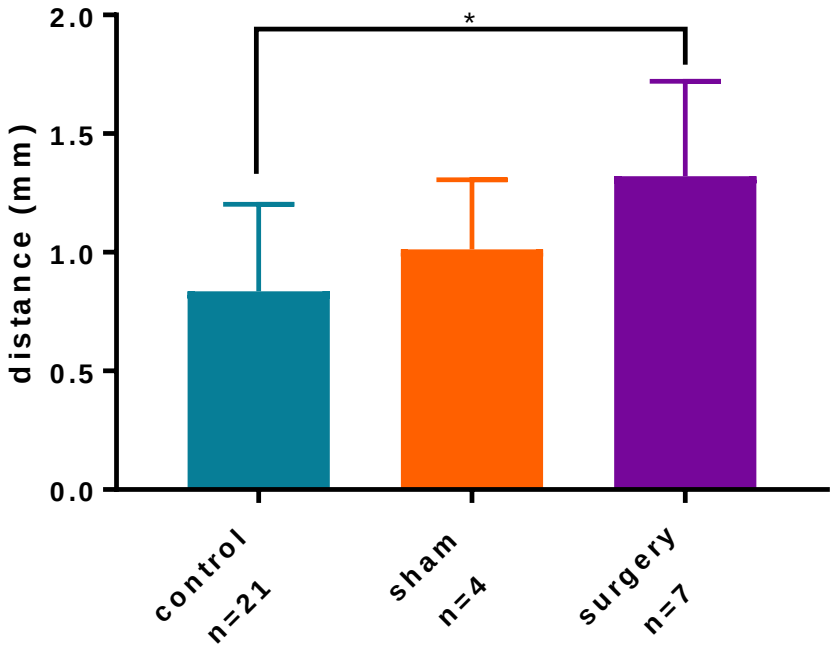

B

	control n=21	sham n=4	surgery n=7
Mean	0.8357	1.013	1.321
Std. Deviation	0.3661	0.2926	0.3999

Figure 5-15: The connectives of locusts that underwent connective cutting at third instar can be pulled a greater distance before breaking. A: The distance moved by the micromanipulator before connectives experienced failure (loss of force) was greater in locusts that had undergone the full connective cutting surgery at third instar than controls (Kruskal Wallis with Dunn's post hoc tests, *$p<0.05$) data is mean ± SD. **B:** mean ± SD (mm) of the distance the connectives were stretched prior to critical failure in each group.

A

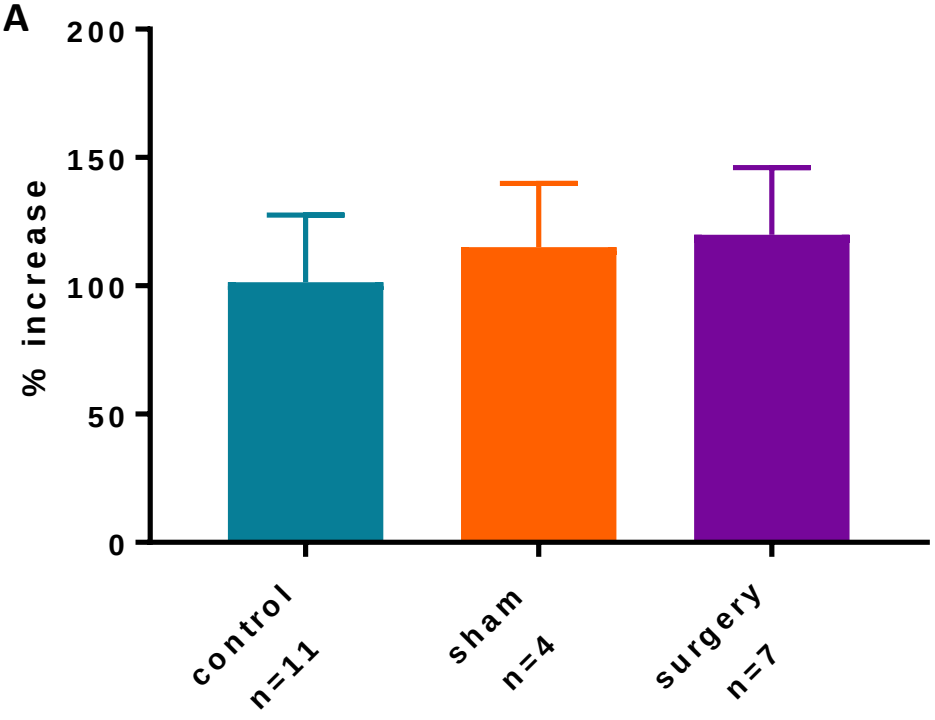

B

	Control	Sham	Surgery
Length of connectives *in vivo* (mm)	0.8695 ± 0.125	0.872 ± 0.1075	1.126 ± 0.3053
Distance stretched (mm)	0.8909 ± 0.299	1.013 ± 0.2926	1.321 ± 0.3999
Percentage increase	101.4 ± 26.16	115.1 ± 24.78	119.9 ± 26.2

Figure 5-16: The percentage increase in connective length before breaking when compared to *in vivo* length is the same across all groups. A: When the length of connectives just prior to breakage is represented as a percentage increase compared to *in vivo* length there is no difference between the three groups of desert locusts (Kruskal Wallis, n.s) data is mean ± SD. **B:** the mean ± SD of the lengths of connectives in surgery, sham and control locusts (mm), the distance they were stretched (mm) and the percentage increase caused by stretch.

A

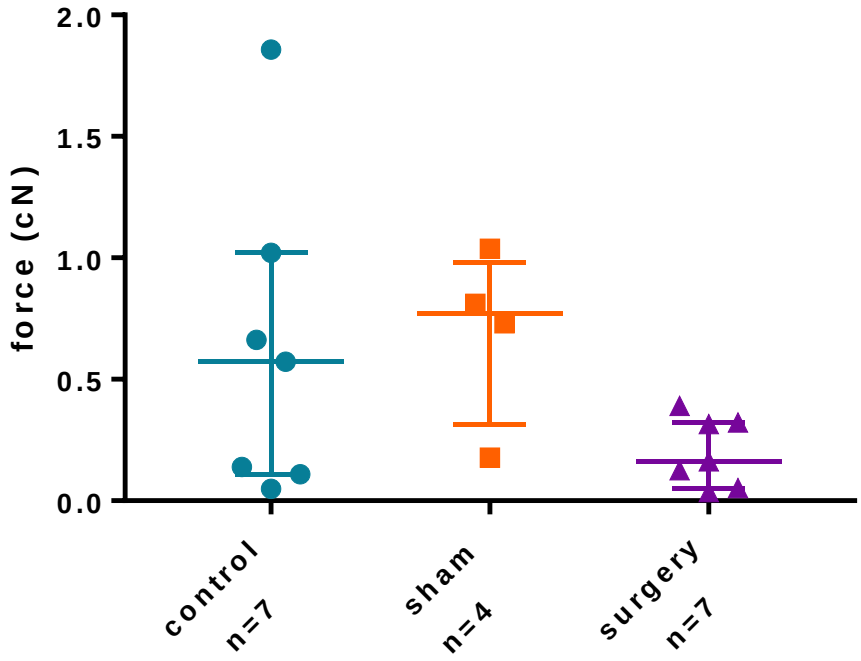

B

	control n=7	sham n=4	surgery n=7
Mean	0.6306	0.6888	0.2006
Std. Deviation	0.6473	0.3644	0.142

Figure 5-17: Forces experienced by connectives *in vivo* are the same across control, sham and full third instar connective cutting surgery. **A:** By measuring the forces experienced at the same length as found *in vivo* we were able to approximate the *in vivo* forces and found no differences across groups (Kruskal Wallis, n.s) data is median and interquartile range. **B:** mean ± SD of the *in vivo* forces (cN) experienced by each bundle.

5.5 Discussion

We have found that tension in the connectives between the meso- and metathoracic ganglia remains the same throughout growth from third instar via microdissections. We have also found that tension is maintained when internal forces are changed by ablation of a single connective at third instar. We find that carrying out connective severing surgery at third instar led to morphological changes, including smaller body size and longer remaining connectives. The composition of the connectives also changed, there were more and smaller axons with a higher number and density of microtubules. Single connectives were also equally as strong as pairs of control and sham connectives, had the same proportional elasticity, and were under similar forces *in vivo.* Together these results suggest that there is a 'set-point' of tension in these connectives that is actively maintained.

5.5.1 Tension in the connectives between the meso- and metathoracic ganglia does not alter throughout growth in desert locusts

Throughout growth, the connectives between the meso- and the metathoracic ganglia grow. At all stages cutting the connectives causes an increase in the separation of the ganglia. This separation remains proportionally similar throughout growth. This consistency throughout development contradicted our hypothesis that the nerve cord would grow reducing tension immediately prior to moulting. This may occur between the late fourth and mid fifth instars, however because these two points are only different to each other and not the ones either side it does not seem like there is a loss of tension in the fourth instar nor again prior to moulting in the fifth instar. We cannot discount this result, however it fails to produce a pattern we can explain. This

experiment only included locusts in the middle of the instar (at least 1 week post moult) and late in the instar (while individuals were pharate). It is possible that, rather than a change prior to moulting, there is a transient increase in tension during and just after moulting due to both the changing body size and the internal pressures (Chapman, 2013). However, investigating this using our current protocol would be impossible as the process of mounting the locusts produces external forces prior to sclerotization (Chapman, 2013; personal observation).

5.5.2 Severing a single connective at third instar altered the composition of the remaining connective at adulthood

Transmission electron microscopy (TEM) study showed revealed a nearly two-fold increase in density of axons in the surgery connective in comparison to sham and control connectives. However, there were more axons in the surgery connectives than the sham and control, these axons were generally smaller and thus the connective remained the same size as control and shams. This is evidence of rewiring in the central nervous system, it is unclear if this a rewiring of damaged neurons or neurogenesis and it is also interesting that the average area of axons decreases, and the connective diameter remains the same rather than the connective increasing in diameter.

In this chapter we further relate the presence of microtubules in the longitudinal orientation with tension on a macroscopic scale and strength of axon bundles. Like axon density, microtubule density also increased around two-fold and average microtubule count also increased in the remaining connective in surgery locusts. Currently we do not know if this represents an increase in overall microtubule production or if a greater proportion of the pool of microtubules are recruited to this orientation. Determining

this would distinguish between whether the change in the cytoskeleton of post-surgery connectives is due to realignment of existing cytoskeletal elements to the increase in applied force, or whether there is active up regulation of the expression of these elements.

We found that when comparing the relationship between the number of microtubules and axon cross-section area that the surgery group had a much steeper relationship than either control or sham and that sham had the least steep relationship. This shows that this relationship is not fixed in axon bundles but can change in response to changing forces/wounding. In chapter 4 we found this relationship was less steep in axon bundles that were not under tension *in vivo* however we did not know if axon bundles under tension therefore produced more microtubules in the longitudinal orientation, or if an increased number of microtubules in orientation for a different reason (for example, increased transport needs) caused increased tension via contraction. The results from this chapter indicate that forces axon bundles experience *in vivo* may drive the production of microtubules in the longitudinal orientation.

5.5.3 Uniaxial loading shows single connectives remaining after third instar surgery are as strong and elastic as control and sham pairs

We found no difference in the strength of pairs of connectives between the meso- and metathoracic ganglia in the sham and control locusts and the singular connectives that remain after third instar surgery. This could suggest that the single connectives adapt to internal forces and become stronger, possibly as a consequence of more tightly packed axons, a higher number of microtubules or a change in cytoskeleton elements not

studied in this thesis. Alternatively, this result could be explained by the fact that we are not simply testing the tensile strength of the connectives via our protocol (see Chapter 4). During the protocol the meso- and metathoracic remain attached to the connectives and are affixed to the equipment. The lack of difference between these connectives could be explained by a lack of change in the strength of the connection between the connectives and the ganglia which would not necessarily alter due to the loss of a connective.

While this result is ambiguous, uniaxial loading also revealed that in real terms the remaining surgery connective could be stretched a further distance, but when corrected for initial length had the same level of elasticity as the sham and surgery connectives. This aligns with previous results from Chapter 4 where we found no difference in elasticity between the connectives between the meso- and metathoracic ganglia, the connectives between the metathoracic ganglia and fourth abdominal ganglia or nerve 5, despite differences in dimension and microtubule numbers. This suggests that the elasticity of axon bundles does not necessarily relate to *in vivo* forces experienced or strength.

We also used uniaxial loading to estimate forces *in vivo*. A similar concept has been used previously to show stress in the lamprey spinal cord (Luna *et al.*, 2013). We found that the forces exerted on the surgery, sham and control connectives did not differ. This further supports our theory that the single connective in the surgery locust was exposed to a greater level of force when surgery was initially carried out but grew to compensate for that change in force and stopped when the 'set point' of tension was reached.

5.5.4 Stretch growth occurs in surgery locusts but some tension remains

Stretch growth is the term given to the growth of integrated axons that occurs after embryogenesis (Smith, 2009). Currently, the mechanisms are poorly understood although two hypotheses have been proposed to explain how stretch growth occurs (Heidemann and Bray, 2015; Purohit and Smith, 2016). Both hypotheses describe stretch growth as a passive process, with axons stretching as they are pulled by surrounding growing tissue. It is the mechanism of this growth that differs between the two hypotheses.

In this chapter we see evidence of stretch growth, upon severing one connective at third instar the remaining connective is exposed to a greater amount of force and increases in length compared to controls and shams at adulthood. However, the remaining connective stops growing at the point it is under the same amount tension and *in vivo* force as occurs in controls. This seems to be incompatible with existing hypotheses that attempt to explain stretch growth. Our results suggest one of two possibilities: (1) stretch growth is passive, but requires a certain amount of force before growth is initiated, (2) axon bundles have a 'set point' of tension that either (a) is actively regulated in a way that prevents or stops stretch growth or (b) is actively regulated in a way that resists stretch growth. The former seems unlikely because other axon bundles in the desert locust are under less or no tension and therefore have grown to a completely unstressed position throughout growth (Chapter 3). Thus, the second hypothesis seems more likely, however whether stretch growth is stopped or resisted is unclear. In the locust, axon bundles grow to a 'set point' of stress that is unique to each bundle. Currently, only the Purohit and Smith (2016) hypothesis has the potential for

such regulation. This suggests that mechanosensitive ion channels in the axon may signal for growth to occur and theoretically these ion channels could be regulated, for example in number or sensitivity. Candidate channels are not suggested in the Purohit and Smith (2016) hypothesis, however Piezo channels may be potential candidates (Coste *et al.*, 2010).

5.5.5 Axonal tension set-points suggest functionality

We suggest that axon bundles have a 'set-point' of tension that is reached prior to third instar and maintained throughout growth. We have found that altering forces that connectives are exposed to, by ablating a single connective, causes anatomical changes such as a lengthening of the connective and cellular changes, including an increase in microtubules in axons, but does not alter tension. The maintenance of a 'set point' of tension in axons may suggest a level of functionality. Currently, despite finding axonal tension in adult vertebrates (Xu *et al.*, 2009, 2010; Luna *et al.*, 2013) no theory of function has been put forward. In individual axons, it has been suggested that tension may lead to efficient arrangements of membrane channels (Xu *et al.*, 2013; Zhang *et al.*, 2017) and proteins linked with maintaining axon tension may be protective against damage caused by motion (Hammarlund *et al.*, 2007).

5.5.6 Axonal tension and ventral nerve cord morphology

Van Essen (1997) hypothesised that axonal tension drives the gross morphology of the nervous system. Although the formation of sulci and gyri in the human brain are thought be explained by other mechanisms that do not involve axon tension (Xu *et al.*, 2010; Ronan and Fletcher, 2014; Kasthuri *et al.*, 2015; Razavi, Zhang, Liu, *et al.*, 2015), axonal

tension may explain the morphology of other nervous system structures. We have previously shown axonal tension present in the *S. gregaria* nervous system (Chapter 3), by altering these forces through connective cutting surgeries at third instar we have drastically altered morphology of the nervous system. The remaining connective between the meso- and metathoracic ganglia increases in length. While we did not fully explore the entire anatomy of these individuals, an increase in the length of one connective must have knock on effects and alter the morphology or positioning of other structures. For example, the metathoracic ganglion may have shifted posteriorly or the mesothoracic ganglion anteriorly. While from these results we cannot say whether axonal tension has driven morphology or if morphology leads to the emergence of tension, the two are closely twinned.

5.5.7 Third instar surgery caused morphological changes but had negligible impact on behaviour

The adults of both the sham and the surgery groups were smaller than their control counterparts, likely because of the healing process diverting resources otherwise required for growth. However, despite smaller body size the surgery locusts grew a longer connective between the meso- and metathoracic ganglia, had a higher number of axons in the connective and an increase in microtubules in longitudinal orientation in these axons. The sham locusts had no obvious morphological changes, however did have a reduced microtubule count. This reduction in microtubules in the longitudinal orientation in sham-operated locusts may be a response to wounding; the consumption of energy for wound repair could consume energy needed for microtubule generation. Alternatively, wounding reduces the overall size of the adult locusts, which may indirectly reduce the microtubule generation. Either alternative implies that the

increase in microtubules in post-surgery locusts that have also experienced wounding is even greater than the difference between these locusts and the control animals.

By the time surgery locusts reached adulthood it was very difficult to tell the difference between them and controls or shams in terms of behaviour, although of course surgery and sham locusts were markedly smaller. Certainly, the surgery locusts were not paralysed in the limbs that should be affected by the loss of the left connective (the second and third legs on the left, see Figure 1-4 in General Introduction, Burrows, 1996). This is perhaps to be expected as previous studies have shown that transection of connectives minimally affects flight behaviour even with hemisection of ganglia in adults (Ronacher *et al.*, 1988; Wolf *et al.*, 1988) suggesting a remarkable robustness to behaviour even without the opportunity for rewiring. Behavioural experiments, such as self-righting studies, would be interesting to see if behaviour was affected to confirm observations. We have observed an increase in axonal density in the connectives of the surgery locusts which may indicate rewiring of damaged neurons or growth of new projections to replace those damaged by the surgery. Previous work has shown regeneration of neurons in developing *L. migratoria* (Patschke *et al.*, 2004) and even axonal sprouting in adult insects after injury (Butler and Lakes-harlan, 2011).

5.5.8 Is tension found in other insects?

We have found that tension is present in the connectives between the meso- and metathoracic ganglia in *S. gregaria* but not in other axon bundles. We have found that this is reflected in the number of microtubules in individual axons of these axon bundles. In this chapter we have also suggested that the tension may be actively regulated and that this regulation may also be linked to an increase in microtubules. To begin to

explore if these traits are more universal we next look to the same connective, between the meso- and metathoracic ganglia in other insects. First, we look at solitary locusts, members of the same species but with different development and slightly different anatomy; *Locusta migratoria* a different species yet with very similar body and VNC anatomy and then branch to other orthopteroid insects to examine if the features found in the locust are applicable elsewhere.

6 Properties of the connectives between the meso- and metathoracic ganglia differ among species

6.1 Abstract

Tension is present in the meso- to metathoracic connectives in the VNC of the desert locust. Whether this tension is conserved among species is currently unknown but could be important for understanding its role. Comparison of homologous axon bundles and their properties could distinguish between whether tension has a function and is selected for during evolution or is a more indirectly emergent property due to surrounding tissue mechanics. Here we compare the homologous meso- to metathoracic connective of solitary desert locusts and migratory locusts, which have a similar VNC structure, to our original findings in the gregarious desert locust. We also compared two more distantly-related species, crickets (*Gryllus bimaculatus*) and cockroaches (*Periplaneta americana*). Tension is similar among the different locusts including the gregarious desert locust, but both *G. bimaculatus* and *P. americana* have significantly different levels of tension within the homologous connectives linking the meso- to metathoracic ganglia. This difference in tension is reflected in the number and density of microtubules. There were also species differences in responses to uniaxial loading *ex vivo*, though these did not reflect tension found via microdissection. We find that a steep relationship between microtubule number and axon size indicates an axon bundle under high tension, whereas a shallow relationship between the two indicates

axon bundles under low or no tension, and that this pattern holds true among species. Our results suggest that axonal tension may, in part, be a functional adaptation, but is constrained by surrounding anatomy.

6.2 Introduction

Tension is present in the connectives between the meso- and metathoracic ganglia of the desert locust, and is related to microtubules in the perpendicular orientation to the plane of tension observed and longitudinal orientation along the axon (Chapters 3, 4). The amount of tension is not universal within the desert locust, with both nerve 5 and the connectives between the metathoracic and fourth abdominal ganglia showing much less tension and different microtubule patterns. Here we investigate if tension and its relation to microtubule number and density is conserved across species. By looking at other species we also begin to address if tension is a universal property or the product of evolution through natural selection. We compare the homologous region of the VNC, the connectives between the meso- and metathoracic ganglia, in several orthopteroid insects. Two of these species have similar VNC structures whereas the other two retain the connectives between the meso- and metathoracic ganglia but differ in the extent of fusion in the metathoracic ganglion (Niven *et al.*, 2008, see General Introduction Figure 1-4).

Solitarious desert locusts are morphologically and behaviourally distinct from their gregarious counterparts; gregarious locusts are generally smaller and have a larger brain size (Pener and Simpson, 2009; Ott and Rogers, 2010), they are diurnal and form swarms whereas solitary locusts are cryptic and actively avoid other locusts (Roessingh *et al.*, 1993; Homberg, 2015), they also differ in colouring which somewhat reflects the

different behaviours (Pener and Simpson, 2009). Migratory locusts (*Locusta migratoria*), another phylogenetically distinct species from the Acrididae family with similar gross anatomical features to *S. gregaria.* Migratory locusts permit comparison of similar VNC morphology and gross anatomy yet distant phylogenetic positions.

The comparison can be extended to more phylogenetically distant orthopteroids (Wheeler *et al.*, 2001): the black cricket (*G. bimaculatus*) and the American cockroach (*P. americana*). Black crickets are orthopterans whereas American cockroaches are from the order Blattodea (though they were previously grouped within the orthopteroidea). The black cricket has a metathoracic ganglion comprised of three neuromeres, whilst the metathoracic ganglion of the cockroach is comprised of only two neuromeres (Niven *et al.*, 2008). In all of these species the metathoracic ganglion is positioned anteriorly to at least some of its peripheral structures.

Here we perform microdissections, severing the connectives between the meso- and metathoracic ganglia in all four of the insect species. TEM and uniaxial loading experiments allowed us to determine the relationship between microtubules and tension of these orthopteroid species. We demonstrate that the slope of the relationship between microtubule number and axon area is indicative of *in vivo* tension exerted on the axon bundle, and this is conserved among species. This supports the hypothesis that tension is actively maintained and functional. We also relate morphology of the VNC to *in vivo* axon bundle tension.

6.3 Methods

Techniques in this chapter are described in Methods 2.2.6, 2.2.9, 2.2.10.

6.4 Results

6.4.1 Desert locust phase does not alter tension between the meso- and metathoracic ganglia

We compared solitary locusts with age and colony matched gregarious locusts and those from our own colony (control). Solitary females were significantly larger than gregarious males (Kruskal Wallis H=23.22, p=0.0003, Dunn's post hoc test solitary female vs colony-match males p=0.0005, solitary female vs control males = 0.0021; Figure 6-1). Severing a single connective had no effect on the separation between the meso- and metathoracic ganglia (one-way ANOVA, F(1.041,15.61)=82.42, p<0.0001 with Geisser-Greenhouse's correction for repeated measures Ɛ=0.5204 and Tukey's multiple comparison test, intact vs left cut p=0.0871; Figure 6-2). Severing both led to a significant separation of the ganglia and an increase in the distance between the two (intact vs both cut p<0.0001, left cut vs both cut p<0.0001).

Due to the larger body size of the female solitary locusts compared to gregarious males, we normalised the data as percentage increase. We also merged males and females in each group because there was no significant difference in body size between sexes in each group (solitary p=0.2350, colony-match gregarious p>0.9999, control gregarious p>0.9999). We measured the distance between the meso- and metathoracic ganglia *in vivo* before and after severing the connectives between them. There was no significant difference in the distance between the ganglia once the connectives between the meso- and metathoracic ganglia were cut when represented as a percentage increase (one-way ANOVA F(2,32)=2.882, p=0.0707; Figure 6-3).

A

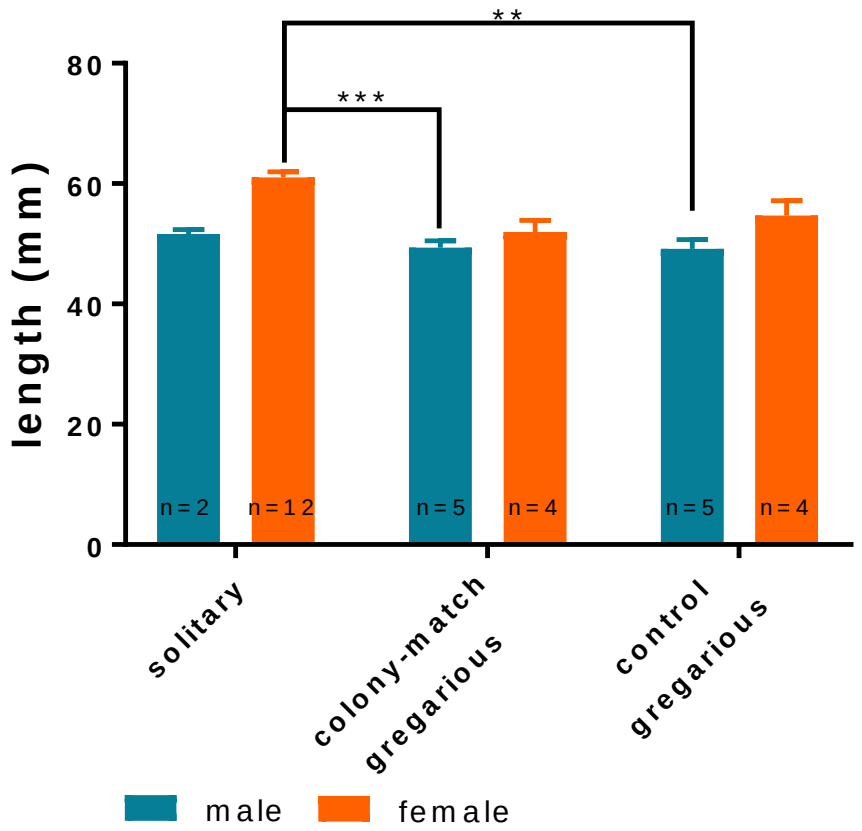

B

	Male		Female	
	Mean	SD	Mean	SD
solitary	51.60	1.38	61.05	3.08
colony-match gregarious	49.36	2.58	51.97	3.88
control gregarious	49.13	3.52	54.70	4.87

Figure 6-1: Solitary female desert locusts are larger than male gregarious desert locusts. **A:** Solitary female locusts were significantly larger than gregarious males (Kruskal Wallis and Dunn's post hoc test, **p<0.01, ***p<0.001) data is mean ± SD. **B:** mean ± SD (mm) of body lengths in solitary, gregarious colony-matched and control desert locusts.

A

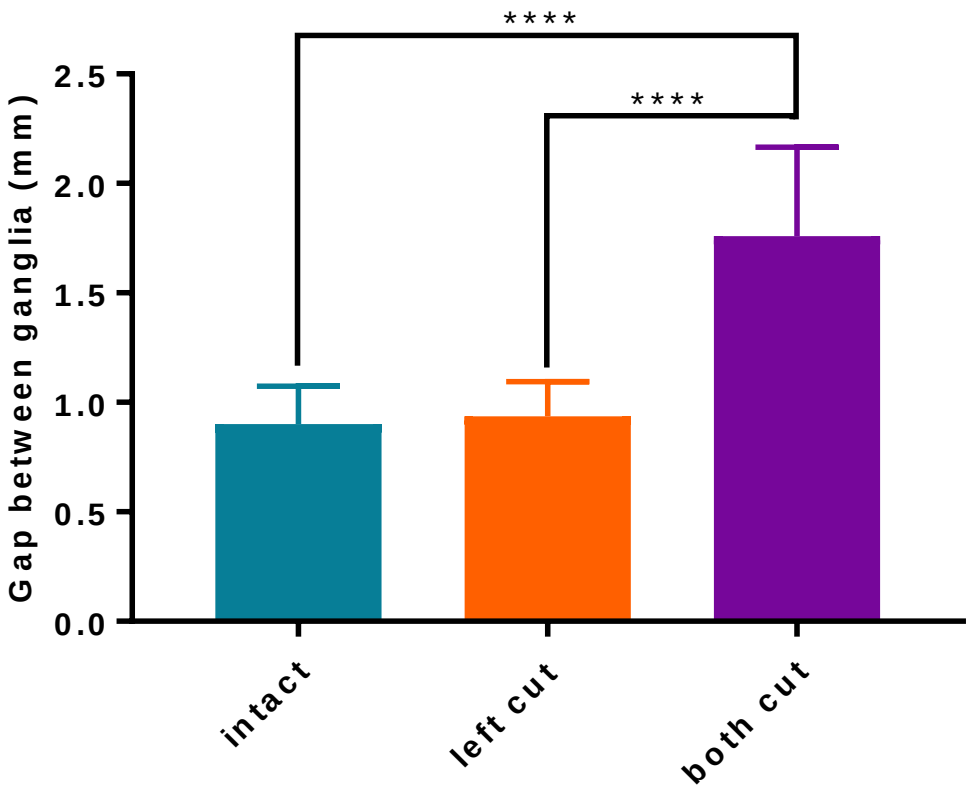

B

	intact	left cut	both cut
Mean	0.9004	0.9371	1.76
Std. Deviation	0.1726	0.1582	0.4053

Figure 6-2: Severing both connectives between the meso- and metathoracic ganglia increases the separation of the ganglia in solitary desert locusts. A: Cutting the left connective had no effect on the distance between the ganglia, but cutting both led to a dramatic increase in the distance (one-way ANOVA with Geisser-Greenhouse's correction for repeated measures and Tukey's post hoc test, ****$p<0.0001$) data is mean ± SD. **B:** mean ± SD (mm) of the separation between the meso- and metathoracic ganglia.

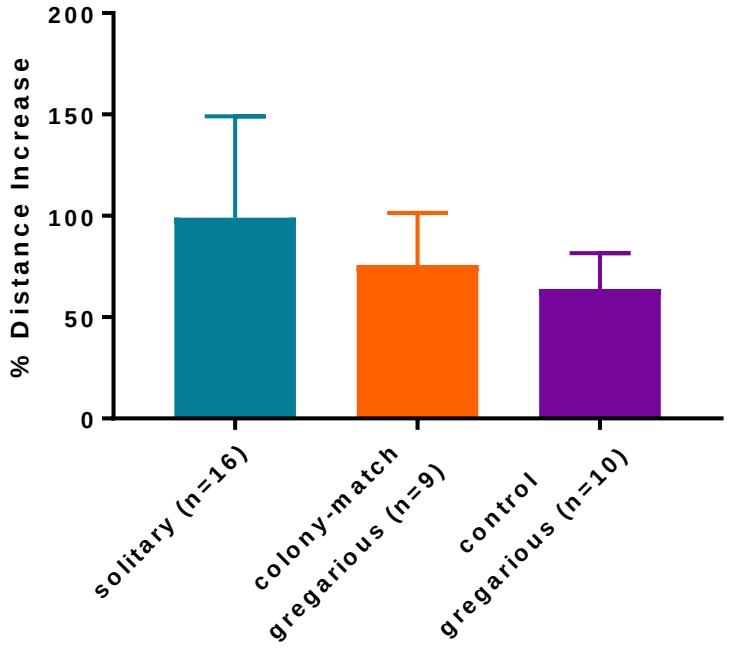

	length of connectives (mm)		Separation after severing connectives (mm)		Separation as percentage increase	
	Mean	SD	Mean	SD	Mean	SD
solitary (n=16)	0.9004	0.1726	1.76	0.4053	99.04	50.01
colony-match gregarious (n=9)	1.016	0.1427	1.799	0.4172	75.83	25.55
control gregarious (n=10)	1.009	0.1165	1.661	0.3179	63.97	17.56

Figure 6-3: The extent the meso- and metathoracic ganglia separate after connectives are severed is the same in gregarious and solitary locusts. A: There is no difference between any of the groups of locusts in regard to the percentage increase when the connectives between the meso- and metathoracic ganglia are cut (one-way ANOVA n.s) data is mean ± SD. **B:** mean ± SD of the length of connectives in each group (mm), the separation of the meso- and metathoracic ganglia after connectives were cut, and the increase in separation represented as a percentage increase.

6.4.2 Tension in connectives between the meso- and metathoracic ganglia does not differ between *S. gregaria* and *Locusta migratoria*

Next we compared the desert locust to another acridid grasshopper with similar morphology. We first measured body length, finding no differences between the sexes of each species (one-way ANOVA $F(3,26)=17.48$, $p<0.0001$; Tukey's multiple comparisons, *L. migratoria* $p=0.2143$, *S. gregaria* $p=0.993$; Figure 6-4). *L. migratoria* were smaller than *S. gregaria* of the same sex (males $p<0.0001$, females $p=0.0038$). Severing a single connective between the meso- and metathoracic ganglia in *L. migratoria* had no effect (one-way ANOVA, $F(1.123,14.6)=82.55$, $p<0.0001$ with Geisser-Greenhouse's correction for repeated measures $\varepsilon=0.5617$ and Tukey's multiple comparison test, intact vs left cut $p=0.3507$; Figure 6-5). Severing both significantly increased the separation between the two ganglia (intact vs both cut $p<0.0001$, left cut vs both cut $p<0.0001$). We normalised the increase in separation of the meso- and metathoracic ganglia as a percentage increase of the length of connectives *in vivo* to compensate for differences in body size. There was no difference in the extent of tension in the connectives between the meso- and metathoracic ganglia between the two species (Mann Whitney test, two-tailed, $U=75$, $df=29$, $p=0.1306$; Figure 6-6**;** Table 9).

A

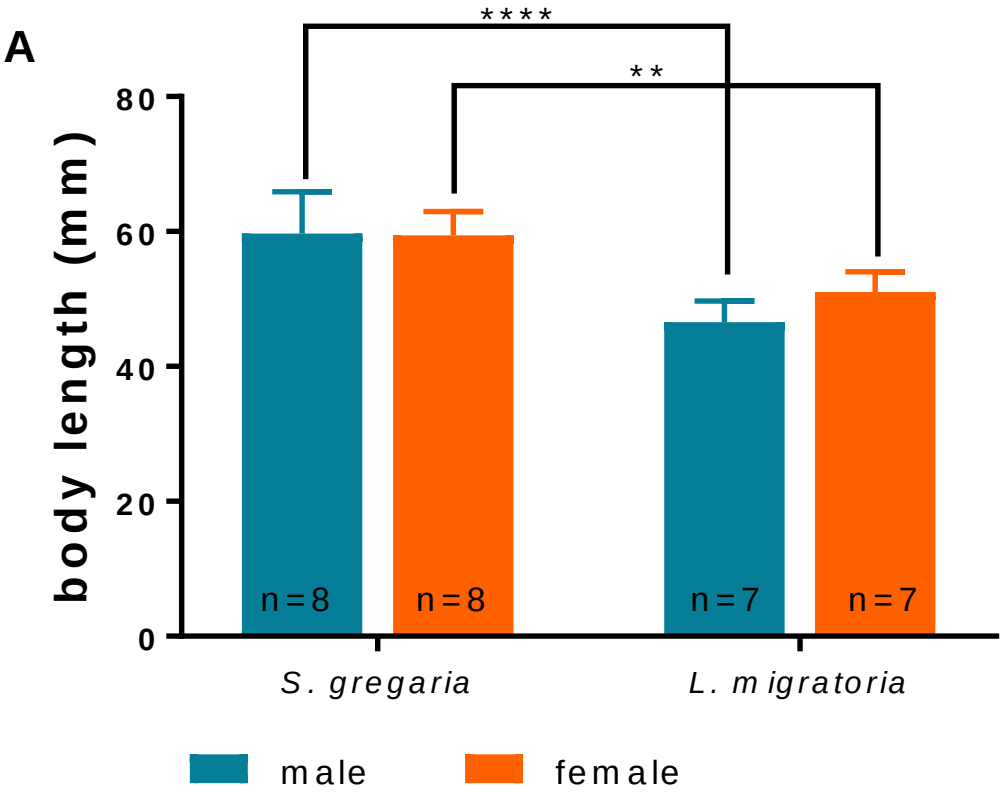

B

	male		female	
	Mean	SD	Mean	SD
S. gregaria	59.70	6.18	59.44	3.51
L. migratoria	46.54	3.14	51.06	2.96

Figure 6-4: Migratory locusts are smaller than desert locusts. **A:** *L. migratoria* were smaller than *S. gregaria* (one-way ANOVA with Tukey's post hoc test, **p<0.01, ****p<0.0001) data is mean ± SD. **B:** mean ± SD of body length (mm) of migratory and desert locusts.

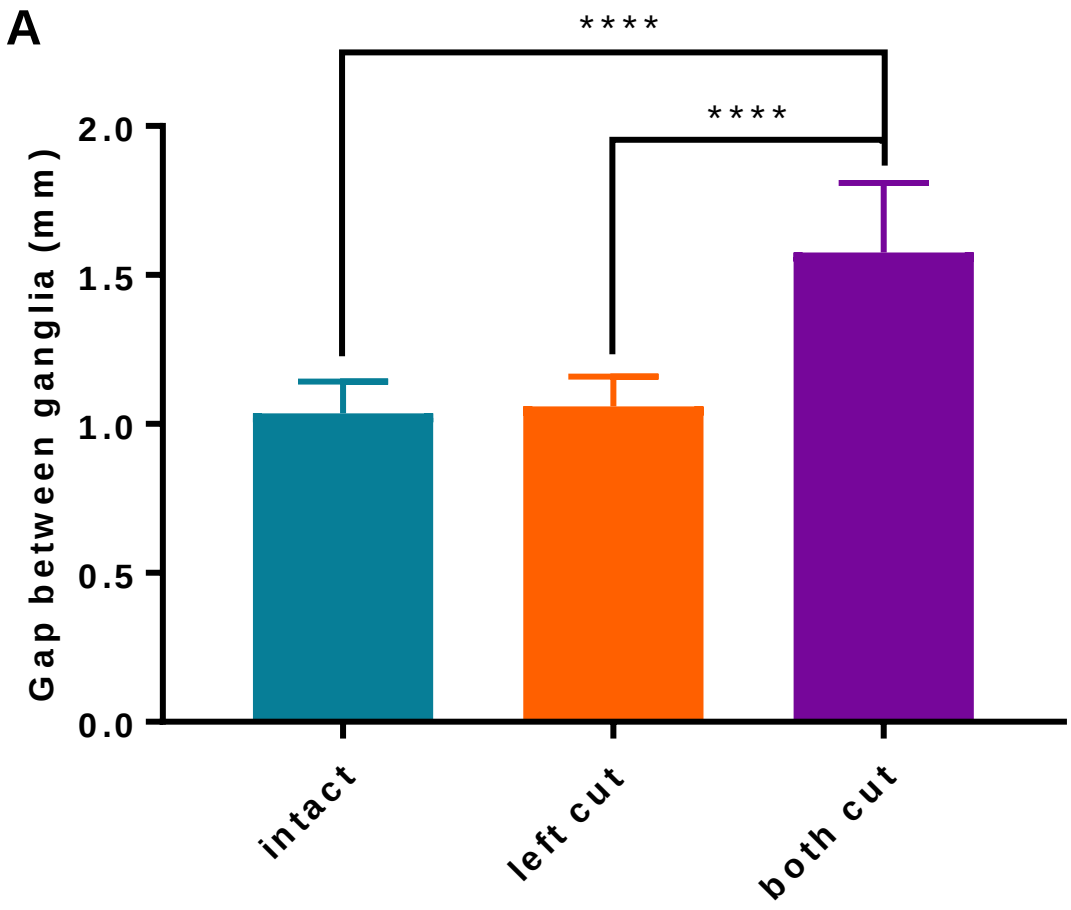

B

	intact	left cut	both cut
Mean	1.036	1.059	1.577
Std. Deviation	0.1072	0.0995	0.233

Figure 6-5: Severing both connectives between the meso- and metathoracic ganglia causes an increase in separation between the ganglia in migratory locusts. **A:** We found that severing the connectives between the meso- and metathoracic ganglia caused an increase in the distance between the two, only when both connectives were cut (one-way ANOVA with Geisser-Greenhouse's correction for repeated measures and Tukey's post hoc test, ****$p<0.0001$) data is mean ± SD. **B:** mean ± SD of the separation between the meso- and metathoracic ganglia (mm).

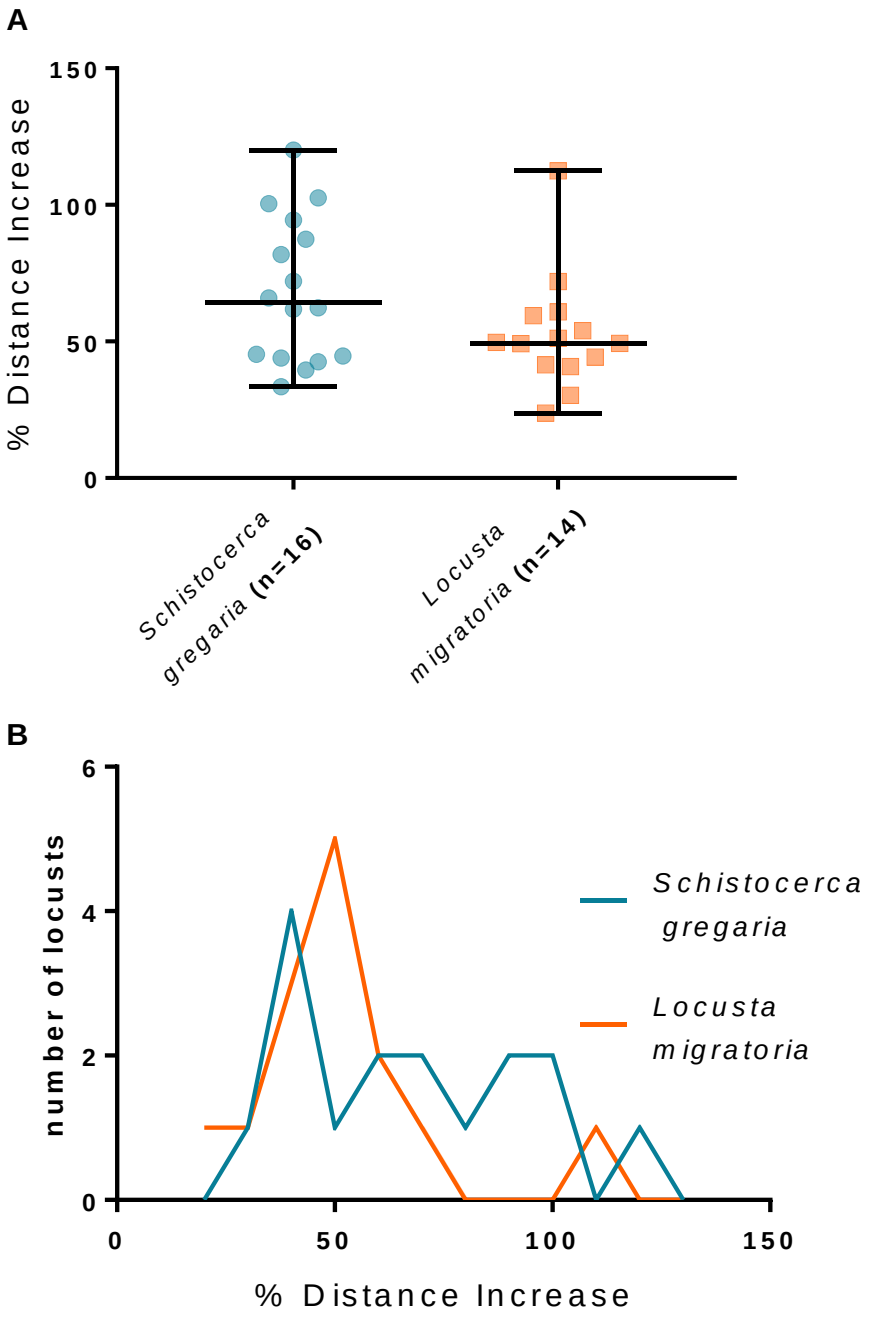

Figure 6-6: Comparison of nerve cutting microdissection between migratory and desert locusts. A: When normalised as a percentage increase in the distance between the meso- and metathoracic ganglia, there is no difference in the tension between *S. gregaria* and *L. migratoria* (Mann Whitney U test, n.s) data is median and range. **B:** Distribution of percentage increase.

Table 9: The increase in separation between the meso- and metathoracic ganglia has a positive skew in the migratory locust. Shown are the means ± SD of the length of connectives between the meso- and metathoracic ganglia (mm) the separation between the ganglia after the connectives are cut (mm) and the separation represented as a percentage increase of the initial length. The distribution of this increase is positively skewed in the migratory locust.

	S. gregaria	*L. migratoria*
Mean length of connectives (mm)	0.9888	1.084
SD length of connectives (mm)	0.07022	0.1296
Mean separation of ganglia after severing connectives (mm)	1.659	1.507
SD separation of ganglia after severing connectives (mm)	0.2214	0.1999
Mean (% increase)	68.67	52.76
SD (% increase)	26.57	21.05
cv	38.69%	39.90%
skew	0.4272	1.745
n	16	14

6.4.3 *Gryllus bimaculatus and Periplaneta americana* connectives between the meso- and metathoracic ganglia are under tension

Severing a single connective in the cricket *Gryllus Bimaculatus* led to a significant increase in the distance between the ganglia (one-way ANOVA, $F(1.352,16.22)=36.69$, $p<0.0001$ with Geisser-Greenhouse's correction for repeated measures $\varepsilon=0.676$ and Tukey's multiple comparison test, intact vs left cut $p=0.0325$; Figure 6-7). Severing the remaining connective led to a further significant increase (intact vs both cut $p<0.0001$, left cut vs both cut $p<0.0002$). We investigated the direction and extent of movement of the meso- and metathoracic ganglia and found no difference between the extent of movement of each after being severed (paired T-test, n=12 pairs, $t=0.9124$, $df=11$, p 0.3811; Figure 6-8).

In *Periplaneta americana* cutting a single nerve had no effect, but cutting both caused a significant increase in the distance between the meso- and metathoracic ganglia (one-way ANOVA, $F(1.29,25.73)=50.13$, $p<0.0001$ with Geisser-Greenhouse's correction for repeated measures $\varepsilon=0.6433$ and Tukey's multiple comparison test, intact vs both cut $p<0.0001$, left cut vs both cut $p<0.0001$, intact vs left cut $p=0.2478$; Figure 6-9). Both ganglia moved to the same extent but in different directions (paired T-test, n=19 pairs, $t=1.731$, $df=18$, $p= 0.1005$; Figure 6-10). Having established tension is present in the connectives between the meso- and metathoracic ganglia of both species, we now compare this to the desert locust.

A

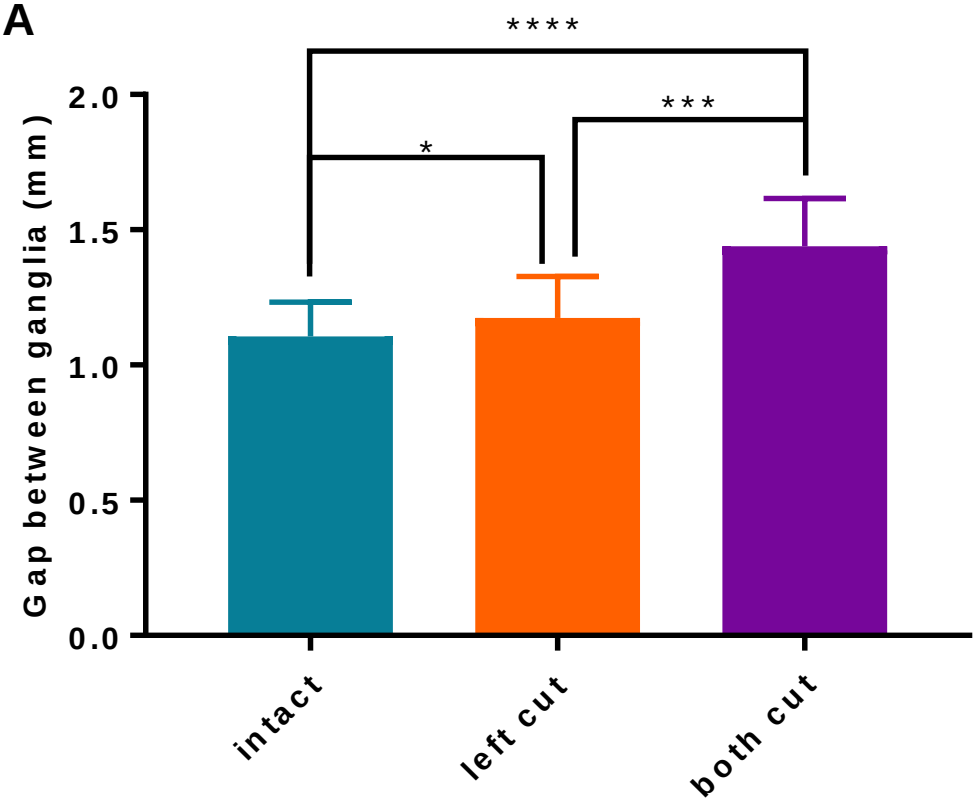

B

	intact	left cut	both cut
Mean	1.105	1.174	1.439
Std. Deviation	0.1276	0.1535	0.1763

Figure 6-7: Severing either one or both connectives between the meso- and metathoracic ganglia leads to an increase in their separation in the black cricket. A: Cutting the left connective causes a significant increase in the gap between the ganglia, cutting both connectives further increases this (One Way ANOVA with Geisser-Greenhouse's correction for repeated measures and Tukey's post hoc test, *p<0.05, ***p<0.001, ****p<0.0001) data is mean ± SD. **B:** mean ± SD of the distance between the meso- and metathoracic ganglia (mm).

A

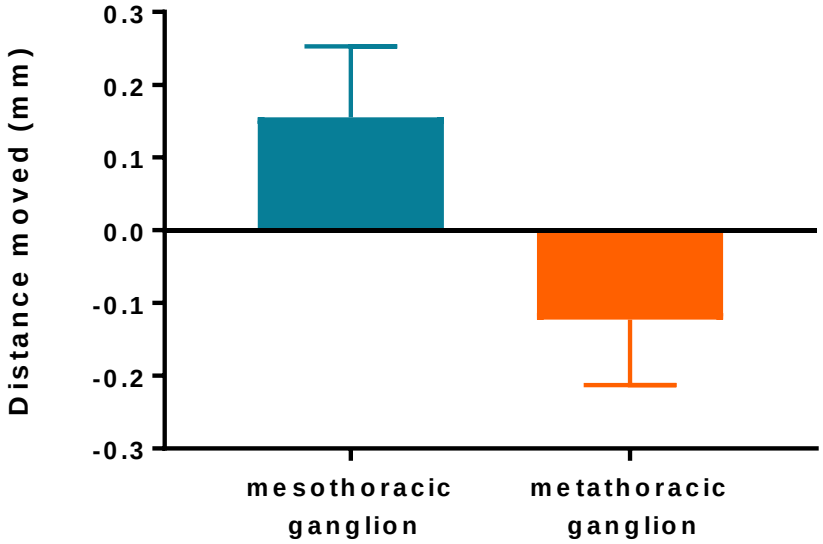

B

	mesothoracic ganglion	metathoracic ganglion
Mean	0.1553	0.1237
Std. Deviation	0.09773	0.08881

Figure 6-8: Both the meso- and metathoracic ganglia move when connectives between them are severed in the black cricket. A: Both the meso- and the metathoracic ganglia move to the same extent (paired T-test, n.s) but in difference directions with the mesothoracic ganglion moving anteriorly and the metathoracic ganglion posteriorly. data is mean ± SD. **B:** absolute mean ± SD of the distance moved by the meso- and metathoracic ganglia after connectives are cut (mm).

A

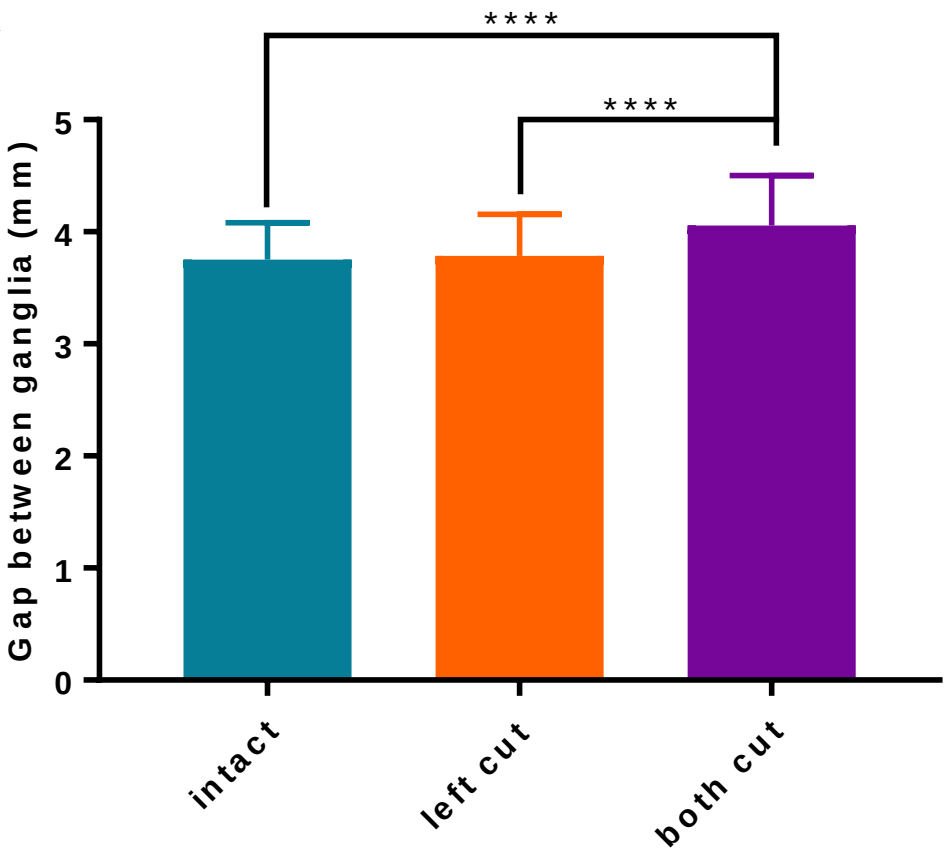

B

	intact	left cut	both cut
Mean	3.751	3.785	4.057
Std. Deviation	0.3282	0.3724	0.4456

Figure 6-9: Severing both connectives between the meso- and metathoracic ganglia leads to an increase in separation between the ganglia in the American cockroach. A: Cutting the left connective has no effect on the gap between the ganglia, cutting both connectives causes a significant increase (One Way ANOVA with Geisser-Greenhouse's correction for repeated measures and Tukey's multiple comparison test, ****$p<0.0001$) data is mean ± SD. **B:** mean ± SD of the separation between the meso- and metathoracic ganglia (mm).

A

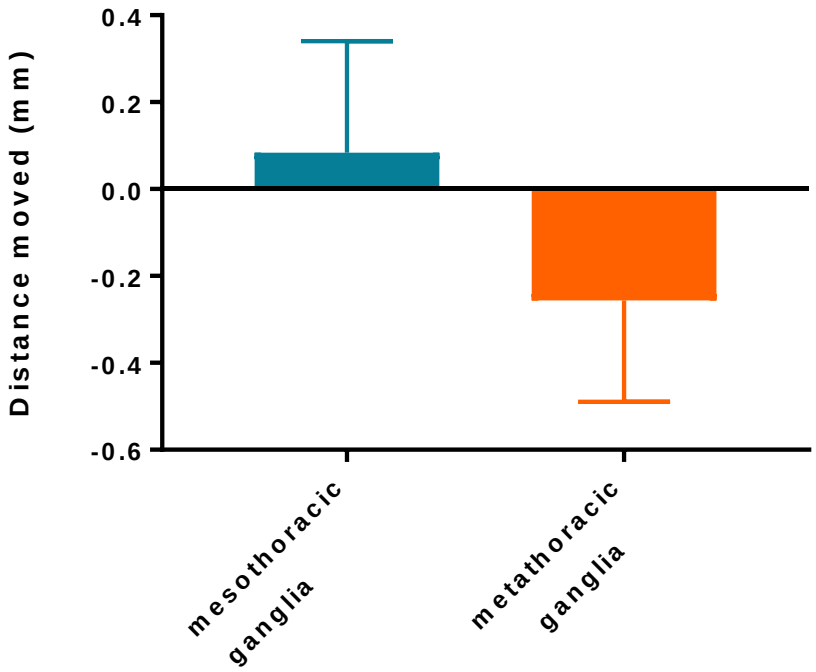

B

	mesothoracic ganglia	metathoracic ganglia
Mean	0.2064	0.2797
Std. Deviation	0.1678	0.2025

Figure 6-10: Both the meso- and metathoracic ganglia move after connectives between them are severed in the American cockroach. A: Both the meso- and the metathoracic ganglia move to the same extent (paired T-test, n.s) but in difference directions with the mesothoracic ganglion moving anteriorly and the metathoracic ganglion posteriorly. Data is mean ± SD. **B:** absolute mean ± SD of the movement of the meso- and metathoracic ganglia after connectives are cut (mm).

6.4.4 Tension is present in the connectives between the meso- and metathoracic ganglia in all species, but the extent varies

The severed ends of the connectives between the meso- and metathoracic ganglia of *S. gregaria* separated significantly more than did the connectives from other species (one-way ANOVA $F(4,68)=8.283$, $p<0.0001$; Figure 6-11; Table 10). After normalising the separation as a percentage increase to account for the differing size of the species there was no difference between *G. bimaculatus* and *S. gregaria* (Kruskal Wallis $H=38.59$, $p<0.0001$, Dunn's multiple comparisons, *S. gregaria* vs *G. bimaculatus* $p=0.083$; Figure 6-12; Table 11). However, the connectives of *P. americana* showed a significantly smaller percentage increase and therefore, a lower tension than either of the other species (against *S. gregaria* $p<0.0001$, *G. bimaculatus* $p=0.0018$).

Retraction of the damaged axons in *S. gregaria* contributed to the gap that forms between the severed ends after nerve cutting (Chapter 3). In *G. bimaculatus* females the retraction of axons was no different from the gap that forms, whereas in males there was a significant difference (paired T-tests were performed for each sex, males $t=7.012$, $df=7$, $p=0.0002$; females $t=2.025$ $df=3$, $p = 0.1360$, Figure 6-13) suggesting in females the separation largely due to axon retraction and not tension. In *P. americana* both male and female connectives showed nerve retraction that was significantly less than the overall gap that formed (paired T-tests were performed for each sex; males $t=3.121$, $df=7$, $p = 0.0168$; females $t=3.47$, $df=10$, $p = 0.0060$; Figure 6-14). This shows that tension is present in the connectives between the meso- and metathoracic ganglia in the American cockroach. We normalised the retraction as a percentage of the entire gap to permit comparison among species and sexes. In *S. gregaria* axonal retraction contributed a significantly smaller amount to the separation of the meso- and

metathoracic ganglia than in *P. americana* (one-way ANOVA, $F(5,40)=9.50$, $p<0.0001$; Tukey's multiple comparisons; males $p=0.0007$, females $p=0.0002$; Figure 6-15). However, there was no difference between the connectives of *G. bimaculatus* and *S. gregaria* (males $p=0.3209$, females $p=0.1380$) or between those of *G. bimaculatus* and *P. americana* (males $p=0.1570$, females $p=0.7047$). There were no differences in the connectives between the sexes of each species (*S. gregaria* $p>0.9999$, *G. bimaculatus* $p=0.9571$, *P. americana* $p=0.9998$). This shows that the connectives between the meso- and metathoracic ganglia in both black crickets and American cockroaches are under less tension than those in the desert locust.

A

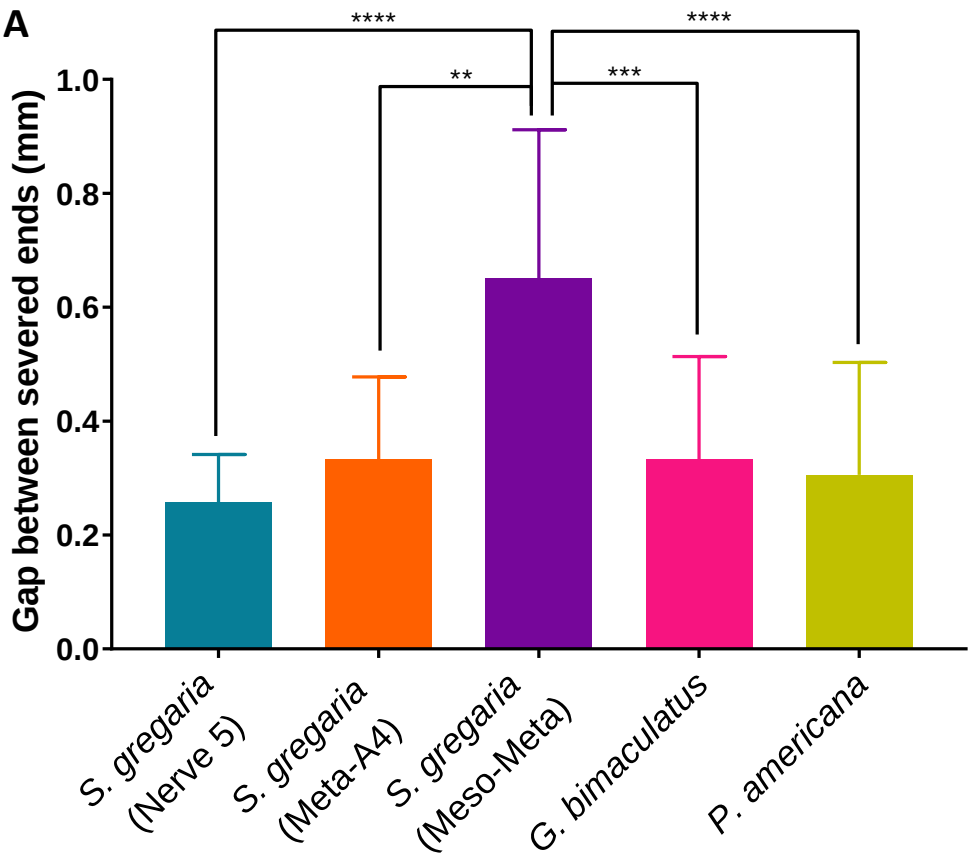

B

	S. gregaria (Nerve 5)	*S. gregaria* (Meta-A4)	*S. gregaria* (Meso-Meta)	*G. bimaculatus*	*P. americana*
Mean	0.2581	0.333	0.65	0.3336	0.3055
SD	0.08313	0.1444	0.2616	0.18	0.1975

Figure 6-11: The connectives between the meso- and metathoracic ganglia in *S. gregaria* separate more than any other bundle studied. A: The connectives between the meso- and metathoracic ganglia (Meso-Meta) in *S. gregaria* separate far more than any other bundle studied. Data for the connectives between the metathoracic and fourth abdominal ganglia (Meta-A4) and Nerve 5 are taken from Chapter 3; none of the other bundles are different from each other. (one-way ANOVA with Tukey's post hoc test, **p<0.01, ***p<0.001, ****p<0.0001) data is mean ± SD. **B:** mean ± SD of the separation of severed ends of axon bundles (mm).

Table 10: Results from multiple comparisons tests on the gaps between severed ends among different axon bundles and species. The gaps between the severed ends of axon bundles were compared using a one-way ANOVA and Tukey's multiple comparison tests, p values are shown below.

	S. gregaria (Meso-Meta)	*S. gregaria* (Nerve 5)	*S. gregaria* (Meta-A4)	*G. bimaculatus*	*P. americana*
S. gregaria (Meso-Meta)		<0.0001	0.0026	0.0007	<0.0001
S. gregaria (Nerve 5)	<0.0001		0.8124	0.7428	0.8281
S. gregaria (Meta-A4)	0.0026	0.8124		0.9936	0.9531
G. bimaculatus	0.0007	0.7428	0.9936		0.9531

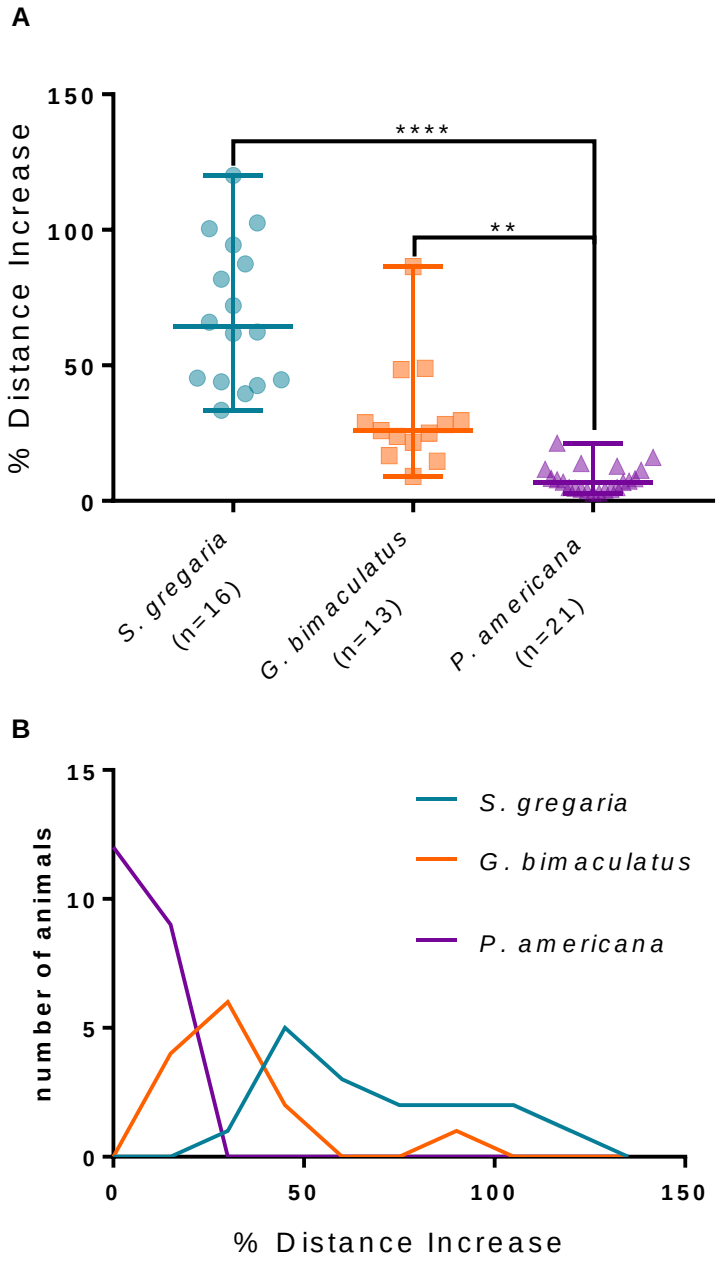

Figure 6-12: The percentage increase in the distance between the meso- and metathoracic ganglia after the connectives are cut across species. A: The percentage increase in distance between the meso- and metathoracic ganglia is significantly smaller in *P. americana* than either of the other two species studied (Kruskal Wallis and Dunn's post hoc tests, **p<0.01, ****p<0.0001) data is median and range. **B:** distributions of % distance increase across species.

Table 11: The distribution of the percentage increase in the separation of the meso- and metathoracic ganglia in the black cricket and American cockroach has a positive skew. Data shown is the mean ± SD of the lengths of the connectives between the meso- and metathoracic ganglia among species (mm), the separation between the two ganglia after connectives are cut (mm), and the increase represented as a percentage of the initial length. The distribution of percentage increase has a positive skew in the black cricket and American cockroach.

	S. gregaria	*G. bimaculatus*	*P. americana*
Mean length of connectives (mm)	0.9888	1.105	3.751
SD length of connectives (mm)	0.07022	0.1276	0.3282
Mean separation of ganglia after severing connectives (mm)	1.659	1.439	4.057
SD separation of ganglia after severing connectives (mm)	0.2214	0.1763	0.4456
Mean (% increase)	68.67	31.33	8.027
SD (% increase)	26.57	20.13	4.853
cv	38.69%	64.25%	60.46%
skew	0.4272	1.898	1.266
n	16	13	21

A

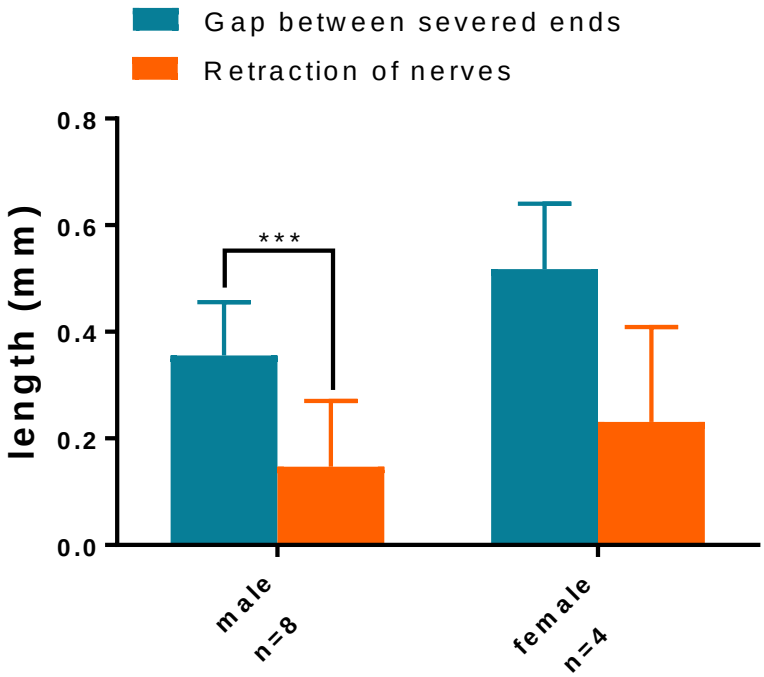

B

	Gap between severed ends		Retraction of nerves	
	Mean	SD	Mean	SD
male	0.36	0.10	0.15	0.12
female	0.52	0.12	0.23	0.18

Figure 6-13: In black cricket males the retraction of nerves accounts for a significantly small portion of overall separation after cutting. **A:** In females the difference between the entire gap between the severed ends of the connectives between the meso- and metathoracic ganglia after nerve cutting and the retraction of the nerves is not significant, however in males the retraction is significantly smaller than the overall gap (Paired T-tests were performed for each sex, ***p<0.001) data is mean ± SD. **B:** mean ± SD of the gap between severed ends of the connectives between the meso- and metathoracic ganglia (mm) and the retraction of the axons (mm).

A

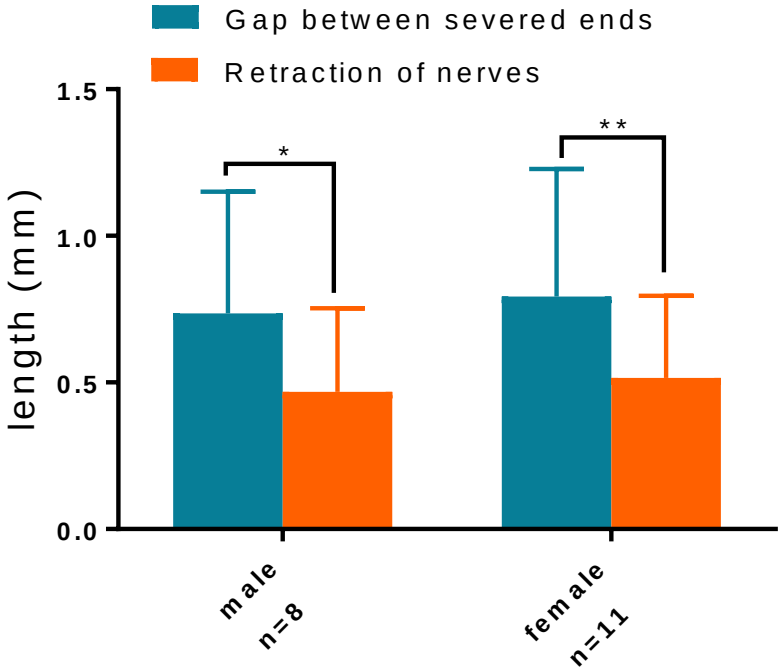

B

	Gap between severed ends		Retraction of nerves	
	Mean	SD	Mean	SD
male	0.74	0.41	0.47	0.29
female	0.79	0.44	0.52	0.28

Figure 6-14: In the American cockroach the retraction of nerves is significantly smaller than the overall separation produced by cutting the connectives between the meso- and metathoracic ganglia. **A:** In both males and females the retraction of axons was significantly less than the overall gap formed between severed ends when the connectives between the meso- and metathoracic ganglia were cut (paired T-tests were performed for each sex, *p<0.5, **p<0.01) data is mean ± SD. **B:** mean ± SD of the gap between the severed ends of the connectives between the meso- and metathoracic ganglia (mm) and the retraction of axons (mm).

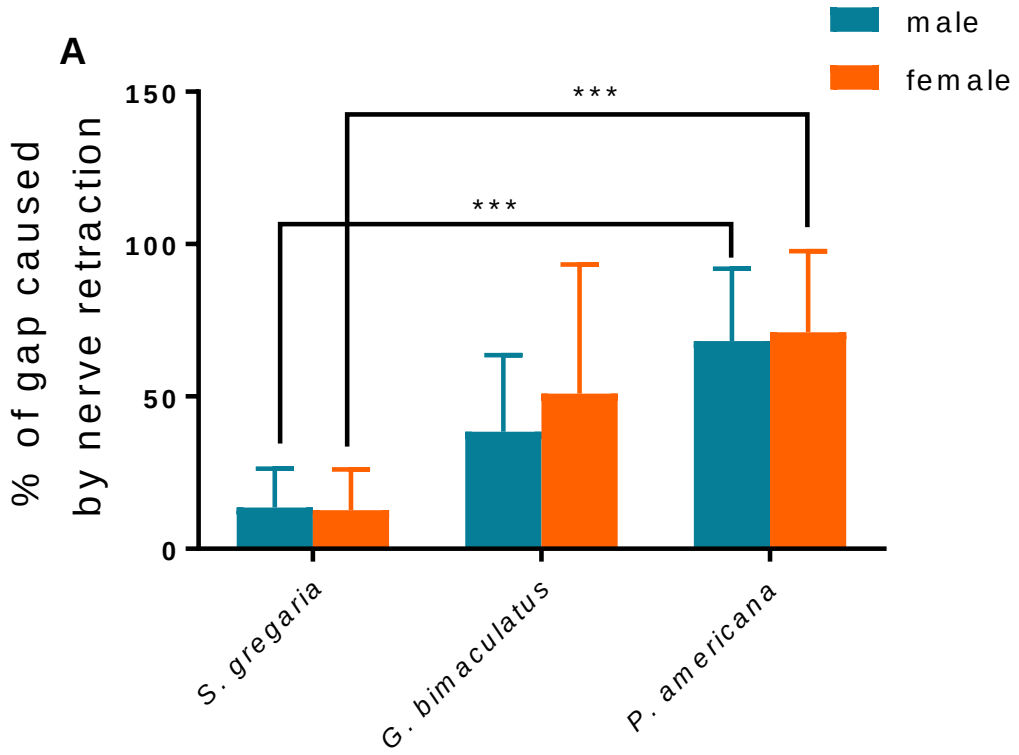

B

	male		female	
	Mean	SD	Mean	SD
S. gregaria	13.55	12.77	12.70	13.31
G. bimaculatus	38.46	25.09	50.89	42.43
P. americana	68.16	23.80	71.05	26.67

Figure 6-15: Nerve retraction contributes significantly more to the separation of severed connectives in the American cockroach than the desert locust. A: When the retraction of axons is represented as a percentage of the overall gap there are no differences between sexes in any species. *S. gregaria* has a significantly smaller percentage of the gap caused by nerve retraction when compared to *P. americana* and *G. bimaculatus* was not different from either other species (one-way ANOVA with Tukey's post hoc tests, ***p<0.001) data is mean ± SD. **B:** mean ± SD of the percentage of the gap between the severed ends of the connectives that is caused by axon retraction. Absolute data of gap size and nerve retraction can be found in Figures 3-1, 6-7, 6-9.

6.4.5 There are differences in the anatomy and composition of the connectives between the meso- and metathoracic ganglia among species.

We compared the anatomy of the connectives between the meso- and metathoracic ganglia among species via TEM imaging, using data for the desert locust from chapter 4. The connective diameters of *P. americana* were significantly larger than those of the other species studied (one-way ANOVA, $F(2,16)=34.63$, $p<0.0001$, Tukey's multiple comparisons *S. gregaria* $p<0.0001$, *G. bimaculatus* $p<0.0001$; Figure 6-16) but there was no difference between the diameters of connectives between *S. gregaria* and *G. bimaculatus* ($p=0.1214$). Conversely, the connectives of *G. bimaculatus* had significantly thinner BBB compared to *S. gregaria* (one-way ANOVA, $F(2,16)=8.555$, $p=0.0030$, Tukey's multiple comparisons, *S. gregaria* vs *G. bimaculatus* $p=0.0021$, *S. gregaria* vs *P. americana* $p=0.1234$, *G. bimaculatus* vs *P. americana* $p=0.1013$; Figure 6-17). After examining gross anatomy we compared the axons in the connectives between the meso- and metathoracic ganglia.

The connectives of *G. bimaculatus* had a significantly higher density of axons than those of *P. americana* (Kruskal Wallis $H=6.066$, $p=0.0482$; Dunn's multiple comparisons *G. bimaculatus* vs *P. americana* $p=0.0426$; Figure 6-18; Table 12). However, there were no differences between the axonal density of the connectives of black crickets and desert locusts ($p=0.7770$) or between those of desert locusts and American cockroaches ($p=0.3210$). *G. bimaculatus* connectives were composed of smaller axons than either of the other species (Kruskal Wallis $H = 51.18$, $p<0.0001$; Dunn's multiple comparisons *G. bimaculatus* vs *S. gregaria* $p<0.0001$, *G. bimaculatus* vs *P. americana* $p<0.0001$, *S. gregaria* vs *P .americana* $p = 0.1601$; Figure 6-19; Table 13).

A

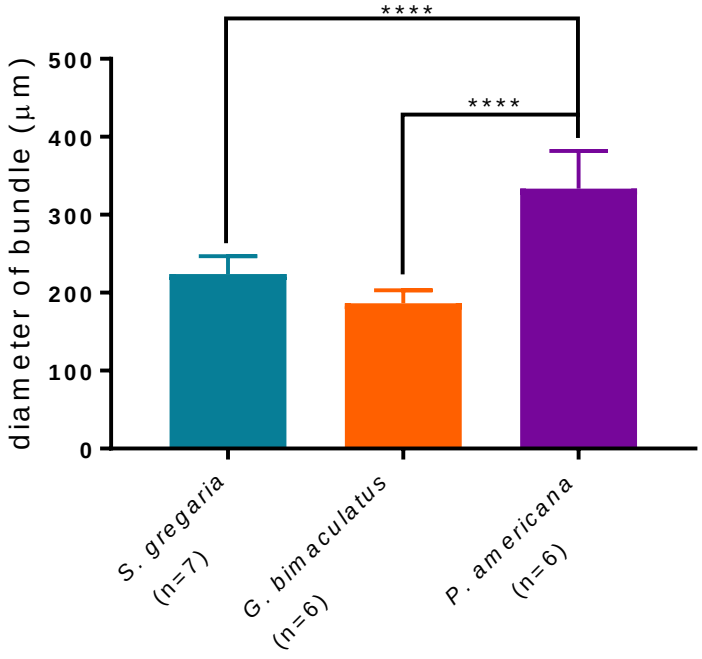

B

	S. gregaria (n=7)	*G. bimaculatus* (n=6)	*P. americana* (n=6)
Mean	223.8	186.5	333.5
Std. Deviation	22.96	16.78	48.47

Figure 6-16: The connectives between the meso- and metathoracic ganglia are the largest in the American cockroach. A: The connectives in *P. americana* are significantly larger than those in *S. gregaria* or *G. bimaculatus* (one-way ANOVA with Tukey's post hoc tests, ****p<0.0001) data is mean ± SD. **B:** mean ± SD of the diameter of the connectives between the meso- and metathoracic ganglia (µm).

A

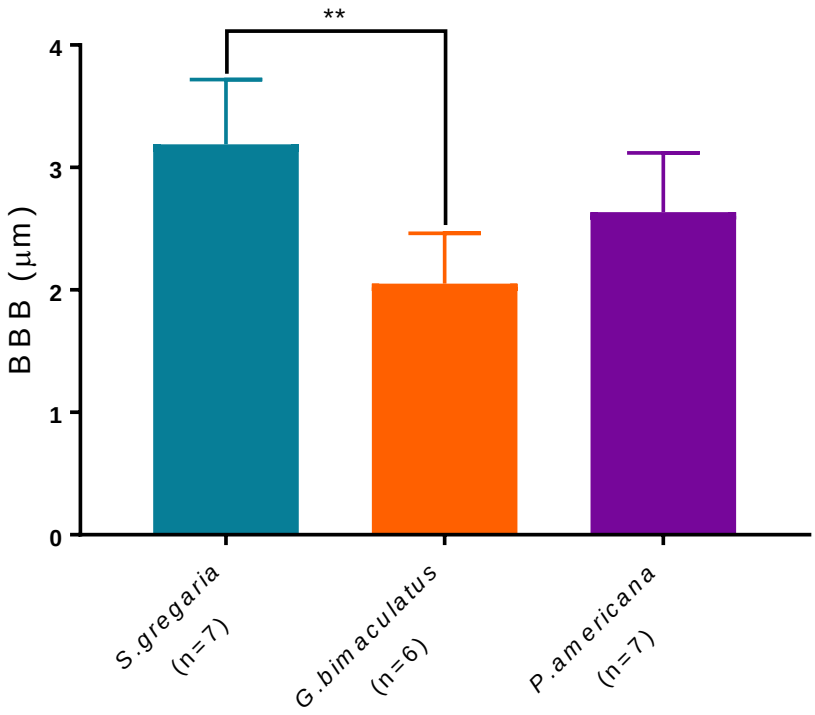

B

	S.gregaria (n=7)	*G.bimaculatus* (n=6)	*P.americana* (n=7)
Mean	3.19	2.052	2.636
Std. Deviation	0.5283	0.4096	0.4833

Figure 6-17: The blood-brain barrier of connectives between the meso- and metathoracic ganglia is thinner in black crickets compared to the desert locust. A: *S. gregaria* has a thicker BBB than *G. bimaculatus* (one-way ANOVA with Tukey's post hoc tests, **p<0.01) data is mean ± SD. **B:** mean ± SD of the thickness of the BBB of the connectives between the meso- and metathoracic ganglia (µm).

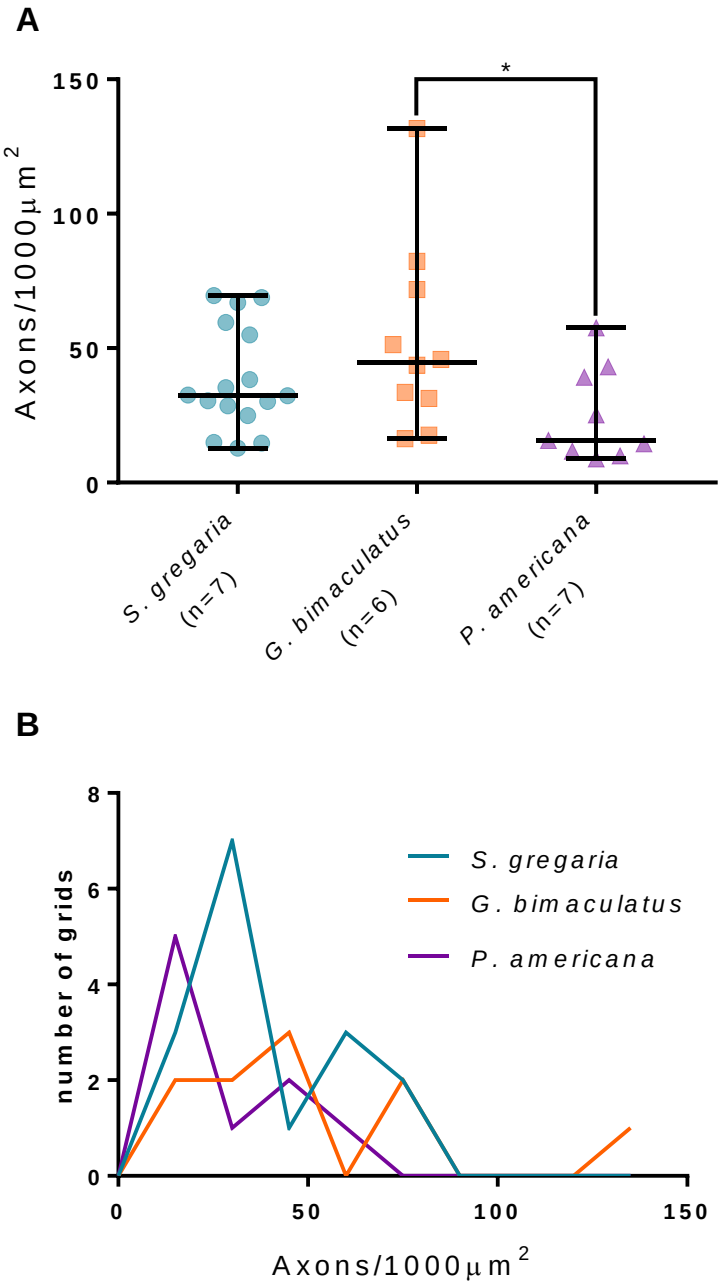

Figure 6-18: Axon density in the connectives between the meso- and metathoracic ganglia across species. A: For each individual 2 or 3 images were counted to count both near the BBB and the centre of the connective. We found that on average there were more axons per 1000 um^2 in *G. bimaculatus* than *P. americana* but no other differences (Kruskal Wallis *p<0.05) data is median and range. **B:** Distribution of axon densities across species.

Table 12: The distribution of axon density in black crickets shows a strong positive skew. Mean ± SD of the axon density in the connectives between the meso- and metathoracic ganglia among species.

	S. gregaria	*G. bimaculatus*	*P. americana*
Mean (axons/1000 um^2)	68.67	31.33	8.027
SD (axons/1000 um^2)	19.47	34.92	17.51
cv	38.69%	64.25%	60.46%
skew	0.4272	1.898	1.266
n	16	13	21

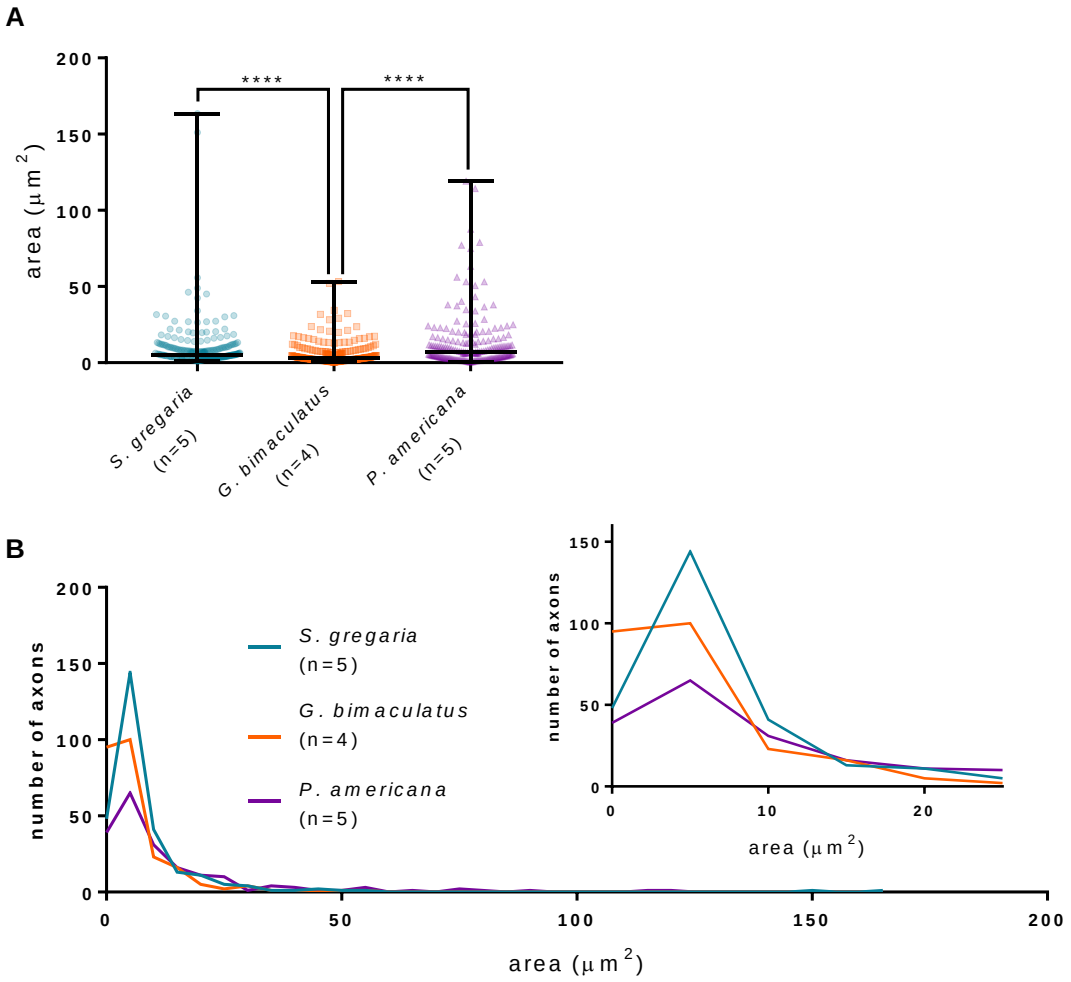

Figure 6-19: Transverse sectional area of axons in the connectives between the meso- and metathoracic ganglia. A*: G. bimaculatus* had significantly smaller axons compared to either other species (Kruskal Wallis and Dunn's post hoc tests, **** p<0.0001) data is median and range. **B:** Distributions of axon size across species in full and under 25 µm^2 (inset).

Table 13: The distribution of axon cross-section area is positively skewed in all species studied. Shown is the mean ± SD of cross-section axon area (μm^2) in the connectives between the meso- and metathoracic ganglia.

	S. gregaria	*G. bimaculatus*	*P. americana*
Mean (axon μm^2)	8.777	5.74	13.18
SD (axon μm^2)	15.2	7.335	18.52
cv	173.21%	127.79%	140.49%
skew	7.32	3.35	3.193
n	274	248	192

6.4.6 Microtubule density and count differs among species

In previous chapters we found a high number of microtubules in the longitudinal orientation, and a steep relationship between microtubule number and axon cross-section area that reflects axon bundles under high tension in the desert locust (chapter 4, 5). To determine if this is a more general relationship, we compared these measures among species. *P. americana* connectives were composed of a lower density of microtubules in the perpendicular orientation then other species (Kruskal Wallis $H=63.08$, $p<0.0001$; Dunn's multiple comparison *S. gregaria* $p<0.0001$, *G. bimaculatus* $p<0.0001$; Figure 6-20). Whereas there is no difference in microtubule density in the connectives of *S. gregaria* and *G. bimaculatus* ($p=0.9445$). *S. gregaria* had a greater number of microtubules in the longitudinal orientation per axon than either other two species (Kruskal Wallis $H = 25.29$, $p<0.0001$; Dunn's multiple comparison *S. gregaria* vs *G. bimaculatus* $p<0.0001$, *S. gregaria* vs *P. americana* $p = 0.0030$, *G. bimaculatus* vs *P. americana* $p = 0.6794$; Figure 6-21; Table 15).

There was a linear relationship between microtubule number and axon cross-section area for each of the connectives from the three species (*S. gregaria* slope =5.017 ± 0.1701, Y-intercept= 5.366±2.982; *G. bimaculatus* slope=2.5±0.1637, Y-intercept =10.06±1.522; *P. americana* slope=1.314±0.1042, Y-intercept=12.03±2.364; Figure 6-22) This relationship between microtubule number and axon size differed significantly among species (ANCOVA, $F(2,708)=219.3$, $p<0.0001$). Indeed, each species was significantly different from the other two (one-way ANOVA of the slopes, $F(2,708)$ 144.3, $p<0.0001$, Tukey's post hoc comparisons, each species $p<0.0001$ from each other species). The relationship between microtubule number and axon cross-section area

was the steepest in the desert locust, followed by the black cricket, followed by the American cockroach.

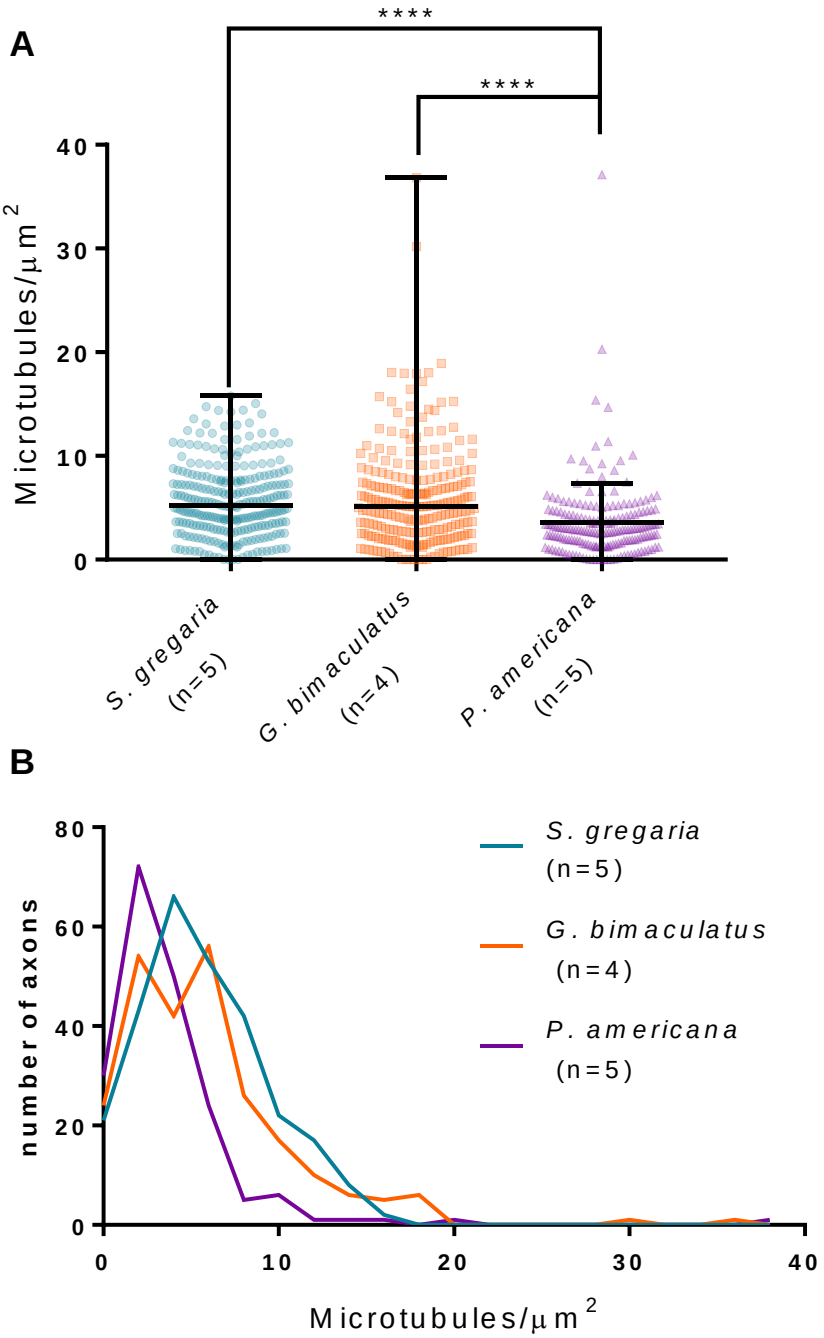

Figure 6-20: Microtubule density in the connectives between the meso- and metathoracic ganglia across species. A: Both *S. gregaria* and *G. bimaculatus* had a higher density of microtubules in the perpendicular orientation compared to *P. americana* (Kruskal Wallis and Dunn's post hoc tests, ****p<0.0001) data is median and range. **B:** Distributions of microtubule density in axons across species.

Table 14: The distribution of microtubule density is positively skewed in all species. The mean ± SD of microtubule density (microtubules/μm^2) in the connectives between the meso- and metathoracic ganglia is shown. The distributions are positively skewed, particularly in the American cockroach.

	S. gregaria	*G. bimaculatus*	*P. americana*
Mean (microtubules/μm^2)	5.712	5.879	3.587
SD (microtubules/μm^2)	3.49	4.844	3.746
cv	61.10%	82.40%	104.42%
skew	0.5969	2.135	4.701
n	274	248	192

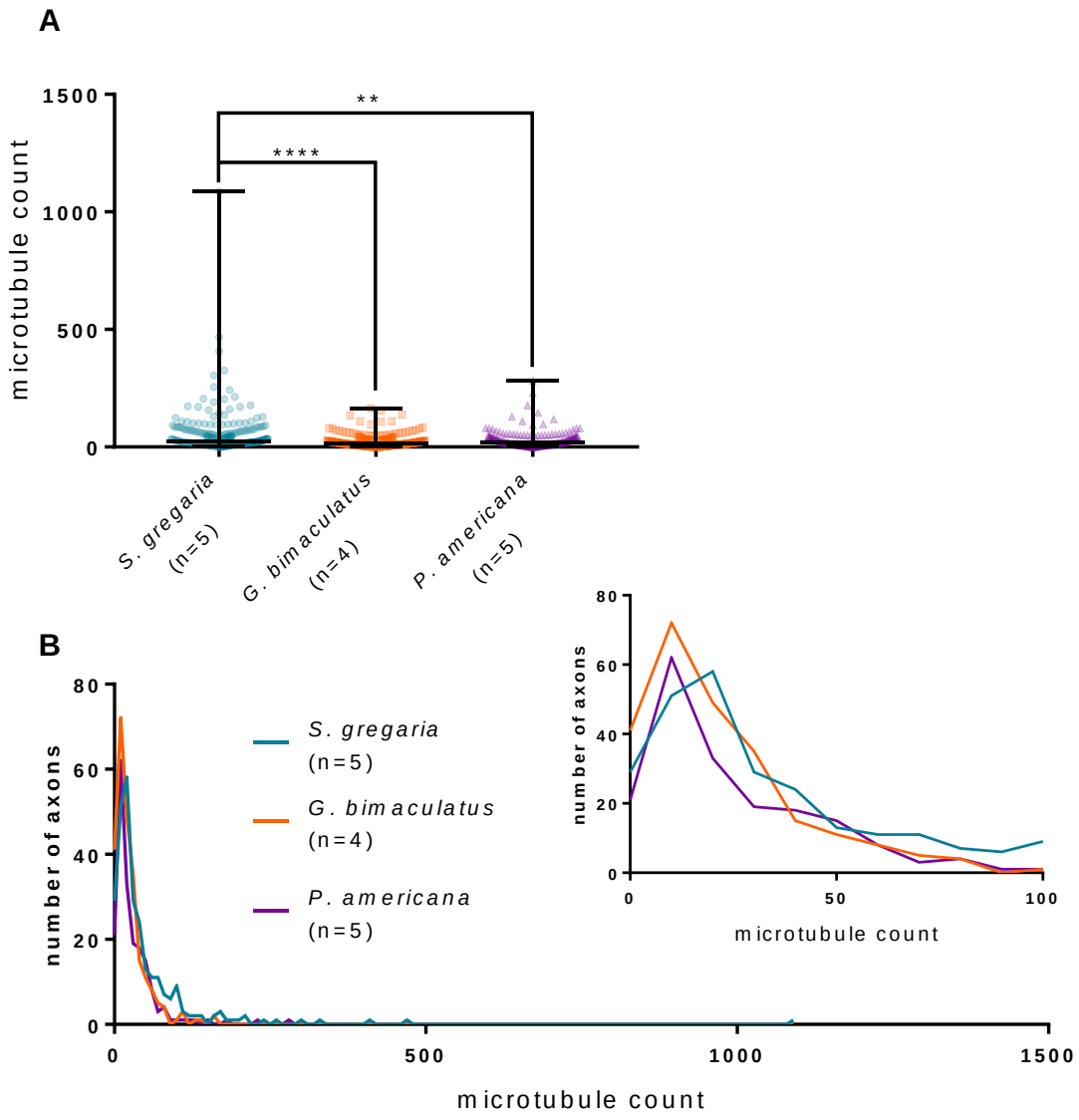

Figure 6-21: Microtubule count in the connectives between the meso- and metathoracic ganglia across species. **A:** *S. gregaria* had an increased number of microtubules per cells than either other species studied (Kruskal Wallis and Dunn's post hoc tests, **p<0.01, ****p<0.0001) data is median and range. B: The distribution of microtubule number per axon across species in full and less than 100 microtubules per axon (inset). **C:** All species show positive skew, particularly *S. gregaria.*

Table 15: The distribution of microtubule count per axon is positively skewed in all species studied. The mean ± SD of the number of microtubules per axon in the connectives between the meso- and metathoracic ganglia in all three species is shown. The distribution of this count is positively skewed.

	S. gregaria	*G. bimaculatus*	*P. americana*
Mean (microtubules/axon)	49.4	24.41	29.35
SD (microtubules/axon)	87.39	26.28	36.05
cv	176.89%	107.65%	122.80%
skew	7.236	2.475	3.582
n	274	248	192

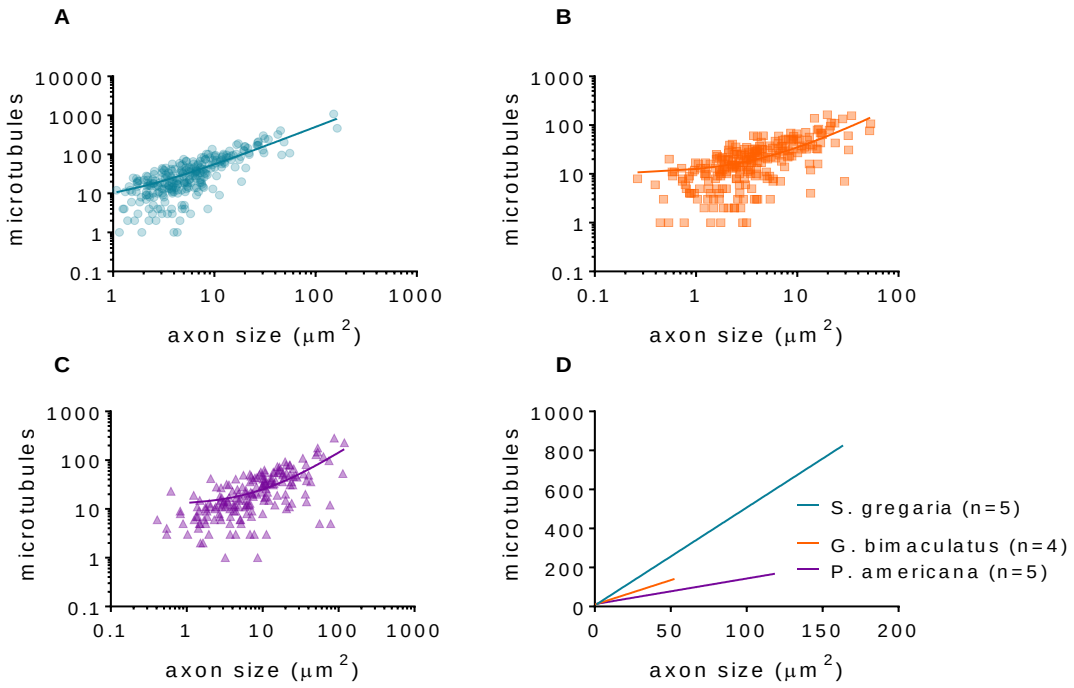

Figure 6-22: Relationship between microtubule number and axon size differs among species. *S. gregaria* R^2=0.7618 (A), *G. bimaculatus* 0.4868 (B), *P. americana* 0.4556 (C). The relationship between microtubule number and axon size differed between each species is plotted on log10 axes (A-C) and the linear regressions shown on linear axes (D).

6.4.7 *S. gregaria* connectives are more elastic but not stronger than those in other orthopteroid species

Using uniaxial loading, we investigated the relationship between tension found *in vivo* and differences in connective composition with mechanical properties *ex vivo* among species. Data for the desert locust comes from chapter 4. We measured the maximum force experienced by connectives prior to critical failure. We found that female *G. bimaculatus* connectives withstood significantly less force than the female connectives of both *S. gregaria* (two-way ANOVA interaction $F(2,56)=4.984$, $p=0.0102$, species $F(2,56)=52.84$, $p<0.0001$, sex $F(1,56)=7.244$, $p=0.0094$; Tukey's multiple comparisons $p<0.0001$; Figure 6-23) and *P. americana* ($p=0.0004$). There was no difference between female *S. gregaria* and *P. americana* connectives ($p=0.8731$) and no differences between the male connectives of any species (*S. gregaria* vs *G. bimaculatus* $p=0.0683$, vs *P. americana* $p>0.9999$; *G. bimaculatus* vs *P. americana* $p=0.0877$).

We also examined the elasticity of the bundle by measuring the distance bundles were stretched prior to breaking. Connectives between the meso- and metathoracic ganglia in *P. americana* could be stretched a significantly greater distance than either of the other two species (two-way ANOVA interaction $F(2,48)=0.329$, $p=0.7212$, sex $F(1,48)=5.614$, $p=0.0219$, species $F(2,48)=95.33$, $p<0.0001$; Tukey's multiple comparison, male *P. americana* vs *S. gregaria* $p<0.0001$, vs *G. bimaculatus* $p<0.0001$, female *P. americana* vs *S. gregaria* $p<0.0001$, vs *G. bimaculatus* $p<0.0001$; Figure 6-24). There were no differences between the distance that the connectives of *S. gregaria* and *G. bimaculatus* could be stretched (males $p>0.9999$, females $p=0.9993$). We normalised the length that the connectives could be stretched as a percentage increase of *in vivo* length, merging data for male and female connectives (Figure 6-25). The connectives of

S. gregaria could be pulled an additional 101.4±26.16% of their length compared to *G. bimaculatus* and *P. americana* which were both closer to only 70% (*G. bimaculatus* 67.89±22.67; *P. americana* 69.11±15.17). The connectives in *S. gregaria* were pulled to a significantly higher extent of their original length (one-way ANOVA, $F(2,35)=9.542$, $p=0.0005$; Tukey's multiple comparison tests *S. gregaria* vs *G. bimaculatus* $p=0.0018$, *S. gregaria* vs *P. americana* $p=0.0011$, *G. bimaculatus* vs *P. americana* $p=0.9879$). Finally, we found that all of the connectives across the species were under approximately the same forces *in vivo* (Kruskal Wallis test $h=1.003$, $p=0.6057$, Dunn's multiple comparison test all comparisons $p>0.9999$; Figure 6-26).

A

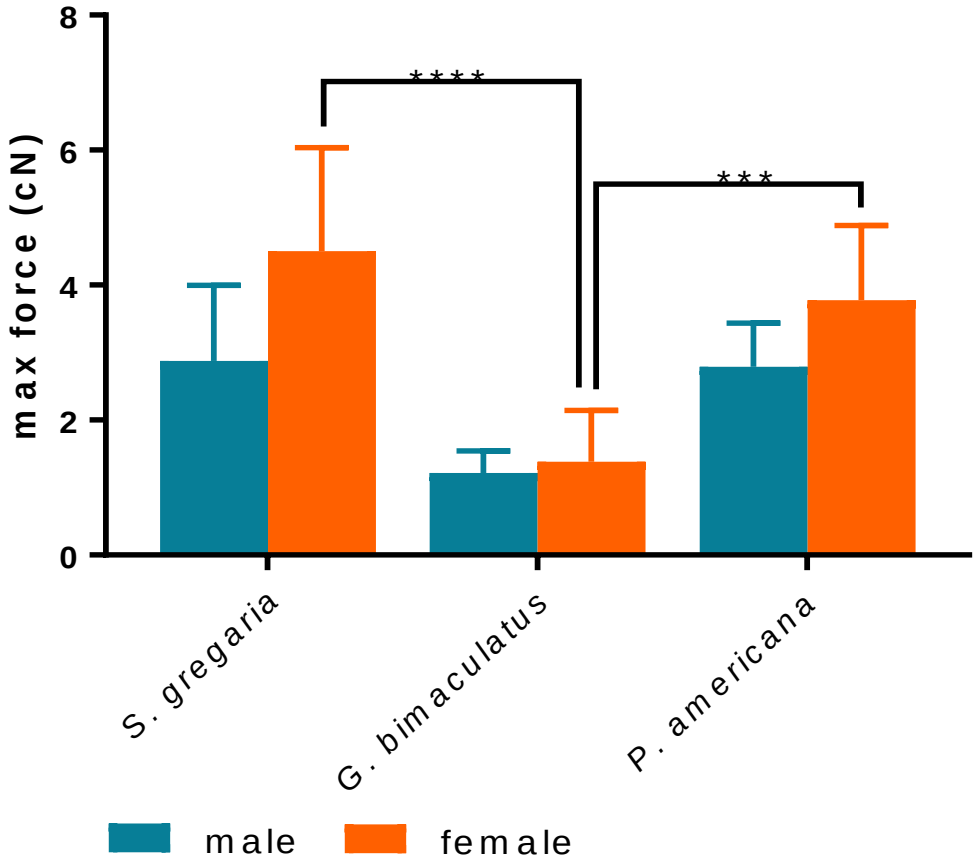

B

	male		female	
	Mean	SD	Mean	SD
S. gregaria	2.88	1.12	4.50	1.54
G. bimaculatus	1.22	0.32	1.38	0.76
P. americana	2.79	0.65	3.78	1.10

Figure 6-23: The maximum force experienced by the connectives between the meso- and metathoracic ganglia is significantly lower in female black crickets. **A:** *G. bimaculatus* females had significantly weaker connectives compared to the other species, while there was no difference between males (two-way ANOVA with Tukey's post hoc tests, ***p<0.001, ****p<0.0001) data is mean ± SD. **B:** mean ± SD of the maximum force measured in the connectives between the meso- and metathoracic ganglia of each species (cN).

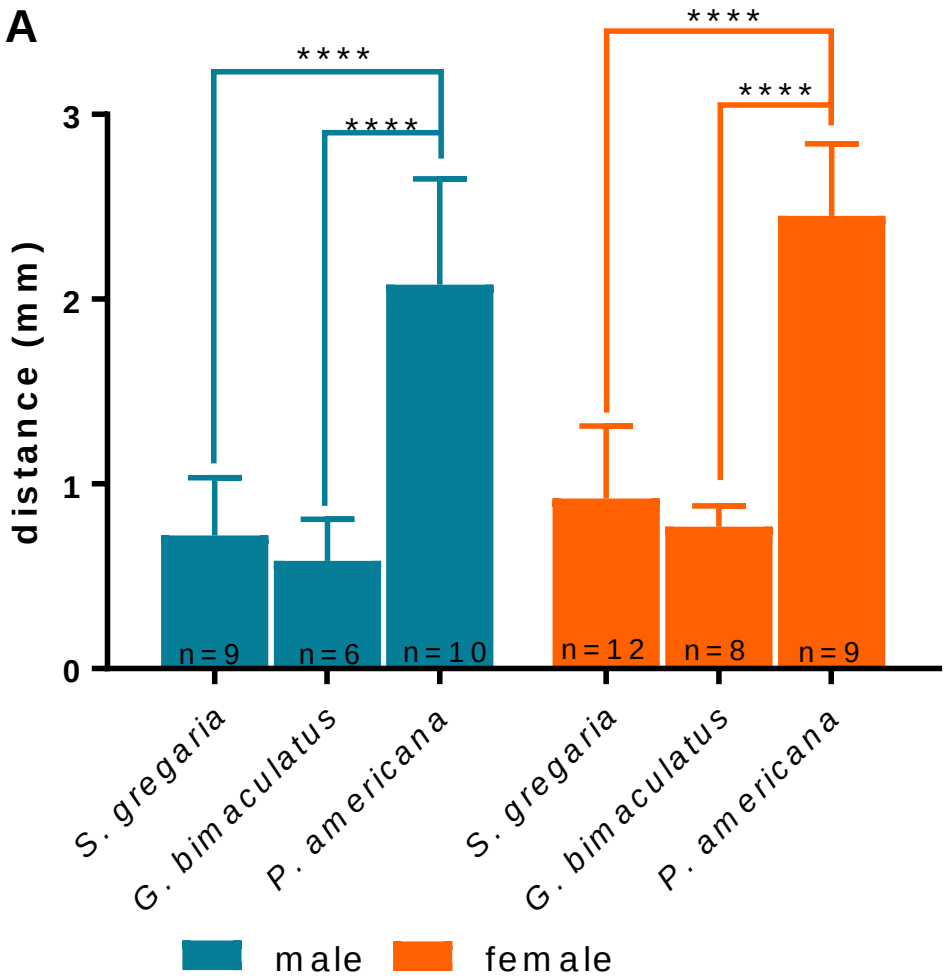

B

	male		female	
	Mean	SD	Mean	SD
S. gregaria	0.72	0.31	0.92	0.39
G. bimaculatus	0.58	0.23	0.77	0.11
P. americana	2.08	0.57	2.45	0.39

Figure 6-24: The connectives between the meso- and metathoracic ganglia can be pulled a greater distance in the American cockroach. **A:** The connectives of *P. americana* were stretched a further distance before breaking than either *S. gregaria* or *G. bimaculatus*, there were no differences between sexes in any species (two-way ANOVA with Tukey's post hoc tests, ****p<0.0001) data is mean ± SD. **B:** mean ± SD of the distance the connectives between the meso- and metathoracic ganglia were stretched (mm).

A

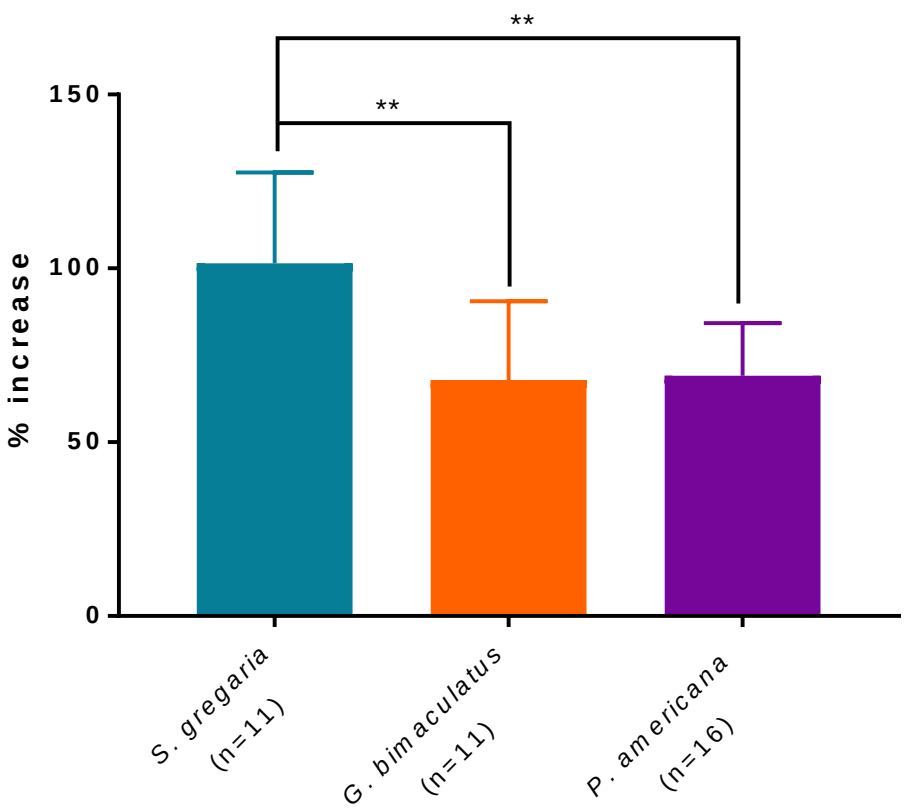

B

	length *in vivo* (mm)		percentage increase	
	Mean	SD	Mean	SD
S. gregaria (n=11)	0.8695	0.1250	101.40	26.16
G. bimaculatus (n=11)	1.0660	0.1779	67.89	22.67
P. americana (n=16)	3.3760	0.3073	69.11	15.17

Figure 6-25: When normalised as a percentage increase, the connectives between the meso- and metathoracic ganglia in the desert locusts are capable of the most stretch. **A:** The connectives between the meso- and metathoracic ganglia in *S. gregaria* were able to be pulled a comparatively greater distance before breaking than the other species (One Way ANOVA with Tukey's post hoc test, **p<0.01) mean ± SD. **B:** the mean ± SD of the length of the connectives between the meso- and metathoracic ganglia *in vivo* and the increase caused by stretched represented as a percentage increase. Data for the absolute distance stretched is in Figure 6-24.

A

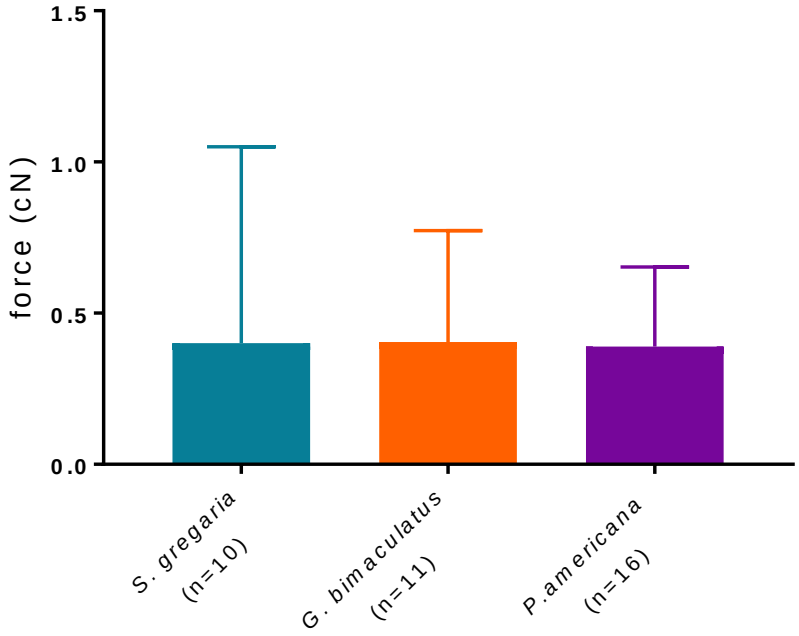

B

	S. gregaria (n=10)	*G. bimaculatus* (n=11)	*P.americana* (n=16)
Mean	0.4011	0.4047	0.39
Std. Deviation	0.6489	0.3687	0.2631

Figure 6-26: Approximate forces experienced by the connectives between the meso- and metathoracic ganglia *in vivo* are similar among species. A: We were able to gather approximate values for the forces experienced by connectives *in vivo* by matching the length of the connectives *ex vivo* in the pulling experiments and recording the force at that point. We found there were no differences between the species studied (Kruskal Wallis n.s) data is mean ± SD. **B:** mean ± SD of the estimated force exerted on the connectives between the meso- and metathoracic ganglia *in vivo* (cN).

6.4.8 Connectives across species are viscoelastic but show different responses to stretch

The material properties of the connectives between the meso- and metathoracic ganglia in *S. gregaria* were discussed in Chapter 4 (4.4.4). In *G. bimaculatus* breakage of the connectives occurred within 20 or so steps, and the forces rise quickly. This was similar to the pattern observed in *S. gregaria* but to a lesser extent depending upon whether the connectives were torn simultaneously or not (Figure 6-27). In *G. bimaculatus* connectives the sudden loss of tension did not necessarily occur simultaneously with the observation of the connectives breaking; in some preparations there was a latency of >30 seconds separating the loss of resistance and breakage of the connectives.

Stretching of the *P. americana* connectives revealed a similar pattern to those of *S. gregaria*: initial steps caused forces to rise sharply and then decrease rapidly (Figure 6-28). Although in *P. americana* connectives this occurs over a longer period of stretching. In some cases the connectives broke at different time points, but did so suddenly with visible retraction from the breaking point, unlike *G. bimaculatus* which tore slowly. In some *P. americana* connectives a small loss of force early in the experiment occurs, which may indicate that an element of the connectives breaking either internally or out of field of view.

Comparison of the responses to single steps of 50 µm at the early stages with steps just prior to breakage showed that all connectives displayed viscoelastic properties (cf. *S. gregaria* in Chapter 4; Figure 4-17) The connectives of all species show an elastic strain response in the penultimate step before maximum force and breakage. There are species specific differences in the recovery of this step; *S. gregaria* connectives showed the fastest recovery followed by those of *P. americana,* and finally those of *G. bimaculatus*, which show comparatively little recovery. *G. bimaculatus* connectives also

showed an elastic strain response during the early steps in the sequences when force is first recorded whereas both *P. americana* and *S. gregaria* show a step up in force with little to no recovery prior to the next step.

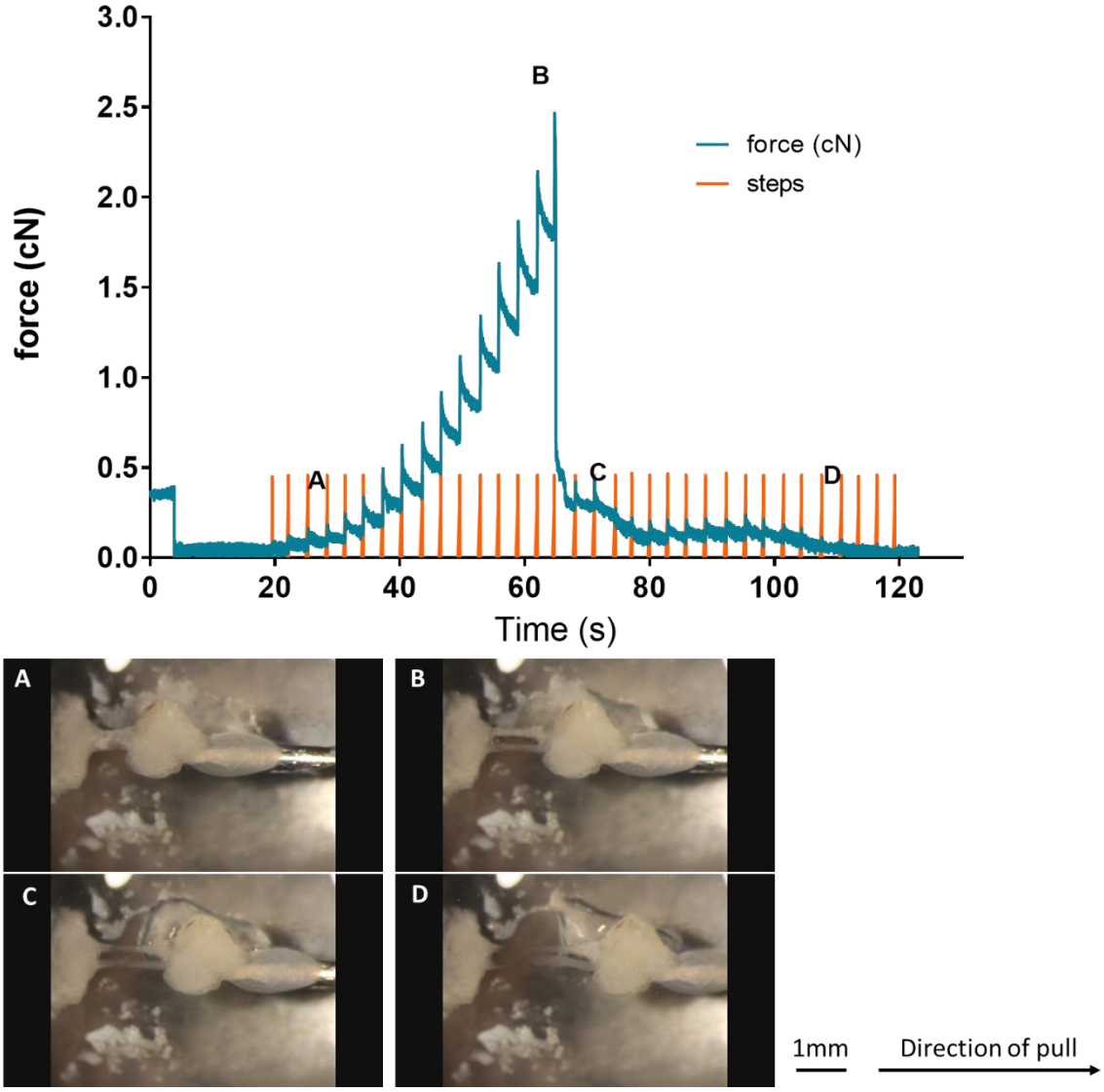

Figure 6-27: Example trace of pulling experiment on the connectives between the meso- and metathoracic ganglia of *G. bimaculatus*. The trace shows the forces (cN) recorded as the metathoracic ganglion was pulled away, causing the connectives to stretch. Areas of interest are (A) when the first forces are recorded, (B) when the connectives reach their maximum force just prior to breaking, (C) the sudden loss of force and (D) the moment the connectives were clearly severed.

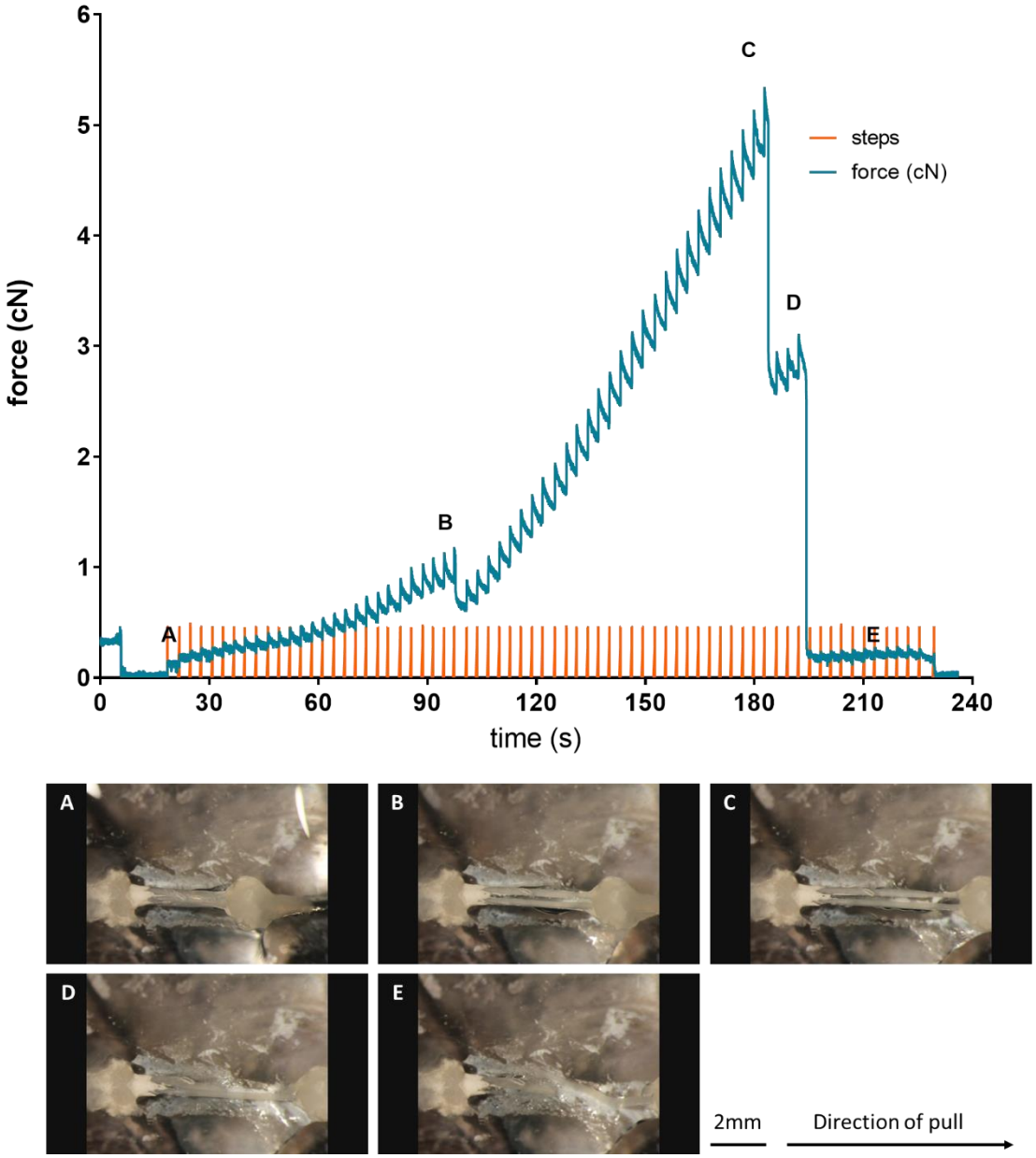

Figure 6-28: Example of pulling experiment in *P. americana*. The trace shows the forces (cN) recorded as the metathoracic ganglion was pulled away, causing the connectives to stretch. Areas of interest are (A) when the first forces are recorded, (B) when an element of the connectives breaks but does not lead to complete loss of force, likely part of the blood brain barrier, (C) the maximum force recorded, (D) the sudden breakage of one connective, and (E) the breakage of the second connective.

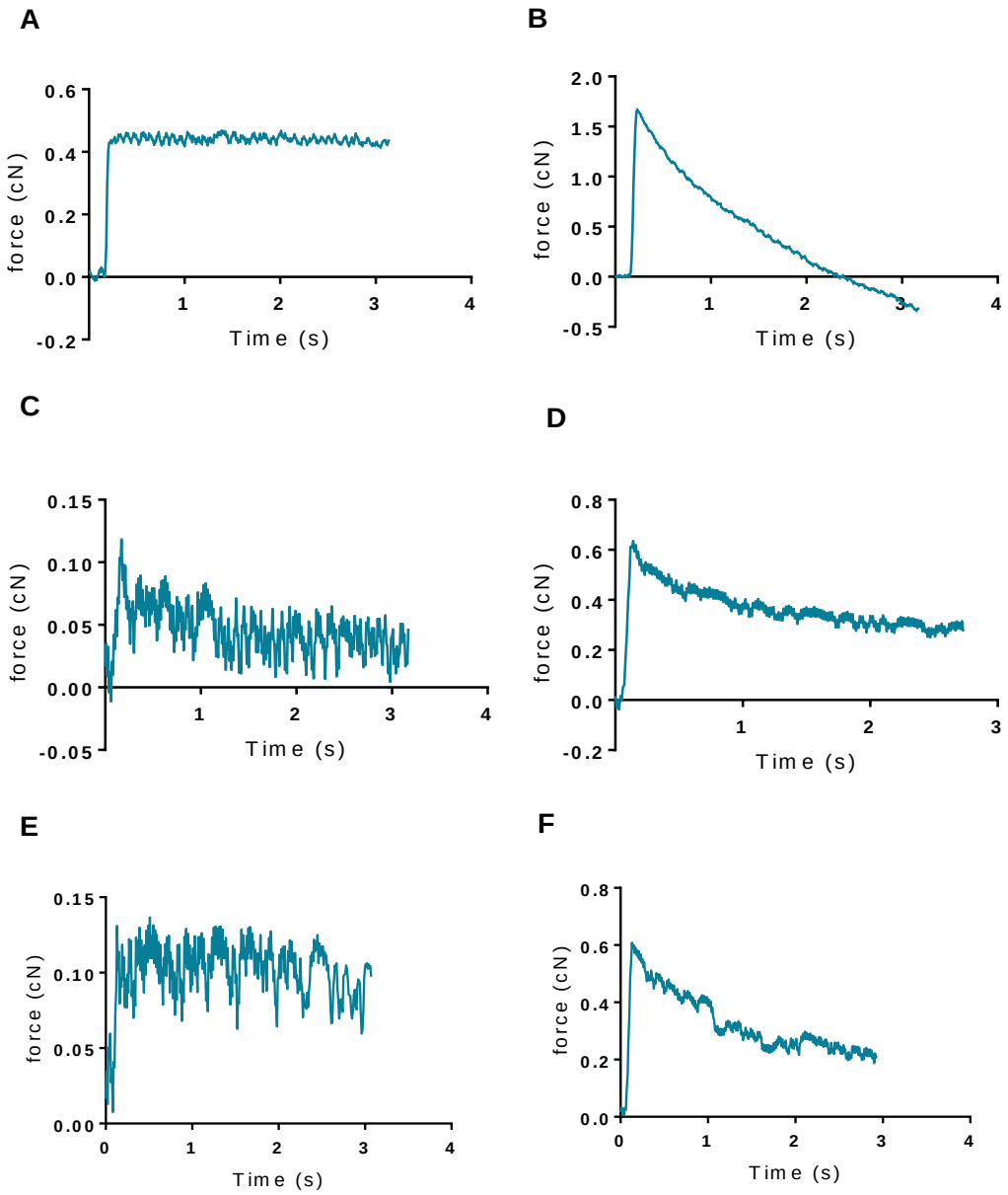

Figure 6-29: Examples of single steps early in the pulling experiments and near maximum force. Examples show the early steps where and increase in force was first detected (A,C,E) and later responses just prior to maximum force and breakage (B,D,F) of *S. gregaria* (A,B), *G. bimaculatus* (C,D) and *P. americana* (E,F). In all cases initial force is corrected to 0 cN.

6.5 Discussion

Tension in the connectives between the meso- and metathoracic ganglia is consistent across locust species, but differs from other orthopteroid species; both *G. bimaculatus* and *P. americana* connectives were under less tension in comparison to *S. gregaria*. The relative amounts of tension in the three connectives could be summarised as *S. gregaria* > *G. bimaculatus* > *P. americana*. These differences in tension relate to differences in the number and density of microtubules among species. However, we find no link between these results and strength or elasticity results from uniaxial loading. There was a consistent relationship between microtubules in longitudinal orientation along individual axons and tension in axon bundles at the macroscopic level. This suggests that tension in axons is related to VNC morphology and/or the anatomy of the organism implying that axon bundle tension has evolved in relation to selective pressures.

6.5.1 Microtubules in individual axons reflect macroscopic properties

To relate anatomy and subcellular components to the tension at the macroscopic scale, we compared the connectives between the meso- and metathoracic ganglia in desert locusts, black crickets and American cockroaches via TEM imaging. Several anatomical differences in the connectives between the meso- and metathoracic ganglion exist among the species: *G. bimaculatus* had small diameter connectives with a thinner BBB, smaller axons and a higher density of axons; *P. americana* had the largest diameter connectives but was otherwise very similar to *S. gregaria* connective composition. None of these differences correlate with the tension revealed by microdissection. Microdissection results show the desert locust has the highest tension exerted on the connectives between the meso- and metathoracic ganglia, however in no case did the

desert locust differ markedly in anatomy from both the American cockroach or the black cricket.

The differences in tension among the connectives of the different species can be explained through differences in the microtubules in longitudinal orientation along individual axons. The lowest density of microtubules occurred in *P. americana*. In regards to microtubules per axon, both *P. americana* and *G. bimaculatus* had a lower overall count per axon than *S. gregaria*. This directly reflects the tension revealed through microdissection, which suggests that microtubules in longitudinal orientation are related to *in vivo* tension. We found slope shifts between axon size and microtubule count among the species. This directly reflected tension revealed by microdissection because *S. gregaria* had the steepest relationship, followed by *G. bimaculatus* and finally *P. americana*. In previous chapters, we showed that the relationship between microtubule number and axon cross-section area was related to the amount of tension that bundle was under in microdissection experiments. This is also the case across species and is a conserved feature of axon bundles; axons under tension will have more microtubules in the longitudinal orientation and a steeper linear relationship between microtubule number and axon-cross section area.

6.5.2 Tensile properties of connectives do not reflect tension *in vivo*

Despite being under the least amount of tension, the connectives between the meso- and metathoracic ganglia of *P. americana* were much stronger than those of *G. bimaculatus* and similar to the high-tension connectives of *S. gregaria*. Uniaxial loading results do not account for size and are not an accurate test of tensile strength because of their dimensions (Davis, 2004). Furthermore, as we include the meso- and

metathoracic ganglia in our experiments, we may also be studying the strength of the connection between ganglia and connective, rather than the tensile strength of the connective itself. *G. bimaculatus* connectives are weaker than either the connectives in *P. americana* or *S. gregaria*, which could be a consequence of their small size, though size does not necessarily correlate with strength. We saw in chapter 4 that nerve 5 and the connectives between the metathoracic and fourth abdominal ganglia are similar strengths despite nerve 5 having a substantially wider diameter.

The observational data from the pulling experiments showed that *G. bimaculatus* exhibited very different responses to the stretching. With all the other axon bundles force would decrease abruptly when one or both of the connectives broke or detached from a ganglion. In *G. bimaculatus* the decrease in force happened as suddenly as other bundles but without visible breakage. Instead the connectives between the meso- and metathoracic ganglia in *G. bimaculatus* slowly tore apart over multiple steps after the initial sudden decrease in force. This suggests that the composition differs from those of the other connectives we tested. The connectives of *G. bimaculatus* are under slight tension and none of our TEM data showed an obvious anatomical difference that would explain their differing response to stretch.

In *S. gregaria* we found that despite absolute distances varying, once normalised as a percentage of the initial length *in vivo* all nerves could be stretched an additional 100% of their length (see Chapter 4). Comparing the connectives between the meso- and metathoracic ganglia among species, we also found variation in absolute length with *P. americana* able to stretch a much greater distance before breaking. When normalised for this increase the connectives in *S. gregaria* were more elastic than either of the others, indicating that elasticity is not conserved between species.

In absolute terms the adult *P. americana* that has the largest capability for stretch and is also the species with the greatest motility and the least tension. This is similar to our results from *S. gregaria,* in which the connectives between the metathoracic and fourth abdominal ganglia were capable of being stretched an empirically greater distance and were also under little or no tension and in the highly motile abdomen. This suggests that absolute capability to stretch may be an important function of axon bundles in motile regions.

6.5.3 Axonal tension and morphology

Despite anatomical differences in brain and body size, there was no difference in the tension in the connectives between the meso- and metathoracic ganglia between solitary or gregarious desert locusts, or migratory locusts. However, tension differed substantially in the other orthopteroid species. There are several possible explanations for these differences in the tension showing by connectives. The differences in tension may be linked to the differences in VNC morphology; while all these insects possess a fused metathoracic ganglion they do so to different extents (Niven *et al.*, 2008). In *S. gregaria* this is a fusion of four neuromeres, *G. bimaculatus* a fusion of three, and *P. americana* a fusion of two (see General Introduction). Van Essen (1997) posited that axonal tension drives morphology but we suggest that the converse relationship is more likely; morphology drives tension. If tension in axons drove morphology, we would expect that the tension would pull anteriorly because this is where morphological fusions of neuromeres have occurred. We would expect that the driving force behind the fusion of the metathoracic ganglion would be caused by anterior axon bundles pulling it. Instead, we see that the tension in the connectives anterior to the metathoracic ganglion is largely caused by a posterior pull.

Nervous system morphology is not the only explanation for the tension seen in the connectives between the meso- and metathoracic ganglia. Another possibility is that tension in axon bundles is linked to motility of the surrounding anatomy. The locust thorax is immotile being composed of rigid cuticle and lacks regions of movement (Albrecht, 1953). However, the abdomen, posterior to the connectives, is far more extensible particularly during mating and egg laying (Snodgrass, 1933), but is also continuously experiencing smaller motions connected to ventilation (Hamilton, 1964; Hustert, 1975; Burrows, 1996). In chapter 3 we found that the tension in the connectives between the meso- and the metathoracic ganglia in the desert locust was, in part, mediated by the VNC posterior to the metathoracic ganglion in the abdomen, while the connectives between the metathoracic and fourth abdominal ganglia that partially sit in the abdomen were under none themselves. This suggests that motile regions may exert forces upon the nerve cord, connectives directly exposed to the force are elastic and lack tension, while those indirectly exposed to those forces are capable of maintaining tension.

In the black cricket there is a region of thinner cuticle on the ventral surface covering the connectives between the meso- and metathoracic ganglia. The cricket is able to bend at this point, allowing movement between the meso- and metathoracic ganglia, with both ganglia then in relatively stable positions due to the apophyses. In the American cockroach, the entire thorax is highly motile with the cockroach able to bend and move along its length, and the VNC is positioned directly under the very thin ventral cuticle between the legs. This suggests that the nerve cord is subject to a range of external forces as the cockroach moves. When considered in the context of data from vertebrates, where tension is found in the central nervous system (Xu *et al.*, 2009, 2010;

Luna *et al.*, 2013), it suggests that tension is only present in axons that are not exposed to large external forces.

A neuron under tension that is exposed to pulling, twisting or other forces may be more prone to damage and therefore difficult to repair. This difficulty to repair occurs in other tissues under tension when they are damaged such as muscles under passive tension (Eccles, 1943; Hersche and Gerber, 1998; Davidson *et al.*, 2000; Luna *et al.*, 2013). However, the repeated discovery of adult axons under tension suggests that it is beneficial if the axon is relatively isolated from external forces. While no such benefit has been identified, tension may ensure an efficient arrangement of channels in vertebrate axons (Xu *et al.*, 2013; Zhang *et al.*, 2017). Moreover, elements of the cytoskeleton known to be involved in maintaining tension have been shown to be protective against damage caused by physical stresses in invertebrates (Hammarlund *et al.*, 2007).

6.5.4 Physical properties of axon bundles

The responses of the connectives to stretch have a profile that is classically viscoelastic (Alexander, 1983). Singular axons and axon bundles have been described repeatedly as viscoelastic (Galbraith *et al.*, 1993; Miller and Chinzei, 2002; Gefen and Margulies, 2004; Bernal *et al.*, 2007; Tamura *et al.*, 2008; Javid *et al.*, 2014) so this is unsurprising. Like the connectives between the meso- and metathoracic ganglia in *S. gregaria*, those in *P. americana* responded initially with an increase in force and no recovery and an elastic strain response at higher forces (Alexander, 1983). It is likely that the recovery response is just much slower at these low level of forces, as we saw in *S. gregaria* (see Chapter 4).

The difference in response to low levels of force versus high levels is intriguing, there are many possible explanations for what could be causing it and why it seems to be something that occurs only in these connectives and not in the other bundles of *S. gregaria* or in the connectives in *G. bimaculatus*. One possible reason we only see this behaviour in the cockroach and locust connectives between the meso- and metathoracic ganglia is that they both reach much higher forces before breaking than any of the other axon bundles studied, it may simply be that the 50 µm steps immediately exert a high enough force on the weaker bundles that they seem to 'skip' this long recovery phase in our current set-up whereas with the 'stronger' bundles we are able to observe all phases. As for why this slow recovery phase exists, it is likely that the axon bundles we have studied are all subject to some level of force change *in vivo*, whether through digestion, mating, egg laying or simply moving. None of the axon bundles are protected from the other internal systems (Chapman, 2013) and most will also be subject to the motility of the segments they are in. As such, it seems reasonable that these bundles may have some level of redundancy that ensures constant functioning at a range of different, low level, forces.

7 Discussion

7.1 Contributions of the thesis

We sought to understand how the nervous system achieves its final position during growth and development, highlighting the importance of mechanical properties that are often overlooked in favour of chemical guidance cues and genetic programmes. A theory proposed by Van Essen (1997) suggested an important role for axonal tension in the formation of the sulci and the gyri in the human cortex. We sought to study the link between the presence of tension within axonal bundles and the morphology of the VNC in orthopteroid insects.

This thesis makes novel contributions to understanding axon biomechanics in insects with implications for understanding the biomechanics of axons more generally. Considered as a whole, this thesis provides the first evidence that the composition of individual axons reflects mechanical properties of the entire axon bundle. The composition of axons within the bundles and, therefore, the mechanical properties of the bundles themselves varies greatly both within the same insect, and in the homologous bundle (specifically the connectives between the meso- and metathoracic ganglia) among closely-related but morphologically distinct insect species. This is the first example of such variance between closely-related species, and evidence of a close link between morphology and axonal tension. Importantly, this suggests that axonal tension is not simply a universal property of all axons but one that can be selected for with a specific function.

In this thesis, we have shown that cellular composition is correlated on the tension present within an entire axon bundle, and that properties at the cellular level

influence tissue mechanics on a macroscopic level. We have found that this influence of cellular composition on tissue mechanics holds true across bundles, growth, species and in response to insult. Our experimental findings also suggest that individual axon bundles have a tension set-point established prior to third instar (as we found consistent levels of tension from third instar throughout growth) that is then actively maintained even in response to perturbations in forces at the cost of surrounding morphology. Within closely-related species all of which are orthopteroid insects, there is substantial variability in the levels of tension among homologous axon bundles. Thus, we suggest that rather than tension driving morphology as suggested by Van Essen (1997), that morphology is driven by other mechanical properties of tissues (Razavi, Zhang, Li, *et al.*, 2015) and consequently leads to axonal tension during embryogenesis. We further suggest 'set-point' of tension then becomes integral to the axonal bundle function and that this can alter morphology in later growth if perturbed.

In chapter 3, we develop the first experimental model of axonal tension in adult insects in entire axon bundles. We show that axonal tension is not a universal property of all axon bundles and is in fact highly variable. Furthermore, we show that tension is largely mediated by connectives within the VNC that link ganglia to one another, and not by peripheral nerves. We also find that starvation or egg laying status do not change this tension, suggesting that other organs may have an influence but not one that is constantly altering the state of the animal.

In chapter 4, we further examined those axon bundles we had identified, finding that the tension to which they were exposed is independent of the composition of the gross morphology of the axon bundle but is instead linked to the number of

microtubules per axon, and the relationship between microtubules and axon area. To our knowledge, this is the first example of the mechanical properties of entire axon bundles being linked to individual axonal compositions. This suggests that other factors, such as bundle size, are less important in generating physical tension than the cytoskeletal composition of the axons within the bundle. This has clear implications for a range of studies including in the field of neurodegeneration in which the cytoskeleton is frequently involved or affected because the cytoskeleton of axons within tracts may be vital to the integrity of the tract itself. Furthermore, when coupled with the species specific differences this emphasises that tension may not be a simple universal property of axons with implications for the modelling of axons.

In chapter 4, we also investigated the mechanical properties of the connectives between the meso- and metathoracic ganglia, the connectives between the metathoracic and fourth abdominal ganglia and nerve 5 via uniaxial loading. In the case of *Schistocerca gregaria*, we found that the maximum amount of force experienced by a bundle prior to breakage also reflected the level of tension the bundle was exposed to *in vivo*. These bundles were also the least elastic empirically, which suggests that the axon bundles under tension resist perturbations to the tension to which they are subject. In all cases, the axon bundles exhibited viscoelastic behaviour as well as strain-stiffening responses as the forces increased per step.

In chapter 5, we studied the tension in the connectives between the meso- and metathoracic ganglia of *S. gregaria* during growth. The tension in these connectives is consistent throughout growth, even close to the moulting period. We also found that when one of the pair of connectives was severed at the third instar, exposing the

remaining connective to greater forces *in vivo*, tension was the same upon adulthood. This was despite massive morphological changes following insult including a reduction in the size of adults, reshaping of the meso- and metathoracic ganglia, invasion of tracheoles to the damaged area, and a likely repositioning of the ganglia and peripheral nerves due to a lengthening of the remaining connective itself. We found this maintenance of tension was twinned with an increase in axon number (suggesting some level of repair and rewiring); bundles contained more and smaller axons, and an increase in the number of microtubules but no change in the overall diameter. Again, this shows the importance of microtubules to the mechanics of an entire axon bundle.

These results show that axon tension is actively and homeostatically maintained throughout the period of growth, and in response to injury and perturbation via compensatory mechanisms such as the upregulation of microtubules in orientation. When considered in combination with the results of chapter 3, this suggests that different bundles are under different levels of tension with different 'set points' of tension that are actively maintained. Again, this has implications beyond understanding the development, growth and physiology of locusts but indicates a generally broader role for tension in axon bundles.

In chapter 6, we extended our findings into other insects by investigating the connectives between the meso- and metathoracic ganglia in other species. We found the differences in morphology, such as the different sizes of the sexes, between gregarious and solitary *S. gregaria* had no effect on the tension, and that *Locusta migratoria* was also very similar. However, the homologous connective in both *Gryllus bimaculatus* and *Periplaneta americana* was exposed to very different levels of tension.

Once again this was correlated with microtubule number and density and not with any other element of connective anatomy that were analysed in this thesis. Data from our uniaxial loading experiments showed that both *S. gregaria* and *P. americana* had similarly strong connectives with regards to the maximum force prior to breakage. The *P. americana* connectives could withstand the greatest stretch but when accounting for size the connectives of *S. gregaria* could withstand greater stretch. Once again, all connectives showed viscoelastic properties and a strain-stiffening response, and were under similar resting forces *in vivo*. The connectives of *G. bimaculatus* behaved differently to the other species; rather than breaking abruptly with a large decrease in force, the connectives split slowly apart and the force decreased gradually.

Our studies into different species show the variable and complex nature of axon bundles, even homologous bundles among species. Once again, we find the relationship between the axonal cytoskeleton and the properties of an axon bundle in its entirety, and this factor remains true across species. We also suggest that the tension within connectives does not necessarily reflect other mechanical properties such as elasticity or resistance to pull. These properties may be mediated by other components of the axon bundle, such as intermediate filaments or actin. We also found similar forces were experienced by the connectives in different species *in vivo*, however this measure does not consider active contraction within the axons nor the different sizes of the connectives studied so may not truly reflect the resulting tension experienced by the connectives. The same amount of force can cause different levels of stress on materials with different properties. While this conflicts with our results from chapter 4, where mechanical properties seemed to reflect tension in the locust, it is possible that axon bundles among species have broadly different compositions that were not accounted

for in this study leading to different mechanical properties. What remains is the clear relationship between microtubules and bundle tension.

Previous studies have found axonal tension in the brain and spinal cord (Xu *et al.*, 2009, 2010; Luna *et al.*, 2013). Both of these structures are protected from external stresses, this matches our findings that axon bundles under tension are those that are protected from motility. It is likely, therefore, that tension confers both a benefit to axonal functioning and a risk if exposed to damage. Therefore there is low or no tension in regions that are motile such as nerve 5 and the connectives between the metathoracic and fourth abdominal ganglia or the connectives between the meso- and metathoracic ganglia in *P. americana.* Axon bundles under tension are likely harder to repair if damaged due to the separation that would occur between severed ends as occurs in muscle tissue (Eccles, 1943; Hersche and Gerber, 1998; Davidson *et al.*, 2000; Luna *et al.*, 2013).

Therefore, having axon bundles under tension in regions that are more likely to experiences stresses (such as motile regions) is a risk. However, the fact that axonal tension is actively maintained suggests it is also beneficial. One possible benefit may be efficiency; an axon under tension is likely shorter requiring less membrane, fewer receptors, a shorter distance for action potentials to travel and for transport. Tension may also permit easier transport of components with less risk of tangles (Hirano, 1995) and a more efficient arrangement of receptors and membrane channels (Hammarlund *et al.*, 2007; Pielage *et al.*, 2009; Xu *et al.*, 2013; Zhang *et al.*, 2017). We also find that the macroscopic properties of axon bundles are determined by the composition of individual axons that varies greatly across closely related species, this contrasts with the

current dogma that treats axons or 'the axon' as a relatively homogenous cellular sub-compartment that is always under longitudinal tension.

7.2 Morphology and tension

We began this project in response to the hypothesis put forward by Van Essen (1997), that the tension of axons drove the morphology of the human brain. Several competing hypotheses have been proposed but early in our investigations a study was published that made this hypothesis far less likely to be correct (Razavi *et al.*, 2015). However, residual tension had been documented within the brain and spinal cord (Xu *et al.*, 2009; Luna *et al.*, 2013) suggesting that it is either an emergent property of these tissues or had an unknown function. We hypothesised that tension in axons and gross morphology are linked but that it is morphology that drives or allows tension to emerge. We found the highest levels of tension in connectives that were well shielded from external forces, and the lowest in those that were subject to motility; both within our primary experimental model *S. gregaria* and among other species. We also found evidence of a relationship between tension in the connectives between the meso- and metathoracic ganglia and the extent of fusion in the metathoracic ganglia, finding that higher tension was found in animals with more neuromeres in the ganglia. This suggests that fusion of neuromeres away from their original parallel segmental placement may induce forces; however, this is not mediated by the peripheral nerves. In retrospect, this makes sense because the peripheral nerves are generated at the peripheral tissues (Caudy and Bentley, 1986) and project to the VNC. If they were generated from the nerve cord and then towed via stretch-growth as the limb grew away from the VNC we would expect them to exert greater forces.

To determine whether morphology is linked to the tensile properties of axon bundles, we would need to expand our studies to other species and connectives insulated from external forces, and to other fused ganglia. Fortunately insects offer a wide range of morphologies with which to accomplish this (Niven *et al.*, 2008). However, if our theory that the risk of exposure to external forces due to motility of the surrounding segment is correct, then this explains the presence of axonal tension in the brain and spinal cord because both structures are well protected from external forces by bone unlike peripheral nerves that are constantly exposed to them. This does not necessarily disagree with the work of Razavi *et al.*, (2015), which shows that cortical folding is driven by mechanical properties of cells other than axonal tension because we do not address the driving forces behind these properties. We suggest that possibly the folding drives tension or that tension occurs independently.

7.3 Microtubules in tension

Microtubules have been shown to play important roles in the tension in axons during post-embryonic growth and development via increasing polymerisation producing a pushing force and depolymerisation creating pulling forces (Gordon *et al.*, 2001; Kulic *et al.*, 2008). They are also involved in cross-talk with other components of the cytoskeleton: actin and intermediate filaments (Kaverina *et al.*, 1998; Small *et al.*, 1999; Wehrle-Haller and Imhof, 2003). We have found a consistent link between the number of microtubules within individual axons in axon bundles and the amount of tension measured from those connectives. Previous work has shown that increasing axon size is linked to an increase in microtubule numbers (Pannese *et al.*, 1984).

We have found that that relationship between microtubule number and axon size differs among bundles in the same species (*S. gregaria)* and among homologous bundles in different species (the connectives between the meso- and metathoracic ganglia). This suggests that microtubule number may not simply be linked to size but also indicates other features of the axon bundle. We show that microtubule number in individual axons is linked to the tension held within the axon bundle. Because microtubules are also important for transport, a higher number could indicate an axon requiring more transport perhaps due to high levels of synaptic activity. It seems unlikely, however, that there would be vastly different transport requirements in the connectives between the meso- and metathoracic ganglia in one species compared to another, or in the connectives between the metathoracic and fourth abdominal ganglia of the same species. Furthermore, previous work has shown a linear relationship between axon diameter, firing rate and mitochondrial density that is maintained across different tracts (Perge *et al.*, 2012), whereas our data shows differences in the linear relationship microtubule number and axon diameter, suggesting that it is not simply a function of firing rate or energy consumption.

Understanding the basis of adult axonal tension will likely be an important step in the field of axonal repair after injury and linking this to microtubules also has many implications for neurodegenerative diseases that either originate from or subsequently cause dysfunction in microtubules. Our results suggest that different axonal bundles rely on microtubules for tension to different extents; perhaps suggesting that certain axons will be more vulnerable to microtubule dysfunction than others.

7.4 Stretch-growth

Although we were not directly studying stretch growth, our investigations have implications for its understanding. Stretch growth, the growth of integrated axons caused by the pulling of surrounding growing tissue (Bray, 1984; Loverde *et al.*, 2011), is poorly understood. A leading hypothesis is that it is a passive reaction to elements of the cytoskeleton being broken by the external pulling forces of tissue and a subsequent accumulation of transported materials at the broken regions and integration of these into the axon (Heidemann and Bray, 2015). However, this theory relies on axonal transport speeds which are not fast enough to account for extreme growth seen in axons (Smith, 2009). A second hypothesis addresses this by suggesting that stretch opens mechanosensitive ion channels in the axon that signals for growth which largely occurs at the junction between the axon and soma (Purohit and Smith, 2016), thus removing the necessity for transport of membrane components down the axon. However, this hypothesis also suggests growth is passive in response to stretch. We suggest that stretch growth is not a passive mechanism, instead axons must reach a set point before they respond with growth or they can actively resist external forces to maintain a set point of tension. Our results show that all of the connectives between the meso- and metathoracic ganglia across the three species that we tested directly were under a small amount of force *in vivo* that did not necessarily reflect the tension of the connectives. However, this small external force apparently was not leading to stretch growth suggesting that either it was not a large enough force to induce it, or the axons were actively resisting. The mechanosensitive ion channel hypothesis (Purohit and Smith, 2016) could, speculatively, include regulation or set-points through regulation of the involved ion channels. Stretch growth has been difficult to study as dysfunction in the

process during embryogenesis is very likely fatal (Smith, 2009). Consequently, we have yet to identify diseases in which an element of the process is disrupted. Therefore, inferences such as the ones presented in this thesis are still important until more direct evidence becomes available.

7.5 Open questions

The aim of this thesis was primarily exploratory, to investigate if indeed tension was held in adult axonal bundles and further investigate the properties of these bundles. As such there are an endless number of open questions as this project has implications for many different fields of study.

A primary question remains; what is the function of the tension held in axons? We have suggested that tension must confer some level of efficiency within a bundle, but that this is paired with a risk of damage, or struggle to repair. An hypothesis presented by Zhang *et al.* (2017) offers one possibility. They suggest that if spectrin filaments, a tetramer associated with the lipid bilayer and linked to structure in other cells such as red blood cells (Mohandas and Evans, 1994), that are found within axons are under tension this could cause irreversible damage if the axon is injured as these filaments do not self-assemble. However, they also hypothesise that the tension in the spectrin filaments limits the thermal motion of the ankyrin proteins. Ankyrin proteins attach to the actin-spectrin cytoskeleton and to various membrane proteins including ion channels (Matsuoka *et al.*, 1998; Malhotra *et al.*, 2000). They have been identified in humans, *C. elegans* and *D. melanogaster* (Hopitzan *et al.*, 2006). Zhang *et al.* (2017) posit that the stability of the ankyrin proteins subsequently stabilises the associated voltage-gated sodium channels along the axon, keeping them in a configuration that may be more efficient. While similar arrangements have yet to be identified in

invertebrate axons, ankyrin lattices have been found in *Drosophila* axons (Pielage *et al.*, 2009) and β-spectrin has been shown to be protective against strain-induced damage in *C. elegans* (Hammarlund *et al.*, 2007). If tension increases the efficiency of sodium channels, then axon bundles not under tension would likely require compensatory mechanisms such as an increased number of channels. It has also been suggested that in humans maintaining tension in the cytoskeleton may protect from formation of tangles seen in diseases such as amyotrophic lateral sclerosis (ALS) (LaMonte *et al.*, 2002; Chevalier-larsen and Holzbaur, 2006), however, identifying the specific function of tension remains difficult as all of the components are involved in various other roles.

Another open question is the role of other cytoskeleton components in the tension of axon bundles. We chose to begin with microtubules due to their involvement in dynamic changes of tension in growth and development (Tanaka *et al.*, 1995; Gordon *et al.*, 2001; Tsaneva-Atanasova *et al.*, 2009), as well as the fact microtubules were easily counted in the perpendicular orientation to the section plane using the same preparation that allowed us to measure axon diameter and macroscopic properties of the bundle. We can now move on to looking at individual factors such as actin amount. We can also begin to investigate the active roles of each component by chemically disrupting them during our microdissections and uniaxial loading experiments to further elucidate individual roles.

A still unanswered question is also the source of the tension we saw. We found that a portion of it seemed to be mediated by the nerve cord posterior to the region of interest, but that this did not account for all the tension. It is possible the residual tension actually arises from the axons themselves in the form of contraction of the

cytoskeleton: this could be further studied by examining the presences of motor proteins in the bundles, again across species and in response to the third instar nerve cutting microsurgery.

We have also questioned whether stretch growth is a passive phenomenon. External force is applied to the connectives between the meso- and metathoracic ganglia from the surrounding nerve cord, yet they do not grow to accommodate this. It is unclear whether this is due to active resistance to stretch-growth, or that a certain threshold of force is required before stretch-growth is initiated. Investigating this would be an important step in understanding a currently poorly understood phenomenon.

8 Bibliography

Abercrombie, M., Heaysman, J. E. M. and Pegrum, S. M. (1971) 'The locomotion of fibroblasts in culture. IV. Electron microscopy of the leading lamella', *Experimental Cell Research*, **67**, pp. 359–367.

Ahmed, W. W., Li, T. C., Rubakhin, S. S., Chiba, A., Sweedler, J. V. and Saif, T. A. (2012) 'Mechanical tension modulates local and global vesicle dynamics in neurons', *Cellular and Molecular Bioengineering*, **5**, pp. 155–164.

Ahmed, W. W., Williams, B. J., Silver, A. M., Saif, T. A., Li, Z., Howard, J. *et al.* (2013) 'Measuring nonequilibrium vesicle dynamics in neurons under tension', *Lab on a Chip*, **13**, p. 570.

Ahmed, W. W. and Saif, T. A. (2014) 'Active transport of vesicles in neurons is modulated by mechanical tension', *Scientific Reports*, **4**, p. 4481.

Akhmanova, A. and Steinmetz, M. O. (2015) 'Control of microtubule organization limelight', *Nature Publishing Group*, **16**, pp. 711–726.

Akhshi, T. K., Wernike, D. and Piekny, A. (2014) 'Microtubules and actin crosstalk in cell migration and division', *Cytoskeleton*, **71**, pp. 1–23.

Alberts, B., Johnson, A., Lewis, J., Morgan, D., Raff, M., Roberts, K. and Walter, P. (2015) *Molecular Biology of the Cell*. Sixth. New York: Garland Science, Taylor & Francis Group.

Albrecht, F. O. (1953) *The Anatomy of the Migratory Locust*. first. London: University of London, Athlone Press.

Alexander, R. M. (1983) *Animal Mechanics*. Second. Chichester: Blackwell Scientific Publications.

Aliee, M., Röper, J. C., Landsberg, K. P., Pentzold, C., Widmann, T. J., Jülicher, F. and Dahmann, C. (2012) 'Physical mechanisms shaping the *Drosophila* dorsoventral compartment boundary', *Current Biology*, **22**, pp. 967–976.

Allen, C. and Borisy, G. G. (1974) 'Structural polarity and directional growth of microtubules of *Chlamydomonas* flagella', *The Journal of Molecular BiologyJournal of Molecular Biology*, **90**, pp. 381–402.

Allodi, I., Udina, E. and Navarro, X. (2012) 'Specificity of peripheral nerve regeneration : Interactions at the axon level', *Progress in Neurobiology*, **98**, pp. 16–37.

Angelillo, F. V. F. F. M. (2006) 'Anisotropic constitutive equations and experimental tensile behavior of brain tissue', *Biomechanics and Modeling in Mechanobiology*, **5**, pp. 53–61.

Anstey, M. L., Rogers, S. M., Ott, S. R., Burrows, M. and Simpson, S. J. (2009a) 'Gregarization underlying swarm formation in desert locusts', *Science*, **323**, pp. 627–630.

Anstey, M. L., Rogers, S. M., Ott, S. R., Burrows, M. and Simpson, S. J. (2009b) 'Serotonin mediates behavioral gregarization underlying swarm formation in desert locusts', *Science*, **323**, pp. 627–631.

Arancibia-ca, I. L., Ford, M. C., Cossell, L., Ishida, K., Tohyama, K. and Attwell, D. (2017) 'Node of Ranvier length as a potential regulator of myelinated axon conduction speed', *eLife*, **6**, pp. 1–15.

Arendt, D. and Nübler-jung, K. (1999) 'Comparison of early nerve cord development in insects and vertebrates', *Development*, **2325**, pp. 2309–2325.

Arnold, E. M., Hamner, S. R., Seth, A., Millard, M. and Delp, S. L. (2013) 'How muscle fiber lengths and velocities affect muscle force generation as humans walk and run at different speeds', *The Journal of Experimental Biology*, **216**, pp. 2150–2160.

Astbury, W. T. (1939) 'X-ray studies of the structure of compounds of biological interest', *Annu. Rev. Biochem*, **8**, pp. 113–133.

Astbury, W. T. and Street, A. (1930) 'X-ray studies of the structure of hair, wool, and related fibres. I. General.', *Philos. Trans. R. Soc. Lond. A.*, **230**, pp. 75–101.

Athamneh, A. I. M. and Suter, D. M. (2015) 'Quantifying mechanical force in axonal growth and guidance.', *Frontiers in cellular neuroscience*, **9**, p. 359.

Ayali, A. and Lange, A. B. (2010) 'Rhythmic behaviour and pattern-generating circuits in the locust: Key concepts and recent updates', *Journal of Insect Physiology*, **56**, pp. 834–843.

Bahler, A. S., Fales, John, T. and Zierler, K. L. (1968) 'The dynamic properties of mammalian skeletal muscle', *The Journal of General Physiology*, **51**, pp. 369–384.

Bannister, J., Kemper, C. M. and Warneke, R. M. (1996) *The action plan for Australian Cetaceans.* Canberra: Australian Nature Conservation Agency.

Bard, L., Lambert, M., Choquet, D., Thoumine, O. and Curie, M. (2008) 'A molecular clutch between the actin flow and N-cadherin adhesions drives growth cone migration', *The Journal of Neuroscience*, **28**, pp. 5879–5890.

Bastiani, M. J., Lac, S. and Goodman, C. S. (1986) 'Guidance of neuronal growth cones in the grasshopper embryo. I. Recognition of a specific axonal pathway by the pCC neuron', *The Journal of Neuroscience*, **6**, pp. 3518–3531.

Bate, B. C. M. (1976) 'Embryogenesis of an insect nervous system I . A map of the thoracic and abdominal neuroblasts in *Locusta migratoria*', *J. Embryol. exp. Morph*, **35**, pp. 107–123.

Bell, W. J. and Adiyodi, K. G. (eds) (1982) *The American Cockroach*. New York: Chapman and Hall Ltd.

Bentley, D. and Toroian-Raymond, A. (1989) 'Pre-axonogenesis migration of afferent pioneer cells in the grasshopper embryo', *Journal of Experimental Zoology*, **251**, pp. 217–223.

Berbel, P. and Innocenti, G. M. (1988) 'The development of the corpus callosum in cats : A light- and electron-microscopic study', *The Journal of comparative neurology*, **276**, pp. 132–156.

Bernal, R., Pullarkat, P. A. and Melo, F. (2007) 'Mechanical properties of axons', *Physical Review Letters*, **99**, pp. 6–9.

Betz, T., Koch, D., Lu, Y.-B., Franze, K. and Käs, J. A. (2011) 'Growth cones as soft and weak force generators.', *Proceedings of the National Academy of Sciences of the United States of America*, **108**, pp. 13420–5.

Bevan, S. and Burrows, M. (2003) 'Localisation of Even-skipped in the mature CNS of the locust, *Schistocerca gregaria*', *Cell and Tissue Research*, **313**, pp. 237–244.

Borisy, G. G. and Taylor, E. W. (1967) 'The mechanism of action of colchicine: Colchicine binding to sea urchin eggs and the mitotic apparatus colchicine binding to intact sea', *Journal of Cell Biology*, **34**, pp. 535–548.

Bragg, W. H. and Bragg, W. L. (1915) *X rays and crystal structure*. London: G. Bell.

Bray, D. (1979) 'Mechanical tension produced by nerve cells in tissue culture.', *Journal of cell science*, **37**, pp. 391–410.

Bray, D. (1984) 'Axonal growth in response to experimentally applied mechanical tension', *Developmental Biology*, **102**, pp. 379–389.

Bray, D. and White, J. G. (1988) 'Cortical flow in animal cells', *Science*, **239**, pp. 883–888.

Bridgman, P. C., Dave, S., Asnes, C. F., Tullio, A. N. and Adelstein, R. S. (2001) 'Myosin IIB is required for growth cone motility', *The Journal of Neuroscience*, **21**, pp. 6159–6169.

Brodland, G. W. (2016) 'The differential interfacial tension hypothesis (DITH): A comprehensive theory for the self-rearrangement of embryonic cells and tissues', *Journal of Biomechanical Engineering*, **124**, pp. 188–197.

Bryan, J. (1972) 'Vinblastine and microtubules II. characterisation of two protein subunits from the isolated crystals', *The Journal of Molecular Biology*, **66**, pp. 157–168.

Bullock, T. H. and Horridge, G. A. (1965) *Structure and Function in the Nervous System of Invertebrates. vol 2.* San Francisco and London: W. H. Freeman a. Comp. Ltd.

Burns, R. G. (1991) 'α-, β- and γ-tubulins: Sequence comparisons and structural constraints', *Cell Motility and the Cytoskeleton*, **20**, pp. 181–189.

Burrows, M. (1979) 'Graded synaptic interactions between local premotor interneurons of the locust', *Journal of neurophysiology*, **42**, pp. 1108–1123.

Burrows, M. (1996) *The Neurobiology of an Insect Brain*. Oxford: Oxford University Press.

Butler, C. S. and Lakes-harlan, R. (2011) 'Morphological and physiological regeneration in the auditory system of adult *Mecopoda elongata* (Orthoptera: Tettigoniidae)', *J Comp Physiol*, **197**, pp. 181–192.

Cajal, S. R. y (1897) 'Leyes de la morphologia y dinamismo de las células nerviosas.', *Rev Trim Micrograf*, **2**.

Cajal, S. R. y (1911) *Histologie du système nerveux de l'homme et des vertébrés*. Paris Maloine.

Carisey, A., Tsang, R., Greiner, A. M., Nijenhuis, N., Heath, N., Nazgiewicz, A., Kemkemer, R., Derby, B. and Spatz, J. (2013) 'Article vinculin regulates the recruitment and release of core focal adhesion proteins in a force-dependent manner', *Current Biology*, **23**, pp. 271–281.

Carpenter, S. (1968) 'Proximal axonal enlargement in motor neuron disease.', *Neurology*, **18**, pp. 841–851.

Cash, A. D., Aliev, G., Siedlak, S. L., Nunomura, A., Fujioka, H., Zhu, X., Raina, A. K., Vinters, H. V, Tabaton, M., Johnson, A. B., Paula-barbosa, M., Av, J., Jones, P. K., Castellani, R. J., Smith, M. A. and Perry, G. (2003) 'Microtubule reduction in Alzheimer's disease and aging is independent of τ filament formation', *American Journal of Pathology*, **162**, pp. 1623–1627.

Cassimeris, L. U., Walker, R. A., Pryer, N. K. and Salmon, E. D. (1987) 'Dynamic instability of microtubules', *BioEssays*, **7**, pp. 149–154.

Castillo, A. E., Rossoni, S. and Niven, J. E. (2018) 'Matched short-term depression and recovery encodes interspike interval at a central synapse', *Scientific Reports*, **8**, pp. 1–12.

Caudy, M. and Bentley, D. (1986) 'Pioneer growth cone steering along a series of neuronal and non-neuronal cues of different affinities', *The Journal of Neuroscience*, **6**, pp. 1781–1795.

Chada, S., Lamoureux, P., Buxbaum, R. E. and Heidemann, S. R. (1997) 'Cytomechanics of neurite outgrowth from chick brain neurons.', *Journal of cell science*, **110**, pp. 1179–86.

Chang, L. and Goldman, R. D. (2004) 'Intermediate filaments mediate cytoskeletal crosstalk', *Nature reviews. Molecular cell biology*, **5**, pp. 601–613.

Chang, P. and Stearns, T. (2000) 'δ -Tubulin and ε -tubulin : two new human centrosomal tubulins reveal new aspects of centrosome structure and function', *Nature cell biology*, **2**, pp. 30–35.

Chapman, R. F. (2013) *The Insects: structure and function*. fifth. Edited by S. J. Simpson and A. E. Douglas. Cambridge: Cambridge University Press.

Cheffings, T. H., Burroughs, N. J. and Balasubramanian, M. K. (2016) 'Actomyosin ring formation and tension generation in eukaryotic cytokinesis', *Current Biology*, **26**, pp. R719–R737.

Cheng, S., Clarke, E. C. and Bilston, L. E. (2008) 'Rheological properties of the tissues of the central nervous system: A review', *Medical Engineering and Physics*, **30**, pp. 1318–1337.

Chevalier-larsen, E. and Holzbaur, E. L. F. (2006) 'Axonal transport and neurodegenerative disease', *Biochimica et Biophysica Acta 1762*, **1762**, pp. 1094–1108.

Chou, S. M. and Fakadej, A. V (1971) 'Ultrastructure of chromatolytic motoneurons and anterior spinal roots in a case of werdnig-hoffman diseases', *J. Neuropathol. Exp. Neurol.*, **30**, pp. 368–379.

Chretien, D., Fuller, S. D., Karsenti, E. and Chem, R. C. W. J. B. (1995) 'Structure of growing microtubule ends: Two-dimensional sheets close into tubes at variable rates', *The Journal of Cell Biology*, **129**, pp. 1311–1328.

Christman, C. W., Grady, M. S., Walker, S. A., Holloway, K. L. and Povlishock, J. T. (1994) 'Ultrastructural studies of diffuse axonal injury in humans', *Journal of Neurotrauma*, **11**, pp. 173–186.

Chugh, P. and Paluch, E. K. (2018) 'The actin cortex at a glance', *Journal of cell science*, **131**, pp. 1–9.

Ciobanasu, C., Faivre, B. and Clainche, C. Le (2014) 'Actomyosin-dependent formation of the mechanosensitive talin–vinculin complex reinforces actin anchoring', *Nature Communications*, **5**, pp. 1–10.

Clarke, R. S. J., Hellon, R. F. and Lind, A. R. (1958) 'The duration of sustained contractions of the human forearm at different muscle temperatures', *Journal of Physiology*, **143**, pp. 454–473.

Clarkson, B., Ota, K., Ohkita, T. and O'Connor, A. (1965) 'Kinetics of proliferation of cancer cells in neoplastic effusions in man', *Cancer*, **18**, pp. 1189–1213.

Cochran, D. G. (2009) 'Chapter 27 - *Blattodea*: (Cockroaches)', in Resh, V. H. and Cardé, R. T. (eds) *Encyclopedia of Insects*. second. Burlington: Academic Press, pp. 108–112.

Cohen, T. S., Smith, A., Massouros, P. G., Bayly, P. V, Amy, Q. and Genin, G. M. (2008) 'Inelastic behaviour in repeated shearing of bovine white matter', *Journal of Biomechanical Engineering*, **130**, pp. 1–10.

Conde, C. and Cáceres, A. (2009) 'Microtubule assembly , organization and dynamics in axons and dendrites', *Nature Reviews. Neuroscience*, **10**, pp. 319–332.

Condron, B. G. and Zinn, K. (1994) 'The grasshopper median neuroblast is a multipotent progenitor cell that generates glia and neurons in distinct temporal phases.', *The Journal of Neuroscience*, **14**, pp. 5766–77.

Condron, B. G. and Zinn, K. (1997) 'Regulated neurite tension as a mechanism for determination of neuronal arbor geometries *in vivo*', *Current Biology*, **7**, pp. 813–816.

Cooke, P. (1976) 'A filamentous cytoskeleton in vertebrate smooth muscle fibers', *The Journal of Cell Biology*, **68**, pp. 539–556.

Coste, B., Mathur, J., Schmidt, M., Earley, T. J., Ranade, S., Petrus, M. J., Dubin, A. E. and Patapoutian, A. (2010) 'Piezo1 and Piezo2 are essential components of distinct mechanically-activated cation channels', *Science*, **330**, pp. 55–60.

Cramer, L. P. (2013) 'Mechanism of cell rear retraction in migrating cells', *Current Opinion in Cell Biology*, **25**, pp. 591–599.

Davidson, P. A., Rivenburgh, D. W. and Petersburg, S. (2000) 'Rotator cuff repair tension as a determinant of functional outcome', *J Shoulder Elbow Surg*, **9**, pp. 502–506.

Davis, J. R. (2004) *Tensile Testing*. second. Materials Park: ASM International.

Deiters, O. F. K. (1865) *Untersuchungen über Gehirn und Rückenmark des Menschen und der Säugethiere.* third. New York: Braunschweig Vieweg.

Demali, K. A., Sun, X. and Bui, G. A. (2014) 'Force transmission at cell−cell and cell−matrix adhesions', *Biochemistry*, **53**, pp. 7706–7717.

Dennerll, T. J., Joshi, H. C., Steel, V. L., Buxbaum, R. E. and Heidemann, S. R. (1988) 'Tension and compression in the cytoskeleton of PC-12 neurites II: Quantitative measurements', *The Journal of Cell Biology*, **107**, pp. 665–674.

Dent, E. W., Gupton, S. L. and Gertler, F. B. (2011) 'The growth cone cytoskeleton in Axon outgrowth and guidance', *Cold Spring Harbor Perspectives in Biology*, **3**, pp. 1–39.

Devine, R. and Anderson, E. (1957) 'Ultrastructure of the nuclear membrane of a gregarine parasitic in grasshoppers', *Experimental Cell Research*, **13**, pp. 200–204.

Dingyu, W., Fanjie, M., Zhengzheng, D., Baosheng, H. and Chao, Y. (2016) 'Regulation of intracellular structural tension by talin in the axon growth and regeneration', *Molecular Neurobiology*, **53**, pp. 4582–4595.

Dittmer, T. and Misteli, T. (2011) 'The lamin protein family', *Genome Biology*, **12**, pp. 1–14.

Dodemont, H., Riemer, D. and Weber, K. (1990) 'Structure of an invertebrate gene

encoding cytoplasmic intermediate filament (IF) proteins: implications for the origin and the diversification of IF proteins', *The EMBO Journal*, **9**, pp. 4083–4094.

Doe, C. Q. and Goodman, C. S. (1985) 'Early events in insect neurogenesis. I. Development and segmental differences in the pattern of neuronal precursor cells', *Developmental Biology*, **111**, pp. 193–205.

Dorfman, J. G. and Cherdantzev, V. G. (1975) 'Mechanical stresses and morphological patterns in amphibian embryos', *J. Embryol. exp. Morph*, **34**, pp. 559–574.

Doring, V. and Stick, R. (1990) 'Gene structure of nuclear lamin Lil of *Xenopus laevis*; a model for the evolution of IF proteins from a lamin-like ancestor', *The EMBO Journal*, **9**, pp. 4073–4081.

Draper, M. H. and Hodge, A. J. (1949) 'Sub-microscopic localisation of minerals in skeletal muscle by internal "micro-incineration" within the electron microscope', *Nature*, **163**, pp. 576–577.

Draper, M. H. and Hodge, A. J. (1950) 'Electron-induced microincineration with the electron microscope. 1. Distribution of residual mineral content in vertebrate striated muscle', *Australian Journal of Experimental Biology & Medical Science*, **28**, pp. 549–558.

Drechsel, D. N., Hyman, A. A., Cobb, M. H. and Kirschner, M. W. (1992) 'Modulation of the dynamic instability of tubulin assembly by the microtubule-associated protein tau', *Molecular biology of the cell*, **3**, pp. 1141–1154.

Duan, Y., Dong, S., Gu, F., Hu, Y. and Zhao, Z. (2012) 'Advances in the pathogenesis of Alzheimer's disease: Focusing on tau-mediated neurodegeneration', *Translational Neurodegeneration*, **1**, pp. 1–7.

Ducuing, A. and Vincent, S. (2016) 'The actin cable is dispensable in directing dorsal closure dynamics but neutralizes mechanical stress to prevent scarring in the *Drosophila* embryo', *Nature cell biology*, **18**, pp. 1149–1160.

Dutcher, S. K. and Trabuco, E. C. (1998) 'The UNI3 gene is required for assembly of basal bodies of *Chlamydomonas* and encodes δ-tubulin, a new member of the tubulin superfamily', *Molecular Biology and Evolution*, **9**, pp. 1293–1308.

Eccles, J. C. (1943) 'Investigations on muscle atrophies arising from disuse and tenotomy', *Journal of Physiology*, **103**, pp. 253–266.

Ecken, J. Von Der, Heissler, S. M., Pathan-chhatbar, S., Manstein, D. J. and Raunser, S. (2016) 'Cryo-EM structure of a human cytoplasmic actomyosin complex at near-atomic resolution', *Nature*, **534**, pp. 724–728.

Edwards, K. A., Demsky, M., Montague, R. A., Weymouth, N. and Kiehart, D. P. (1997) 'GFP-Moesin illuminates actin cytoskeleton dynamics in living tissue and demonstrates cell shape changes during morphogenesis in *Drosophila*', *Developmental Biology*, **117**,

pp. 103–117.

Eibl, E. and Huber, F. (1979) 'Central projections of tibial sensory fibers within the three thoracic ganglia of crickets (*Gryllus campestris* L., *Gryllus bimaculatus* DeGeer)', *Zoomorphologie*, **17**, pp. 1–17.

Elder, G. A., Friedrich, V. L., Bosco, P., Kang, C., Gourov, A., Tu, P., Lee, V. M. and Lazzarini, R. A. (1998) 'Absence of the mid-sized neurofilament subunit decreases axonal calibers, levels of light neurofilament (NF-L), and neurofilament content', *The Journal of Cell Biology*, **141**, pp. 727–739.

Elkin, B. S., Gabler, L. F., Panzer, M. B. and Siegmund, G. P. (2018) 'Brain tissue strains vary with head impact location : A possible explanation for increased concussion risk in struck versus striking football players', *Clinical Biomechanics*, **0**, pp. 1–9.

Engler, A., Bacakova, L., Newman, C., Hategan, A., Griffin, M. and Discher, D. (2004) 'Substrate compliance versus ligand density in cell on gel responses', *Biophysical journal*, **86**, pp. 15–25.

Erber, A., Riemer, D., Hofemeister, H., Bovenschulte, M., Stick, R., Panopoulou, G., Lehrach, H. and Weber, K. (1999) 'Characterization of the *Hydra* lamin and its gene: A molecular phylogeny of metazoan lamins', *J Mol Evol*, **49**, pp. 260–271.

Van Essen, D. C. (1997) 'A tension-based theory of morphogenesis and compact wiring in the central nervous system.', *Nature*, **385**, pp. 313–318.

Estecha, A., Sánchez-martín, L., Puig-kröger, A., Bartolomé, R. A., Teixidó, J., Samaniego, R. and Sánchez-mateos, P. (2009) 'Moesin orchestrates cortical polarity of melanoma tumour cells to initiate 3D invasion', *Journal of cell science*, **122**, pp. 3492–3501.

Evans, L. L., Lee, A. J., Bridgman, P. C. and Mooseker, M. S. (1998) 'Vesicle-associated brain myosin-V can be activated to catalyze actin-based transport', *Journal of cell science*, **111**, pp. 2055–2066.

Fadic, R., Vergara, J. and Alvarez, J. (1985) 'Microtubules and caliber of central and peripheral processes of sensory axons', *The Journal of comparative neurology*, **236**, pp. 258–264.

Faisal, A. A., White, J. A. and Laughlin, S. B. (2005) 'Ion-channel noise places limits on the miniaturization of the brain's wiring', *Current Biology*, **15**, pp. 1143–1149.

Fan, A., Tofangchi, A., Kandel, M., Popescu, G. and Saif, T. (2017) 'Coupled circumferential and axial tension driven by actin and myosin influences *in vivo* axon diameter', *Scientific Reports*, **7**, pp. 1–12.

Farhadifar, R., Ro, J., Aigouy, B. and Eaton, S. (2007) 'The influence of cell mechanics, cell-cell interactions, and proliferation on epithelial packing', *Current Biology*, **17**, pp. 2095–2104.

Fatt, I. and Weissman, B. A. (1992) *Physiology of the Eye: an introduction to the vegetative functions*. second. Stoneham: Butterworth-Heinemann.

Fawcett, D. W. (1966) 'On the occurrence of a fibrous lamina on the inner aspect of the nuclear envelope in certain cells of vertebrates', *Am. J. Anat.*, **119**, pp. 129–146.

Ferreira, M. and Ferguson, J. W. H. (2002) 'Geographic variation in the calling song of the field cricket *Gryllus bimaculatus* (Orthoptera: Gryllidae) and its relevance to mate recognition and mate choice', *J. Zool. Lond*, **257**, pp. 163–170.

Findeisen, P., Mu, S., Dempewolf, S., Hertzog, J., Zietlow, A., Carlomagno, T. and Kollmar, M. (2014) 'Six subgroups and extensive recent duplications characterize the evolution of the eukaryotic tubulin protein family', *Genome Biol. Evol.*, **6**, pp. 2274–2288.

Franze, K., Gerdelmann, J., Weick, M., Betz, T., Pawlizak, S., Lakadamyali, M., Bayer, J., Rillich, K., Gögler, M., Lu, Y. B., Reichenbach, A., Janmey, P. and Käs, J. (2009) 'Neurite branch retraction is caused by a threshold-dependent mechanical impact', *Biophysical Journal*, **97**, pp. 1883–1890.

Franze, K. (2013) 'The mechanical control of nervous system development.', *Development*, **140**, pp. 3069–77.

Franze, K. and Guck (2010) 'The biophysics of neuronal growth', *Reports on Progress in Physics*, **73**, p. 094601.

Fraser, R. D. B. and Macrae, T. P. (1961) 'The molecular configuration of α-Keratin', *Journal of Molecular Biology*, **3**, pp. 640–647.

Galbraith, J. A., Thibault, L. E. and Matteson, D. R. (1993) 'Mechanical and electrical responses of the squid giant axon to simple elongation', *Journal of Biomechanical Engineering*, **115**, pp. 13–22.

Galvani, L. (1791) 'De viribus electricitatis in motu musculari commentarius.', *Sci Art Inst Acad Comm*, **7**, pp. 363–418.

Garcia-Bellido, A., Ripoll, P. and Morata, G. (1973) 'Developmental compartmentalisation of the cing disk of *Drosophila*', *Nature New Biology*, **245**, pp. 251–253.

Gefen, A. and Margulies, S. S. (2004) 'Are *in vivo* and *in situ* brain tissues mechanically similar?', *Journal of Biomechanics*, **37**, pp. 1339–1352.

Gere, J. M. (2004) *Mechanics of Materials*. Sixth. Belmont: Thomson Learning Inc.

Gianola, D. S. and Eberl, C. (2009) 'micro- and nanoscale tensile testing of materials', *JOM*, **16**, pp. 24–35.

Gibbons, I. R. and Rowe, A. J. (1965) 'Dynein: A protein with adenosine triphosphatase activity from cilia', *Science*, **149**, pp. 424–426.

Goldberg, J. (1992) 'Microtubule-based filopodium-like protrusions form after axotomy', *The Journal of Neuroscience*, **12**, pp. 4800–4807.

Goldman, R. D. and Follett, E. A. C. (1970) 'Birefringent filamentous organelle in BHK-21 cells and its possible role in cell spreading and motility', *Science*, **169**, pp. 286–288.

Gonzalez-perez, F., Udina, E. and Navarro, X. (2013) 'Extracellular matrix components in peripheral nerve regeneration', *International Review of Neurobiology*, **108**, pp. 257–275.

Goodyear, R. J., Marcotti, W., Krose, C. J. and Richardson, G. P. (2005) 'Development and properties of stereociliary link types in hair cells of the mouse cochlea', *The Journal of comparative neurology*, **485**, pp. 75–85.

Gordon, A. M., Huxley, A. F. and Julian, F. J. (1966) 'The variation inisometric tension with sarcomere length in vertebrate muscle fibres', *Journal of Physiology*, **184**, pp. 170–192.

Gordon, M. B., Howard, L. and Compton, D. A. (2001) 'Chromosome movement in mitosis requires microtubule anchorage at spindle poles', *The Journal of Cell Biology*, **152**, pp. 425–434.

Gotz, K. G. (1987) 'Course-control, metabolism and wing interference during ultralong tethered flight in *Drosophilia melanogaster*', *The Journal of Experimental Biology*, **128**, pp. 35–46.

Grandpré, T., Strittmatter, S. M. and Strittmatter, S. M. (2001) 'Nogo: A molecular determinant of axonal growth and regeneration', *Neuroscientist*, **7**, pp. 377–386.

Granzier, H. L. M. and Wang, K. (1993) 'Passive tension and stiffness of vertebrate skeletal and insect flight muscles: the contribution of weak cross-bridges and elastic filaments', *Biophysical Journal*, **65**, pp. 2141–2159.

Grashoff, C., Hoffman, B. D., Brenner, M. D., Zhou, R., Parsons, M., Yang, M. T., Mclean, M. A., Sligar, S. G., Chen, C. S., Ha, T. and Schwartz, M. A. (2010) 'Measuring mechanical tension across vinculin reveals regulation of focal adhesion dynamics', *Nature*, **466**, pp. 263–266.

Gregory, G. E. (1974) 'Neuroanatomy of the mesothoracic ganglion of the cockroach *Periplaneta americana* (L) I . The roots of the peripheral nerves', *Philosophical transactions of the Royal Society London B*, **267**, pp. 421–465.

Grevesse, T., Dabiri, B. E., Parker, K. K. and Gabriele, S. (2015) 'Opposite rheological properties of neuronal microcompartments predict axonal vulnerability in brain injury', *Scientific Reports*, **5**, pp. 1–10.

Gunst, S. J. and Zhang, W. (2008) 'Actin cytoskeletal dynamics in smooth muscle : a new paradigm for the regulation of smooth muscle contraction', *American Journal of Physiology-Cell Physiology*, **295**, pp. 576–587.

Guo, Y. C., Wang, Y. X., Ge, Y. P., Yu, L. J. and Guo, J. (2018) 'Analysis of subcellular structural tension in axonal growth of neurons', *Reviews in the Neurosciences*, **29**, pp. 125–137.

Hackman, R. H. and Goldberg, M. (1987) 'Comparative study of some expanding arthropd cuticles: the relation between composition, structure and function', *Journal of Insect Physiology*, **33**, pp. 39–50.

Hamilton, A. G. (1953) 'Thelytokous parthenogenesis for four generations in the desert locust (*Schistocerca gregaria* Forsk) (Acrididæ).', *Nature*, **172**, pp. 1153–1154.

Hamilton, A. G. (1964) 'The occurrence of periodic or continuous discharge of carbon dioxide by male desert locusts (*Schistocerca gregaria* Forskal) measured by an infra-red gas analyser', *Proceedings of the Royal Society of London. Series B. Biological Sciences*, **160**, pp. 373–395.

Hammarlund, M., Jorgensen, E. M. and Bastiani, M. J. (2007) 'Axons break in animals lacking β-spectrin', *The Journal of Cell Biology*, **176**, pp. 269–275.

Hanein, Y., Tadmor, O., Anava, S. and Ayali, A. (2011) 'Neuronal soma migration is determined by neurite tension', *Neuroscience*, **172**, pp. 572–579.

Hanson, J. and Lowy, J. (1963) 'The structure of F-actin and of actin filaments', *Journal of Molecular Biology*, **6**, pp. 46–60.

Harden, N., Ricos, M., Yee, K., Sanny, J., Langmann, C., Yu, H., Chia, W. and Lim, L. (2002) 'Drac1 and Crumbs participate in amnioserosa morphogenesis during dorsal closure in *Drosophila*', *Journal of cell science*, **115**, pp. 2119–2128.

Harris, W. A., Holt, C. E. and Bonhoeffer, F. (1987) 'Retinal axons with and without their somata , growing to and arborizing in the tectum of *Xenopus* embryos: a time-lapse video study of single fibres *in vivo*', *Development*, **101**, pp. 123–133.

Heidemann, S. R. and Bray, D. (2015) 'Tension-driven axon assembly: a possible mechanism', *Frontiers in Cellular Neuroscience*, **9**, p. e316.

Hellal, F., Hurtado, A., Ruschel, J., Flynn, K., Umlauf, M., Strikis, D., Lemmon, V., Bixby, J. and Hoogenraad, C. (2012) 'Microtubule stabilisation reduces scarring and enables axon regeneration after spinal cord injury', *Science*, **331**, pp. 928–931.

Hersche, O. and Gerber, C. (1998) 'Passive tension in the supraspinatus musculotendinous unit after long-standing rupture of its tendon: A preliminary report', *Journal of Shoulder and Elbow Surgery*, **7**, pp. 393–396.

Hindle, S. J. and Bainton, R. J. (2014) 'Barrier mechanisms in the *Drosophila* blood-brain barrier', *Frontiers in Neuroscience*, **8**, pp. 1–12.

Hintzman, D. L. (2003) 'Robert Hooke's model of memory', *Psychonomic Bulletin & Review*, **10**, pp. 3–14.

Hirano, A., Nakano, I., Kurland, L. T., Mulder, D. W., Holley, P. W. and Saccomanno, G. (1984) 'Fine structural study of neurofibrillary changes in a family with amytrophic laterial sclerosis', *Journal of Neuropathology and Experimental Neurology*, **5**, pp. 471–480.

Hirano, A. (1995) 'Cytopathology of amyotrophic lateral sclerosis: A personal perspective of recent developments', *Neuropathology*, **15**, pp. 1–6.

Hodge, A. J., Huxley, H. E. and Spiro, D. (1953) 'Electron microscope studies on ultrathin sections of muscle', *The Journal of Experimental Medicine*, **99**, pp. 201–206.

Hodgkin, A. L. and Huxley, A. F. (1939) 'Action potentials recorded from inside a nerve fibre', *Nature*, **144**, pp. 710–711.

Hodgkin, A. L. and Huxley, A. F. (1952) 'A quantative description of membrane current and its application to conduction and excitation in nerve', *J. Physiol*, **117**, pp. 500–544.

Hodgkin, A. L. and Katz, B. (1948) 'The effect of sodium ions on the electrical activity of the giant axon of the squid', *J. Physiol*, **108**, pp. 37–77.

Homberg, U. (2015) 'Sky compass prientation in desert locusts-evidence from field and laboratory studies.', *Frontiers in behavioral neuroscience*, **9**, p. 346.

Hong, M., Zhukareva, V., Vogelsberg-Ragaglia, V., Wszolek, Z., Reed, L., Miller, B. I., Ceschwind, D. H., Bird, T. D., Mckeel, D., Coate, A., Morris, J. C., Wilhelmsen, K. C., Schellenberg, G. D., Trojanowski, J. Q. and Lee, V. M.-Y. (1998) 'Mutation-specific functional impairments in distinct tau isoforms of hereditary FTDP-17', *Science*, **282**, pp. 18–21.

Hooke, R. (1665) *Micrographia: or Some Physiological Descriptions of Minute Bodies Made by Magnifying Glasses. With Observations and Inquiries Thereupon*. The Royal Society.

Hopitzan, A. A., Baines, A. J. and Kordeli, E. (2006) 'Molecular evolution of ankyrin: Gain of function in vertebrates by acquisition of an obscurin/titin-binding-related domain', *Molecular Biology and Evolution*, **23**, pp. 46–55.

Horio, T. and Hotani, H. (1986) 'Visualisation of the dynamic instability of individual microtubules by dark-field microscopy', *Nature*, **321**, pp. 605–607.

Horowitz, A. and Barazany, D. (2014) '*In vivo* correlation between axon diameter and conduction velocity in the human brain', *Brain Structure and Function*, **220**, pp. 1777–1788.

Horridge, G. A. (1960) 'Pitch discrimination in Orthoptera (Insecta) demonstrated by responses of centrel auditory neurones', *Nature*, **185**, pp. 623–624.

Horridge, G. A. (1964) 'Multimodal interneurones of locust optic lobe', *Nature*, **204**, pp. 499–500.

Hoyle, G. and Burrows, M. (1973) 'Neural mechanisms underlying behaviour in the locust *Schistocerca gregaria*. I. Physiology of identified motorneurons in the metathoracic ganglion', *Journal of Neurobiology*, **4**, pp. 3–41.

Hursh, J. B. (1939) 'Conduction velocity and diameter of nerve fibers', *Am J Physiol*, **127**, pp. 131–139.

Hustert, R. (1975) 'Neuromuscular coordination and proprioceptive control of rhythmical abdominal ventilation in intact *Locusta migratoria migratorioides*', *Journal of Comparative Physiology*, **97**, pp. 159–179.

Hutson, M. S., Tokutake, Y., Chang, M.-S., Bloor, J. W., Venakides, S., Kiehart, D. P. and Edwards, G. S. (2003) 'Forces for morphogenesis investigated with laser microsurgery and quantitative modeling', *Science*, **300**, pp. 145–149.

Huxley, A. F. and Niedergerke, R. (1954) 'Structural changes in muscle during contraction', *Nature*, **173**, pp. 971–973.

Huxley, A. F. and Simmons, R. M. (1971) 'Proposed mechanism of force generation in striated muscle', *Nature*, **233**, pp. 533–538.

Huxley, H. E. (1969) 'The mechanism of muscular contraction', *Science*, **164**, pp. 1356–1366.

Huxley, H. and Hanson, J. (1954) 'Changes in the cross-striations of muscle during contraction and stretch and their structural interpretation', *Nature*, **173**, pp. 973–976.

Ikenaka, K., Katsuno, M., Kawai, K., Ishigaki, S., Tanaka, F. and Sobue, G. (2012) 'Disruption of axonal transport in motor neuron diseases', *International Journal of Molecular Sciences*, **13**, pp. 1225–1238.

Ingrisch, S. and Rentz, D. C. F. (2009) 'Chapter 187 - Orthoptera: Grasshoppers, Locusts, Katydids, Crickets', in Resh, V. H. and Cardé, R. T. (eds) *Encyclopedia of Insects*. second. Burlington: Academic Press, pp. 732–743.

Inoue, S., Fuseler, J., Salmon, E. D. and Ellis, G. W. (1975) 'Functional organization of mitotic microtubules: Physical chemistry of the *in vivo* equilibrium system', *Biophysical Chemistry*, **15**, pp. 3–5.

Inoue, S. and Salmon, E. D. (1995) 'Force generation by microtubule assembly/disassembly in mitosis and related movements', *Molecular biology of the cell*, **6**, pp. 1619–1640.

Ishihara, T., Hong, M., Zhang, B., Nakagawa, Y., Lee, M. K., Trojanowski, J. Q. and Lee, V. M. (1999) 'Age-dependent emergence and progression of a tauopathy in transgenic mice overexpressing the shortest human tau isoform', *Neuron*, **24**, pp. 751–762.

Ishikawa, H., Bischoff, R. and Holtzer, H. (1968) 'Mitosis and intermediate-sized filaments in developing skeletal muscle', *The Journal of Cell Biology*, **38**, pp. 538–555.

Jacinto, A., Wood, W., Balayo, T., Turmaine, M., Martinez-arias, A. and Martin, P. (2000) 'Dynamic actin-based epithelial adhesion and cell matching during *Drosophila* dorsal closure', *Current Biology*, **10**, pp. 1420–1426.

Jacinto, A., Wood, W., Woolner, S., Hiley, C., Turner, L., Wilson, C., Martinez-arias, A. and Martin, P. (2002) 'Dynamic analysis of actin cable function during *Drosophila* dorsal closure', *Current Biology*, **12**, pp. 1245–1250.

Jacinto, A., Woolner, S., Martin, P. and Grande, Q. (2002) 'Dynamic analysis of dorsal closure in *Drosophila*: from genetics to cell biology', *Developmental Cell*, **3**, pp. 9–19.

Jakobs, M., Franze, K. and Zemel, A. (2015) 'Force generation by microtubule bundles; implications for neuronal polarization and growth', *Frontiers in cellular neuroscience*, **9**, pp. 1–14.

Jankovics, F. and Brunner, D. (2006) 'Transiently reorganized microtubules are essential for zippering during dorsal closure in *Drosophila melanogaster*', *Developmental Cell*, **11**, pp. 375–385.

Janmey, P. A., Euteneuer, U., Traub, P. and Schliwa, M. (1991) 'Viscoelastic properties of vimentin compared with other filamentous biopolymer networks', *The Journal of Cell Biology*, **113**, pp. 155–160.

Javid, S., Rezaei, A. and Karami, G. (2014) 'A micromechanical procedure for viscoelastic characterization of the axons and ECM of the brainstem', *Journal of the Mechanical Behavior of Biomedical Materials*, **30**, pp. 290–299.

Jin, L., Zhang, G., Jamison, C., Takano, H., Haydon, P. G. and Selzer, M. E. (2009) 'Axon regeneration in the absence of growth cones: Acceleration by cyclic AMP', *The Journal of comparative neurology*, **312**, pp. 295–312.

Johnson, V. E., Stewart, W. and Smith, D. H. (2013) 'Axonal pathology in traumatic brain injury', *Experimental Neuroscience*, **246**, pp. 35–43.

Jonas, O. and Duschl, C. (2010) 'Force propagation and force generation in cells', *Cytoskeleton*, **67**, pp. 555–563.

Jorgensen, W. K. and Rice, M. J. (1983) 'Morphology of a very extensible insect muscle', *Tissue & Cell*, **15**, pp. 639–644.

Kabsch, W., Mannherz, H. G., Suck, D., Pai, E. F. and Holmes, K. C. (1990) 'Atomic structure of the actin:DNase I complex', *Nature*, **347**, pp. 37–44.

Kaltschmidt, J. A., Lawrence, N., Morel, V., Balayo, T., Fernández, B. G., Pelissier, A., Jacinto, A. and Arias, A. M. (2002) 'Planar polarity and actin dynamics in the epidermis of *Drosophila*', *Nature cell biology*, **4**, pp. 937–944.

Kapitein, L. C. and Hoogenraad, C. C. (2011) 'Which way to go? Cytoskeletal organization and polarized transport in neurons', *Molecular and Cellular Neuroscience*, **46**, pp. 9–20.

Kasthuri, N., Hayworth, K. J., Berger, D. R., Schalek, R. L., Conchello, J. A., Knowles-Barley, S., Lee, D., Vazquez-Reina, A., Kaynig, V., Jones, T. R., Roberts, M., Morgan, J. L., Tapia, J. C., Seung, H. S., Roncal, W. G., Vogelstein, J. T., Burns, R., Sussman, D. L., Priebe, C. E., Pfister, H. and Lichtman, J. W. (2015) 'Saturated reconstruction of a volume of neocortex', *Cell*, **162**, pp. 648–661.

Kaverina, I., Rottner, K. and Small, J. V. (1998) 'Targeting, capture, and stabilization of microtubules at early focal adhesions', *Journal of Cell Biology*, **142**, pp. 181–190.

Keener, J. P. and Shtylla, B. (2014) 'A mathematical model of force generation by flexible kinetochore-microtubule attachments.', *Biophysical journal*, **106**, pp. 998–1007.

Keil, T. A. and Steinbrecht, R. A. (2010) 'Insects as model systems in cell biology', *Methods in Cell Biology*, **96**, pp. 363–394.

Kendrew, J. C., Bodo, G., Dintzis, H. M., Parrish, R. G., Wyckoff, H. and Phillips, D. C. (1958) 'A three-dimensional model of the myoglobin molecule obtained by X-ray analysis', *Nature*, **181**, pp. 662–666.

Kerssemakers, J. W. J., Munteanu, E. L., Laan, L., Noetzel, T. L., Janson, M. E. and Dogterom, M. (2006) 'Assembly dynamics of microtubules at molecular resolution', *Nature*, **442**, pp. 2–5.

Keshishian, H. (1980) 'The origin and morphogenesis of pioneer neurons in the grasshopper metathoracic leg', *Developmental Biology*, **80**, pp. 388–397.

Keshishian, H. and Bentley, D. (1983) 'Embryogenesis of peripheral nerve pathways in grasshopper legs. II. The major nerve routes', *Developmental Biology*, **96**, pp. 103–115.

Kiecker, C. and Lumsden, A. (2005) 'Compartments and their boundaries in vertebrate brain development', *Nature Reviews. Neuroscience*, **6**, pp. 553–564.

Kiehart, D. P., Galbraith, C. G., Edwards, K. A., Rickoll, W. L. and Montague, R. A. (2000) 'Multiple forces contribute to cell sheet morphogenesis for dorsal closure', *The Journal of Cell Biology*, **149**, pp. 471–490.

Kioussi, C., Appu, M., Christiane, V. L., Fischer, K. A., Bajaj, G., Leid, M. and Ishmael, J. E. (2007) 'Co-expression of myosin II regulatory light chain and the NMDAR1 subunit in neonatal and adult mouse brain', *Brain Research Bulletin*, **74**, pp. 439–451.

Koser, D. E., Moeendarbary, E., Hanne, J., Kuerten, S. and Franze, K. (2015) 'CNS cell distribution and axon orientation determine local spinal cord mechanical properties', *Biophysical Journal*, **108**, pp. 2137–2147.

Koster, S., Weitz, D., Goldman, R. D., Aebi, U. and Herrmann, H. (2015) 'Intermediate filament mechanics in vitro and in the cell: From coiled coils to filaments, fibers and networks', *Curr Opin Cell Biol*, **0**, pp. 82–91.

Kraning-rush, C. M., Carey, S. P., Califano, J. P., Smith, B. N. and Reinhart-king, C. A.

(2011) ‘The role of the cytoskeleton in cellular force generation in 2D and 3D environments’, *Physical biology*, **8**, pp. 1–19.

Krieg, M., Stuhmer, J., Cueva, J. G., Fetter, R., Spilker, K., Creners, D., Shen, K., Dunn, A. R. and Goodman, M. B. (2017) ‘Genetic defects in β-spectrin and tau sensitise *C. elegans* axons to movement-induced damage via torque-tension coupling’, *eLife*, **6**.

Krogh, A. (1929) ‘The progress of physiology’, *The American Journal of Physiology*, **90**, pp. 243–251.

Kulic, I. M., Brown, E. X., Kim, H., Kural, C., Blehm, B., Selvin, P. R., Nelson, P. C. and Gelfand, V. I. (2008) ‘The role of microtubule movement in bidirectional organelle transport’, *pnas*, **105**, pp. 10011–10016.

Kutsch, W. (1989) ‘Formation of the receptor system in the hind limb of the locust embryo’, *Roux’s Arch Dev Biol*, **198**, pp. 39–47.

LaMonte, B. H., Wallace, K. E., Holloway, B. A., Shelly, S. S., Ascaño, J., Tokito, M., Van Winkle, T., Howland, D. S. and Holzbaur, E. L. F. (2002) ‘Disruption of dynein/dynactin inhibits axonal transport in motor neurons causing late-onset progressive degeneration’, *Neuron*, **34**, pp. 715–727.

Lamoureux, P., Heidemann, S. R., Martzke, N. R. and Miller, K. E. (2010) ‘Growth and elongation within and along the axon’, *Developmental Neurobiology*, **70**, pp. 135–149.

Lamoureux, P., Buxbaum, R. E. and Heidemann, S. R. (1989) ‘Direct evidence that growth cones pull’, *Nature*, **340**, pp. 159–162.

Landsberg, K. P., Farhadifar, R., Ranft, J., Umetsu, D., Widmann, T. J., Bittig, T., Said, A., Jülicher, F. and Dahmann, C. (2009) ‘Increased cell bond tension governs cell sorting at the *Drosophila* anteroposterior compartment boundary’, *Current Biology*, **19**, pp. 1950–1955.

Laplaca, M. C., Cullen, D. K., Mcloughlin, J. J. and Cargill, R. S. (2005) ‘High rate shear strain of three-dimensional neural cell cultures: a new in vitro traumatic brain injury model’, *Journal of Biomechanics*, **38**, pp. 1093–1105.

Lasek, R. J., Paggi, P. and Katz, M. J. (1993) ‘The maximum rate of neurofilament transport in axons: a view of molecular transport mechanisms continuously engaged’, *Brain Research*, **616**, pp. 58–64.

LaVan, D. A. and Sharpe Jr, W. N. (1999) ‘Tensile testing of microsamples’, *Experimental Mechanics*, **39**, pp. 210–216.

Lavoie, T. L., Dowell, M. L., Lakser, O. J., Gerthoffer, W. T., Fredberg, J. J., Seow, C. Y., Mitchell, R. W. and Solway, J. (2009) ‘State of the art disrupting actin-myosin-actin connectivity in airway smooth muscle as a treatment for asthma?’, *Proceedings of the American Thoracic Society*, **6**, pp. 295–300.

Lazarus, C., Soheilypour, M. and Mofrad, M. R. K. (2015) ‘Torsional behavior of axonal

microtubule bundles', *Biophysical Journal*, **109**, pp. 231–239.

Ledbetter, M. C. and Porter, K. R. (1963) 'A "microtubule" in plant cell fine structure', *The Journal of Cell Biology*, **19**, pp. 239–250.

Ledbetter, M. C. and Porter, K. R. (1964) 'Morphology of microtubules of plant cell', *Science*, **144**, pp. 872–874.

Lee, J. C. and Frigon, R. P. (1973) 'The chemical characterization of calf brain microtubule protein subunits', *The Journal of Biological Chemistry*, **248**, pp. 7253–7262.

Legerlotz, K., Riley, G. P. and Screen, H. R. C. (2010) 'Specimen dimensions influence the measurement of material properties in tendon fascicles', *Journal of Biomechanics*, **43**, pp. 2274–2280.

Lehmann, F. and Dickinson, M. H. (1997) 'The changes in power requirements and muscle efficiency during elevated force production in the fruit fly *Drosophila melanogaster*', *The Journal of Experimental Biology*, **1143**, pp. 1133–1143.

Lemke, S. B. and Schnorrer, F. (2017) 'Mechanical forces during muscle development', *Mechanisms of Development*, **144**, pp. 92–101.

Lester, R. L., Grach, C., Paul, M. and Simpson, S. J. (2005) 'Stimuli inducing gregarious colouration and behaviour in nymphs of *Schistocerca gregaria*', *Journal of Insect Physiology*, **51**, pp. 737–747.

Lewellyn, L., Dumont, J., Desai, A. and Oegema, K. (2010) 'Analyzing the effects of delaying aster separation on furrow formation during cytokinesis in the *Caenorhabditis elegans* embryo', *Molecular biology of the cell*, **21**, pp. 50–62.

Lewellyn, L., Carvalho, A., Desai, A., Maddox, A. S. and Oegema, K. (2011) 'The chromosomal passenger complex and centralspindlin independently contribute to contractile ring assembly', *Journal of Cell Biology*, **193**, pp. 155–169.

Li, X., Xu, Q., Wang, Y., Chen, F. and He, J. (2016) 'Development of a new miniaturized bioreactor for axon stretch growth', *Journal of Integrative Neuroscience*, **15**, pp. 365–380.

Lin, C. H., Espreafico, E. M. and Mooseker, M. S. (1996) 'Myosin drives retrograde F-actin flow in neuronal growth cones', *Neuron*, **16**, pp. 769–782.

Lindstedt, S. and Nishikawa, K. (2017) 'Huxleys' missing filament: form and function of titin in vertebrate striated muscle', *Annu. Rev. Physiol*, **79**, pp. 145–166.

Ling, H., Hardy, J. and Zetterberg, H. (2015) 'Neurological consequences of traumatic brain injuries in sports', *Molecular and Cellular Neuroscience*, **66**, pp. 114–122.

Linke, W. A., Ivemeyer, M., Mundel, P., Stockmeier, M. R. and Kolmerer, B. (1998) 'Nature of PEVK-titin elasticity in skeletal muscle', *Proceedings of the National*

Academy of Sciences USA, **95**, pp. 8052–8057.

Linke, W. A., Popov, V. I. and Pollack, G. H. (1994) 'Passive and active tension in single cardiac myofibrils', *Biophysical journal*, **67**, pp. 782–792.

Linnaeus, C. (1758) *Systema Naturae*. tenth. Stockholm: Hes & de Graaf.

Litchy, W. J. and Brimijoin, S. (1983) 'Concentration dependence of rapid axonal transport: a study of the transport kinetics of [35s]methionine-labeled protein in postganglionic sympathic fibers of the bullfrog', *The Journal of Neuroscience*, **3**, pp. 2075–2082.

Löffek, S., Franzke, C. W. and Helfrich, I. (2016) 'Tension in cancer', *International Journal of Molecular Sciences*, **17**, pp. 1–14.

Loisel, T. P., Boujemaa, R., Pantaloni, D. and Carlier, M. (1999) 'Reconstitution of actin-based motility of *Listeria* and *Shigella* using pure proteins', *Nature*, **401**, pp. 613–616.

Lomer, C. J., Bateman, R. P., Johnson, D. L., Langewald, J. and Thomas, M. (2001) 'Biological control of locusts and grasshoppers', *Annual review of entomology*, **46**, pp. 667–702.

Loverde, J. R. and Pfister, B. J. (2015) 'Developmental axon stretch stimulates neuron growth while maintaining normal electrical activity, intracellular calcium flux, and somatic morphology', *Frontiers in Cellular Neuroscience*, **9**, p. 308.

Loverde, J. R., Tolentino, R. E. and Pfister, B. J. (2011) 'Axon stretch growth: the mechanotransduction of neuronal growth.', *Journal of visualized experiments : JoVE*, pp. 1–6.

Lowery, L. A. and Van Vactor, D. (2009) 'The trip of the tip: understanding the growth cone machinery.', *Nature reviews. Molecular cell biology*, **10**, pp. 332–43.

Loza, M. C. D. De and Thompson, B. J. (2017) 'Mechanisms of development forces shaping the *Drosophila* wing', *Mechanisms of Development*, **144**, pp. 23–32.

Lu, H., Sokolow, A., Kiehart, D. P. and Edwards, G. S. (2015) 'Remodeling tissue interfaces and the thermodynamics of zipping during dorsal closure in *Drosophila*', *Biophysical Journal*, **109**, pp. 2406–2417.

Lu, W., Lakonishok, M., Gelfand, V. I. and Fehon, R. (2015) 'Kinesin-1 – powered microtubule sliding initiates axonal regeneration in *Drosophila* cultured neurons', *Molecular biology of the cell*, **26**, pp. 1296–1307.

Luduena, R. F. and Woodward, D. O. (1973) 'Isolation and partial characterization of α- and β-tubulin from outer doublets of sea-urchin sperm and microtubules of chick-embryo brain', *Proceedings of the National Academy of Sciences USA*, **70**, pp. 3594–3598.

Luna, C., Detrick, L., Shah, S. B., Cohen, A. H. and Aranda-espinoza, H. (2013) 'Mechanical properties of the lamprey spinal cord : Uniaxial loading and physiological strain', *Journal of Biomechanics*, **46**, pp. 2194–2200.

Ma, X., Kovács, M., Anne, M., Wang, A., Zhang, Y. and Sellers, J. R. (2012) 'Nonmuscle myosin II exerts tension but does not translocate actin in vertebrate cytokinesis', *PNAS*, **109**, pp. 4509–4514.

Maddrell, S. H. P. and Klunsuwan, S. (1973) 'Fluid secretion by in vitro preparations of the malpighian tubules of the desert locust *Schistocerca gregaria*', *Journal of Insect Physiology*, **19**, pp. 1369–1376.

Magid, A. and Law, D. J. (1985) 'Myofibrils bear most of the resting tension in frog skeletal muscle', *Science*, **230**, pp. 1280–1282.

Magie, C. R., Meyer, M. R., Gorsuch, M. S. and Parkhurst, S. M. (1999) 'Mutations in the Rho1 small GTPase disrupt morphogenesis and segmentation during early *Drosophila* development', *Development*, **5364**, pp. 5353–5364.

Major, R. J. and Irvine, K. D. (2006) 'Localization and requirement for myosin II at the dorsal-ventral compartment boundary of the *Drosophila* wing', *Developmental Dynamics*, **235**, pp. 3051–3058.

Malhotra, J. D., Kazen-Gillespie, K., Hortsch, M. and Isom, L. L. (2000) 'Sodium channel β subunits mediate homophilic cell adhesion and recruit ankyrin to points of cell-cell contact', *Journal of Biological Chemistry*, **275**, pp. 11383–11388.

Mallo, M. and Alonso, C. R. (2013) 'The regulation of Hox gene expression during animal development', *Development*, **140**, pp. 3951–3963.

Margolis, R. L. and Wilson, L. (1978) 'Opposite end assembly and disassembly microtubules at steady state *in vitro*', *Cell*, **13**, pp. 1–8.

Marszalek, J. R., Lee, M. K., Wong, P. C., Folmer, J., O.Crawford, T., Hsieh, S.-T., Griffin, J. W. and Cleveland, D. W. (1996) 'Subunit composition of neurofilaments specifies axonal diameter', *The Journal of Cell Biology*, **133**, pp. 1061–1069.

Martin, A. C. and Wieschaus, E. F. (2010) 'Tensions divide', *Nature Cell Biology*, **12**, pp. 5–7.

Martin, P. and Parkhurst, S. M. (2004) 'Parallels between tissue repair and embryo morphogenesis', *Development*, **131**, pp. 3021–3034.

Martın-Blanco, E., Gampel, A., Ring, J., Virdee, K., Kirov, N., Tolkovsky, A. M. and Martinez-arias, A. (1998) '*puckered* encodes a phosphatase that mediates a feedback loop regulating JNK activity during dorsal closure in *Drosophila*', *Genes & Development*, **12**, pp. 557–570.

Matsuoka, Y., Li, X. and Bennet, V. (1998) 'Adducin is an *in vivo* substrate for protein kinase C: Phosphorylation in the MARCKS-related domain inhibits activity in promoting

spectrin–actin complexes and occurs in many cells, including dendritic spines of neurons', *The Journal of Cell Biology*, **142**, pp. 485–497.

Mcintosh, A. S., Patton, D. A., Fréchède, B., Pierré, P., Ferry, E. and Barthels, T. (2014) 'The biomechanics of concussion in unhelmeted football players in Australia: a case–control study', *BMJ Open*, **4**, pp. 1–9.

McIntosh, J. R., Hepler, P. K. and Van Wie, D. G. (1969) 'Model for mitosis', *Nature*, **224**, pp. 659–663.

Mehta, A. D., Rock, R. S., Rief, M., Spudich, J. A., Mooseker, M. S. and Cheney, R. E. (1999) 'Myosin-V is a processive actin-based motor', *Nature*, **400**, pp. 590–593.

Meier, I. (2007) 'Composition of the plant nuclear envelope: theme and variations', *Journal of Ethnopharmacology*, **58**, pp. 27–34.

Meier, T., Therianos, S., Zacharias, D. and Reichert, H. (1993) 'Developmental expression of TERM-1 glycoprotein on growth cones and terminal arbors of individual identified neurons in the grasshopper', *J Neurosci*, **13**, pp. 1498–1510.

Melcer, S., Gruenbaum, Y. and Krohne, G. (2007) 'Invertebrate lamins', *Experimental Cell Research*, **3**, pp. 2157–2166.

Mercer, E. H. (1958) 'An electron microscopic study of *Amoeba proteus*', *Proceedings of the Royal Society of London. Series B: Biological Sciences*, **150**, pp. 216–232.

Millard, T. H. and Martin, P. (2008) 'Dynamic analysis of filopodial interactions during the zippering phase of *Drosophila* dorsal closure', *Development*, **135**, pp. 621–626.

Miller, G. A., Islam, M. S., Claridge, T. D. W., Dodgson, T. and Simpson, S. J. (2008) 'Swarm formation in the desert locust *Schistocerca gregaria*: isolation and NMR analysis of the primary maternal gregarizing agent', *The Journal of Experimental Biology*, **211**, pp. 370–376.

Miller, K. and Chinzei, K. (2002) 'Mechanical properties of brain tissue in tension', *Journal of Biomechanics*, **35**, pp. 483–490.

Miller, P. L. (1960a) 'Respiration in the desert locust: I. The control of ventilation', *J. Exp. Biol.*, **37**, pp. 237–263.

Miller, P. L. (1960b) 'Respiration in the desert locust: II. The control of the spiracles', *J. Exp. Biol.*, **37**, pp. 237–263.

Mitchison, T. and Kirschner, M. (1984a) 'Dynamic instability of microtubule growth', *Nature*, **312**, pp. 237–242.

Mitchison, T. and Kirschner, M. (1984b) 'Microtubule assembly nucleated by isolated centrosomes', *Nature*, **312**, pp. 232–237.

Mohandas, N. and Evans, E. (1994) 'Mechanical properties of the red cell membrane

in relation to molecular structure and genetic defects', *Annual Review of Biophysics and Biomolecular Structure*, **23**, pp. 787–818.

Mohri, H. (1968) 'Amino-acid composition of "tubulin" constituting microtubules of sperm flagella', *Nature*, **217**, pp. 1053–1054.

Munoz-Diz, A., Fletcher, D. A. and Weiner, O. D. (2013) 'Use the force: Membrane tension as an organizer of cell shape and motility', *Trend*, **23**, pp. 47–53.

Navarro, X., Vivo, M. and Valero-Cabre, A. (2007) 'Neural plasticity after peripheral nerve injury and regeneration ´', *Progress in Neurobiology*, **82**, pp. 163–201.

Neuhaus, J.-M., Wanger, M., Keiser, T. and Wegner, A. (1983) 'Treadmilling of actin', *Journal of Muscle Research and Cell Motility*, **4**, pp. 507–508.

Nguyen, T. D., Hogue, I. B., Cung, K., Purohit, P. K. and McAlpine, M. C. (2013) 'Tension-induced neurite growth in microfluidic channels.', *Lab on a chip*, **13**, pp. 3735–40.

Nia, H. T., Datta, M., Seano, G., Huang, P., Munn, L. L. and Jain, R. K. (2018) 'Quantifying solid stress and elastic energy from excised or *in situ* tumors', *Nature protocols*, **13**, pp. 1091–1105.

Nijhout, H. F. and Callier, V. (2015) 'Developmental mechanisms of body size and wing-body scaling in insects', *Annual review of entomology*, **60**, pp. 141–156.

Niven, J. E. and Farris, S. M. (2012) 'Miniaturization of nervous systems and neurons', *Current Biology*, **22**, pp. R323–R329.

Niven, J. E., Graham, C. M. and Burrows, M. (2008) 'Diversity and evolution of the insect ventral nerve cord.', *Annual review of entomology*, **53**, pp. 253–271.

North, G. and Greenspan, R. J. (2007) *Invertebrate Neurobiology*. first. Edited by G. North and R. J. Greenspan. New York: Cold Spring Harbor Labratory Press.

Nüsslein-Volhard, C., Lohs-Schardin, M., Sander, K. and Cremer, C. (1980) 'A dorso-ventral shift of embryonic primordia in a new maternal-effect mutant of Drosophila', *Nature*, **283**, pp. 474–476.

Nüsslein-Volhard, C. and Wieschaus, E. (1980) 'Mutations affecting segment number and polarity in *Drosophila*', *Nature*, **287**, pp. 795–801.

O'Toole, M., Lamoureux, P. and Miller, K. E. (2015) 'Measurement of subcellular force generation in neurons', *Biophysical Journal*, **108**, pp. 1027–1037.

Oakley, C. E. and Oakley, B. R. (1989) 'Identification of γ-tubulin, a new member of the tubulin superfamily encoded by mipA gene of *Aspergillus nidulans*', *Nature*, **338**, pp. 662–664.

Okazaki, T., Kanchiku, T. and Nishida, N. (2018) 'Age-related changes of the spinal

cord: A biomechanical study', *Experimental and Therapeutic Medicine*, **15**, pp. 2824–2829.

Ott, S. R. and Rogers, S. M. (2010) 'Gregarious desert locusts have substantially larger brains with altered proportions compared with the solitarious phase.', *Proceedings. Biological sciences / The Royal Society*, **277**, pp. 3087–96.

Oyama, K., Zeeb, V., Kawamura, Y., Arai, T. and Gotoh, M. (2015) 'Triggering of high-speed neurite outgrowth using an optical microheater', *Scientific reports*, **5**, pp. 1–11.

Pannese, E., Ledda, M., Rigamonti, L. and Procacci, P. (1984) 'A comparison of the density of microtubules in the central and peripheral axonal branches of the pseudounipolar neurons of lizard spinal ganglia', *The Anatomical Record*, **605**, pp. 595–605.

Parry, D. A. D. and Steinert, P. M. (1999) 'Intermediate filaments: molecular architecture, assembly, dynamics and polymorphism', *Quaterly Reviews of Biophysics*, **2**, pp. 99–187.

Pasakarnis, L., Frei, E., Caussinus, E., Affolter, M. and Brunner, D. (2016) 'Amnioserosa cell constriction but not epidermal actin cable tension autonomously drives dorsal closure', *Nature cell biology*, **18**, pp. 1161–1172.

Patschke, A., Bicker, G. and Stern, M. (2004) 'Axonal regeneration of proctolinergic neurons in the central nervous system of the locust', *Developmental Brain Research*, **150**, pp. 73–76.

Pelham, R. J. and Wang, Y.-L. (1997) 'Cell locomotion and focal adhesions are regulated by substrate flexibility', *Proceedings of the National Academy of Sciences of the USA*, **94**, pp. 13661–13665.

Pélissié, B., Piou, C., Jourdan-Pineau, H., Pagès, C., Blondin, L. and Chapuis, M. P. (2016) 'Extra molting and selection on nymphal growth in the desert locust', *PLoS ONE*, **11**, pp. 1–18.

Pener, M. P. (1991) 'Locust phase polymorphism and its endocrine relations', *Advances in Insect Physiology*, **23**, pp. 1–79.

Pener, M. P. and Simpson, S. J. (2009) 'Locust phase polyphenism : An update', *Advances in Insect Physiology*, **36**, pp. 1–272.

Perge, J. a, Niven, J. E., Mugnaini, E., Balasubramanian, V. and Sterling, P. (2012) 'Why do axons differ in caliber?', *The Journal of Neuroscience*, **32**, pp. 626–638.

Peters, A., Palay, S. F. and Webster, H. F. (1991) *The fine structure of the nervous system, in: Neurons and their supporting cells.* Oxford University Press.

Pfister, B. J. (2004) 'Extreme stretch growth of integrated axons', *Journal of Neuroscience*, **24**, pp. 7978–7983.

Pfister, B. J., Iwata, A., Taylor, A. G., Wolf, J. A., Meaney, D. F. and Smith, D. H. (2006) 'Development of transplantable nervous tissue constructs comprised of stretch-grown axons', *Journal of Neuroscience Methods*, **153**, pp. 95–103.

Pfister, B. J., Bonislawski, D. P., Smith, D. H. and Cohen, A. S. (2006) 'Stretch-grown axons retain the ability to transmit active electrical signals', *FEBS Letters*, **580**, pp. 3525–3531.

Pflüger, H. J. and Watson, A. H. . (1988) 'Structure and distribution of dorsal unpaired median (DUM) neurones in the abdominal nerve cord of male and female locusts', *The Journal of comparative neurology*, **268**, pp. 329–345.

Phillips, D. M. (1966) 'Structure of flagellar tubules', *Journal of Cell Biology*, **31**, pp. 635–638.

Piel, M., Chavrier, P., Hawkins, R. J., Poincloux, R. and Be, O. (2011) 'Spontaneous contractility-mediated cortical flow generates cell migration in three-dimensional environments', *Biophysical journal*, **101**, pp. 1041–1045.

Pielage, J., Cheng, L., Fetter, R. D., Carlton, P. M., Sedat, J. W. and Graeme, W. (2009) 'A novel presynaptic giant ankyrin stabilizes the NMJ through regulation of presynaptic microtubules and trans-synaptic cell adhesion', *Neuron*, **58**, pp. 195–209.

Polackwich, R. J., Koch, D., McAllister, R., Geller, H. M. and Urbach, J. S. (2015) 'Traction force and tension fluctuations in growing axons.', *Frontiers in cellular neuroscience*, **9**, p. 417.

Prosser, C. L. (1934) 'The nervous system of the earthworm', *The Quarterly Review of Biology*, **9**, pp. 181–200.

Protti, D. A., Flores-herr, N. and Gersdorff, H. Von (2000) 'Light evokes Ca2+ spikes in the axon terminal of a retinal bipolar cell', *Neuron*, **25**, pp. 215–227.

Pumphrey, R. J. and Young, J. Z. (1938) 'The rates of conduction of nerve fibres of various diameters in cephalopods', *Journal of Experimental Biology*, **15**, pp. 453–466.

Purohit, P. K. and Smith, D. H. (2016) 'A model for stretch growth of neurons', *Journal of Biomechanics*, **49**, pp. 3934–3942.

Pyrpassopoulos, S., Arpağ, G., Feeser, E. A., Shuman, H., Tüzel, E. and Ostap, E. M. (2016) 'Force generation by membrane- associated myosin-I', *Scientific Reports*, **6**, pp. 1–14.

Rajagopalan, J., Tofangchi, A. and Saif, M. T. A. (2010) 'Drosophila neurons actively regulate axonal tension *in vivo*', *Biophysical Journal*, **99**, pp. 3208–3215.

Ranatunga, K. W. and Offer, G. (2017) 'The force-generation process in active muscle is strain sensitive and endothermic: a temperature-perturbation study', *Journal of Experimental Biology*, **220**, pp. 4733–4742.

Ranatunga, K. W. and Wylie, S. R. (1983) 'Temperature-dependent transitions in isometric contractions of rat muscle', *Journal of Physiology*, **339**, pp. 87–95.

Randolph, C. (2018) 'Chronic traumatic encephalopathy is not a real disease', *Archives of Clinical Neuropsychology*, **33**, pp. 644–648.

Rashid, B., Destrade, M. and Gilchrist, M. D. (2014) 'Mechanical characterization of brain tissue in tension at dynamic strain rates', *Journal of the Mechanical Behavior of Biomedical Materials*, **33**, pp. 43–54.

Rauch, P., Heine, P., Goettgens, B. and Käs, J. A. (2013) 'Forces from the rear: Deformed microtubules in neuronal growth cones influence retrograde flow and advancement', *New Journal of Physics*, **15**.

Razavi, M. J., Zhang, T., Liu, T. and Wang, X. (2015) 'Cortical folding pattern and its consistency induced by biological growth', *Scientific Reports*, **5**, p. 14477.

Razavi, M. J., Zhang, T., Li, X., Liu, T. and Wang, X. (2015) 'Role of mechanical factors in cortical folding development', *Physical Review E - Statistical, Nonlinear, and Soft Matter Physics*, **92**, pp. 1–8.

Reconditi, M., Brunello, E., Linari, M., Bianco, P., Narayanan, T., Panine, P., Piazzesi, G., Lombardi, V. and Irving, M. (2011) 'Motion of myosin head domains during activation and force development in skeletal muscle', *PNAS*, **108**, pp. 7236–7240.

dos Remedios, C. and Gilmour, D. (2017) 'An historical perspective of the discovery of titin filaments', *Biophys Rev*, **9**, pp. 179–188.

Ridley, A. J., Schwartz, M. A., Burridge, K., Firtel, R. A., Mark, H., Borisy, G., Parsons, J. T., Horwitz, A. R., Ridley, A. J., Schwartz, M. A., Burridge, K., Firtel, R. A., Ginsberg, M. H., Borisy, G., Parsons, J. T. and Horwitz, A. R. (2016) 'Cell migration: Integrating signals from front to back', *Science*, **302**, pp. 1704–1709.

Rodionov, V. I. and Borisy, G. G. (1997) 'Microtubule treadmilling *in vivo*', *Science*, **275**, pp. 215–218.

Roessingh, P., Simpson, S. J. and James, S. (1993) 'Analysis of phase-related changes in behaviour of desert locust nymphs', *Proceedings of the Royal Society B: Biological Sciences*, **252**, pp. 43–49.

Rogers, S. L. and Gelfand, V. I. (1998) 'Myosin cooperates with microtubule motors during organelle transport in melanophores', *Current Biology*, **8**, pp. 161–164.

Ronacher, B., Harald, W. and Reichert, H. (1988) 'Locust flight behavior after hemisection of individual thoracic ganglia: evidence for hemiganglionic premotor centers', *J Comp Physiol*, **163**, pp. 749–759.

Ronan, L., Voets, N., Rua, C., Alexander-Bloch, A., Hough, M., Mackay, C., Crow, T. J., James, A., Giedd, J. N. and Fletcher, P. C. (2014) 'Differential tangential expansion as a mechanism for cortical gyrification', *Cerebral Cortex*, **24**, pp. 2219–2228.

Ronan, L. and Fletcher, P. C. (2014) 'From genes to folds: a review of cortical gyrification theory', *Brain Structure and Function*, **220**, pp. 2475–2483.

Rooij, R. De and Kuhl, E. (2018) 'Microtubule polymerization and cross-link dynamics explain axonal stiffness and damage', *Biophysical Journal*, **114**, pp. 201–212.

Roth, L. M. (1982) 'The American Cockroach: Introduction', in Bell, W. J. and Adiyodi, K. G. (eds) *The American Cockroach*. New York, pp. 1–15.

Rowell, C. H. F. and Dorey, A. E. (1967) 'The number and size of axons in the thoracic connectives of the desert locust, Schistocerca gregaria Forsk .', *Zeitschrift fur Zellforschung*, **83**, pp. 288–294.

Rueden, C. T., Schindelin, J., Hiner, M. C., Dezonia, B. E., Walter, A. E., Arena, E. T. and Eliceiri, K. W. (2017) 'ImageJ2 : ImageJ for the next generation of scientific image data', *BMC Bioinformatics*, **18**, pp. 1–26.

Sabry, J. H., O'Connor, T. P., Evans, L., Toroian-Raymond, A., Kirschner, M. and Bentley, D. (1991) 'Microtubule behavior during guidance of pioneer neuron growth cones *in situ*', *Journal of Cell Biology*, **115**, pp. 381–395.

Sahoo, D., Deck, C. and Willinger, R. (2016) 'Brain injury tolerance limit based on computation of axonal strain', *Accident Analysis and Prevention*, **92**, pp. 53–70.

Saitua, F. and Alvarez, J. (1988) 'Do axons grow during adulthood? a study of caliber and microtubules of sural nerve axons in young, mature, and aging rats', *The Journal of Cell Biology*, **269**, pp. 203–209.

Salmon, E. D. (1976) 'Pressure-induced depolymerisation of spindle microtubules: IV. Production and regulation of chromosome movement', *Cell Motility*, **3**, pp. 1329–1340.

Santamaria, P. and Nüsslein-Volhard, C. (1983) 'Partial rescue of dorsal, a maternal effect mutation affecting the dorso-ventral pattern of the *Drosophila* embryo, by the injection of wild-type cytoplasm.', *The EMBO journal*, **2**, pp. 1695–9.

Savin, T., Kurpios, N. a, Shyer, A. E., Florescu, P., Liang, H., Mahadevan, L. and Tabin, C. J. (2011) 'On the growth and form of the gut.', *Nature*, **476**, pp. 57–62.

Schiaffino, S. and Reggiani, C. (2018) 'Fiber types in mammalian skeletal muscles', *Physiol Rev*, **91**, pp. 1447–1531.

Schindelin, J., Arganda-carreras, I., Frise, E., Kaynig, V., Longair, M., Pietzsch, T., Preibisch, S., Rueden, C., Saalfeld, S., Schmid, B., Tinevez, J., White, D. J., Hartenstein, V., Eliceiri, K., Tomancak, P. and Cardona, A. (2012) 'Fiji : an open-source platform for biological-image analysis', *Nature Methods*, **9**, pp. 676–682.

Schneider, C. A., Rasband, W. S. and Eliceiri, K. W. (2012) 'NIH Image to ImageJ : 25 years of image analysis', *Nature Methods*, **9**, pp. 671–675.

Scholtz, G. and Edgecombe, G. D. (2006) 'The evolution of arthropod heads:

reconciling morphological, developmental and palaeontological evidence', *Development Genes and Evolution*, **216**, pp. 395–415.

Schroeder, T. E. (1972) 'The contractile ring II. Determining its brief existence, volumetric changes, and vital role in cleaving *Arbacia* eggs', *The Journal of Cell Biology*, **53**, pp. 419–434.

Schroeder, T. E. (1990) 'The contractile ring and furrowing in dividing cells', *Annals New York Academy of Sciences*, **582**, pp. 78–87.

Seidl, A. H. (2014) 'Regulation of conduction time along axons', *Neuroscience*, **0**, pp. 126–134.

Sens, P. and Plastino, J. (2015) 'Membrane tension and cytoskeleton organization in cell motility', *Journal of Physics Condensed Matter*, **27**, pp. 1–13.

Shahinnejad, A., Haghpanahi, M. and Farmanzad, F. (2013) 'Finite element analysis of axonal microtubule bundle under tension and torsion', *Procedia Engineering*, **59**, pp. 16–24.

Shreiber, D. I., Hao, H. and Elias, R. A. I. (2009) 'Probing the influence of myelin and glia on the tensile properties of the spinal cord', *Biomechanics and Modeling in Mechanobiology*, **8**, pp. 311–321.

Siechen, S., Yang, S., Chiba, A. and Saif, T. (2009) 'Mechanical tension contributes to clustering of neurotransmitter vesicles at presynaptic terminals.', *Proceedings of the National Academy of Sciences of the United States of America*, **106**, pp. 12611–12616.

Sigurdson, W. J. and Morris, E. (1989) 'Stretch-activated ion channels in growth cones of snail neurons', *The Journal of Neuroscience*, **9**, pp. 2801–2808.

da Silva, R. and Lange, A. B. (2011) 'Evidence of a central pattern generator regulating spermathecal muscle activity in *Locusta migratoria* and its coordination with oviposition.', *The Journal of experimental biology*, **214**, pp. 757–63.

Simmons, L. W. and Zuk, M. (1992) 'Variability in call structure and pairing success of male field crickets, *Gryllus bimaculatus*: the effects of age, size and parasite load', *Animal Behaviour*, **44**, pp. 1145–1152.

Simpson, S. J., Despland, E., Hagele, B. F. and Dodgson, T. (2001) 'Gregarious behavior in desert locusts is evoked by touching their back legs', *PNAS*, **98**, pp. 3895–3897.

Slautterback, D. B. (1963) 'Cytoplasmic microtubules I . Hydra', *The Journal of Cell Biology*, **18**, pp. 367–388.

Small, J. V., Kaverina, I., Krylyshkina, O. and Rottner, K. (1999) 'Cytoskeleton cross-talk during cell motility', *FEBS Letters*, **452**, pp. 96–99.

Smarandache-Wellman, C. R. (2016) 'Arthropod neurons and nervous system', *Current Biology*, **26**, pp. 960–965.

Smirnov, M. S., Cabral, K. A., Geller, H. M. and Urbach, J. S. (2014) 'The effects of confinement on neuronal growth cone morphology and velocity', *Biomaterials*, **35**, pp. 6750–6757.

Smith, D. H., Chen, X.-H., Nonaka, M., Trojanowski, J. Q., Lee, V.-Y., Saatman, K. E., Leoni, M. J., Xu, B.-N., Wolf, J. A. and Meaney, D. F. (1999) 'Accumulation of amyloid β and tau and the formation of neurofilament inclusions following diffuse brain injury in the pig', *Journal of Neuropathology and Experimental Neurology*, **58**, pp. 982–992.

Smith, D. H. (2009) 'Stretch growth of integrated axon tracts: Extremes and exploitations', *Progress in Neurobiology*, **89**, pp. 231–239.

Smith, D. H., Wolf, J. A. and Meaney, D. F. (2001) 'A new strategy to produce sustained growth of central nervous system axons: Continuous mechanical tension', *Tissue Engineering*, **7**, pp. 131–139.

Smith, D. S. (1972) *Muscle*. New York: Academic Press.

Snodgrass, R. E. (1933) *Morphology of the insect abdomen. Part II. The genital ducts and the ovipositor*. Smithsonian Miscellaneous Collections, 89.

Soellner, P., Quinlan, R. A. and Franke, W. W. (1985) 'Identification of a distinct soluble subunit of an intermediate filament protein: Tetrameric vimentin from living cells', *Proceedings of the National Academy of Sciences of the USA Biochemistry*, **82**, pp. 7929–7933.

Song, W., Ranjan, R., Dawson-Scully, K., Bronk, P., Marin, L., Seroude, L., Lin, Y. J., Nie, Z., Atwood, H. L., Benzer, S. and Zinsmaier, K. E. (2002) 'Presynaptic regulation of neurotransmission in *Drosophila* by the G protein-coupled receptor Methuselah', *Neuron*, **36**, pp. 105–119.

Squire, J. M. (2016) 'Muscle contraction: Sliding filament history, sarcomere dynamics and the two Huxleys', *Global Cardiology Science and Practice*, **11**, pp. 1–23.

Starger, J. M., Brown, W. E., Goldman, A. E. and Goldman, R. D. (1978) 'Biochemical and immunological analysis of rapidly purified 10nm filaments from baby hamster kidney (BHK-21) cells', *Journal of Cell Biology*, **78**, pp. 93–109.

Steinert, P. M. and Roop, D. R. (1988) 'Molecular and cellular biology of intermediate filaments', *Annu. Rev. Biochem*, **57**, pp. 593–625.

Stokin, G. B., Raman, R., Davies, P. and Masliah, E. (2014) 'Axonopathy and transport deficits early in the pathogenesis of Alzheimer's disease', *Science*, **307**, pp. 1282–1288.

Stone, J. R., Okonkwo, D. O., Dialo, A. O., Rubin, D. G., Mutlu, L. K., Povlishock, J. T. and Helm, G. A. (2004) 'Impaired axonal transport and altered axolemmal permeability occur in distinct populations of damaged axons following traumatic brain injury', *Experimental Neu*, **190**, pp. 59–69.

Straub, F. B. (1942) *Studies from the Institute of Medical Chemistry University Szeged*

Vol. 2. Edited by A. Szent-Györgyi. Basel: S. Karger AG.

Straub, F. B. (1943) *Studies from the Institute of Medical Chemistry University Szeged Vol. 3*. Edited by A. Szent-Györgyi. Basel: S. Karger AG.

Sugimura, K., Lenne, P. and Graner, F. (2016) 'Measuring forces and stresses *in situ* in living tissues', *Development*, **143**, pp. 186–196.

Suraneni, P., Rubinstein, B., Unruh, J. R., Durnin, M., Hanein, D. and Li, R. (2012) 'The Arp2/3 complex is required for lamellipodia extension and directional fibroblast cell migration', *The Journal of Cell Biology*, **197**, pp. 239–251.

Sweitzer, N. K. and Moss, R. L. (1993) 'Determinants of loaded shortening velocity in single cardiac myocytes permeabilized with alpha-hemolysin.', *Circulation Research*, **73**, pp. 1150–1162.

Sword, G. A., Lecoq, M. and Simpson, S. J. (2010) 'Phase polyphenism and preventative locust management', *Journal of Insect Physiology*, **56**, pp. 949–957.

Tabb, J. S., Molyneaux, B. J., Cohen, D. L., Kuznetsov, S. A. and Langford, G. M. (1998) 'Transport of ER vesicles on actin filaments in neurons by myosin V', *Journal of cell science*, **3234**, pp. 3221–3234.

Tamura, A., Hayashi, S., Nagayama, K. and Matsumoto, T. (2008) 'Mechanical characterization of brain tissue in high-rate extension', *Journal of Biomechanical and Science Engineering*, **3**, pp. 263–274.

Tanaka, E., Ho, T. and Kirschner, M. W. (1995) 'The role of microtubule dynamics in growth cone motility and axonal growth', *Journal of Cell Biology*, **128**, pp. 139–155.

Tang-Schomer, M. D., Patel, A. R., Baas, P. W. and Smith, D. H. (2010) 'Mechanical breaking of microtubules in axons during dynamic stretch injury underlies delayed elasticity, microtubule disassembly, and axon degeneration.', *The FASEB journal*, **24**, pp. 1401–1410.

Theriot, J. and Mitchison, T. J. (1991) 'Actin microfilament dynamics in locomoting cells', *Nature*, **352**, pp. 126–131.

Thompson, D. W. (1917) *On Growth and Form*. London: Cambridge University Press.

Thompson, K. J. (1986) 'Oviposition digging in the grasshopper. I. Functional anatomy and the motor programme.', *The Journal of experimental biology*, **122**, pp. 387–411.

Tilney, L. G., Bryan, J., Bush, D. J., Fujiwara, K., Mooseker, M. S., Murphy, D. B. and Snyder, D. H. (1973) 'Microtubules: Evidence for 13 protofilaments', *The Journal of Cell Biology*, **59**, pp. 267–275.

Tofangchi, A., Fan, A. and Saif, M. T. A. (2016) 'Mechanism of axonal contractility in embryonic *Drosophila* motor neurons *in vivo*', *Biophysical Journal*, **111**, pp. 1519–1527.

Tojkander, S., Gateva, G. and Lappalainen, P. (2012) 'Actin stress fibers – assembly , dynamics and biological roles', *Journal of cell science*, **125**, pp. 1855–1864.

Tooley, A. J., Gilden, J., Jacobelli, J., Beemiller, P., Trimble, W. S., Kinoshita, M. and Krummel, M. F. (2013) 'Amoeboid T lymphocytes require the septin cytoskeleton for cortical integrity and persistent motility', *Nature cell biology*, **11**, pp. 17–26.

Toro, R. and Burnod, Y. (2005) 'A morphogenetic model for the development of cortical convolutions', *Cerebral Cortex*, **15**, pp. 1900–1913.

Tracey, W. D., Wilson, R. I., Laurent, G. and Benzer, S. (2003) 'painless, a *Drosophila* gene essential for nociception', *Cell*, **113**, pp. 1–13.

Tsaneva-Atanasova, K., Burgo, A., Galli, T. and Holcman, D. (2009) 'Quantifying neurite growth mediated by interactions among secretory vesicles, microtubules, and actin networks', *Biophysical Journal*, **96**, pp. 840–857.

Turk, E., Wills, A. A., Kwon, T., Sedzinski, J., Wallingford, J. B. and Stearns, T. (2015) 'Zeta-tubulin is a member of a conserved tubulin module and is a component of the centriolar basal foot in multiciliated cells', *Curr Biol.*, **25**, pp. 2177–2183.

Umetsu, D., Aigouy, B., Aliee, M., Sui, L., Eaton, S., Jülicher, F. and Dahmann, C. (2014) 'Local increases in mechanical tension shape compartment boundaries by biasing cell intercalations', *Current Biology*, **24**, pp. 1798–1805.

Usukura, J. and Kusumi, A. (2006) 'Three-dimensional reconstruction of the membrane skeleton at the plasma membrane interface by electron tomography', *The Journal of Cell Biology*, **174**, pp. 851–862.

Uvarov, B. P. (1966) *Grasshoppers and Locusts, vol. 1*. Cambridge: Cambridge University Press.

Van Veen, M. P. and Van Pelt, J. (1994) 'Neuritic growth rate described by modeling microtubule dynamics', *Bulletin of Mathematical Biology*, **56**, pp. 249–273.

Vehoff, T., Glisovic, H., Schollmeyer, H., Zippelius, A. and Salditt, T. (2007) 'Mechanical Properties of Spider Dragline Silk: Humidity, Hysteresis, and Relaxation', *Biophysical Journal*, **93**, pp. 4425–4432.

Vicente-manzanares, M., Ma, X., Adelstein, R. S. and Horwitz, A. R. (2010) 'Non-muscle myosin II takes centre stage in cell adhesion and migration', *Nature reviews. Molecular cell biology*, **10**, pp. 778–790.

Vierk, R., Pflueger, H. J. and Duch, C. (2009) 'Differential effects of octopamine and tyramine on the central pattern generator for *Manduca* flight', *J Comp Physiol*, **195**, pp. 265–277.

Vincent, J. F. V and Wood, S. D. E. (1972) 'Mechanism of abdominal extension during oviposition in *Locusta*', *Nature*, **235**, pp. 167–168.

Vincent, J. and Irons, D. (2009) 'Developmental biology: Tension at the border', *Curr Biol.*, **19**, pp. 1028–1030.

Vogel, S. (2003) *Comparative Biomechanics: Life's Physical World*. first. New Jersey: Princeton University Press.

Vogel, V. (2006) 'Mechanotransduction involving multimodular proteins: Converting force into biochemical signals', *Annual Review of Biophysics and Biomolecular Structure*, **35**, pp. 459–488.

Vosseler, J. (1905) 'Die Wanderheuschrecken in Usambara im Jahre 1903/1904, zugleich ein Beitrag zu ihre Biologie', *Ber. Ld. u. Forstw. D.-Ostafrica*, **2**, pp. 291–374.

Wada, A., Kato, K., Uwo, M. F., Yonemura, S. and Hayashi, S. (2007) 'Specialized extraembryonic cells connect embryonic and extraembryonic epidermis in response to Dpp during dorsal closure in *Drosophila*', *Developmental Biology*, **301**, pp. 340–349.

Walker, R. A., O'Brien, E. T., Pryer, N. K., Soboeiro, M. F., Voter, W. A., Erickson, H. P. and Salmon, E. D. (1988) 'Dynamic instability of individual microtubules analyzed by video light microscopy: Rate constants and transition frequencies', *The Journal of Cell Biology*, **107**, pp. 1437–1448.

Wang, K., Mcclure, J. and Tu, A. (1979) 'Titin: Major myofibrillar components of striated muscle', *Proceedings of the National Academy of Sciences USA*, **76**, pp. 3698–3702.

Wang, S. S., Shultz, J. R., Burish, M. J., Harrison, K. H., Hof, P. R., Towns, L. C., Wagers, M. W. and Wyatt, K. D. (2008) 'Functional trade-offs in white matter axonal scaling', *The Journal of Neuroscience*, **28**, pp. 4047–4056.

Wang, Y. (1985) 'Exchange of actin subunits at the leading edge of living fibroblasts: possible role of treadmilling', *The Journal of Cell Biology*, **101**, pp. 597–602.

Watson, A. H. D. and Burrows, M. (1982) 'The ultrastructure of identified locust motor neurones and their synaptic relationships', *Journal of Comparative Neurology*, **205**, pp. 383–397.

Wegner, A. (1982) 'Treadmilling of actin at physiological salt concentrations. An analysis of the critical concentrations of actin filaments', *Journal of Molecular Biology*, **161**, pp. 607–615.

Wehrle-Haller, B. and Imhof, B. A. (2003) 'Actin, microtubules and focal adhesion dynamics during cell migration', *International Journal of Biochemistry and Cell Biology*, **35**, pp. 39–50.

Weisenberg, R. C., Deery, W. J. and Dickinson, P. J. (1976) 'Tubulin-nucleotide interactions during the polymerization and depolymerization of microtubules', *Biochemistry*, **15**, pp. 4248–4254.

Wheeler, W. C., Whiting, M., Wheeler, Q. D. and Carpenter, J. M. (2001) 'The

phylogeny of the extant hexapod orders', *Cladistics*, **17**, pp. 113–169.

Wieschaus, E., Nusslein-Volhard, C. and Kluding, H. (1984) 'Krüppel, a gene whose activity is required early in the zygotic genome for normal embryonic segmentation', *Developmental Biology*, **104**, pp. 172–186.

Wilson, D. M. (1961) 'The central nervous control of flight in a locust', *Journal of Experimental Biology*, **38**, pp. 471–490.

Wilson, E. B. (1928) *The cell in development and heredity*. third. New York: Macmillan Company.

Windoffer, R. and Leube, R. E. (1999) 'Detection of cytokeratin dynamics by time-lapse fluorescence microscopy in living cells', *Journal of Cell Science*, **112**, pp. 4521–4534.

Winter, C. G., Wang, B., Ballew, A., Royou, A., Karess, R., Axelrod, J. D. and Luo, L. (2001) '*Drosophila* Rho-associated kinase (Drok) links Frizzled-mediated planar cell polarity signaling to the actin cytoskeleton', *Cell*, **105**, pp. 81–91.

Witte, H., Neukirchen, D. and Bradke, F. (2008) 'Microtubule polarization stabilization specifies initial neuronal polarization', *Journal of Cell Biology*, **180**, pp. 619–632.

Wolbarsht, M. L. (1960) 'Electrical characteristics of insect mechanoreceptors', *The Journal of General Physiology*, **44**, pp. 105–122.

Wolf, H., Ronacher, B. and Reichert, H. (1988) 'Patterned synaptic drive to locust flight motoneurons after hemisection of thoracic ganglia', *J Comp Physiol*, **163**, pp. 761–769.

Wong, R. and Lange, A. B. (2014) 'Octopamine modulates a central pattern generator associated with egg-laying in the locust, *Locusta migratoria*', *Journal of Insect Physiology*, **63**, pp. 1–8.

Wootton, R. J., Herbert, R. C., Young, P. G. and Evans, K. E. (2003) 'Approaches to the structural modelling of insect wings', *Philosophical transactions of the Royal Society London B*, **358**, pp. 1577–1587.

Xu, G., Knutsen, A. K., Dikranian, K., Kroenke, C. D., Bayly, P. V and Taber, L. A. (2010) 'Axons pull on the brain, but tension does not drive cortical folding', *Journal of Biomechanical Engineering*, **132**, pp. 1–17.

Xu, G., Bayly, P. V. and Taber, L. A. (2009) 'Residual stress in the adult mouse brain', *Biomechanics and Modeling in Mechanobiology*, **8**, pp. 253–262.

Xu, K., Zhong, G. and Zhuang, X. (2013) 'Actin, spectrin and associated proteins form a periodic cytoskeletal structure in axons', *Science*, **339**, pp. 1–11.

Xu, Q., Chen, F., Wang, Y., Li, X. and He, J. (2014) 'Development of a miniaturized bioreactor for neural culture and axon stretch growth', *Conf Proc IEEE Eng Med Biol Soc*, **2014**, pp. 1416–1419.

Yoon, K. H., Yoon, M., Moir, R. D., Khuon, S., Flitney, F. W. and Goldman, R. D. (2001) 'Insights into the dynamic properties of keratin intermediate filaments in living epithelial cells', *The Journal of Cell Biology*, **153**, pp. 503–516.

Yoon, M., Moir, R. D., Prahlad, V. and Goldman, R. D. (1998) 'Motile properties of vimentin intermediate filament networks in living cells', *The Journal of Cell Biology*, **143**, pp. 147–157.

Young, P. E., Richman, A. M., Ketchum, A. S. and Kiehart, D. P. (1993) 'Morphogenesis in *Drosophila* requires nonmuscle myosin heavy chain function', *Genes & Development*, **7**, pp. 29–41.

Yusko, E. C. and Asbury, C. L. (2014) 'Force is a signal that cells cannot ignore.', *Mol. Biol. Cell*, **25**, pp. 3717–25.

Zacharias, D., Leslie, J., Williams, D., Meier, T. and Reichert, H. (1993) 'Neurogenesis in the insect brain: cellular identification and molecular characterization of brain neuroblasts in the grasshopper embryo', *Development*, **118**, pp. 941–955.

Zarei, S., Carr, K., Reiley, L., Diaz, K., Guerra, O., Altamirano, P. F., Pagani, W., Lodin, D., Orozco, G. and Chinea, A. (2015) 'A comprehensive review of amyotrophic lateral sclerosis', *Surg Neurol Int*, **6**, pp. 1–23.

Zhang, B., Maiti, A., Shively, S., Lakhani, F., Mcdonald-jones, G., Bruce, J., Lee, E. B., Xie, S. X., Joyce, S., Li, C., Toleikis, P. M., Lee, V. M. and Trojanowski, J. Q. (2005) 'Microtubule-binding drugs offset tau sequestration by stabilizing microtubules and reversing fast axonal transport deficits in a tauopathy model', *PNAS*, **102**, pp. 227–231.

Zhang, Y., Abiraman, K., Li, H., Pierce, D. M., Tzingounis, A. V. and Lykotrafitis, G. (2017) 'Modeling of the axon membrane skeleton structure and implications for its mechanical properties', *PLOS Computational Biology*, **13**, p. e1005407.

Zheng, J., Lamoureux, P., Heidemann, S. R. and Buxbaum, E. (1991) 'Tensile regulation of axonal elongation and initiation', *The Journal of Neuroscience*, **11**, pp. 1117–1125.

Zhou, F., Zhou, J., Dedhar, S., Wu, Y., Snider, W. D., Hill, C. and Carolina, N. (2004) 'NGF-induced axon growth is mediated by localized inactivation of GSK-3β and functions of the microtubule plus end binding protein APC', *Neuron*, **42**, pp. 897–912.

Zhu, Q., Couillard-Despres, S. and Julien, J.-P. (1997) 'Delayed maturation of regenerating myelinated axons in mice lacking neurofilaments', *Experimental Neurology*, **316**, pp. 299–316.

Ziegler, C. (1994) 'Titin-related proteins in invertebrate muscles', *Comparative Biochemistry and Physiology*, **109**, pp. 823–833.

Zinn, K. and Condron, B. G. (1994) 'Cell fate decisions in the grasshopper central nervous system', *Current Opinion in Cell Biology*, **6**, pp. 783–787.